



Structural and compositional effects on tree-water relation

Strukturelle und Zusammensetzungseffekte auf die Beziehung zwischen Baum und Wasser

Doctoral thesis for a doctoral degree
at the Graduate School of Life Sciences,
Julius-Maximilians-Universität Würzburg,
Section Integrative Biology

Submitted by
Manish Kumar
from Sitamarhi, India

Würzburg, 2023



Submitted on:

Office stamp

Members of the Thesis Committee

Chairperson : Prof Dr Thomas Schmitt
University of Würzburg
Department of Animal Ecology and
Tropical Biology, Biocenter, Würzburg, Germany

Primary Supervisor : Prof Dr Bernhard Schuldt
Chair of Forest Botany,
Technical University of Dresden, Germany.

Supervisor (Second) : Prof. Dr. Dirk Holscher
Institute for tropical silviculture and forest ecology,
Georg-August-Universität Göttingen, Germany.

Supervisor (Third) : Prof. Dr. Juliano Sarmiento Cabral
School of Biosciences,
Biodiversity Modelling and Environmental Change,
Birmingham, United Kingdom.

Date of Public defense:

Date of Receipt of Certificates:

Table of Contents

Contents

| | |
|--|-----------|
| Table of Contents | i |
| General Summary | iv |
| Zusammenfassung | vi |
| Symbols, abbreviations and acronyms | ix |
| Chapter-1: General Introduction | 1 |
| 1.1 Forest ecosystems in a context of changing climate and droughts | 1 |
| 1.2 Drought-induced tree mortality in European forests..... | 1 |
| 1.3 Advantages of mixed-species reforestation for ecological restoration | 2 |
| 1.4 The plant hydraulic system and drought susceptibility..... | 4 |
| 1.5 Growth rate trade-off with xylem safety–efficiency association | 5 |
| 1.6 Wood anatomy trade-off with hydraulic efficiency–safety association..... | 6 |
| 1.7 Stomatal stringency in the framework of iso-anisohydric continuum | 8 |
| 1.8 Plant desiccation time and traits coordination | 8 |
| 1.9 Research site, experimental design, and species description | 9 |
| 1.10 General study hypothesis, objectives, and thesis structure | 12 |
| References:..... | 15 |
| Chapter-2: | 26 |
| Influence of Juvenile Growth on Xylem Safety and Efficiency in Three Temperate Tree Species | 26 |
| Abstract..... | 27 |
| 2.1 Introduction..... | 28 |
| 2.2 Material and Methods | 30 |
| 2.2.1 Study Site, Microclimatic Measurements, and Plant Material | 30 |
| 2.2.2 Sample Collection, Structural Measurements, and Growth Rate | 33 |
| 2.2.3 Leaf Traits | 33 |
| 2.2.4 Hydraulic Conductivity..... | 34 |
| 2.2.5 Vulnerability Curves..... | 35 |
| 2.2.6 Wood Anatomy | 36 |
| 2.2.7 Statistical Analyses | 37 |
| 2.3 Results..... | 37 |
| 2.3.1 Growth and Structural Differences across Species and Treatments..... | 37 |
| 2.3.2 Effects of Climatic Stress on Hydraulic, Wood Anatomical, and Leaf Morphological Traits | 37 |

| | |
|--|------------|
| 2.3.3 Relationships of Hydraulic Safety-Efficiency, Leaf and Anatomical Traits with Species Growth Performance | 38 |
| 2.3.4 Hydraulic Safety-Efficiency Trade-Offs and Their Relations to Wood Anatomy and Leaf Traits | 41 |
| 2.4 Discussion | 45 |
| 2.4.1 Relationship of Juvenile Growth with Hydraulic Safety and Efficiency | 45 |
| 2.4.2 Relationship of Juvenile Growth with Leaf-Related Traits | 46 |
| 2.4.3 Trade-Off between Hydraulic Efficiency and Safety and Anatomic Determinants | 47 |
| 2.4.4 Variability in Hydraulic and Foliar Traits in Response to Environmental Stress | 48 |
| 2.5 Conclusions | 48 |
| Supplementary information | 50 |
| References: | 57 |
| Chapter-3: | 63 |
| Coordinated drought responses determine the time to hydraulic failure in five temperate tree species differing in their degree of isohyry | 63 |
| Abstract | 64 |
| 3.1 Introduction | 65 |
| 3.2 Material and methods | 68 |
| 3.2.1 Species description | 68 |
| 3.2.2 Drying-out experiments | 69 |
| 3.2.3 Plant stomatal response during drought | 70 |
| 3.2.4 Embolism resistance and hydraulic safety margin | 71 |
| 3.2.5 Determination of plant desiccation times | 71 |
| 3.2.6 Plant hydroscape | 72 |
| 3.2.7 Shoot hydraulic capacitance | 72 |
| 3.2.8 Leaf traits | 73 |
| 3.2.9 Data analysis | 74 |
| 3.3 Results | 76 |
| 3.3.1 Stomatal behaviour and relative degree of isohyry | 76 |
| 3.3.2 Species differences in drought response traits | 77 |
| 3.3.3 Coordination between drought response traits | 80 |
| 3.4 Discussion | 83 |
| 3.4.1 The temporal progression of plant drought responses | 83 |
| 3.4.2 Coordination of drought response traits | 84 |
| 3.4.3 Metrics of the degree of isohyry | 86 |
| 3.5 Conclusion | 88 |
| Supplementary information | 90 |
| References: | 93 |
| Chapter-4: Synthesis (General discussion) | 102 |
| 4.1 Juvenile growth trade-off with hydraulic efficiency-safety | 102 |
| 4.2 Xylem safety-efficiency trade-off and anatomical factors | 104 |
| 4.3 Adjustment of leaf traits in response to environmental stress | 105 |

| | |
|---|------------|
| 4.4 Stomatal stringency and relative degree of isohydry | 109 |
| 4.4.1 Metrics and proxies for plant water potential regulation | 110 |
| 4.4.2 Estimating plant degree of isohydry and testing species-specific variability using linear mixed-effects models..... | 111 |
| 4.4.3 Challenges to the isohydry concept and variability in plant water potential dynamics..... | 112 |
| 4.5 Plant desiccation time thresholds | 117 |
| 4.6 Traits significance and their coordination along the spectrum | 118 |
| 4.6.1 Turgor loss point and stomata closure | 120 |
| 4.6.2 Embolism resistance and hydraulic safety margin | 121 |
| 4.6.3 Cuticular conductance..... | 121 |
| 4.6.4 Shoot capacitance..... | 122 |
| Supplementary information | 124 |
| References:..... | 133 |
| Chapter-5: General conclusion..... | 143 |
| 5.1 Conclusion | 143 |
| 5.2 Scopes and Limitations | 145 |
| 5.3 Future perspectives | 146 |
| References:..... | 147 |
| Index of Figures..... | 150 |
| Index of Tables | 151 |
| Publications: | 152 |
| Acknowledgements | 153 |
| Affidavit | 154 |
| Curriculum vitae..... | 155 |
| Authors contributions statement..... | 158 |

General Summary

Forests are essential sources of tangible and intangible benefits, but global climate change associated with recurrent extreme drought episodes severely affects forest productivity due to extensive tree die-back. On that, it appeals to an urgency for large-scale reforestation efforts to mitigate the impact of climate change worldwide; however, there is a lack of understanding of drought-effect on sapling growth and survival mechanisms. It is also challenging to anticipate how long trees can survive and when they succumb to drought. Hence, to ensure success of reforestation programs and sustainable forest productivity, it is essential to identify drought-resistant saplings. For that, profound knowledge of hydraulic characteristics is needed. To achieve this, the study was split into two phases which seek to address (1) how the hydraulic and anatomical traits influence the sapling's growth rate under drought stress. (2) how plant water potential regulation and physiological traits are linked to species' water use strategies and their drought tolerance.

The dissertation is assembled of two study campaigns carried out on saplings at the Chair of Botany II, University of Würzburg, Germany. The first study involved three ecologically important temperate broadleaved tree species — saplings of 18-month (*Acer pseudoplatanus*, *Betula pendula*, and *Sorbus aucuparia*) — grown from seeds in contrasting conditions (inside a greenhouse and outside), with the latter being subjected to severe natural heat waves. In the second study, two additional temperate species (*Fagus sylvatica* and *Tilia cordata*) were added. The drying-out event was conducted using a randomised blocked design by monitoring plant water status in a climate-controlled chamber and a greenhouse.

In campaign I, I present the result based on analysed data of 82 plants of temperate deciduous species and address the juvenile growth rate trade-off with xylem safety-efficiency. Our results indicate biomass production varies considerably due to the contrasted growing environment. High hydraulic efficiency is necessary for increased biomass production, while safety-efficiency traits are decoupled and species-specific. Furthermore, productivity was linked considerably to xylem safety without revealing a well-defined pattern among species. Moreover, plasticity in traits differed between stressed and non-stressed plants. For example, safety-related characteristics were more static than efficiency-related traits, which had higher intra-specific variation. Moreover, we recorded anatomical and leaf traits adjustments in response to a stress condition, but consistency among species is lacking.

In campaign II, I combined different ways to estimate the degree of isohydry based on water potential regulation and connected the iso-anisohydic spectrum (i.e., hydroscape area, HSA) to hydraulic traits to elucidate actual plant performance during drought. We analysed plant water potential regulation (Ψ_{pd} and Ψ_{md}) and stomatal conductance of 28-29 month saplings of five species. I used a linear mixed modelling approach that allowed to control individual variations to describe the water potential regulation and tested different conceptual definitions of isohydricity. The combined methods allowed us to estimate species' relative degree of isohydry. Further, we examined the traits coordination, including hydraulic safety margin, HSM; embolism resistance, P_{88} ; turgor loss, Ψ_{tlp} ; stomata closure, P_{s90} ; capacitance, C ; cuticular conductance, g_{min} , to determine time to hydraulic failure (T_{hf}). T_{hf} is the cumulative effect of time to stomata closure (T_{sc}) and time after stomatal closure to catastrophic hydraulic failure (T_{crit}).

Our results show the species' HSA matches their stomatal stringency, which confirms the relationship between stomatal response and leaf water potential decline. Species that close stomata at lower water potential notably had a larger HSA. Isohydry behaviour was mostly associated with leaf hydraulic traits and poorly to xylem safety traits. Species' degree of isohydry was also unrelated to the species' time to death during drying-out experiments. This supports the notion that isohydry behaviours are linked to water use rather than drought survival strategies. Further, consistent with our assumptions, more isohydry species had larger internal water storage and lost their leaf turgor at less negative water potentials. Counter to our expectations, neither embolism resistance nor the associated hydraulic safety margins were related to metrics of isohydry. Instead, our results indicate traits associated with plant drought response to cluster along two largely independent axes of variation (i.e., stomatal stringency and xylem safety). Furthermore, on the temporal progression of plant drought responses, stomatal closure is critical in coordinating various traits to determine species' hydraulic strategies. Desiccation avoidance strategy was linked to T_{sc} and coordinated traits response of P_{s90} , Ψ_{tlp} , and HSA, whereas desiccation tolerance was related to T_{crit} and traits such as lower P_{88} value, high HSM, and lower g_{min} . Notably, the shoot capacitance (C) is crucial in T_{hf} and exhibits dichotomous behaviour linked to both T_{sc} and T_{crit} .

In conclusion, knowledge of growth rate trade-offs with xylem safety-efficiency combined with traits linked to species' hydraulic strategies along the isohydry could substantially enhance our ability to identify drought-resistant saplings to ensure the success of reforestation programs and predicting sensitivity to drought for achieving sustainable forest ecosystems.

Zusammenfassung

Wälder sind wichtige Quellen materieller und immaterieller Vorteile, aber der globale Klimawandel, der mit wiederkehrenden extremen Dürreperioden einhergeht, beeinträchtigt die Produktivität der Wälder aufgrund des starken Absterbens von Bäumen erheblich. Deshalb werden dringend groß angelegte Aufforstungsmaßnahmen gefordert, um die Auswirkungen des Klimawandels weltweit abzumildern. Allerdings fehlt es an Kenntnissen über die Auswirkungen von Dürre auf das Wachstum und die Überlebensmechanismen von Jungbäumen. Es ist auch schwierig, vorherzusehen, wie lange Bäume überleben können und wann sie der Trockenheit erliegen. Um den Erfolg von Wiederaufforstungsprogrammen und die nachhaltige Produktivität der Wälder zu gewährleisten, ist es daher unerlässlich, trockenheitsresistente Setzlinge zu identifizieren. Dazu ist eine profunde Kenntnis der hydraulischen Eigenschaften erforderlich. Um dies zu erreichen, wurde die Studie in zwei Phasen aufgeteilt, in denen untersucht werden soll, (1) wie die hydraulischen und anatomischen Merkmale die Wachstumsrate der Setzlinge unter Trockenstress beeinflussen. (2) wie die Regulierung des pflanzlichen Wasserpotenzials und die physiologischen Merkmale mit den Wassernutzungsstrategien der Arten und ihrer Trockentoleranz zusammenhängen.

Die Dissertation setzt sich aus zwei Studienkampagnen zusammen, die am Lehrstuhl für Botanik II der Universität Würzburg an Setzlingen durchgeführt wurden. In der ersten Studie wurden drei ökologisch wichtige Laubbaumarten der gemäßigten Zonen - 18-monatige Setzlinge (*Acer pseudoplatanus*, *Betula pendula* und *Sorbus aucuparia*) - aus Samen unter unterschiedlichen Bedingungen (in einem Gewächshaus und im Freien) aufgezogen, wobei letztere schweren natürlichen Hitzewellen ausgesetzt waren. In der zweiten Studie wurden zwei weitere gemäßigte Arten (*Fagus sylvatica* und *Tilia cordata*) hinzugefügt. Der Austrocknungsversuch wurde in einem randomisierten Blockdesign durchgeführt, bei dem der Wasserhaushalt der Pflanzen in einer klimatisierten Kammer und einem Gewächshaus überwacht wurde.

In Kampagne I präsentiere ich die Ergebnisse, die auf den analysierten Daten von 82 Pflanzen gemäßigter Laubbaumarten basieren, und gehe auf den Kompromiss zwischen der Wachstumsrate von Jungpflanzen und der Sicherheitseffizienz des Xylems ein. Unsere Ergebnisse zeigen, dass die Biomasseproduktion aufgrund der unterschiedlichen Wachstumsbedingungen stark variiert. Eine hohe hydraulische Effizienz ist für eine erhöhte Biomasseproduktion

notwendig, während die Sicherheitseffizienz entkoppelt und artspezifisch ist. Darüber hinaus war die Produktivität in erheblichem Maße mit der Xylemsicherheit verknüpft, ohne dass sich ein klar definiertes Muster zwischen den Arten ergab. Darüber hinaus war die Plastizität der Merkmale zwischen gestressten und nicht gestressten Pflanzen unterschiedlich. So waren beispielsweise sicherheitsbezogene Merkmale statischer als effizienzbezogene Merkmale, die eine stärkere intra-spezifische Variation aufwiesen. Darüber hinaus haben wir Anpassungen der anatomischen Merkmale und der Blatteigenschaften als Reaktion auf eine Stressbedingung festgestellt, aber es fehlt die Konsistenz zwischen den Arten.

In Kampagne II kombinierte ich verschiedene Methoden zur Schätzung des Isohydrierungsgrads auf der Grundlage der Wasserpotenzialregulierung und verknüpfte das iso-anisohydrische Spektrum (d. h. die Hydroscape-Fläche, HSA) mit hydraulischen Merkmalen, um die tatsächliche Leistung der Pflanzen bei Trockenheit zu ermitteln. Wir analysierten die Regulierung des pflanzlichen Wasserpotenzials (Ψ_{pd} und Ψ_{md}) und die stomatäre Leitfähigkeit von 28-29 Monate alten Setzlingen von fünf Arten. Ich verwendete einen linearen gemischten Modellierungsansatz, der die Kontrolle individueller Variationen zur Beschreibung der Wasserpotenzialregulierung ermöglichte, und testete verschiedene konzeptionelle Definitionen der Isohydrität. Die kombinierten Methoden ermöglichten es uns, den relativen Grad der Isohydrität der Arten zu schätzen. Darüber hinaus untersuchten wir die Koordination der Merkmale, einschließlich der hydraulischen Sicherheitsspanne (HSM), des Embolieresistenz (P_{88}), des Turgorverlustes (Ψ_{tlp}), des Spaltöffnungsgrades (P_{s90}), der Kapazität (C) und des kutikulären Leitwertes (g_{min}), um die Zeit bis zum hydraulischen Versagen (T_{hf}) zu bestimmen. T_{hf} ist der kumulative Effekt der Zeit bis zum Schließen der Spaltöffnungen (T_{sc}) und der Zeit nach dem Schließen der Spaltöffnungen bis zum katastrophalen hydraulischen Versagen (T_{crit}).

Unsere Ergebnisse zeigen, dass die HSA der Arten mit ihrer Spaltöffnungsintensität übereinstimmt, was die Beziehung zwischen der Spaltöffnungsreaktion und dem Rückgang des Wasserpotenzials der Blätter bestätigt. Arten, die ihre Spaltöffnungen bei einem niedrigeren Wasserpotenzial schließen, hatten einen deutlich größeren HSA. Das isohydrische Verhalten stand hauptsächlich mit den hydraulischen Eigenschaften der Blätter in Verbindung und kaum mit den Sicherheitsmerkmalen des Xylems. Der Grad der Isohydrierung der Arten stand auch in keinem Zusammenhang mit der Zeit bis zum Absterben der Arten während der Austrocknungsversuche. Dies unterstützt die Annahme, dass das Isohydrie-Verhalten eher mit der Wassernutzung als mit

Überlebensstrategien bei Trockenheit zusammenhängt. Darüber hinaus wiesen isohydrische Arten, wie von uns angenommen, einen größeren internen Wasserspeicher auf und verloren ihren Blattturgor bei weniger negativen Wasserpotentialen. Entgegen unseren Erwartungen standen weder die Embolieresistenz noch die damit verbundenen hydraulischen Sicherheitsspannen in Zusammenhang mit Isohydratisierungsmerkmalen. Stattdessen deuten unsere Ergebnisse darauf hin, dass sich die Merkmale, die mit der Reaktion der Pflanzen auf Trockenheit in Verbindung stehen, entlang zweier weitgehend unabhängiger Variationsachsen (d. h. stomatäre Strenge und Xylem-Sicherheit) gruppieren. Was den zeitlichen Verlauf der pflanzlichen Reaktionen auf Trockenheit betrifft, so ist der Stomataverschluss für die Koordinierung der verschiedenen Merkmale entscheidend, um die hydraulischen Strategien der Arten zu bestimmen. Die Strategie zur Vermeidung von Austrocknung war mit T_{sc} und koordinierten Merkmalen wie P_{s90} , Ψ_{tlp} und HSA verbunden, während die Austrocknungstoleranz mit T_{crit} und Merkmalen wie einem niedrigeren P_{88} -Wert, einem hohen HSM und einem niedrigeren g_{min} zusammenhing. Insbesondere die Sprosskapazität (C) ist für T_{hf} entscheidend und zeigt ein dichotomes Verhalten, das sowohl mit T_{sc} als auch mit T_{crit} zusammenhängt.

Zusammenfassend lässt sich sagen, dass das Wissen um die Wechselwirkungen zwischen der Wachstumsrate und der Sicherheitseffizienz des Xylems in Verbindung mit Merkmalen, die mit den hydraulischen Strategien der Arten entlang der Isohydrie zusammenhängen, unsere Fähigkeit, trockenheitsresistente Setzlinge zu identifizieren, erheblich verbessern könnte, um den Erfolg von Aufforstungsprogrammen zu gewährleisten und die Empfindlichkeit gegenüber Trockenheit vorherzusagen, um nachhaltige Waldökosysteme zu erreichen.

Symbols, abbreviations and acronyms

| Symbol | Particulars |
|-------------------------------------|---|
| % | Percentage |
| °C | Degree celsius |
| µm | micrometre |
| ABI | Aboveground biomass increment |
| ACPS | <i>Acer pseudoplatanus</i> |
| AGB | Aboveground biomass |
| AIC | Akaike information criterion |
| A_{leaf} | Mean leaf size |
| $A_{\text{lumen}}:A_{\text{xylem}}$ | Lumen-to-sapwood area ratio |
| amsl | above mean sea level |
| ANOVA | Analysis of Variance |
| BEPE | <i>Betula pendula</i> |
| BIC | Bayesian information criterion |
| C | Shoot capacitance |
| cm | centimeter |
| d | days |
| D | Mean vessel diameter |
| D_h | Hydraulically weighted vessel diameter |
| FASY | <i>Fagus sylvatica</i> |
| g | gram |
| g_{min} | Cuticular conductance |
| g_s | Percent stomatal conductance |
| g_{s90} | Loss of 90 % stomatal conductance |
| $g_{s\text{max}}$ | Absolute maximal stomatal conductance |
| $g_{s\text{mean}}$ | Mean maximal stomatal conductance |
| HSA | Hydroscape area |
| HSM | Hydraulic safety margin ($P_{s90} - P_{s88}$) |
| HV | Huber value (Sapwood-to-Leaf area ratio) |
| ICAR | Indian Council of Agricultural Research |
| IPCC | Intergovernmental panel on climate change |
| kg | kilogram |

| Symbol | Particulars |
|---------------|--|
| K_L | Leaf-specific conductivity |
| K_p | Potential conductivity |
| kPa | Kilopascal |
| K_{pit} | Pit conductivity |
| K_S | Stem-specific conductivity |
| L_A | Mean Leaf area |
| L_D | Leaf density |
| L_m | Maximum leaf area |
| m | meter |
| mg | milligram |
| ML | Maximum likelihood |
| mm | millimeter |
| MPa | megapascal |
| OLS | Ordinary least squares |
| P_{12} | Ψ_x at 12 % loss of conductance |
| P_{50} | Ψ_x at 50 % loss of conductance |
| P_{88} | Ψ_x at 88 % loss of conductance |
| P_{s90} | Proxy to stomatal closure point |
| RCD | Collar diameter of the stem above the ground |
| REML | Restricted maximum likelihood |
| Shoot length | Shoot length from ground to uppermost leaf |
| SLA | Specific leaf area |
| SOAU | <i>Sorbus aucuparia</i> |
| SSM | Stomata safety margin ($P_{s90} - \Psi_{tip}$) |
| SWC | Saturated water content |
| T_{crit} | Standardized time to hydraulic failure from stomatal closure |
| T_{hf} | Standardized total time to hydraulic failure |
| TICO | <i>Tilia Cordata</i> |
| T_{sc} | Standardized time to stomatal closure |
| VCs | Vulnerability curves |
| VD | Vessel density |
| VIFs | Variance inflation factors |
| VPD | Vapor pressure deficit |
| V_w | Amount of water contained in plant |

| Symbol | Particulars |
|---------------|---|
| $\Delta\Psi$ | Diurnal range water potential ($\Psi_{pd} - \Psi_{md}$) |
| ρ | Wood density |
| σ | Slope of Ψ_{pd} vs. Ψ_{md} |
| Ψ_L | Leaf water potential |
| Ψ_{md} | Midday water potential |
| Ψ_{pd} | Pre-dawn water potential |
| Ψ_{tlp} | Turgor loss point |

Chapter-1: General Introduction

1.1 Forest ecosystems in a context of changing climate and droughts

Climate change is a crucial global issue of the 21st century that has been scientifically linked to anthropogenic greenhouse gas emissions. According to the Intergovernmental Panel on Climate Change, climate change is predicted to intensify, resulting in changes in the hydrological cycle and extreme weather events (IPCC 2021). The changing climate is causing Earth and ocean temperatures to rise, altering the hydrological cycle (Betts *et al.* 2007). If the increase continues at the current speed, the intensity and duration of warm summers due to heat waves and cold winter extremes due to snow will further increase (Stanturf *et al.* 2014, Dosio *et al.* 2018, IPCC 2021). This situation will exacerbate the effects of drought, which is already considered a significant detrimental for terrestrial ecosystems globally (Dai 2013, Trenberth *et al.* 2014, Cook *et al.* 2020). Forests are globally important due to various tangible and intangible benefits, such as food, timber, medicine, and biodiversity conservation. They are essential in regulating the water regime, carbon sequestration, and air quality (Morales-Hidalgo *et al.* 2015, Vacek *et al.* 2023). However, forests are vulnerable to climate change-induced disturbances like droughts and heat waves, and insect-pest attacks, which have decreased gross primary production, increased tree mortality, and alterations in forest ecosystems worldwide (Zhang *et al.* 2012, Huang *et al.* 2021, Vacek *et al.* 2023). Drought severely affects the vitality of the forest ecosystem by influencing plant physiological processes, plant growth, and survivability, and weakens the carbon sink function of ecosystems, leading to declines in carbon sequestration (Allen *et al.* 2010, Aroca and Ruiz-Lozano 2012, Anderegg *et al.* 2013, Allen *et al.* 2015, Adams *et al.* 2017, Yuan *et al.* 2019). Drought-induced tree mortality is widespread and has already been reported for different forest ecosystems such as boreal, tropical, and temperate forests across the globe, leading to significant carbon emissions and reduced forest carbon sink capacity (Phillips *et al.* 2009, Allen *et al.* 2010, Carnicer *et al.* 2011, Michaelian *et al.* 2011, Peng *et al.* 2011, Anderegg *et al.* 2013, Matusick *et al.* 2013, Williams *et al.* 2013, Duke *et al.* 2017, Aleixo *et al.* 2019, Hammond *et al.* 2022, McDowell *et al.* 2022).

1.2 Drought-induced tree mortality in European forests

Forestry is a vital economic sector in many European nations. European forest ecosystems are characterized by a comparatively low diversity of tree species. Due to climatic fluctuations, it

is crucial to understand the drought-related impacts on important species. *Acer pseudoplatanus* (Sycamore) is considered well-adapted to current and predicted future climatic changes in Central Europe (Kölling 2007). The more frequent heatwaves and droughts will impact the development and survival of forest ecosystems throughout Europe (Ciais *et al.* 2005, Schuldt *et al.* 2020, Schnabel *et al.* 2022, Rukh *et al.* 2023). Drought significantly reduces forest ecosystems' capacity to store carbon. The 2003 drought event in Europe resulted in the release of 0.5 Pg (petagram, 10^{15} g) of carbon into the atmosphere (Ciais *et al.* 2005). Further, the severe summer drought of 2018 in Central Europe resulted in significant tree mortality among adult trees of multiple species, particularly dominant deciduous European beech (*Fagus sylvatica*) (Schuldt *et al.* 2020, Rukh *et al.* 2023). Additionally, millions of planted saplings over the years were lost during the drought episode. As a legacy effect of drought-induced dieback, forest trees are highly prone to fungal-pathogen or insect attacks, especially by bark beetles (Allen *et al.* 2010, Hart *et al.* 2014, Huang *et al.* 2020). The economic penalties are heavy on the forest-based industries due to mass dieback. An estimate suggested a loss of 3.5 billion Euros (press release by the Association of German Foresters; BDF 2019), and at least 2,450 km² of forests were affected (BMEL 2020) during the 2018 drought episode in Germany. To mitigate the devastating effect, the European Green Deal and EU biodiversity have planned to plant at least 3 billion additional trees in Europe by 2030 to respond to the continent's growing environmental challenges. In addition, to meet these ambitious goals, Germany has increased its funding for international biodiversity conservation to 1.5 billion Euros (an increase of € 0.87 billion) annually (Gilbert 2022). Reforestation efforts at a large scale are a welcome step to mitigate global climate change. Tree planting initiatives require proper species selection and an understanding sapling's drought resistance mechanisms. Also, without appropriate knowledge, such efforts may be riskier for sustainable forest productivity on a long-term scale.

1.3 Advantages of mixed-species reforestation for ecological restoration

Conventional tree plantations have limited success in restoring ecological functions and biodiversity, as highlighted by studies (Lamb *et al.* 2005, Bristow *et al.* 2006, Felton *et al.* 2016, Liu *et al.* 2018). Consequently, mixed-species reforestation consisting of native tree species to overcome forest degradation has gained recognition as it is more productive and more tolerant to

drought stress than monoculture plantation (Vitali *et al.* 2018, Grossiord 2019, Feng *et al.* 2022, Hajek *et al.* 2022). This approach addresses rural poverty, ecological problems and economic functions in changing climate (Felton *et al.* 2016, Liu *et al.* 2018). Still, concerns about its impact on seasonal water use patterns, complementarity, and selection effect on stand growth, especially maintaining ecosystem functions such as carbon and water cycling (Felton *et al.* 2016, Grossiord 2019). Multispecies plantations have emerged as a new way to address rural poverty and environmental change through carbon sequestration, storage, and meeting the growing demand for food, fodder, fuelwood, and timber (Liu *et al.* 2018).

Three types of interactions, namely competition, complementary, and supplementary interactions, play significant roles in determining tree productivity and mortality under water scarcity. Mixed forests have an advantage over monocultures, mainly through the complementary and selection effects (Isbell *et al.* 2009, Grossiord *et al.* 2014, Grossiord 2019, Hajek *et al.* 2022). Complementarity, for example, occurs when different tree species partition temporal or spatial resources, resulting in higher water availability access in polycultures than in monocultures. This, in turn, mitigates drought impacts and enhances the survival of trees (Grossiord 2019). Furthermore, neighbourhood interspecific interactions have been found to play a crucial role in tree survival by either mitigating or enhancing drought effects, depending on the surrounding species (Hajek *et al.* 2022). Mixed stands benefit from species' sensitivity to drought, which causes early mortality or leaf fall, giving neighbouring tree species an advantage by reducing resource competition. For instance, *Betula* spp and *Larix* spp have been found to benefit from this mechanism in mixed stands (Hajek *et al.* 2022). Water uptake by trees at different depths has been found to be complementary in mixed-species plots (Schwendenmann *et al.* 2015, Grossiord 2019), was strategically useful for the survival of species under drought which may be related to percentage foliage and leaf shedding (Schwendenmann *et al.* 2015, Hajek *et al.* 2022). However, information on species growing under plantation conditions is limited, and research is needed to understand better the physiological and morphological traits and neighbourhood effects linked to resource complementarity (Dierick and Hölscher 2009, Kunert *et al.* 2012, Grossiord 2019). Species selection, species richness, and stand composition are critical for designing plantations that maximize wood production while conserving water assets and maintaining ecological function (Kunert *et al.* 2012).

1.4 The plant hydraulic system and drought susceptibility

Photosynthesis, the process by which plants convert light energy into organic matter, depends on water absorption. Stomata, tiny pores on leaves, allow CO₂ to enter and react with water to produce carbon for growth and function. Nevertheless, hydraulic capacity is connected to the plant's photosynthetic capacity and is located at the soil-plant-atmospheric continuum (SPAC) interface (Figure 1.1). Transpiration drives sap ascent in plants and varies across species based on water use efficiency (Wullschleger *et al.* 1998), which is essential for the plant's hydraulic system (McElrone *et al.* 2013). Evaporative demand produces tension in the water column, causing water to move from the soil to the leaves through roots (SPAC). In this process, water enters the plant's closed system from the soil via its roots. Primarily, water movement occurs through passive diffusion (i.e., an apoplastic pathway through cell walls, Steudle 2001) and the osmosis process (i.e., symplastic pathways through cytoplasm or plasmodesmata, Steudle 2001). Secondly, vertical movement occurs within a specialized tissue, the xylem, consisting of interconnected conduits in vascular plants.

The plant's internal water transport system strives to be more efficient to achieve higher stomatal conductance and increase fitness. However, resistance to water flow through SPAC increases under drought conditions. The tension of xylem vessels rises with drought stress which causes a drop in leaf water potential (more negative). So, declining water potential assists in developing the pressure gradient to pull the water from the soil-roots interface via the stem-leaf interface to fulfil the necessary transpiration demand. In that case, the conducting xylem, therefore, continuously persists stress due to increasing tension. However, cavitation occurs when the strain of xylem vessels exceeds its limit, which is the change of water state from liquid to vapour. This leads to the formation of "air bubbles" within xylem conduits, resulting in embolism and a loss of hydraulic conductivity. In this connection, Vulnerability curves (VCs) are constructed to evaluate the sensitivity of cavitation, and the P_{50} value is commonly measured as an index of drought resistance. It signifies that 50 % of the vessels no longer contribute to conductivity at the given xylem water potential due to cavitation and embolized vessels. It is a more static functional trait (Lamy *et al.* 2011) due to less noticeable phenotypic variation for a species. However, P_{88} , representing an 88% loss of xylem conductivity, indicates complete hydraulic failure associated with plant death (Barigah *et al.* 2013, Urli *et al.* 2013). Therefore, understanding the VCs is crucial

in determining the plant's drought resistance and survival ability under varying environmental conditions. (Sperry *et al.* 1988, Lamy *et al.* 2011, Choat *et al.* 2012, Barigah *et al.* 2013).

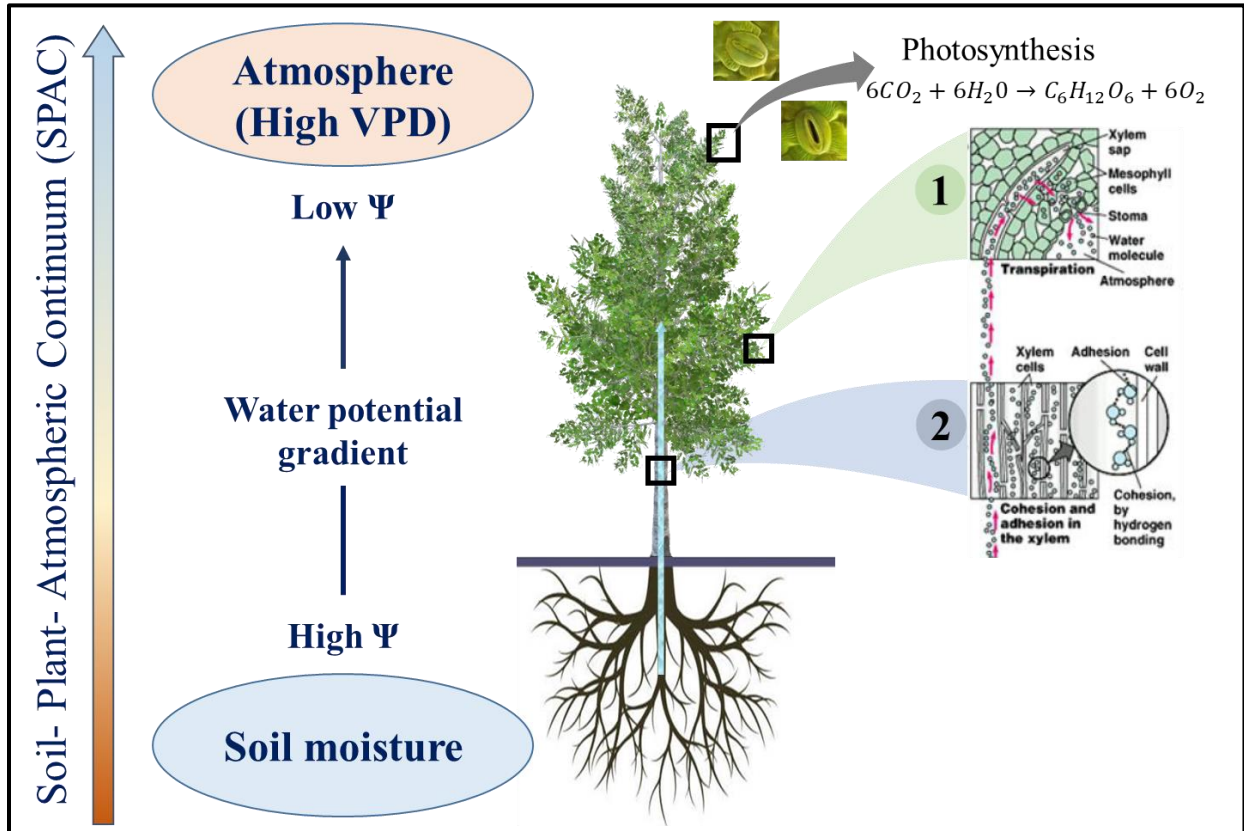


Figure 1.1: Water transportation routes, in general, along the soil-to-plant-to-atmosphere continuum (SPAC) are depicted. Water flows along the pressure potential gradient from the areas with a high-water potential to the areas with a low-water potential in plants. The inset panels display the Cohesion-Tension process, (1) showing how tension is produced by water molecule evaporation during leaf transpiration and is transferred (2) along continuous, cohesive water columns via the interconnected conduits (vessels or tracheids). (Source: McElone *et al.* 2013).

1.5 Growth rate trade-off with xylem safety–efficiency association

The xylem, a network of interconnected conduits, is crucial to plant productivity and survival (Choat *et al.* 2018). Xylem safety can be understood from the context of VCs and P_{50} value, whereas xylem efficiency is linked to stem-specific hydraulic conductivity (i.e., K_S). The link between tree growth and hydraulic conductivity is well established and has been tested empirically at the stem level (Tyree 2003, Domec and Gartner 2003, Wikberg and Ögren 2004, Zhang and Cao 2009, Fichot *et al.* 2010, Russo *et al.* 2010, Fichot *et al.* 2011, Fan *et al.* 2012, Gleason *et al.* 2012). The hydraulic conductivity in vessels increases with the fourth power of its diameter (Tyree and Zimmermann 2002), but larger diameters also increase the risk of hydraulic

failure due to cavitation under drought (Tyree *et al.* 1994, Wheeler *et al.* 2005, Awad *et al.* 2010, Hajek *et al.* 2014). Growth and water-use relationship for plant productivity are more closely related to the vascular plant's water transport capacity, which is influenced by wood anatomy such as larger vessel diameter (Brodribb 2009, Russo *et al.* 2010, Hoeber *et al.* 2014, Eller *et al.* 2018, Gleason *et al.* 2018, Kotowska *et al.* 2021). Wider conduit diameters increase hydraulic efficiency (Pittermann *et al.* 2006), and conduit widening from tip to base minimizes hydraulic resistance in water transport (Olson *et al.* 2014, Kotowska *et al.* 2015, Olson *et al.* 2021). Furthermore, xylem safety is assumed to compromise as the growth rate increases due to competition for carbon allocation, as carbon must be used to reinforce cell walls or support growth (Wikberg and Ögren 2004, Brodribb 2009).

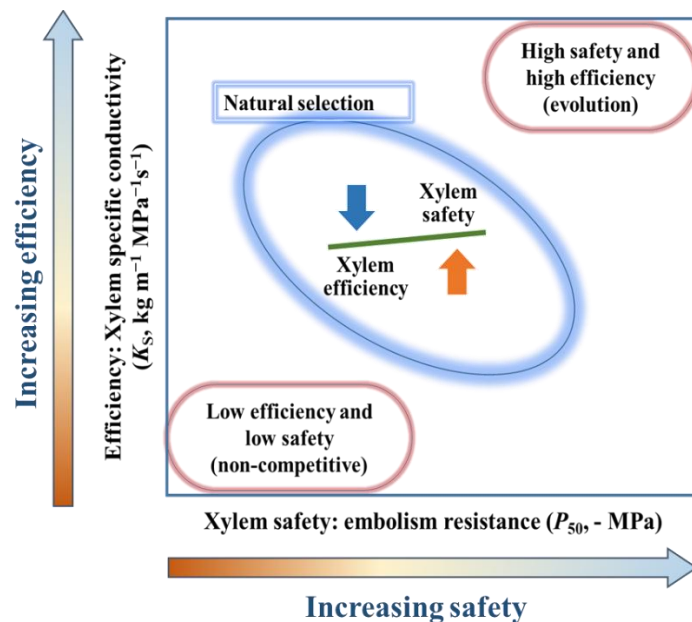


Figure 1.2: A conceptual perspective of the eco-evolutionary trade-off association between xylem safety and efficiency in a species (Source: adapted from Gleason *et al.* 2016).

1.6 Wood anatomy trade-off with hydraulic efficiency–safety association

Xylem safety and efficiency appears as one of the most detrimental for maximising the plant's growth rate. A high efficiency and high safety are advantageous for plant growth and productivity; however, it can not be achieved in the same species. Natural selection is expected to drive species upwards and rightwards, likely causing trade-offs to certain extent (Figure 1.2, Gleason *et al.* 2016). The association between hydraulic efficiency and safety depends on various factors associated with conduit diameter (Figure 1.3), such as pit wall and pit membrane thickness and spatial clustering (Sperry and Tyree 1988, Tyree *et al.* 1994, Hacke *et al.* 2006, Christman *et*

al. 2009, Lens *et al.* 2011, Choat *et al.* 2012, Schuldt *et al.* 2016, Kaack *et al.* 2021). Under increasing water stress, cavitation occurrence is a more frequent phenomenon, which could result in substantial losses in hydraulic conductance. Wood anatomy plays a crucial role in balancing xylem safety and efficiency, which is explained by the rare pit hypothesis (Wheeler *et al.* 2005, Christman *et al.* 2009). The hypothesis predicts that wider vessels with a larger area are more vulnerable to cavitation due to thinner and more porous pit membranes than narrower vessels (Hacke *et al.* 2017). However, pit features such as thicker membranes, shallower chambers, and fewer and smaller apertures can support greater cavitation resistance (Lens *et al.* 2011). While vessel connectivity decreases cavitation resistance by increasing the probability of embolism spread (Loepfe *et al.* 2007). Further, bordered pit characteristics, including pit membrane thickness, pore size, and area, likely explain variations in hydraulic conductivity and plant embolism resistance (Domec *et al.* 2006, Jansen *et al.* 2009, Lens *et al.* 2011, Scholz *et al.* 2013, Gleason *et al.* 2016). Species with thin pit membranes are typically more vulnerable to embolism than those with thick pit membranes (Scholz *et al.* 2013, Li *et al.* 2016b, Schuldt *et al.* 2016). Pit membrane thickness could be uncoupled from the hydraulic safety-efficiency trade-off association (Kaack *et al.* 2021).

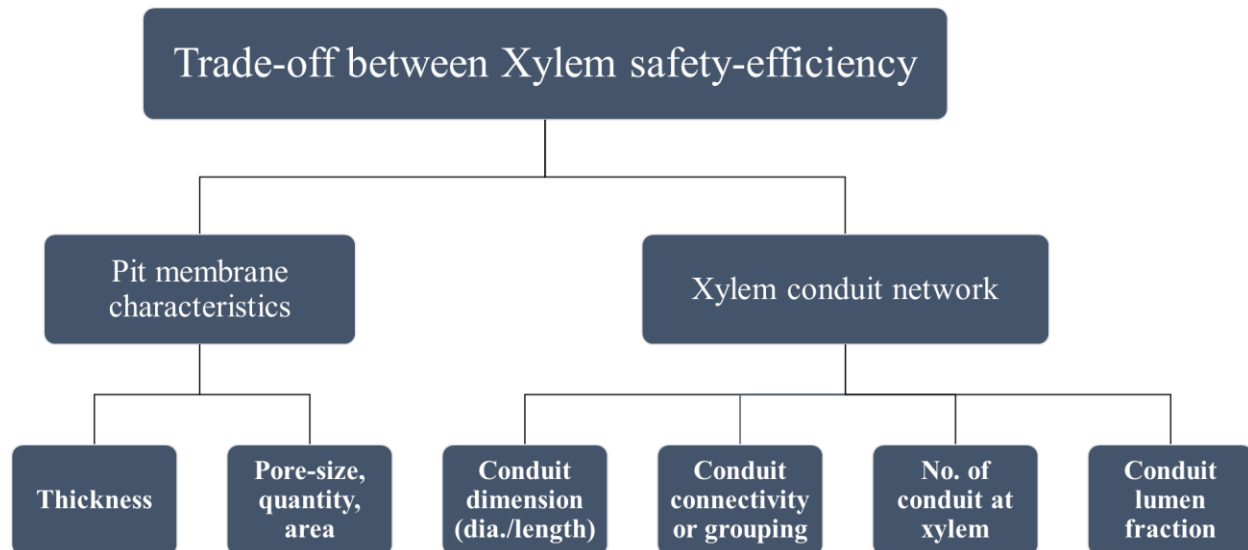


Figure 1.3: Anatomical traits affecting the relationship between xylem safety and efficiency. (Sources: Wheeler *et al.* 2005, Loepfe *et al.* 2007, Lens *et al.* 2011, Gleason *et al.* 2016).

1.7 Stomatal stringency in the framework of iso-anisohydric continuum

Stomata are tiny apertures available in the leaves, which control the exchange of gases through transpiration. Plants lose water mainly through gas exchange via stomata, which became pivotal to elucidating the time to hydraulic failure by coordinating hydraulic traits and stomatal regulations (Choat *et al.* 2012, Blackman *et al.* 2019a, Blackman *et al.* 2019b). Even knowledge beyond stomatal closure remains critical, as this delay between the inception of cavitation and catastrophic hydraulic breakdown, which extends desiccation times (Anderegg *et al.* 2013, Delzon and Cochard 2014, Blackman *et al.* 2016, Martin-StPaul *et al.* 2017, Sperry *et al.* 2017, Choat *et al.* 2018, Blackman *et al.* 2019b). Stomatal stringency is typically categorized along a continuous axis of isohydric (drought avoidance) to anisohydric (drought tolerance). Isohydric plants have greater water use efficiency by conserving water and preventing wilting, while anisohydric plants have greater growth efficiency by taking advantage of periods of high-water availability to grow quickly and efficiently but are more susceptible to water stress (McDowell *et al.* 2008, Arend *et al.* 2021, Hartmann *et al.* 2021). Anisohydric species are assumed to be prone to hydraulic failure, while isohydric species are more prone to carbon failure. However, there is a debate on the drivers of plant mortality between carbon starvation and hydraulic failure (McDowell *et al.* 2008, Garcia-Fomer *et al.* 2017, Choat *et al.* 2018, McDowell *et al.* 2022). Therefore, iso-anisohydric categorization of plants provides a framework for understanding plant hydraulic strategies to water stress.

1.8 Plant desiccation time and traits coordination

Stomata, mostly used for gas exchange, are essential for revealing the time to hydraulic failure in plants. Stomatal stringency is an important strategy for plants to adapt to prolonged desiccation time. However, understanding the traits associated with desiccation time is challenging and complex along the continuum from isohydry to anisohydry. Trees can regulate water use and safety by coordinating hydraulic and stomatal regulations (Choat *et al.* 2012, Brodribb and McAdam 2013, Martin-StPaul *et al.* 2017). When plants experience drought, stomata may counteract to various physical and chemical signals such as leaf turgor loss and the phytohormone abscisic acid in the xylem and foliar levels (Brodribb and McAdam 2013, Speirs *et al.* 2013). High transpiration rates can lead to an increased risk of hydraulic failure, which is why the significance of hydraulic failure increases when plants close their stomata during periods of high evaporative

demand to maintain productivity (Meinzer *et al.* 2016, Fu and Meinzer 2019). Recent studies have shown that stomatal closure and xylem embolism resistance are closely related in response to drought (Klein 2014, Mencuccini *et al.* 2015, Bartlett *et al.* 2016). Species having larger hydraulic safety margins have more survival chances (Plaut *et al.* 2012, Martin-StPaul *et al.* 2017).

Plant desiccation tolerance is determined by two critical stages, before and after stomatal closure, which impact water loss (Blackman *et al.* 2019b). Stomatal behaviour and environmental conditions limit water flux, creating a selective force on the xylem and producing Ψ_{\min} in plants (Bhaskar and Ackerly 2006, Joshi *et al.* 2022). The time to hydraulic failure is influenced by hydraulic and allometric traits (Blackman *et al.* 2019b). Leaf area and total water storage in plants, which are determined by allometric traits, play a crucial role in tissue desiccation, as they provide the surface area for water loss (Blackman *et al.* 2019b, Challis *et al.* 2022). Several factors can potentially increase the desiccation time, including increasing the total volume of water in sapwood relative to leaf area, reducing cuticular conductance, higher embolism, increasing shoot capacitance, lower turgor loss point, or a combination of these factors (Blackman *et al.* 2016, Hammond and Adams 2019, Lemaire *et al.* 2021, Challis *et al.* 2022, Ruffault *et al.* 2022). RWC triggers the time to hydraulic failure at P_{88} , and internal cell water storage in a species could delay hydraulic failure for a longer time (Meinzer *et al.* 2009, Blackman *et al.* 2016, Mantova *et al.* 2022). Studies have indicated that longer desiccation times to extreme drought stress level would be related to traits linked with high drought tolerance, either via drought avoidance (e.g., early stomatal closure or high capacitance) or drought tolerance strategy (e.g., embolism resistance, HSM) (Hacke and Sperry 2001, Tyree 2003, Choat *et al.* 2018, Blackman *et al.* 2019b).

1.9 Research site, experimental design, and species description

This study was conducted in two phases (2020-2021 and 2021-2022) at the Chair of Ecophysiology and Vegetation Ecology, Julius-von-Sachs-Institute of Biological Sciences, Würzburg, Germany. The study focused on five economically, and ecologically important temperate broadleaved tree species: *Acer pseudoplatanus* (sycamore maple), *Betula pendula* (silver birch), *Tilia cordata* (small-leaved lime or linden), *Sorbus aucuparia* (rowan or mountain ash) and *Fagus sylvatica* (European beech), hereafter referred to as ACPS, BEPE, TICO, SOAU, and FASY respectively. These species were chosen due to their extensive distribution across the European continent and varied adaptation to drought conditions (Figure 1.4). *Acer pseudoplatanus*

is commonly found in deciduous forests, river valleys, and mountainous regions. *Betula pendula* is a typical pioneer species that colonize various climatic and ecological conditions. *Sorbus aucuparia* is a tree or shrub found in alpine meadows and moorlands. *Tilia cordata* is distributed in various habitats, such as river valleys and parks, apart from the temperate forest. Among the species, *Fagus sylvatica* is the most commercially valued species, has high shade tolerance and naturally covers more than 60 % of Germany's area (Bohn *et al.* 2003, Christensen *et al.* 2005, Leuschner 2020).

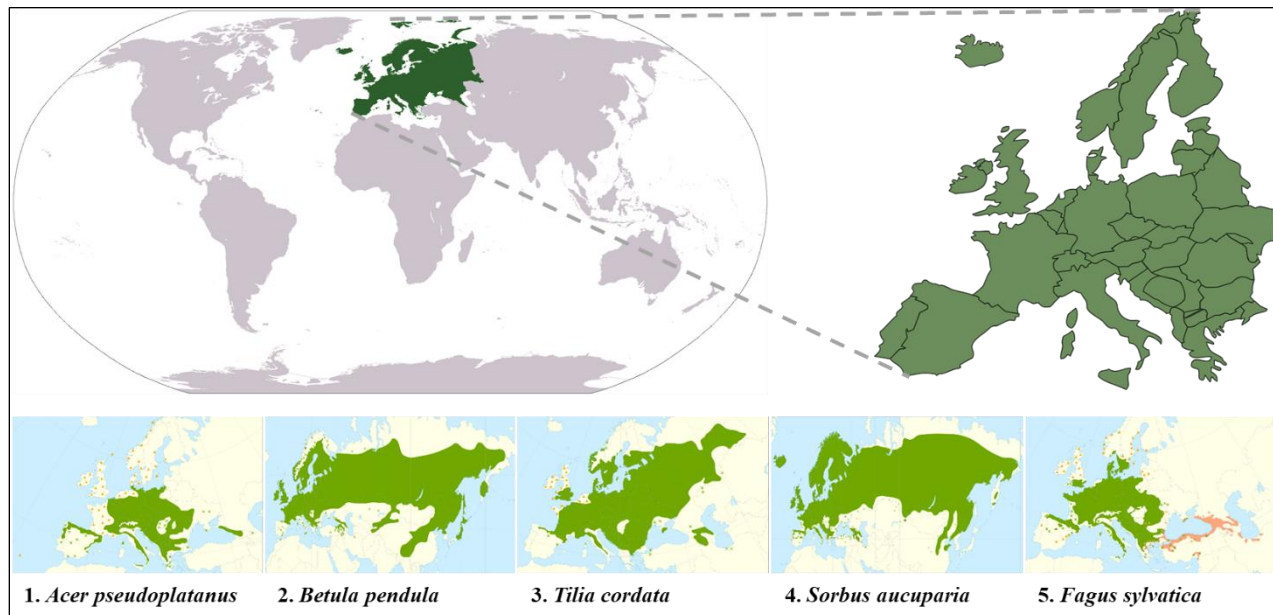


Figure 1.4: Exemplary distribution maps of investigated five temperate broadleaves tree species across Europe. (Source: <https://en.wikipedia.org/wiki/>, Caudullo *et al.* 2017 (date accessed, December 2022)).

ACPS is moderately drought and heat-sensitive (Leuschner and Meier 2018) and well-adapted to current and future climatic in Central Europe (Kölling 2007). However, water stress could enhance the tree's susceptibility to fungi (Schmidt and Roloff 2014). BEPE exhibits a relatively high degree of adaptation to drought, as evidenced by its widest physiological traits amplitude and geographic distribution across Central Europe, and species has shown the ability to maintain growth under both wet and dry conditions (Aspelmeier and Leuschner 2004, Hannus *et al.* 2021). However, according to the UK Forestry Commission (2015), BEPE shows intolerance to prolonged periods of drought. SOAU can experience wide water potential variations during droughts and shows high resistance to cavitation (Vogt 2001). On the iso-anisohydric continuum, ACPS and BEPE are considered to follow an isohydric stomatal control strategy (Robson *et al.*

2015, Li *et al.* 2016a, Leuschner *et al.* 2019, Beikircher *et al.* 2021). FASY and SOAU have been described as anisohydric (Vogt 2001, Rötzer *et al.* 2017, Leuschner *et al.* 2019, 2022). TICO received mixed characterization; fairly isohydric behaviour (Köcher *et al.* 2013, Leuschner *et al.* 2019), while an anisohydric strategy has also been reported (Moser *et al.* 2016, 2017, Gillner *et al.* 2017, Moser-Reischl *et al.* 2019). This study, therefore, aimed to explore the differences in growth and survival in response to drought, their mechanisms, stomatal stringency, and hydraulic behaviour among five economically and ecologically important temperate broadleaved tree species. The study findings are crucial in understanding and managing forest ecosystems and the selection of resistant saplings for reforestation programs in the face of changing climate conditions.

The first study investigated the growth trade-off between xylem safety-efficiency traits under different water regimes in three temperate deciduous tree species: ACPS, BEPE, and SOAU. The saplings used in the study were grown from collected seeds in a botanical garden and subjected to either stress or control treatments. The stress treatment involved subjecting the saplings to high temperatures and VPD in a growing chamber. In contrast, the control treatment involved growing saplings outside under a transparent roof with open sides exposed to natural environmental conditions. The study examined the structural, functional, and hydraulic traits of 18-month-old saplings, including various xylem traits such as embolism resistance, xylem-specific hydraulic conductivity, and xylem anatomy. First, stem segments were water-flushed using the Xylem apparatus. The same stem segments were then used to construct xylem VCs using the flow-centrifuge technique (Cochard *et al.* 2005). The basipetal cut stem portion (VCs sample) was used for xylem anatomy. In addition, leaf morphological and functional traits such as specific leaf area, huber value, and mean leaf size were measured. Total aboveground biomass was also recorded to estimate the aboveground biomass increment (ABI, mg d^{-1}) by dividing their growth periods. Table 2.1 in Chapter II provides a list of the variables measured in the study, along with their definitions and units.

In second study, two additional species, FASY and TICO, were included to investigate the time to hydraulic failure (T_{hf}) under increasing drought stress with the framework of the iso-anisohydric continuum. Among the five species, FASY and SOAU were considered anisohydric (drought tolerant), while ACPS and BEPE were described as isohydric (drought avoider) and highly water-efficient. However, TICO has not clearly distinguished on the continuum. The experiments were conducted in a climate-controlled chamber and greenhouse at the University of

Würzburg, using a randomized blocked design. After setup, irrigation was suspended entirely. Plant water status was monitored by Ψ_{md} and Ψ_{pd} using a pressure chamber (Model 1505D, PMS Instruments). Stomatal regulation was measured using a portable porometer (Delta-T Device), and various drought tolerance and leaf traits were recorded, including Capacitance, P_{s90} , P_{88} , Ψ_{tlp} , g_{min} , HSA, HSM, leaf area, SLA, and HV. The study also explored the association between traits before and after stomatal closure in response to the drought. (Refer to Chapter III for a detailed description).

1.10 General study hypothesis, objectives, and thesis structure

This dissertation seeks to address the knowledge gaps in identifying the drought-resistant sapling in massive reforestation efforts to mitigate global climate change by converting monocultural stands to mixed forests composed of native broad-leaved tree species. A thorough understanding of the drought resistance mechanisms and species selection for saplings is essential for developing more effective strategies for reforestation efforts. On this note, expanding the current knowledge of species adaptation and strategies for drought response is imperative. So, this study endeavours to bridge the gaps in knowledge by pursuing the following objectives:

- I. To expand our understanding of how the hydraulic traits are associated with a species' growth rate under drought stress.
- II. To widen our knowledge of plant water potential regulation and traits linked to species' hydraulic strategies and drought tolerance.

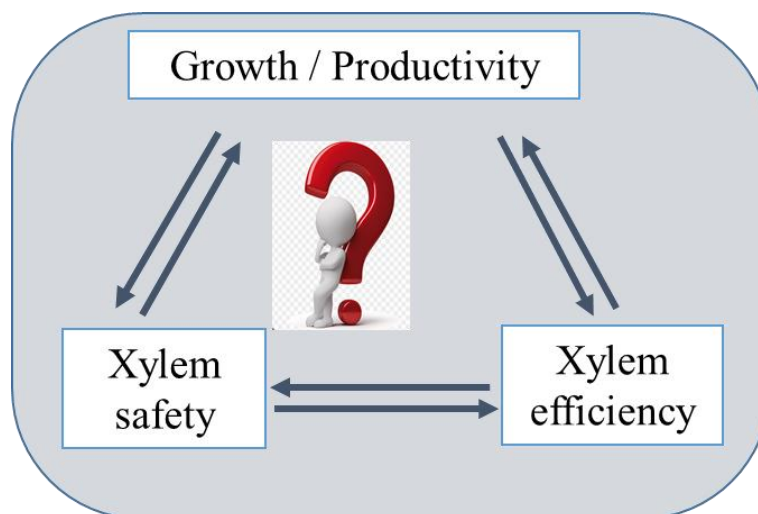


Figure 1.5: Plausible growth trade-offs within conducting xylem system.

To achieve the knowledge gaps, the study proposes to answer the following questions (Figure 1.5).

1. How is juvenile growth rate associated with hydraulic efficiency and safety?
2. How are hydraulic safety–efficiency traits related to xylem anatomy?
3. How do plants regulate the water potential and stomatal stringency along the iso - anisohydric continuum framework under increasing drought stress?
4. How do more anisohydric and more isohydric species differ in their hydraulic traits, and what are the repercussions for the time to hydraulic failure?
5. How are hydraulic traits coordinated to the stomatal stringency?

To address these questions, the overall objective of this study is to examine the juvenile growth trade-off with xylem safety-efficiency and stomatal stringency in an association of trait coordination determining the time to hydraulic failure. Specifically, the study proposes to:

- 1) Investigate the association between low hydraulic safety (P_{50}) and high hydraulic efficiency (K_s) with high juvenile growth rates.
- 2) Examine the trade-off between hydraulic safety and efficiency in seed-grown saplings.
- 3) Explore the relationship between hydraulic safety–efficiency traits and xylem anatomy in saplings.
- 4) Analyze how HSA differs consistently along the iso-anisohydric continuum.
- 5) Compare the hydraulic traits of more anisohydric and isohydric species, including C , P_{88} , HSM, and Ψ_{tlp} , to understand their implications for the time to hydraulic failure.
- 6) Investigate the association between the time to stomatal closure (T_{sc}) with traits such as P_{s90} , Ψ_{tlp} , HSA, and C ; and
- 7) Examine the relationship between the time to critical hydraulic failure (T_{crit}) with traits such as g_{min} , HSM, critical embolism thresholds, and C .
- 8) Examine the regulation of water potential and stomatal stringency on the framework of the iso-anisohydric spectrum under increasing drought stress.

This dissertation is organized (Figure 1.6) into several chapters compiled based on either published articles or proposed to submit in a peer-review journal (draft). Chapter I provides an overview of the research, including the research background, literature review, objectives, and dissertation structure. In Chapter II, we addressed the relationship between juvenile growth and xylem safety-efficiency and their anatomical traits (objective specifically 1-3). This chapter has been published (Kumar *et al.* 2022 “*Influence of Juvenile Growth on Xylem Safety and Efficiency in Three*

Temperate Tree Species.” *Forests*, 13, 909. <https://doi.org/10.3390/f13060909>). Chapter III focuses on stomatal stringency on the iso-anisohydric continuum and the coordination of deterministic traits for the time to hydraulic failure. This chapter is highly suitable for standalone publication and will be submitted to a peer-reviewed journal (Kumar *et al.* “*Coordinated drought responses determine the time to hydraulic failure in five temperate tree species differing in their degree of isohydry*”). Chapter IV presents a detailed synthesis of the dissertation, exploring the regulation of water potential and discussing the definition and concepts of the iso-anisohydric continuum. Additionally, this chapter provides an overview of the general findings of Chapters II and III. Finally, Chapter V concludes, discusses the limitations of the study findings, and outlines potential future research directions.

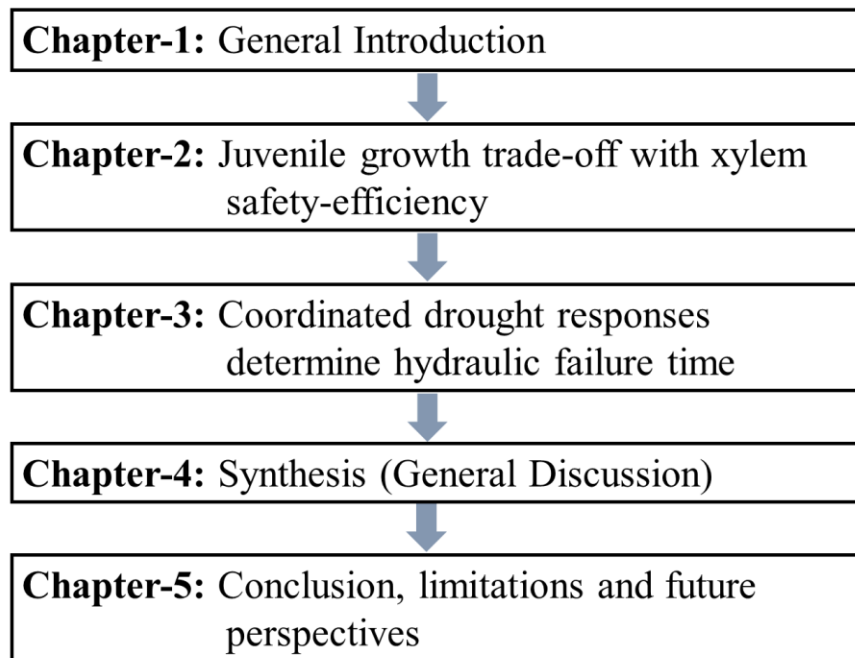


Figure 1.6: Logical flow of the chapters in the dissertation.

Note: This thesis is structured as a chapter-based compilation of published or submitted peer-reviewed journal articles, resulting in some overlap in content between the introduction, the conclusion, and the central body of the chapters in general.

References:

- Adams HD, Barron-Gafford GA, Minor RL, Gardea AA, Bentley LP, Law DJ, Breshears DD, McDowell NG, Huxman TE (2017) Temperature response surfaces for mortality risk of tree species with future drought. *Environmental Research Letters* 12:115014.
- Aleixo I, Norris D, Hemerik L, Barbosa A, Prata E, Costa F, Poorter L (2019) Amazonian rainforest tree mortality driven by climate and functional traits. *Nature Climate Change* 9:384–388.
- Allen CD, Breshears DD, McDowell NG (2015) On underestimation of global vulnerability to tree mortality and forest die-off from hotter drought in the Anthropocene. *Ecosphere* 6:129.
- Allen CD, Macalady AK, Chenchouni H, Bachelet D, McDowell N, Vennetier M, Kitzberger T, Rigling A, Breshears DD, Hogg EH (Ted), Gonzalez P, Fensham R, Zhang Z, Castro J, Demidova N, Lim J-H, Allard G, Running SW, Semerci A, Cobb N (2010) A global overview of drought and heat-induced tree mortality reveals emerging climate change risks for forests. *Forest Ecology and Management* 259:660–684.
- Anderegg WRL, Kane JM, Anderegg LDL (2013) Consequences of widespread tree mortality triggered by drought and temperature stress. *Nature Climate Change* 3:30–36.
- Arend M, Link RM, Patthey R, Hoch G, Schuldt B, Kahmen A (2021) Rapid hydraulic collapse as cause of drought-induced mortality in conifers. *Proceedings of the National Academy of Sciences* 118:e2025251118.
- Aroca R, Ruiz-Lozano JM (2012) Regulation of Root Water Uptake Under Drought Stress Conditions. In: Aroca R (ed) *Plant Responses to Drought Stress: From Morphological to Molecular Features*. Springer, Berlin, Heidelberg, pp 113–127.
- Aspelmeier S, Leuschner C (2004) Genotypic variation in drought response of silver birch (*Betula pendula*): leaf water status and carbon gain. *Tree Physiology* 24:517–528.
- Awad H, Barigah T, Badel E, Cochard H, Herbette S (2010) Poplar vulnerability to xylem cavitation acclimates to drier soil conditions. *Physiologia Plantarum* 139:280–288.
- Adams HD, Barron-Gafford GA, Minor RL, Gardea AA, Bentley LP, Law DJ, Breshears DD, McDowell NG, Huxman TE (2017) Temperature response surfaces for mortality risk of tree species with future drought. *Environment Research Letters* 12:115014.
- Barigah TS, Charrier O, Douris M, Bonhomme M, Herbette S, Améglio T, Fichot R, Brignolas F, Cochard H (2013) Water stress-induced xylem hydraulic failure is a causal factor of tree mortality in beech and poplar. *Annals of Botany* 112:1431–1437.
- Bartlett MK, Klein T, Jansen S, Choat B, Sack L (2016) The correlations and sequence of plant stomatal, hydraulic, and wilting responses to drought. *Proceedings of the National Academic Sciences USA* 113:13098–13103.
- BDF (Bund Deutscher Forstleute) (2019) Der Wald ist in Gefahr -Die Politik muss handeln. Pressemitteilung: Marshallplan für den Wald. 29.03.2019 https://www.bdf-online.de/fileadmin/user_upload/www_bdf-online_de/pdf/2019/19-05_Wald_in_Gefahr_-_Marshallplan_fuer_den_Wald_noetig.pdf.

- Beikircher B, Sack L, Ganthaler A, Losso A, Mayr S (2021) Hydraulic-stomatal coordination in tree seedlings: tight correlation across environments and ontogeny in *Acer pseudoplatanus*. *New Phytologist* 232:1297–1310.
- Betts RA, Boucher O, Collins M, Cox PM, Falloon PD, Gedney N, Hemming DL, Huntingford C, Jones CD, Sexton DMH, Webb MJ (2007) Projected increase in continental runoff due to plant responses to increasing carbon dioxide. *Nature* 448:1037–1041.
- Bhaskar R, Ackerly D D (2006) Ecological relevance of minimum seasonal water potentials. *Physiologia Plantarum* 127:353–359.
- Blackman CJ, Creek D, Maier C, Aspinwall MJ, Drake JE, Pfautsch S, O’Grady A, Delzon S, Medlyn BE, Tissue DT, Choat B (2019a) Drought response strategies and hydraulic traits contribute to mechanistic understanding of plant dry-down to hydraulic failure. *Tree Physiology* 39:910–924.
- Blackman CJ, Li X, Choat B, Rymer PD, De Kauwe MG, Duursma RA, Tissue DT, Medlyn BE (2019b) Desiccation time during drought is highly predictable across species of *Eucalyptus* from contrasting climates. *New Phytologist* 224:632–643.
- Blackman CJ, Pfautsch S, Choat B, Delzon S, Gleason SM, Duursma RA (2016) Toward an index of desiccation time to tree mortality under drought: Desiccation time to tree mortality. *Plant, Cell & Environment* 39:2342–2345.
- BMEL (Bundesministerium für Ernährung und Landwirtschaft) (2020) Waldschäden: Bundesministerium veröffentlicht aktuelle Zahlen, Pressemitteilung Nr 40/2020. (<https://www.bmel.de/SharedDocs/Pressemitteilungen/DE/2020/040-waldschaeden.html>).
- Bohn U, Neuhäusl R, Gollub G, Hettwer C, Neuhäuslová Z, Schlüter H, Weber H, (2003) Map of the Natural Vegetation of Europe–Scale 1:2 500 000. Landwirtschaftsverlag, Münster, Map and Explanatory Text.
- Bristow M, Vanclay JK, Brooks L, Hunt M (2006) Growth and species interactions of *Eucalyptus pellita* in a mixed and monoculture plantation in the humid tropics of north Queensland. *Forest Ecology and Management* 233:285–294.
- Brodribb TJ (2009) Xylem hydraulic physiology: The functional backbone of terrestrial plant productivity. *Plant Science* 177:245–251.
- Brodribb TJ, McAdam SAM (2013) Abscisic Acid Mediates a Divergence in the Drought Response of Two Conifers. *Plant Physiology* 162:1370–1377.
- Carnicer J, Coll M, Ninyerola M, Pons X, Sánchez G, Peñuelas J (2011) Widespread crown condition decline, food web disruption, and amplified tree mortality with increased climate change-type drought. *Proceedings of the National Academy of Sciences* 108:1474–1478.
- Caudullo G, Welk E, San-Miguel-Ayanz J (2017) Chorological maps for the main European woody species. *Data in Brief* 12:662–666.
- Challis A, Blackman C, Ahrens C, Medlyn B, Rymer P, Tissue D (2022) Adaptive plasticity in plant traits increases time to hydraulic failure under drought in a foundation tree. *Tree Physiology* 42:708–721.

- Choat B, Brodribb TJ, Brodersen CR, Duursma RA, López R, Medlyn BE (2018) Triggers of tree mortality under drought. *Nature* 558:531–539.
- Choat B, Jansen S, Brodribb TJ, Cochard H, Delzon S, Bhaskar R, Bucci SJ, Feild TS, Gleason SM, Hacke UG, Jacobsen AL, Lens F, Maherali H, Martínez-Vilalta J, Mayr S, Mencuccini M, Mitchell PJ, Nardini A, Pittermann J, Pratt RB, Sperry JS, Westoby M, Wright IJ, Zanne AE (2012) Global convergence in the vulnerability of forests to drought. *Nature* 491:752–755.
- Christensen M, Hahn K, Mountford EP, Ódor P, Standovár T, Rozenbergar D, Diaci J, Wijdeven S, Meyer P, Winter S, Vrska T (2005) Dead wood in European beech (*Fagus sylvatica*) forest reserves. *Forest Ecology and Management* 210:267–282.
- Christman MA, Sperry JS, Adler FR (2009) Testing the ‘rare pit’ hypothesis for xylem cavitation resistance in three species of *Acer*. *New phytologist* 182:664–674.
- Ciais P, Reichstein M, Viovy N, Granier A, Ogée J, Allard V, Aubinet M, Buchmann N, Bernhofer C, Carrara A, Chevallier F, de NOBLET N, Friend A, Friedlingstein P, Grünwald T, Heinesch B, Keronen P, Knohl A, Krinner G, Valentini R (2005) Europe-wide reduction in primary productivity caused by the heat and drought in 2003. *Nature* 437:529–33.
- Cochard H, Damour G, Bodet C, Tharwat I, Poirier M, Améglio T (2005) Evaluation of a new centrifuge technique for rapid generation of xylem vulnerability curves. *Physiologia Plantarum* 124:410–418.
- Cook BI, Mankin JS, Marvel K, Williams AP, Smerdon JE, Anchukaitis KJ (2020) Twenty-First Century Drought Projections in the CMIP6 Forcing Scenarios. *Earth’s Future* 8:e2019EF001461.
- Dai A (2013) Increasing drought under global warming in observations and models. *Nature Climate Change* 3:52–58.
- Delzon S, Cochard H (2014) Recent advances in tree hydraulics highlight the ecological significance of the hydraulic safety margin. *New Phytologist* 203:355–358.
- Dierick D, Hölscher D (2009) Species-specific tree water use characteristics in reforestation stands in the Philippines. *Agricultural and Forest Meteorology* 149:1317–1326.
- Domec J-C, Gartner BL (2003) Relationship between growth rates and xylem hydraulic characteristics in young, mature and old-growth ponderosa pine trees. *Plant, Cell & Environment* 26:471–483.
- Domec J-C, Lachenbruch B, Meinzer FC (2006) Bordered pit structure and function determine spatial patterns of air-seeding thresholds in xylem of Douglas-Fir (*Pseudotsuga menziesii*; Pinaceae) trees. *American Journal of Botany* 93:1588–1600.
- Dosio A, Mentaschi L, Fischer EM, Wyser K (2018) Extreme heat waves under 1.5 °C and 2 °C global warming. *Environment Research Letters* 13:054006.
- Duke N (2017) Mangrove Floristics and Biogeography Revisited: Further Deductions from Biodiversity Hot Spots, Ancestral Discontinuities, and Common Evolutionary Processes. In: *Mangrove Ecosystems: A Global Biogeographic Perspective: Structure, Function, and Services*. pp 17–53.

- Eller CB, Rowland L, Oliveira RS, Bittencourt PRL, Barros FV, da Costa ACL, Meir P, Friend AD, Mencuccini M, Sitch S, Cox P (2018) Modelling tropical forest responses to drought and El Niño with a stomatal optimization model based on xylem hydraulics. *Philosophical Transactions of the Royal Society B: Biological Sciences* 373:20170315.
- Fan Z-X, Zhang S-B, Hao G-Y, Ferry Slik JW, Cao K-F (2012) Hydraulic conductivity traits predict growth rates and adult stature of 40 Asian tropical tree species better than wood density. *Journal of Ecology* 100:732–741.
- Felton A, Nilsson U, Sonesson J, Felton AM, Roberge J-M, Ranius T, Ahlström M, Bergh J, Björkman C, Boberg J, Drössler L, Fahlvik N, Gong P, Holmström E, Kesitalo ECH, Klapwijk MJ, Laudon H, Lundmark T, Niklasson M, Nordin A, Pettersson M, Stenlid J, Sténs A, Wallertz K (2016) Replacing monocultures with mixed-species stands: Ecosystem service implications of two production forest alternatives in Sweden. *Ambio* 45:124–139.
- Feng Y, Schmid B, Loreau M, Forrester DI, Fei S, Zhu J, Tang Z, Zhu J, Hong P, Ji C, Shi Y, Su H, Xiong X, Xiao J, Wang S, Fang J (2022) Multispecies forest plantations outyield monocultures across a broad range of conditions. *Science* 376:865–868.
- Fichot R, Barigah TS, Chamaillard S, Le Thiec D, Laurans F, Cochard H, Brignolas F (2010) Common trade-offs between xylem resistance to cavitation and other physiological traits do not hold among unrelated *Populus deltoides*×*Populus nigra* hybrids: Xylem resistance to cavitation and water relations in poplar. *Plant, Cell & Environment*:1553–1568.
- Fichot R, Chamaillard S, Depardieu C, Le Thiec D, Cochard H, Barigah TS, Brignolas F (2011) Hydraulic efficiency and coordination with xylem resistance to cavitation, leaf function, and growth performance among eight unrelated *Populus deltoides*×*Populus nigra* hybrids. *Journal of Experimental Botany* 62:2093–2106.
- Fu X, Meinzer FC (2019) Metrics and proxies for stringency of regulation of plant water status (iso/anisohydry): a global data set reveals coordination and trade-offs among water transport traits. *Tree Physiology* 39:122–134.
- Garcia-Forner N, Biel C, Savé R, Martínez-Vilalta J (2017) Isohydric species are not necessarily more carbon limited than anisohydric species during drought. *Tree Physiology* 37:441–455.
- Gilbert N (2022) Troubled biodiversity plan gets billion-dollar funding boost. *Nature* 610:19–20.
- Gillner S, Korn S, Hofmann M, Roloff A (2017) Contrasting strategies for tree species to cope with heat and dry conditions at urban sites. *Urban Ecosystems* 20:853–865.
- Gleason SM, Butler DW, Ziemińska K, Waryszak P, Westoby M (2012) Stem xylem conductivity is key to plant water balance across Australian angiosperm species. *Functional Ecology* 26:343–352.
- Gleason SM, Stephens AEA, Tozer WC, Blackman CJ, Butler DW, Chang Y, Cook AM, Cooke J, Laws CA, Rosell JA, Stuart SA, Westoby M (2018) Shoot growth of woody trees and shrubs is predicted by maximum plant height and associated traits. *Functional Ecology* 32:247–259.
- Gleason SM, Westoby M, Jansen S, Choat B, Hacke UG, Pratt RB, Bhaskar R, Brodribb TJ, Bucci SJ, Cao K, Cochard H, Delzon S, Domec J, Fan Z, Feild TS, Jacobsen AL, Johnson DM,

- Lens F, Maherali H, Martínez-Vilalta J, Mayr S, McCulloh KA, Mencuccini M, Mitchell PJ, Morris H, Nardini A, Pittermann J, Plavcová L, Schreiber SG, Sperry JS, Wright IJ, Zanne AE (2016) Weak tradeoff between xylem safety and xylem-specific hydraulic efficiency across the world's woody plant species. *New Phytologist* 209:123–136.
- Grossiord C (2019) Having the right neighbors: how tree species diversity modulates drought impacts on forests. *New Phytologist* 228:42–49.
- Grossiord C, Granier A, Ratcliffe S, Bouriaud O, Bruelheide H, Čečko E, Forrester DI, Dawud SM, Finér L, Pollastrini M, Scherer-Lorenzen M, Valladares F, Bonal D, Gessler A (2014) Tree diversity does not always improve resistance of forest ecosystems to drought. *Proceedings of the National Academy of Sciences* 111:14812–14815.
- Hacke UG, Sperry JS (2001) Functional and ecological xylem anatomy. *Perspectives in Plant Ecology, Evolution and Systematics* 4:97–115.
- Hacke UG, Sperry JS, Wheeler JK, Castro L (2006) Scaling of angiosperm xylem structure with safety and efficiency. *Tree physiology* 26:689–701.
- Hacke UG, Spicer R, Schreiber SG, Plavcová L (2017) An ecophysiological and developmental perspective on variation in vessel diameter: Variation in xylem vessel diameter. *Plant, Cell & Environment* 40:831–845.
- Hajek P, Leuschner C, Hertel D, Delzon S, Schuldt B (2014) Trade-offs between xylem hydraulic properties, wood anatomy and yield in *Populus*. *Tree Physiology* 34:744–756.
- Hajek P, Link RM, Nock CA, Bauhus J, Gebauer T, Gessler A, Kovach K, Messier C, Paquette A, Saurer M, Scherer-Lorenzen M, Rose L, Schuldt B (2022) Mutually inclusive mechanisms of drought-induced tree mortality. *Global Change Biology* 28:3365–3378.
- Hammond WM, Adams HD (2019) Dying on time: traits influencing the dynamics of tree mortality risk from drought. *Tree Physiology* 39:906–909.
- Hammond WM, Williams AP, Abatzoglou JT, Adams HD, Klein T, López R, Sáenz-Romero C, Hartmann H, Breshears DD, Allen CD (2022) Global field observations of tree die-off reveal hotter-drought fingerprint for Earth's forests. *Nature Communications* 13:1761.
- Hannus S, Hiron A, Baxter T, McAllister HA, Wiström B, Sjöman H (2021) Intraspecific drought tolerance of *Betula pendula* genotypes: an evaluation using leaf turgor loss in a botanical collection. *Trees* 35:569–581.
- Hart SJ, Veblen TT, Eisenhart KS, Jarvis D, Kulakowski D (2014) Drought induces spruce beetle (*Dendroctonus rufipennis*) outbreaks across northwestern Colorado. *Ecology* 95:930–939.
- Hartmann H, Link RM, Schuldt B (2021) A whole-plant perspective of isohydry: stem-level support for leaf-level plant water regulation. *Tree Physiology* 41:901–905.
- Hoerber S, Leuschner C, Köhler L, Arias-Aguilar D, Schuldt B (2014) The importance of hydraulic conductivity and wood density to growth performance in eight tree species from a tropical semi-dry climate. *Forest Ecology and Management* 330:126–136.

- Huang J, Hammerbacher A, Gershenson J, van Dam NM, Sala A, McDowell NG, Chowdhury S, Gleixner G, Trumbore S, Hartmann H (2021) Storage of carbon reserves in spruce trees is prioritized over growth in the face of carbon limitation. *Proceedings of National Academic Sciences USA* 118:e2023297118.
- Huang J, Kautz M, Trowbridge AM, Hammerbacher A, Raffa KF, Adams HD, Goodsman DW, Xu C, Meddens AJH, Kandasamy D, Gershenson J, Seidl R, Hartmann H (2020) Tree defence and bark beetles in a drying world: carbon partitioning, functioning and modelling. *New Phytologist* 225:26–36.
- IPCC (2021) *Climate Change 2021: The Physical Science Basis. Contribution of Working Group I to the Sixth Assessment Report of the Intergovernmental Panel on Climate Change* Masson-Delmotte V, Zhai P, Pirani A, Connors SL, Péan C, Berger S, Caud N, Chen Y, Goldfarb L, Gomis MI, Huang M, Leitzell K, Lonnoy E, Matthews JBR, Maycock TK, Waterfield T, Yelekçi R, Yu R, Zhou B (eds). Cambridge University Press: Cambridge, UK.
- Isbell FI, Polley HW, Wilsey BJ (2009) Biodiversity, productivity and the temporal stability of productivity: patterns and processes. *Ecology Letters* 12:443–451.
- Jansen S, Choat B, Pletsers A (2009) Morphological variation of intervessel pit membranes and implications to xylem function in angiosperms. *American Journal of Botany* 96:409–419.
- Joshi J, Stocker BD, Hofhansl F, Zhou S, Dieckmann U, Prentice IC (2022) Towards a unified theory of plant photosynthesis and hydraulics. *Nature Plants*:1–13.
- Kaack L, Weber M, Isasa E, Karimi Z, Li S, Pereira L, Trabi CL, Zhang Y, Schenk HJ, Schuldt B, Schmidt V, Jansen S (2021) Pore constrictions in intervessel pit membranes provide a mechanistic explanation for xylem embolism resistance in angiosperms. *New Phytologist* 230:1829–1843.
- Klein T (2014) The variability of stomatal sensitivity to leaf water potential across tree species indicates a continuum between isohydric and anisohydric behaviours. *Functional Ecology* 28:1313–1320.
- Köcher P, Horna V, Leuschner C (2013) Stem water storage in five coexisting temperate broad-leaved tree species: significance, temporal dynamics and dependence on tree functional traits. *Tree Physiology* 33:817–832.
- Kölling C (2007) Klimahüllen für 27 waldbaumarten. *AFZ-DerWald* 23:1242–1245.
- Kotowska MM, Hertel D, Rajab YA, Barus H, Schuldt B (2015) Patterns in hydraulic architecture from roots to branches in six tropical tree species from cacao agroforestry and their relation to wood density and stem growth. *Frontiers in Plant Science* 6.
- Kotowska MM, Link RM, Röhl A, Hertel D, Hölscher D, Waite P-A, Moser G, Tjoa A, Leuschner C, Schuldt B (2021) Effects of wood hydraulic properties on water use and productivity of tropical rainforest trees. *Frontiers in Forests and Global Change* 3:598759.
- Kunert N, Schwendenmann L, Potvin C, Hölscher D (2012) Tree diversity enhances tree transpiration in a Panamanian forest plantation. *Journal of Applied Ecology* 49:135–144.

- Lamb D, Erskine PD, Parrotta JA (2005) Restoration of Degraded Tropical Forest Landscapes. *Science* 310:1628–1632.
- Lamy J-B, Bouffier L, Burlett R, Plomion C, Cochard H, Delzon S (2011) Uniform Selection as a Primary Force Reducing Population Genetic Differentiation of Cavitation Resistance across a Species Range Ingvarsson PK (ed). *PLoS ONE* 6:e23476.
- Lemaire C, Blackman CJ, Cochard H, Menezes-Silva PE, Torres-Ruiz JM, Herbette S (2021) Acclimation of hydraulic and morphological traits to water deficit delays hydraulic failure during simulated drought in poplar. *Tree Physiology* 8:2008-2021.
- Lens F, Sperry JS, Christman MA, Choat B, Rabaey D, Jansen S (2011) Testing hypotheses that link wood anatomy to cavitation resistance and hydraulic conductivity in the genus *Acer*. *New Phytologist* 190:709–723.
- Leuschner C (2020) Drought response of European beech (*Fagus sylvatica* L.)—A review. *Perspectives in Plant Ecology, Evolution and Systematics* 47:125576.
- Leuschner C, Meier IC (2018) The ecology of Central European tree species: Trait spectra, functional trade-offs, and ecological classification of adult trees. *Perspectives in Plant Ecology, Evolution and Systematics* 33:89–103.
- Leuschner C, Schipka F, Backes K (2022) Stomatal regulation and water potential variation in European beech: challenging the iso/anisohdry concept. *Tree Physiology* 42:365–378.
- Leuschner C, Wedde P, Lübke T (2019) The relation between pressure–volume curve traits and stomatal regulation of water potential in five temperate broadleaf tree species. *Annals of Forest Science* 76:1–14.
- Li S, Feifel M, Karimi Z, Schuldt B, Choat B, Jansen S (2016a) Leaf gas exchange performance and the lethal water potential of five European species during drought. *Tree Physiology* 36:179–192.
- Li S, Lens F, Espino S, Karimi Z, Klepsch M, Schenk HJ, Schmitt M, Schuldt B, Jansen S (2016b) Intervessel pit membrane thickness as a key determinant of embolism resistance in angiosperm xylem. *IAWA Journal* 37:152–171.
- Liu CLC, Kuchma O, Krutovsky KV (2018) Mixed-species versus monocultures in plantation forestry: Development, benefits, ecosystem services and perspectives for the future. *Global Ecology and Conservation* 15:e00419.
- Loepfe L, Martinez-Vilalta J, Piñol J, Mencuccini M (2007) The relevance of xylem network structure for plant hydraulic efficiency and safety. *Journal of Theoretical Biology* 247:788–803.
- Mantova M, Herbette S, Cochard H, Torres-Ruiz JM (2022) Hydraulic failure and tree mortality: from correlation to causation. *Trends in Plant Science* 27:335–345.
- Martin-StPaul N, Delzon S, Cochard H (2017) Plant resistance to drought depends on timely stomatal closure. *Ecology Letters* 20:1437–1447.

- Matusick G, Ruthrof KX, Brouwers NC, Dell B, Hardy GSJ (2013) Sudden forest canopy collapse corresponding with extreme drought and heat in a mediterranean-type eucalypt forest in southwestern Australia. *European Journal of Forest Resources* 132:497–510.
- McDowell N, Pockman WT, Allen CD, Breshears DD, Cobb N, Kolb T, Plaut J, Sperry J, West A, Williams DG, Yepez EA (2008) Mechanisms of plant survival and mortality during drought: why do some plants survive while others succumb to drought? *New Phytologist* 178:719–739.
- McDowell NG, Sapes G, Pivovarov A, Adams HD, Allen CD, Anderegg WRL, Arend M, Breshears DD, Brodribb T, Choat B, Cochard H, De Cáceres M, De Kauwe MG, Grossiord C, Hammond WM, Hartmann H, Hoch G, Kahmen A, Klein T, Mackay DS, Mantova M, Martínez-Vilalta J, Medlyn BE, Mencuccini M, Nardini A, Oliveira RS, Sala A, Tissue DT, Torres-Ruiz JM, Trowbridge AM, Trugman AT, Wiley E, Xu C (2022) Mechanisms of woody-plant mortality under rising drought, CO₂ and vapour pressure deficit. *Nature Reviews Earth and Environment* 3:294–308.
- McElrone AJ, Choat B, Gambetta GA, Brodersen CR (2013) Water Uptake and Transport in Vascular Plants. *Nature Education Knowledge* 4(5):6.
- Meinzer FC, Johnson DM, Lachenbruch B, McCulloh KA, Woodruff DR (2009) Xylem hydraulic safety margins in woody plants: coordination of stomatal control of xylem tension with hydraulic capacitance. *Functional Ecology* 23:922–930.
- Meinzer FC, Woodruff DR, Marias DE, Smith DD, McCulloh KA, Howard AR, Magedman AL (2016) Mapping ‘hydroscares’ along the iso- to anisohydric continuum of stomatal regulation of plant water status. *Ecology Letters* 19:1343–1352.
- Mencuccini M, Minunno F, Salmon Y, Martínez-Vilalta J, Hölttä T (2015) Coordination of physiological traits involved in drought-induced mortality of woody plants. *New Phytologist* 208:396–409.
- Michaelian M, Hogg EH, Hall RJ, Arsenault E (2011) Massive mortality of aspen following severe drought along the southern edge of the Canadian boreal forest. *Global Change Biology* 17:2084–2094.
- Morales-Hidalgo D, Oswalt SN, Somanathan E (2015) Status and trends in global primary forest, protected areas, and areas designated for conservation of biodiversity from the Global Forest Resources Assessment 2015. *Forest Ecology and Management* 352:68–77.
- Moser A, Rahman MA, Pretzsch H, Pauleit S, Rötzer T (2017) Inter- and intraannual growth patterns of urban small-leaved lime (*Tilia cordata* mill.) at two public squares with contrasting microclimatic conditions. *International Journal of Biometeorology* 61:1095–1107.
- Moser A, Rötzer T, Pauleit S, Pretzsch H (2016) The Urban Environment Can Modify Drought Stress of Small-Leaved Lime (*Tilia cordata* Mill.) and Black Locust (*Robinia pseudoacacia* L.). *Forests* 7:71.
- Moser-Reischl A, Rahman MA, Pauleit S, Pretzsch H, Rötzer T (2019) Growth patterns and effects of urban micro-climate on two physiologically contrasting urban tree species. *Landscape and Urban Planning* 183:88–99.

- Olson ME, Anfodillo T, Gleason SM, McCulloh KA (2021) Tip-to-base xylem conduit widening as an adaptation: causes, consequences, and empirical priorities. *New Phytologist* 229:1877–1893.
- Olson ME, Anfodillo T, Rosell JA, Petit G, Crivellaro A, Isnard S, León-Gómez C, Alvarado-Cárdenas LO, Castorena M (2014) Universal hydraulics of the flowering plants: vessel diameter scales with stem length across angiosperm lineages, habits and climates Enquist B (ed). *Ecology Letters* 17:988–997.
- Peng S, Chen A, Xu L, Cao C, Fang J, Myneni RB, Pinzon JE, Tucker CJ, Piao S (2011) Recent change of vegetation growth trend in China. *Environment Research Letters* 6:044027.
- Phillips OL, Aragão LEOC, Lewis SL, Fisher JB, Lloyd J, López-González G, Malhi Y, Monteagudo A, Peacock J, Quesada CA, van der Heijden G, Almeida S, Amaral I, Arroyo L, Aymard G, Baker TR, Bánki O, Blanc L, Bonal D, Brando P, Chave J, de Oliveira ÁCA, Cardozo ND, Czimczik CI, Feldpausch TR, Freitas MA, Gloor E, Higuchi N, Jiménez E, Lloyd G, Meir P, Mendoza C, Morel A, Neill DA, Nepstad D, Patiño S, Peñuela MC, Prieto A, Ramírez F, Schwarz M, Silva J, Silveira M, Thomas AS, Steege H ter, Stropp J, Vásquez R, Zelazowski P, Dávila EA, Andelman S, Andrade A, Chao K-J, Erwin T, Di Fiore A, C. EH, Keeling H, Killeen TJ, Laurance WF, Cruz AP, Pitman NCA, Vargas PN, Ramírez-Angulo H, Rudas A, Salamão R, Silva N, Terborgh J, Torres-Lezama A (2009) Drought Sensitivity of the Amazon Rainforest. *Science* 323:1344–1347.
- Pittermann J, Sperry JS, Hacke UG, Wheeler JK, Sikkema EH (2006) Inter-tracheid pitting and the hydraulic efficiency of conifer wood: the role of tracheid allometry and cavitation protection. *American journal of botany* 93:1265–1273.
- Plaut JA, Yopez EA, Hill J, Pangle R, Sperry JS, Pockman WT, McDowell NG (2012) Hydraulic limits preceding mortality in a piñon-juniper woodland under experimental drought: Hydraulic limits in a piñon-juniper woodland. *Plant, Cell & Environment* 35:1601–1617.
- Robson TM, Hartikainen SM, Aphalo PJ (2015) How does solar ultraviolet-B radiation improve drought tolerance of silver birch (*Betula pendula* Roth.) seedlings? *Plant, Cell & Environment* 38:953–967.
- Rötzer T, Häberle KH, Kallenbach C, Matyssek R, Schütze G, Pretzsch H (2017) Tree species and size drive water consumption of beech/spruce forests - a simulation study highlighting growth under water limitation. *Plant Soil* 418:337–356.
- Ruffault J, Pimont F, Cochard H, Dupuy J-L, Martin-StPaul N (2022) SurEau-Ecos v2.0: a trait-based plant hydraulics model for simulations of plant water status and drought-induced mortality at the ecosystem level. *Geoscience Model Development* 15:5593–5626.
- Rukh S, Sanders TGM, Krüger I, Schad T, Bolte A (2023) Distinct Responses of European Beech (*Fagus sylvatica* L.) to Drought Intensity and Length—A Review of the Impacts of the 2003 and 2018–2019 Drought Events in Central Europe. *Forests* 14:248.
- Russo SE, Jenkins KL, Wiser SK, Uriarte M, Duncan RP, Coomes DA (2010) Interspecific relationships among growth, mortality and xylem traits of woody species from New Zealand. *Functional Ecology* 24:253–262.

- Schmidt O, Roloff A (2014) *Acer pseudoplatanus*. In: Enzyklopädie der Holzgewächse: Handbuch und Atlas der Dendrologie. John Wiley & Sons, Ltd, pp 1–26.
- Schnabel F, Purruicker S, Schmitt L, Engelmann RA, Kahl A, Richter R, Seele-Dilbat C, Skiadaresis G, Wirth C (2022) Cumulative growth and stress responses to the 2018–2019 drought in a European floodplain forest. *Global Change Biology* 28:1870–1883.
- Scholz A, Rabaey D, Stein A, Cochard H, Smets E, Jansen S (2013) The evolution and function of vessel and pit characters with respect to cavitation resistance across 10 *Prunus* species. *Tree Physiology* 33:684–694.
- Schuldt B, Buras A, Arend M, Vitasse Y, Beierkuhnlein C, Damm A, Gharun M, Grams TEE, Hauck M, Hajek P, Hartmann H, Hiltbrunner E, Hoch G, Holloway-Phillips M, Körner C, Larysch E, Lübke T, Nelson DB, Rammig A, Rigling A, Rose L, Ruehr NK, Schumann K, Weiser F, Werner C, Wohlgemuth T, Zang CS, Kahmen A (2020) A first assessment of the impact of the extreme 2018 summer drought on Central European forests. *Basic and Applied Ecology* 45:86–103.
- Schuldt B, Knutzen F, Delzon S, Jansen S, Müller-Haubold H, Burlett R, Clough Y, Leuschner C (2016) How adaptable is the hydraulic system of European beech in the face of climate change-related precipitation reduction? *New Phytologist* 210:443–458.
- Schwendenmann L, Pendall E, Sanchez-Bragado R, Kunert N, Hölscher D (2015) Tree water uptake in a tropical plantation varying in tree diversity: interspecific differences, seasonal shifts and complementarity. *Ecohydrology* 8:1–12.
- Speirs J, Binney A, Collins M, Edwards E, Loveys B (2013) Expression of ABA synthesis and metabolism genes under different irrigation strategies and atmospheric VPDs is associated with stomatal conductance in grapevine (*Vitis vinifera* L. cv Cabernet Sauvignon). *Journal of Experimental Botany* 64:1907–1916.
- Sperry JS, Donnelly JR, Tyree MT (1988) A method for measuring hydraulic conductivity and embolism in xylem. *Plant, Cell & Environment* 11:35–40.
- Sperry JS, Tyree MT (1988) Mechanism of water stress-induced xylem embolism. *Plant Physiology* 88:581–587.
- Sperry JS, Venturas MD, Anderegg WRL, Mencuccini M, Mackay DS, Wang Y, Love DM (2017) Predicting stomatal responses to the environment from the optimization of photosynthetic gain and hydraulic cost: A stomatal optimization model. *Plant, Cell & Environment* 40:816–830.
- Stanturf JA, Palik BJ, Dumroese RK (2014) Contemporary forest restoration: A review emphasizing function. *Forest Ecology and Management* 331:292–323.
- Steudle E (2001) The Cohesion-Tension Mechanism and the Acquisition of Water by Plant Roots. *Annual Review of Plant Physiology and Plant Molecular Biology* 52:847–875.
- Trenberth KE, Dai A, van der Schrier G, Jones PD, Barichivich J, Briffa KR, Sheffield J (2014) Global warming and changes in drought. *Nature Climate Change* 4:17–22.
- Tyree MT (2003) Hydraulic limits on tree performance: transpiration, carbon gain and growth of trees. *Trees* 17:95–100.

- Tyree MT, Davis SD, Cochard H (1994) Biophysical Perspectives of Xylem Evolution: is there a Tradeoff of Hydraulic Efficiency for Vulnerability to Dysfunction? *IAWA Journal* 15:335–360.
- Tyree MT, Zimmermann MH (2002) *Xylem Structure and the Ascent of Sap*, 2nd edn. Springer-Verlag, Berlin Heidelberg, Germany, pp. 143-174.
- UK Forestry Commission (2015) Right Trees for Changing Climate Database, web page. Available at: <http://www.righttree4cc.org.uk>.
- Urli M, Porte AJ, Cochard H, Guengant Y, Burlett R, Delzon S (2013) Xylem embolism threshold for catastrophic hydraulic failure in angiosperm trees. *Tree Physiology* 33:672–683.
- Vacek Z, Vacek S, Cukor J (2023) European forests under global climate change: Review of tree growth processes, crises and management strategies. *Journal of Environmental Management* 332:117353.
- Vitali V, Forrester DI, Bauhus J (2018) Know Your Neighbours: Drought Response of Norway Spruce, Silver Fir and Douglas Fir in Mixed Forests Depends on Species Identity and Diversity of Tree Neighbourhoods. *Ecosystems* 21:1215–1229.
- Vogt UK (2001) Hydraulic vulnerability, vessel refilling, and seasonal courses of stem water potential of *Sorbus aucuparia* L. and *Sambucus nigra* L. *Journal of Experimental Botany* 52:1527–1536.
- Wheeler JK, Sperry JS, Hacke UGWE, Hoang N (2005) Inter-vessel pitting and cavitation in woody Rosaceae and other vesselless plants: a basis for a safety versus efficiency trade-off in xylem transport. *Plant, Cell & Environment* 28:800–812.
- Wikberg J, Ögren E (2004) Interrelationships between water use and growth traits in biomass-producing willows. *Trees - Structure and Function* 18:70–76.
- Williams AP, Allen CD, Macalady AK, Griffin D, Woodhouse CA, Meko DM, Swetnam TW, Rauscher SA, Seager R, Grissino-Mayer HD, Dean JS, Cook ER, Gangodagamage C, Cai M, McDowell NG (2013) Temperature as a potent driver of regional forest drought stress and tree mortality. *Nature Climate Change* 3:292–297.
- Wullschlegel SD, Meinzer FC, Vertessy RA (1998) A review of whole-plant water use studies in tree. *Tree Physiology* 18:499–512.
- Yuan W, Zheng Y, Piao S, Ciais P, Lombardozzi D, Wang Y, Ryu Y, Chen G, Dong W, Hu Z, Jain AK, Jiang C, Kato E, Li S, Lienert S, Liu S, Nabel JEMS, Qin Z, Quine T, Sitch S, Smith WK, Wang F, Wu C, Xiao Z, Yang S (2019) Increased atmospheric vapor pressure deficit reduces global vegetation growth. *Science Advances* 5:eaax1396.
- Zhang J-L, Cao K-F (2009) Stem hydraulics mediates leaf water status, carbon gain, nutrient use efficiencies and plant growth rates across dipterocarp species. *Functional Ecology* 23:658–667.
- Zhang Y, Oren R, Kang S (2012) Spatiotemporal variation of crown-scale stomatal conductance in an arid *Vitis vinifera* L. cv. Merlot vineyard: direct effects of hydraulic properties and indirect effects of canopy leaf area. *Tree Physiology* 32:262–279.

Chapter-2:

Influence of Juvenile Growth on Xylem Safety and Efficiency in Three Temperate Tree Species

Manish Kumar^{1,2}, Pierre-André Waite¹, Sharath Shyamappa Paligi^{1,3}, Bernhard Schuldt^{1*}

¹ *University of Würzburg, Julius-von-Sachs-Institute of Biological Sciences, Ecophysiology and Vegetation Ecology, Julius-von-Sachs-Platz 3, 97082 Würzburg, Germany.*

² *ICAR—Central Soil Salinity Research Institute (CSSRI), Karnal, 132001, India.*

³ *Plant Ecology and Ecosystems Research, Albrecht von Haller Institute for Plant Sciences, University of Göttingen, 37073, Göttingen, Germany.*

Forests 2022, 13, 909. <https://doi.org/10.3390/f13060909>.

(The published article is open access, under licence CC BY 4.0)

Abstract

The evolution of the internal water transport system was a prerequisite for high plant productivity. In times of climate change, understanding the dependency of juvenile growth on xylem hydraulic physiology is, therefore, of high importance. Here, we explored various wood anatomical, hydraulic, and leaf morphological traits related to hydraulic safety and efficiency in three temperate broadleaved tree species (*Acer pseudoplatanus*, *Betula pendula*, and *Sorbus aucuparia*). We took advantage of a severe natural heat wave that resulted in different climatic growing conditions for even-aged plants from the same seed source growing inside a greenhouse and outside. Inside the greenhouse, the daily maximum vapour pressure deficit was on average 36% higher than outside during the growing seasons. Because of the higher atmospheric moisture stress, the biomass production differed up to 5.6-fold between both groups. Except for one species, a high productivity was associated with a high hydraulic efficiency caused by large xylem vessels and a large, supported leaf area. Although no safety-efficiency trade-off was observed, productivity was significantly related to P_{50} in two of the tree species but without revealing any clear pattern. A considerable plasticity in given traits was observed between both groups, with safety-related traits being more static while efficiency-related traits revealed a higher intra-specific plasticity. This was associated with other wood anatomical and leaf morphological adjustments. We confirm that a high hydraulic efficiency seems to be a prerequisite for a high biomass production, while our controversial results on the growth–xylem safety relationship confirm that safety-efficiency traits are decoupled and that their relationship with juvenile growth and water regime is species-specific.

Keywords: hydraulic efficiency, biomass, growth rate, hydraulic variability, phenotypic plasticity, safety-efficiency trade-off, vulnerability curve.

2.1 Introduction

Worldwide, trees in forested ecosystems are increasingly exposed to drought and heat stress due to the rise in intensity and frequency of global change-type drought events (IPCC 2021). Thereby, prolonged drought exposure may affect plant productivity and biomass allocation (Eziz *et al.* 2017), survival (McDowell *et al.* 2008, Rowland *et al.* 2015), and potentially future species abundance and distributions (Clark *et al.* 2016). During drought exposure, plants close their stomata to maintain high xylem water potentials and to reduce transpirational water loss (Choat *et al.* 2018). However, prolonged drought conditions might ultimately lead to hydraulic failure because of continuous residual water loss via the cuticle and bark (Duursma *et al.* 2019). Under severe and prolonged water stress, xylem tensions therefore ultimately reach critical thresholds causing water-filled vessels to embolize, which disrupts the continuous water column and ultimately causes plant death (Nolan *et al.* 2021, Britton *et al.* 2022, Hajek *et al.* 2022). Thus, the likelihood of hydraulic failure and xylem characteristics are supposed to be highly interconnected. The ability to resist embolism formation is mainly depicted by the water potential at a 50% loss of conductivity (P_{50}) and referred to as hydraulic safety. Although it is meanwhile well-established that pit membrane thickness is directly related to the P_{50} -value (Li *et al.* 2016b, Kaack *et al.* 2021), wide vessels have likewise commonly been associated with low hydraulic safety, both within (Awad *et al.* 2010, Hajek *et al.* 2014) and across species (Maherali *et al.* 2006, Domec *et al.* 2010). Therefore, species with thin pit membranes and large vessels may be more vulnerable to water stress-induced cavitation (Isasa *et al.* 2021). However, large vessels are directly linked to the maximal capacity of the xylem to transport water, i.e., the xylem-specific hydraulic conductivity (K_S ; hereafter ‘hydraulic efficiency’), which scales to the fourth power of conduit diameter.

Hence, a trade-off between hydraulic efficiency and safety has traditionally been hypothesized (Sperry and Tyree 1990, Hacke *et al.* 2006, Gleason *et al.* 2016). Both a high hydraulic efficiency and a high safety, are advantageous for plant growth and drought-tolerance. However, because of their contrasting anatomical needs, both are supposedly not achievable by the same species, and natural selection is expected to drive species towards one extreme or another (Choat *et al.* 2012, Gleason *et al.* 2016). In fact, empirical evidence is ambiguous, and a majority of recent studies could find only weak or no relations between hydraulic efficiency and safety in trees (Maherali *et al.* 2006, Hajek *et al.* 2014, Gleason *et al.* 2016, Schumann *et al.* 2019, Liu *et*

al. 2021). Most likely, such a safety–efficiency trade-off depends on a range of wood anatomical properties and not just vessel diameter (Schuldt *et al.* 2016). Accordingly, hydraulic safety–efficiency relationships are more likely to appear in interspecific studies with species from different habitats than in samples of co-occurring, phylogenetically related taxa or in intraspecific studies.

Although safety–efficiency trade-offs are scale-dependent, the water status of plants is highly related to xylem characteristics, and xylem physiology has been termed the backbone of terrestrial plant productivity because of the close connection between carbon uptake and water release via the stomata (Brodribb 2009). This is in line with (Tyree 2003), hypothesizing that high productivity should be closely associated with a high hydraulic efficiency. In the case of a safety–efficiency trade-off, this might mean that productive trees favour hydraulic efficiency over safety to ensure high growth rates. Since then, a plausible link between stem growth rate and hydraulic efficiency and safety has been tested empirically revealing close, yet contrasting, associations (Domec and Gartner 2003, Wikberg and Ögren 2004, Zhang and Cao 2009, Fichot *et al.* 2011, Fan *et al.* 2012, Gleason *et al.* 2012). For example, no relationship between growth and hydraulic efficiency was found in *Populus nigra* across different genotypes at the intra-population level (Guét *et al.* 2015). Nonetheless, relations between productivity and hydraulic efficiency seem to be closely related to plant water transport capacity and therefore wood anatomical features such as a large vessel diameter (Hoeber *et al.* 2014, Eller *et al.* 2018, Gleason *et al.* 2018, Kotowska *et al.* 2021). On the other hand, xylem safety may also decline with an increasing growth rate. Firstly, due to the anticipated trade-off between hydraulic safety and efficiency, but also because of carbon allocation conflicts. In plants, assimilated carbon might either be allocated to cell walls to resist the higher hydraulic tensions (Brodribb 2009) or to foliar and axial tissues for a higher productivity (Wikberg and Ögren 2004). However, most studies did not observe any relationship between hydraulic safety and growth (Fichot *et al.* 2010, Sterck *et al.* 2012, Hajek *et al.* 2014, Guét *et al.* 2015, Hajek *et al.* 2016) although exceptions exist (Cochard *et al.* 2007, Eller *et al.* 2018).

In view of current and future climate change impacts on the Central European forests, the selected minor timber tree species—Sycamore maple (*Acer pseudoplatanus*), European rowan (*Sorbus aucuparia*), and Silver birch (*Betula pendula*)—are ecologically important because of their different habitat preferences (Ellenberg and Leuschner 2010), highlighting their potential suitability for the establishment of climate-resilient forests.

In order to test whether differences in juvenile growth affect xylem efficiency and/or safety, we measured 17 structural, functional, and hydraulic traits in evenly-aged young trees differing up to 5.6-fold in biomass production, which was induced by different climatic growing conditions during an exceptional heat wave in the year 2019. We analysed the association of structural parameters and hydraulic safety–efficiency traits as well as other functional traits linked to resource acquisition and partitioning. We studied interactions across and within species including the plastic response of the plants to contrasting growing conditions. We asked whether (i) a low hydraulic safety (P_{50}) and a high hydraulic efficiency (K_S) are associated with high juvenile growth rates, (ii) a trade-off exists between hydraulic safety and efficiency in seed-grown saplings, and whether (iii) hydraulic safety–efficiency traits are related to xylem anatomy.

2.2 Material and Methods

2.2.1 Study Site, Microclimatic Measurements, and Plant Material

The present study was conducted at the Chair of Ecophysiology and Vegetation Ecology, Julius-von-Sachs-Institute of Biological Sciences, Würzburg, Germany (180 m a.s.l; mean annual temperature: 10°C; mean annual precipitation: 625 mm). From seeds collected in the Botanical Garden Würzburg in 2018, we grew 82 plants of three temperate deciduous angiosperm species, namely *Acer pseudoplatanus* (ACPS), *Betula pendula* (BEPE), and *Sorbus aucuparia* (SOAU) for 18 months. These three tree species were selected because of their anticipated differences in growth performance and hydraulic traits. *B. pendula* is a typical pioneer, broad-leaved tree species in the temperate and boreal forests of Europe. It has the ability to grow in both wet and dry habitats but has high needs for light. It can survive under fairly extreme conditions through physiological adaptation and is considered to follow an isohydric stomatal control strategy (Robson *et al.* 2015). The second species selected, *A. pseudoplatanus*, prefers a humid climate, high rainfall, and moderately moist to wet site up to 1800 m elevation. The species has a high-water demand and needs large rooting space. The species is considered as moderately drought and heat sensitive (Leuschner and Meier 2018) and is defined as isohydric (Leuschner *et al.* 2019). The last species of our sample, *S. aucuparia*, occurs as a tree or a shrub and can experience wide water potential variations during droughts (*i.e.*, related to an anisohydric behavior), and shows a high resistance to cavitation (Vogt 2001). In the Botanical Garden, open-field air temperature and air humidity is

continuously measured at 2 m height aboveground (Umweltmeßtechnik Adolf Thies GmbH & Co. KG, Göttingen, Germany). Micro-climatic conditions inside the growing chamber of the greenhouse are likewise continuously recorded (RAM GmbH Mess-und Regeltechnik, Herrsching, Germany), but unfortunately the data for the 2019 and 2020 growing seasons were lost due to a fatal computer crash. We therefore used the data from the 2021 growing season, which also became a dry and warm growing season in Würzburg, to model the microclimatic conditions in 2019 and 2020 (Figures S2.1 and S2.2); both were highly interrelated according to a linear model ($R^2 = 0.85$, $p < 0.001$; data not shown).

After initial sowing in March 2019 and transplanting in May 2019, the seedlings were grown in 7.5 L pots in an Euroham soil mixture (Eurohum Faser, Article no. 12-03200-xx) containing N, P, K in a proportion of 14, 16, and 18 kg m⁻³, respectively. For the duration of the growing phase (i.e., 18 months), a subset of randomly selected 10 to 12 plants per species ($n = 34$) were placed in a small chamber of a greenhouse with an area of 18 m², hereafter named ‘inside’ or ‘stress treatment’. We took advantage of the severe climatic conditions in 2019, an unprecedented heat and drought event since more than 250 years (Hari *et al.* 2020), which exposed these plants to stressful environmental conditions resulting in reduced growth rates. This stress was mainly caused by high temperatures and high atmospheric moisture stress inside the growing chamber (Figure 2.1). Meanwhile, the remaining 14 to 18 plants per species ($n = 48$) were grown outside under a transparent roof but with completely open sites, enabling air exchange due to wind, hereafter named ‘outside’ or ‘control treatment’. These plants were therefore exposed to more natural environmental conditions. As a consequence of the different growing locations, saplings that were grown inside the greenhouse chamber were strongly affected by the heat wave (i.e., stress treatment) while the plants outside experienced more natural growing conditions (control treatment), which was mirrored in large differences in growth rates. During the growing season in 2019, the daily maximum temperature (T_{\max}) differed on average by 15.9% between inside and outside (mean \pm SE: 29.5 ± 0.4 °C versus 24.8 ± 0.5 °C), and vapour pressure deficit (VPD_{\max}) differed by 36.2% (3.04 ± 0.12 kPa versus 1.94 ± 0.08 kPa). Similar differences were observed during the growing season in 2020, where T_{\max} differed by 15.8 % (29.7 ± 0.3 °C versus 25.0 ± 0.4 °C) and VPD by 36.0 % (3.08 ± 0.10 kPa versus 1.97 ± 0.07 kPa). During the 10 % of the hottest days in 2019 and 2020, a daily VPD_{\max} of 5.89 ± 0.27 kPa or 5.64 ± 0.23 kPa was reached inside the greenhouse, indicative for severe atmospheric moisture stress. Average outside values

stayed below 4 kPa (3.93 ± 0.19 kPa in 2019 and 3.75 ± 0.16 kPa in 2020, respectively; Figure 2.1).

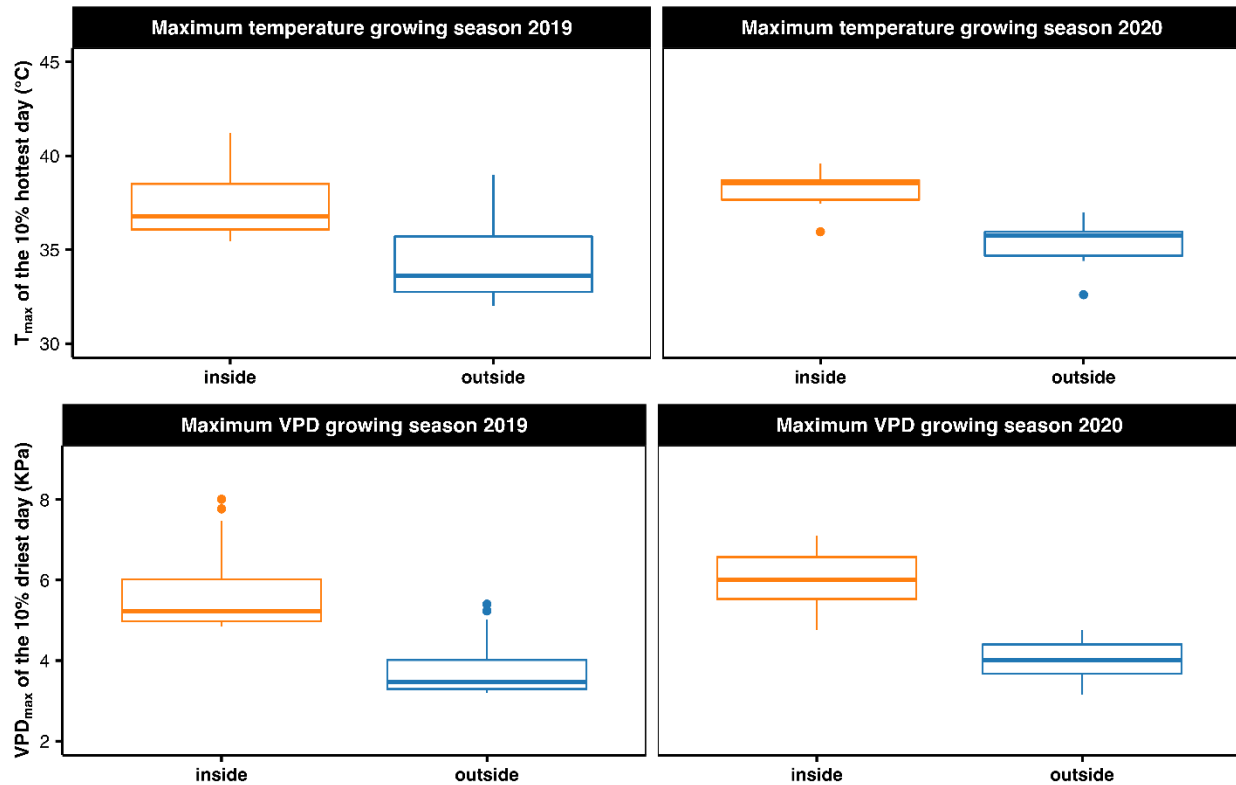


Figure 2.1: Boxplots showing the micro-climatic growing conditions in the greenhouse (inside) and open-field measurements at 2 m height (outside) during the growing season from May to September in 2019 and 2020. Given are the daily maximum temperature (T_{\max} , °C) for 10 % of the hottest days as well as the daily maximum vapour pressure deficit (VPD_{\max} , kPa) for 10 % of the driest days of each growing season. Please note that only the outside microclimatic data are available for both years, the inside values have been modelled based on data from 2021 (refer to Figures S2.1 and S2.2 for details).

None of the plants inside the greenhouse showed signs of leaf discoloration, indicating that frequent stomatal closure due to a high evaporative demand explains observed differences in biomass production as all other growing conditions were comparable (e.g., light exposure, soil composition and volume, and irrigation schedule). Please note that the plant material from both groups was even-aged and seeds originated from the same parental trees. After 18 months of growth under the different conditions, we collected plant material for structural, functional, and hydraulic measurements in August 2020.

2.2.2 Sample Collection, Structural Measurements, and Growth Rate

Before the hydraulic measurements, saplings were watered overnight to ensure full turgor and a relaxed state to minimize measurement artefacts associated with cutting under tension. We performed all measurements on the main shoot of most saplings (*i.e.*, structural measurements were performed on all 82 trees, while hydraulic and leaf morphological measurements were carried out on a subset of 57 to 64 trees including side branches (see Table S2.1 for more details). We first measured structural parameters of each sapling, *i.e.*, the root collar diameter (RCD) and shoot length, and then proceeded to cut-off the main shoot at the root collar and to recut it under water several times in order to relax the xylem, thereby avoiding measurement artefacts associated with sample excision (Torres-Ruiz *et al.* 2015). On this shoot, we labelled a targeted segment to be used for hydraulic measurements, and collected and separated (*i.e.*, divided in two groups: basal and apical leaves) all leaves above and below the proximal end of the targeted section and stored them in plastic bags at 4 °C until scanning. Furthermore, the distance from the segment used for hydraulic and wood anatomical measurements to the tip was recorded. Directly below the proximal end of the targeted segment, we stored a ~3 cm segment in 70 % ethanol for subsequent wood anatomical analyses. After hydraulic measurements, the segment used and the remaining woody samples were oven-dried at 70 °C for 72 h. Subsequently, total aboveground biomass (AGB, g) was estimated by adding the total leaf dry mass per plant, and aboveground biomass increment (ABI, mg d⁻¹) estimated by dividing AGB by the growth period, *i.e.*, the difference between seed sowing and sapling harvesting time. A list of all traits measured with the corresponding acronyms and units is given in Table 2.1.

2.2.3 Leaf Traits

All leaves from basal and apical group (see the previous section for details) were scanned separately with an A3 high-resolution scanner (Expression 12000XL, EPSON, Nagano, Japan). We divided the leaves into two groups to relate hydraulic conductivity measurements to the leaf area that is supported by the measured segment (*i.e.*, apical group). We then computed the areas to obtain total leaf area (A_L^{total} , cm²) and mean leaf area (A_{leaf} , cm²) per sapling using the ImageJ software. The Huber value (HV, 10⁻⁴ m² m⁻²), *i.e.*, the sapwood-to-leaf-area ratio, was calculated

by dividing the sapwood area (i.e., obtained from anatomical cross-sections) by the distal leaf area. All leaves were then oven-dried at 70 °C for 48 h to calculate specific leaf area (SLA, cm² g⁻¹).

Table 2.1: List of variables included in this study with their definitions and units.

| Abbreviation | Units | Definitions |
|--------------------------|---|--|
| <i>Growth attributes</i> | | |
| RCD | mm | Collar diameter of the stem above the ground |
| Shoot length | cm | Shoot length from ground to uppermost leaf |
| AGB | g | Aboveground biomass |
| ABI | mg d ⁻¹ | Aboveground biomass increment |
| <i>Hydraulic traits</i> | | |
| P_{12} | MPa | Xylem pressure at 12 % loss of hydraulic conductance |
| P_{50} | MPa | Xylem pressure at 50 % loss of hydraulic conductance |
| P_{88} | MPa | Xylem pressure at 88 % loss of hydraulic conductance |
| K_S | kg m ⁻¹ MPa ⁻¹ s ⁻¹ | Specific conductivity |
| K_L | 10 ⁻⁴ kg m ⁻¹ MPa ⁻¹ s ⁻¹ | Leaf-specific conductivity |
| K_{pit} | kg m ⁻¹ MPa ⁻¹ s ⁻¹ | Pit conductivity |
| K_p | kg m ⁻¹ MPa ⁻¹ s ⁻¹ | Potential conductivity |
| <i>Foliar traits</i> | | |
| HV | 10 ⁻⁴ m ² m ⁻² | Huber value, i.e., the sapwood-to-leaf area ratio |
| A_{leaf} | cm ² | Mean leaf size |
| SLA | cm ² g ⁻¹ | Specific leaf area |
| <i>Anatomical traits</i> | | |
| D | μm | Mean vessel diameter |
| D_h | μm | Hydraulically weighted mean vessel diameter |
| VD | n mm ⁻² | Vessel density |
| $A_{lumen} : A_{xylem}$ | % | Lumen-to-sapwood area ratio |

2.2.4 Hydraulic Conductivity

In the laboratory, stem segments were shortened under water (mean length ± SD: 307.3 ± 2.07 mm), lateral branches cut off, and scars sealed with quick-drying contact adhesive (Loctite

431 with Loctite activator SF 7452, Henkel, Düsseldorf, Germany). Segment diameters were measured twice at the basal and distal ends of the segment and four times along the segment (mean diameter \pm SD: 8.30 ± 0.79 mm). Subsequently, the bark was removed at the basal end and segments connected to the Xylem apparatus (Bronkhorst France, Montigny les Corneilles, France) to measure hydraulic conductivity (K_h ; $\text{kg m MPa}^{-1} \text{s}^{-1}$). We used filtered ($0.2 \mu\text{m}$) and degassed demineralized water mixed with 10 mM KCl and 1 mM CaCl_2 . We initially measured the actual hydraulic conductivity (K_h^{act}) at a low pressure of 6 kPa and then measured maximum hydraulic conductivity (K_h^{max}) after repetitively water-flushing the segments at a high pressure of 120 kPa for 10 min until K_h remained constant. The hydraulic conductivity and flow rate data were analyzed with the software XylWin 3.0 (Bronkhorst France, Montigny les Corneilles, France). We calculated sapwood-specific hydraulic conductivity (K_s ; $\text{kg m}^{-1} \text{MPa}^{-1} \text{s}^{-1}$) by dividing K_h^{max} with the basal sapwood cross-sectional area without pith and bark (Hajek *et al.* 2014, Schuldt *et al.* 2016). We also calculated leaf-specific hydraulic conductivity (K_L ; $\text{kg m}^{-1} \text{MPa}^{-1} \text{s}^{-1}$) by dividing K_h^{max} by the supported leaf area.

2.2.5 Vulnerability Curves

The flow-centrifuge technique (Cochard *et al.* 2005) was used to construct xylem vulnerability curves (VCs) of the same stem segments used for hydraulic conductivity measurements. The samples were shortened to a length of ca. 27 cm and the bark was removed at both ends and had a basal diameter of 7.91 ± 0.09 mm and an apical diameter of 6.57 ± 0.09 mm (mean \pm SD). The segments were then inserted into a custom-made Cavitron rotor chamber attached to a centrifuge (Cavitron device built from a Sorvall RC-5C series centrifuge, customised) and measurements were made using the Cavisoft software (Cavisoft version 5.2.1, University of Bordeaux, Bordeaux, France).

Measurements started at a xylem pressure of -0.37 MPa for *B. pendula*, and -0.83 MPa for *A. pseudoplatanus* and *S. aucuparia*. We then stepwise raised the rotation speed corresponding to 0.2 – 0.3 MPa until the percentage loss of hydraulic conductivity (PLC) reached at least 90%. By plotting PLC against xylem pressure (Ψ_x), vulnerability curves were generated for each branch. We used an exponential-sigmoidal function provided by (Pammenter and Van der Willigen 1998) to derive the Ψ_x causing 50% loss of conductivity (P_{50}):

$$\text{PLC} = 100 / (1 + \exp(s/25 \times (P_i - P_{50}))),$$

with s (% MPa⁻¹) being slope of the curve at P_{50} and P_i , the applied xylem pressure. Subsequently, the Ψ_x at 12% and 88% loss of conductivity (P_{12} and P_{88}) were obtained by following (Domec and Gartner 2003) as: $P_{12} = P_{50} - 50/s$ and $P_{88} = P_{50} + 50/s$. Values of P_{12} and P_{88} represent the thresholds of xylem tension at the onset and offset of cavitation, respectively.

2.2.6 Wood Anatomy

A sliding microtome (G.S.L.1, Schenkung Dapples, Zürich, Switzerland) was used to cut three transverse sections of 10–20 μm thickness from ethanol-stored segments. Sections were stained with safranin alcian blue (1% safranin in ethanol), rinsed with distilled water and ethanol (95%), and permanently embedded on glass slides using Euparal (Carl Roth, Karlsruhe, Germany). Slides were oven-dried at 50 °C for ten days. Complete cross-sections were digitalized at 100x magnification with a resolution of 1.33 pixels μm^{-1} using a stereo-microscope equipped with an automatic stage and a digital camera (Observer.Z1, Carl Zeiss MicroImaging GmbH, Jena, Germany; Software: AxioVision c4.8.2, Carl Zeiss MicroImaging GmbH). The digitalized images were then analyzed using GIMP (version 2.10.14) and ImageJ (Version 1.51h) for anatomical traits using the particle analysis function. The recorded parameters include sapwood area (A_{xylem} , μm^2), lumen-to-sapwood area ratio ($A_{\text{lumen}}: A_{\text{xylem}}$, %), vessel density (VD, n mm^{-2}), and vessel diameter (D , μm) from major (a) and minor (b) vessel radii using the equation (White 1991):

$$D = ((32 \times (\mathbf{a} \times \mathbf{b})^3) / (\mathbf{a}^2 + \mathbf{b}^2))^{1/4}$$

D was then used to obtain the hydraulically-weighted vessel diameter (D_h , μm) according to (Sperry *et al.* 1994) as $D_h = \Sigma D^5 / \Sigma D^4$. Standardized D_h was calculated according to (Anfodillo *et al.* 2013) as $D_h^{\text{std}} = D_h / L^b$, where L is the distance of the segment to the apex and b is the exponent constant (0.2) according to the metabolic scaling theory (West *et al.* 1999). The potential conductivity (K_P ; $\text{kg m}^{-1} \text{MPa}^{-1} \text{s}^{-1}$) was derived using the Hagen–Poiseuille equation:

$$K_P = \pi \times p \times \Sigma D^4 / (128 \times \eta \times A_{\text{xylem}}),$$

where η is the viscosity (1.002×10^{-9} MPa s) and p the density of water (998.2 kg m^{-3}), both at 20 °C, and A_{xylem} (mm^2) is the analysed sapwood area. Pit conductivity was estimated as per equation given by (Larter *et al.* 2017):

$$K_{\text{pit}} = ((1/K_S) - (1/K_P))^{-1}$$

A low K_{pit} indicates that higher resistance to water flow has to be overcome.

2.2.7 Statistical Analyses

All statistical analyses were carried out with R version 4.0.3 (R CoreTeam, 2020) in the framework of the tidyverse package (Wickham *et al.* 2019). First descriptive statistics were applied, and then data were tested for normal distribution with a Shapiro–Wilk normality test. For inferential statistics, significant differences were tested by adopting a t-test or welch test within species as per treatment basis. However, Wilcoxon test was performed if normality assumptions were not met. We also performed linear models to test the effect of predictors on target variables, e.g., effect of growth rate on hydraulic traits. We log transformed variables that did not met normality assumptions.

2.3 Results

2.3.1 Growth and Structural Differences across Species and Treatments

Because the species were monitored from seed sowing, the juvenile growth performance could be assessed in terms of shoot length and aboveground biomass increment per day (i.e., growth rate). For all species, we recorded significantly different growth-related parameters ($p < 0.001$) between the control and stressed treatment (Figure 2.2, Table S2.1). All control plants had a higher growth compared to the stressed plants. In *B. pendula*, *A. pseudoplatanus*, and *S. aucuparia*, the shoot length was smaller in the stress treatment than in the control and differed by 47%, 50%, and 33%, respectively. For the aboveground biomass increment (ABI), the differences were even more pronounced and differed on average 2.8- to 5.3-fold between the control and stress treatment, i.e., 287 mg d⁻¹ versus 61 mg d⁻¹ for *A. pseudoplatanus*, 424 mg d⁻¹ versus 79 mg d⁻¹ for *B. pendula*, and 324 mg d⁻¹ versus 117 mg d⁻¹ for *S. aucuparia* (Figure 2.2, Table S2.1).

2.3.2 Effects of Climatic Stress on Hydraulic, Wood Anatomical, and Leaf Morphological

Traits

We found significant, yet contrasting, intra-specific differences between trees grown under stressed and optimal control conditions. Notably, P_{50} was more negative (i.e., higher resistance) in stressed *S. aucuparia* compared to the control ($p < 0.01$, Figure 2.3a), while for *B. pendula*, we found that stressed plants were slightly less resistant to embolism formation ($p < 0.05$). We did not

find differences in hydraulic safety between the two groups of *A. pseudoplatanus*. Likewise, we found that hydraulic efficiency (i.e., specific conductivity, K_s) was significantly higher in optimally-grown saplings of two of the three species (Figure 2.3b; *B. pendula* and *A. pseudoplatanus*) while the last one (*S. aucuparia*) showed no significant difference (Figure 2.3b); similar trends were found for K_{pit} (Figure S2.3). These differences in hydraulic efficiency were mirrored by xylem anatomical differences between groups as we found wider vessels in controlled plants of *A. pseudoplatanus* and *B. pendula* but not in *S. aucuparia* (Figure 2.3c, Figure S2.4). Similar patterns were observed for the hydraulically-weighted vessel diameter standardized by the distance to the tip (D_h^{std} ; Table S2.1), which was highly related to D_h (Figure S2.5). However, the vessel density (VD) did not change with growing conditions in any of the species (Figure 2.3d).

We found significant differences between treatments with regards to leaf characteristics. For example, the specific leaf area (SLA) was lower in the stressed plants of *B. pendula* and *S. aucuparia* compared to the control (Figure 2.3f), but higher in stressed *A. pseudoplatanus* (Figure 2.3f). Nonetheless, both *A. pseudoplatanus* and *B. pendula* had a significantly higher Huber value (HV) when stressed (Figure 2.3e), i.e., a reduced leaf area per cross-sectional sapwood area.

2.3.3 Relationships of Hydraulic Safety-Efficiency, Leaf and Anatomical Traits with

Species Growth Performance

In our study, *S. aucuparia* was the most embolism-resistant species with a mean P_{50} of -4.05 MPa and a mean P_{88} of -5.17 MPa (Figure 2.3, Table S2.1). *A. pseudoplatanus* was found to be less resistant ($P_{50} = -3.54$ MPa, $P_{88} = -4.14$ MPa), followed by *B. pendula* ($P_{50} = -1.91$ MPa, $P_{88} = -2.14$ MPa). However, *A. pseudoplatanus* was the least sensitive species regarding the onset of cavitation ($P_{12} = -2.93$ MPa; Table S2.1). Although being vulnerable to embolism, *B. pendula* presented the highest hydraulic efficiency ($K_s = 1.40$ kg m⁻¹ MPa⁻¹ s⁻¹), followed by *S. aucuparia* (1.18 kg m⁻¹ MPa⁻¹ s⁻¹) and *A. pseudoplatanus* (0.56 kg m⁻¹ MPa⁻¹ s⁻¹). Linear regressions depicted significant associations of hydraulic safety with growth traits, although no general trend across species existed (Figure 2.4a, b). We found that P_{50} was related to log-transformed ABI in *B. pendula* ($p < 0.01$, $R^2 = 0.42$) and in *S. aucuparia* ($p < 0.05$, $R^2 = 0.32$) but not in *A. pseudoplatanus* (Figure 2.4a).

A positive relationship in *B. pendula* suggests that a higher embolism resistance was associated with a higher growth, while a negative relationship in *S. aucuparia* indicates the opposite, i.e., a low hydraulic safety was related to high growth rates. Similar trends were found between P_{50} and the shoot length (Figure 2.4b). In *B. pendula* and *A. pseudoplatanus*, we found that hydraulic conductivity (K_S) was significantly affected by growth-related parameters (*B. pendula*: $p < 0.01$, $R^2 = 0.41$ with ABI and $p < 0.001$, $R^2 = 0.50$ with shoot length; *A. pseudoplatanus*: $p < 0.05$, $R^2 = 0.35$ with ABI and $R^2 = 0.30$ with shoot length; Figure 2.4c, d). This indicates that a higher hydraulic efficiency was associated with a high juvenile growth. In *S. aucuparia*, on the other hand, K_S was not related to any of the growth-related variables investigated (Figure 2.4c, d).

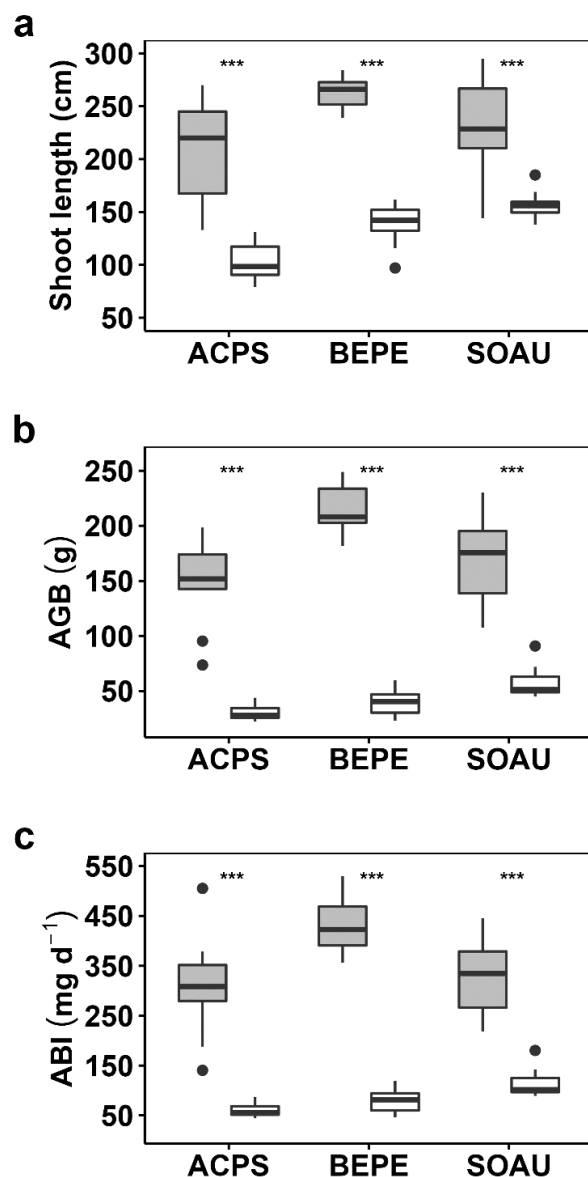


Figure 2.2: Boxplots of growth-related traits of *Acer pseudoplatanus* (ACPS), *Betula pendula* (BEPE), and *Sorbus aucuparia* (SOAU) for the control (grey) and stress (white) treatment. Presented are (a) shoot length, (b) aboveground biomass (AGB), and (c) aboveground biomass increment (ABI). Asterisks indicate the level of significance (***, $p < 0.001$; ns, for non-significant).

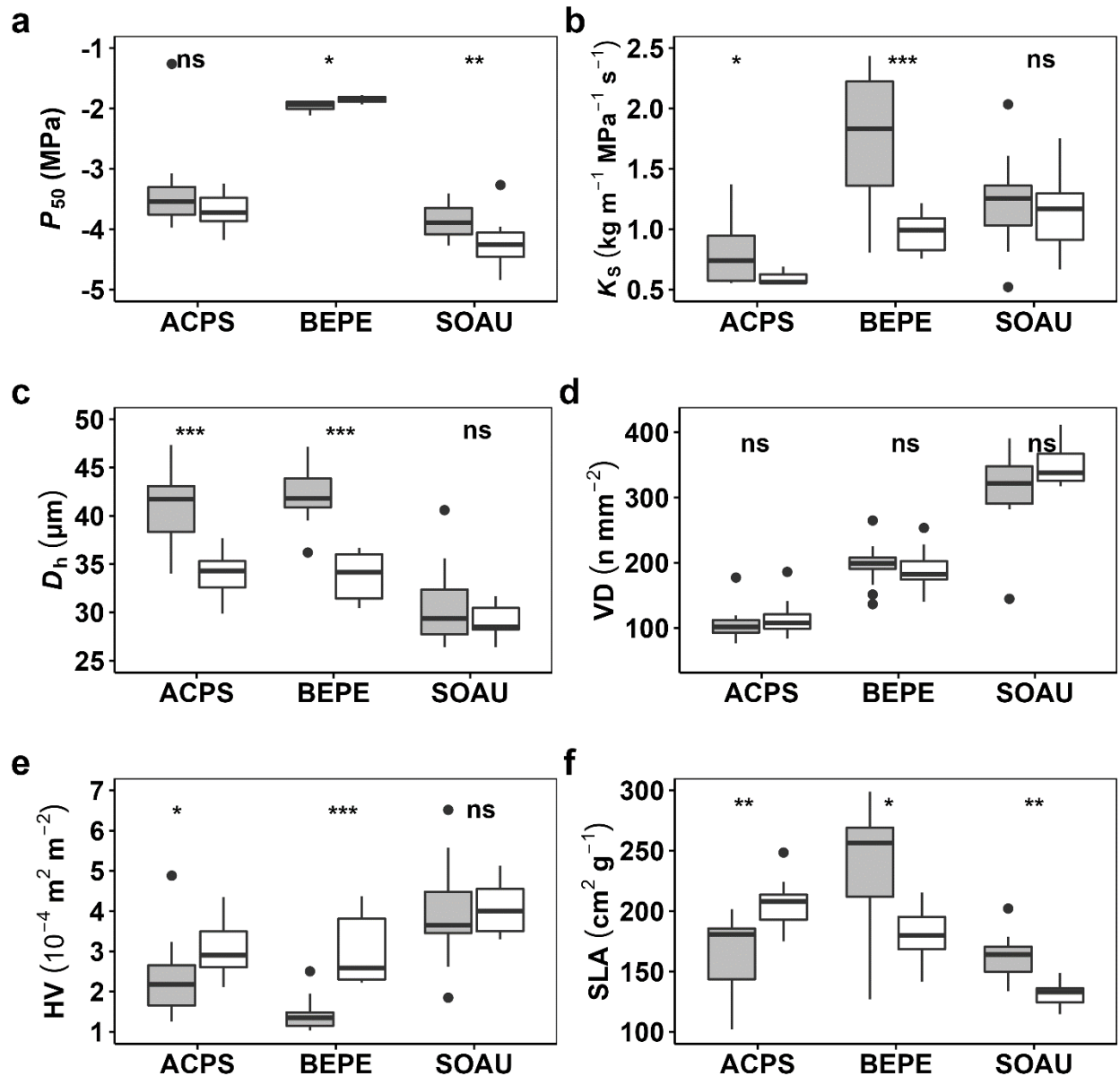


Figure 2.3: Boxplot depicting the variability between treatments for hydraulic, wood anatomical, and leaf morphological traits for the three species. Given are (a) water potential at 50% loss of hydraulic conductivity (P_{50}), (b) specific conductivity (K_s), (c) hydraulically-weighted vessel diameter (D_h), (d) vessel density (VD), (e) Huber value (HV), and (f) specific leaf area (SLA) for the control (grey) and stress (white) treatment. Asterisks indicate the level of significance (*, $p < 0.05$; **, $p < 0.01$; ***, $p < 0.001$; ns, for non-significant). For traits abbreviations, see Table 2.1.

The analysis of other hydraulic efficiency traits (K_{pit}) and anatomical traits (D_h and VD) associated with the growth rate revealed similar contrasting patterns across species (Figure 2.5). We found that a higher aboveground biomass increment (ABI) was associated with a higher K_{pit} in *A. pseudoplatanus* and *B. pendula* but not in *S. aucuparia*. Likewise, D_h was related to higher

ABI in *A. pseudoplatanus* and *B. pendula* only. VD, however, was not linked to the growth performance for any of the species (Figure 2.5c, d). We also found that leaf traits such as the HV were well related to the growth rate in the case of *A. pseudoplatanus* and *B. pendula* but not in *S. aucuparia* (Figure 2.5f). In the first two species, a lower Huber value was associated with a high growth. The SLA was always related to the ABI, although the nature of the relationship was different across species. *B. pendula* and *S. aucuparia* had a higher SLA associated with a higher growth performance, while the *A. pseudoplatanus* that performed better had a reduced SLA (Figure 2.5e).

2.3.4 Hydraulic Safety-Efficiency Trade-Offs and Their Relations to Wood Anatomy and Leaf Traits

In all three species, we found that P_{50} was unrelated to K_S , indicating the absence of any trade-off between hydraulic safety and efficiency (Figure 2.6a). As expected from the Hagen–Poiseuille equation, K_S was well related to D_h in all species (Figure 2.6c; $p < 0.01$ and $R^2 = 0.35, 0.71$ and 0.37 in *A. pseudoplatanus*, *B. pendula*, and *S. aucuparia*, respectively). More interesting was that none of the species showed the relationship between D_h and P_{50} , indicating that xylem embolism likely does not depend on vessel diameter in the investigated species of our sample (Figure 2.6b). We also found that xylem safety was associated with a higher specific leaf area (SLA) in *B. pendula* but a lower one in *S. aucuparia* (Figure S2.6).

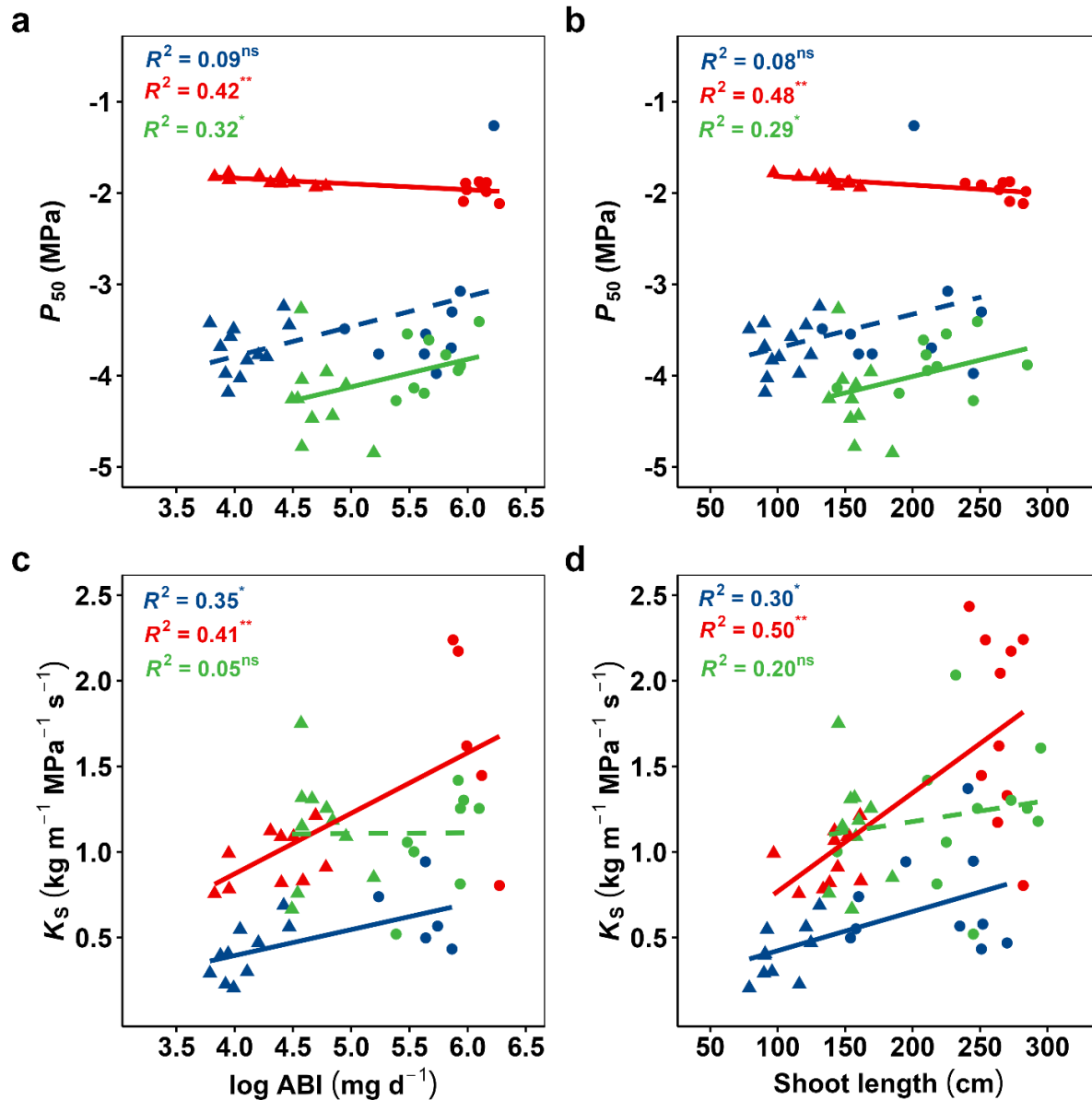


Figure 2.4: Effect of growth performance on the water potential at 50% loss of hydraulic conductivity (P_{50}) and specific conductivity (K_S). Given are linear regression analyses between (a) P_{50} or (c) K_S and log-transformed growth rate, and (b) P_{50} or (d) K_S and shoot length. Indicated for each species are the coefficients of determination, *i.e.*, R^2 , for the investigated relationships. Different colours and symbols represent different species and treatments (blue: *A. pseudoplatanus*; red: *B. pendula*; green: *S. aucuparia*; filled circles: control treatment; triangles: stress treatment). Full lines indicate significant effects of variable x on variable y; dashed lines indicate a non-significant relationship. Asterisks indicate the level of significance (*, $p < 0.05$; **, $p < 0.01$; ns, for non-significant).

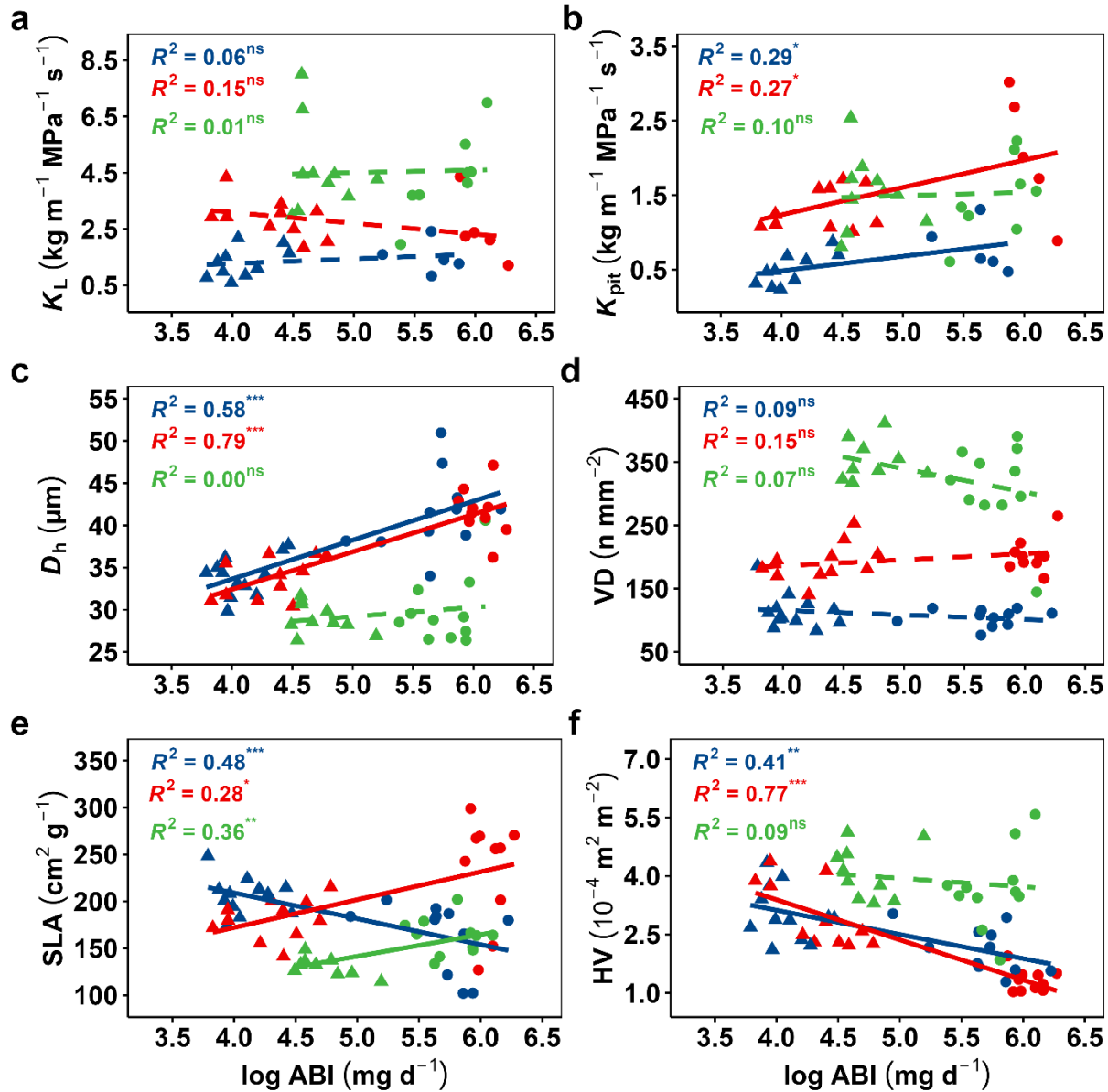


Figure 2.5: Dependency of growth rate on wood anatomical and leaf morphological traits. Given are linear regression analyses of log-transformed growth rate against (a) leaf-specific conductivity (K_L), (b) pit conductivity (K_{pit}), (c) hydraulically-weighted vessel diameter (D_h), (d) vessel density (VD), (e) specific leaf area (SLA), and (f) Huber value (HV). Different colours and symbols represent different species and treatments (blue: *A. pseudoplatanus*; red: *B. pendula*; green: *S. aucuparia*; filled circles: control treatment; triangles: stress treatment). Indicated for each species are the coefficients of determination, i.e., R^2 , for the investigated relationships. Full lines indicate significant effects of variable x on variable y; dashed lines indicate a non-significant relationship. Asterisks indicate the level of significance (*, $p < 0.05$; **, $p < 0.01$; ***, $p < 0.001$; ns, for non-significant).

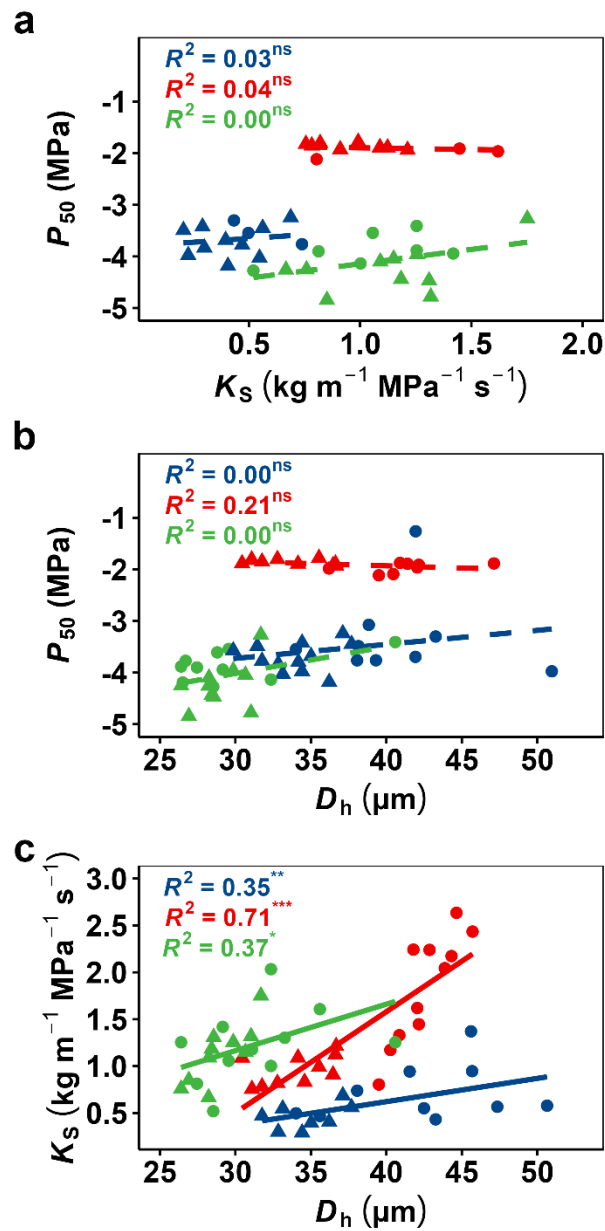


Figure 2.6: Water potential at 50% loss of hydraulic conductivity (P_{50}) in relation to (a) specific conductivity (K_s) and (b) hydraulically-weighted vessel diameter (D_h), as well as (c) specific conductivity (K_s) in relation to hydraulically-weighted vessel diameter (D_h). The results from the linear regression analyses are given. Different colours and symbols represent different species and treatments (blue: *A. pseudoplatanus*; red: *B. pendula*; green: *S. aucuparia*; filled circles: control treatment; triangles: stress treatment). Indicated for each species are the coefficients of determination, i.e., R^2 , for the investigated relationships. Full lines indicate significant effects of variable x on variable y; dashed lines indicate a non-significant relationship. Asterisks indicate the level of significance (*, $p < 0.05$; **, $p < 0.01$; ***, $p < 0.001$; ns, for non-significant).

2.4 Discussion

2.4.1 Relationship of Juvenile Growth with Hydraulic Safety and Efficiency

In our study, significant growth rate and biomass allocation differences were observed for all three species in contrasting growing conditions. We found that juvenile growth was related to either or both hydraulic efficiency and safety in all species. This might suggest a close dependency of juvenile growth on xylem characteristics, but the nature of these relationships contrasted across species. While the growth rate (aboveground biomass increment and shoot length) was negatively related to the xylem pressure at 50 % loss of hydraulic conductivity (P_{50}) in *B. pendula*, no clear pattern emerged as a positive relationship was found in the case of *S. aucuparia*. However, growth performance was notably associated to a higher hydraulic efficiency in two of the three species, most likely through an increase in hydraulically-weighted vessel diameter (D_h), which was strongly and positively related to sapwood-specific hydraulic conductivity (K_s). In *B. pendula* and *A. pseudoplatanus*, two species with an isohydric water potential regulation strategy (Leuschner *et al.* 2019, Beikircher *et al.* 2021, and Kumar *et al.* unpublished), efficiency-related variables (e.g., D_h and K_s) were associated with higher growth. This is consistent with earlier intra- and inter-specific studies reporting a close association of growth biomass increment to hydraulic efficiency rather than to other wood traits (Hajek *et al.* 2014, Hoerber *et al.* 2014, Kotowska *et al.* 2015, Kotowska *et al.* 2021). However, the growth performance was decoupled from hydraulic efficiency in *S. aucuparia*. This was the only species following a rather anisohydric water potential regulation strategy in our study (Vogt 2001, and Kumar *et al.* unpublished).

In the case of *A. pseudoplatanus*, which has large leaves with a high conductance but a stringent control of its stomates, only hydraulic efficiency and not safety was related to the growth performance. Although *B. pendula* likewise follows an isohydric strategy, a lower embolism resistance was found in stressed individuals with a lower growth performance. In *B. pendula*, no intra-specific variation in P_{50} has been observed at various stands across Europe, strongly differing in microclimatic conditions (González-Muñoz *et al.* 2018). Consequently, we likewise observed a marginal increase in P_{50} by 0.11 MPa only in *B. pendula*, but counterintuitively plants in the control group developed a slightly more embolism-resistant xylem ($P_{50} = -1.97$ MPa versus -1.86 MPa, respectively). This might explain why hydraulic safety counterintuitively was negatively, and not positively, related to growth as hypothesized. In the case of *S. aucuparia*, the most

embolism-resistant species with the least stringent stomatal control, we found that hydraulic safety was positively associated with growth as speculated, i.e., fast-growing individuals developed a less embolism-resistant xylem ($P_{50} = -3.87$ MPa versus -4.24 MPa in the control versus the stress treatment, respectively). The disparities in the growth–hydraulic safety trade-off between species observed here was also reported in previous studies. While a negative relationship was found for willow genotypes (Wikberg and Ögren 2004, Cochard *et al.* 2007) and provenances of cedar (Ducrey *et al.* 2008), a positive relationship was reported for poplar hybrids (Fichot *et al.* 2010) and European beech (Herbette *et al.* 2020), and other studies did not find any link at all (Sterck *et al.* 2012, Hajek *et al.* 2014, Guet *et al.* 2015, Schuldt *et al.* 2016, Schumann *et al.* 2019).

Contrasting results across studies suggest that relationships between growth performance and hydraulic safety, but also efficiency, do not necessarily present a general trend across species but may be linked to species-specific hydraulic strategies (Hartmann *et al.* 2021).

2.4.2 Relationship of Juvenile Growth with Leaf-Related Traits

Leaf traits are often used as an indicator of plant growth performance since they are responsive to the local environment (Chaturvedi *et al.* 2013, Weithmann *et al.* 2022). For example, the specific leaf area (SLA) is often assumed to be a central trait under species-selection, and species with large and thin but short-lived leaves tend to have a resource-acquisition strategy based on a quick return on leaf investments (Markesteyn *et al.* 2011, Schreiber *et al.* 2016). In this study, we found the SLA to be linked to growth performance, but once more without revealing any clear trend. While we found that a reduction of SLA was associated with a higher growth performance in *A. pseudoplatanus*, the opposite was found in the other two species. In our study, stressed individuals of *A. pseudoplatanus* developed larger and/or lighter leaves compared to the control, although the opposite relationship is usually associated with environmental stress (Cunningham *et al.* 1999, Wright *et al.* 2004).

We also found that two of the three species, namely *A. pseudoplatanus* and *B. pendula*, had Huber values (HV), i.e., the sapwood-to-leaf area ratios, that decreased with the growth performance as one would expect. While the third species, *S. aucuparia*, showed the same tendency, this relationship was non-significant. Thus, all species of our sample adjusted their leaf-level water supply in response to more stressful climatic conditions by reducing the size of single leaves (Table S2.1), and potentially their numbers. Our results suggest that all three foliar traits

covered are highly plastic and responsive to climatic stress conditions, consistent with studies reporting that leaf traits respond to gradients of water availability (Gleason *et al.* 2012, Weithmann *et al.* 2022).

2.4.3 Trade-Off between Hydraulic Efficiency and Safety and Anatomic Determinants

In agreement with a growing body of evidence, we did not find any relationship between the hydraulic safety and efficiency across the three species of our sample (cf. Larter *et al.* 2017, Torres-Ruiz *et al.* 2017, Lübbe *et al.* 2022 but see Schumann *et al.* 2019). Although we only investigated siblings originating from the same parental tree, our results support the assumption that different evolutionary pathways exist for achieving xylem safety and efficiency, and that the safety–efficiency trade-off may be species- and scale-dependent (Isasa *et al.* 2021, Lübbe *et al.* 2022). Furthermore, hydraulic safety appears to be a rather conservative trait in temperate broad-leaved tree species (cf. Rosas *et al.* 2019, Fuchs *et al.* 2021), while hydraulic efficiency is more plastic in order to meet the water demand of the supported foliage at the place of growth.

Therefore, the majority of recent results support a divergence from the classical paradigm of plant hydraulics, postulating that plant hydraulic functioning is dependent on a trade-off between xylem safety and efficiency (Tyree *et al.* 1994). It is evident that some species might have both a low safety and a low efficiency, which means that the anatomical basis for a high efficiency could be trading off with traits other than embolism resistance (Gleason *et al.* 2016). Hence, a question arises on the significance of given anatomical features that play a role. On that matter, the vessel diameter was initially proposed as the primary anatomical determinant of the safety–efficiency trade-off since vessel conductivity increases in the proportion of its diameter at the fourth power according to the Hagen–Poiseuille equation (Tyree and Zimmermann 2002). This is supported by our study, as D_h was related to K_S in all three species. However, it seems that vessel diameter is not universally linked to embolism resistance. While several studies observed a dependency of P_{50} on D_h within or across species (Hacke *et al.* 2006, Maherali *et al.* 2006, Awad *et al.* 2010, Sterck *et al.* 2012, Hajek *et al.* 2014), others could not (Choat *et al.* 2008, Fichot *et al.* 2010, Lens *et al.* 2011, Schuldt *et al.* 2016, Hajek *et al.* 2016). It is meanwhile well-established that embolism resistance is only indirectly related to vessel diameter through an increased number of interconnected vessels, while it is directly related to pit membrane thickness (Kaack *et al.* 2021). Thus, the focus has shifted from conduit diameter to inter-vessel transport and pit membrane

characteristics such as pore size and membrane thickness for determining embolism resistance. Further work is needed to shed light on these controversies.

2.4.4 Variability in Hydraulic and Foliar Traits in Response to Environmental Stress

As shown and discussed, the three species exhibited significant differences in their hydraulic and leaf functional attributes between both treatments. Because genetic material was similar within a species, those differences can be imputed to a plastic response of the plants to heat stress. Knowledge of the degree of phenotypic plasticity of given traits is essential to better understand tree responses to climate change. In *B. pendula*, the highest degree of variability was found. Here, 14 of the 17 growth-related, wood anatomical, hydraulic, and leaf morphological traits differed between treatments, while only six differed in the case of *S. aucuparia* (Table S2.1). Although stressed plants of *S. aucuparia* developed a more embolism-resistant xylem, other traits such as hydraulic efficiency and its main anatomical determinant, vessel diameter, were unaffected by the growing conditions. Because *S. aucuparia* relies on its high resistance to embolism to survive drought, this might explain why mainly xylem safety responded plastically. In *B. pendula*, on the other hand, both embolism resistance and specific conductivity decreased in stressed plants. This was associated with a reduction in the vessel diameter, and this effect remained even after standardizing for the distance to the tip (Table S2.1). Altogether, this matches the expected growth strategy of this pioneer tree species. In *A. pseudoplatanus*, we found a strong reduction of hydraulic conductivity and vessel diameter but not xylem safety. This species seems to have a stringent stomatal control (Kumar *et al.* unpublished) associated with a fairly embolism-resistant xylem.

2.5 Conclusions

This study on the association of juvenile growth with xylem safety and efficiency revealed considerable inter-specific differences. The distinguishable relationships across species could be related to their habitat preferences and ecological strategies. We found species-specific links between growth performances and hydraulic safety and efficiency in two of the tree species but without revealing any clear pattern. The safety-related traits appeared more static, while efficiency traits revealed a higher intra-specific plasticity. In all species, the hydraulic efficiency was strongly dependent on vessel diameter but was unrelated to xylem safety.

Overall, understanding the links among hydraulic traits and their specific association with juvenile growth performance during stress is necessary to understand plant behaviour in a warmer and drier environment and to improve breeding programs.

Funding: This work was financially supported by the Indian Council of Agricultural Research (ICAR), New Delhi, India, through the Netaji Subhash-ICAR International Fellowship granted to Manish Kumar (F.No.: 18(20)/2018-EQR/Edn).

Acknowledgments: This publication was supported by the Open Access Publication Fund of the University of Würzburg. The first author gratefully acknowledges the financial support provided by the Indian Council of Agricultural Research (ICAR), New Delhi, India, through the Netaji Subhash-ICAR International Fellowship for his doctoral programme. The logistical and scientific assistance received from the University of Würzburg, Germany, is gratefully acknowledged. Additionally, we thank Roman Mathias Link for his guidance with statistical analysis. Special thanks to Christine Gernert and Yvonne Heppenstiel for their skillful support in preparing transverse sections and microscopic work for wood anatomy, and to Jutta Winkler-Steinbeck for taking care of the plants.

Supplementary information

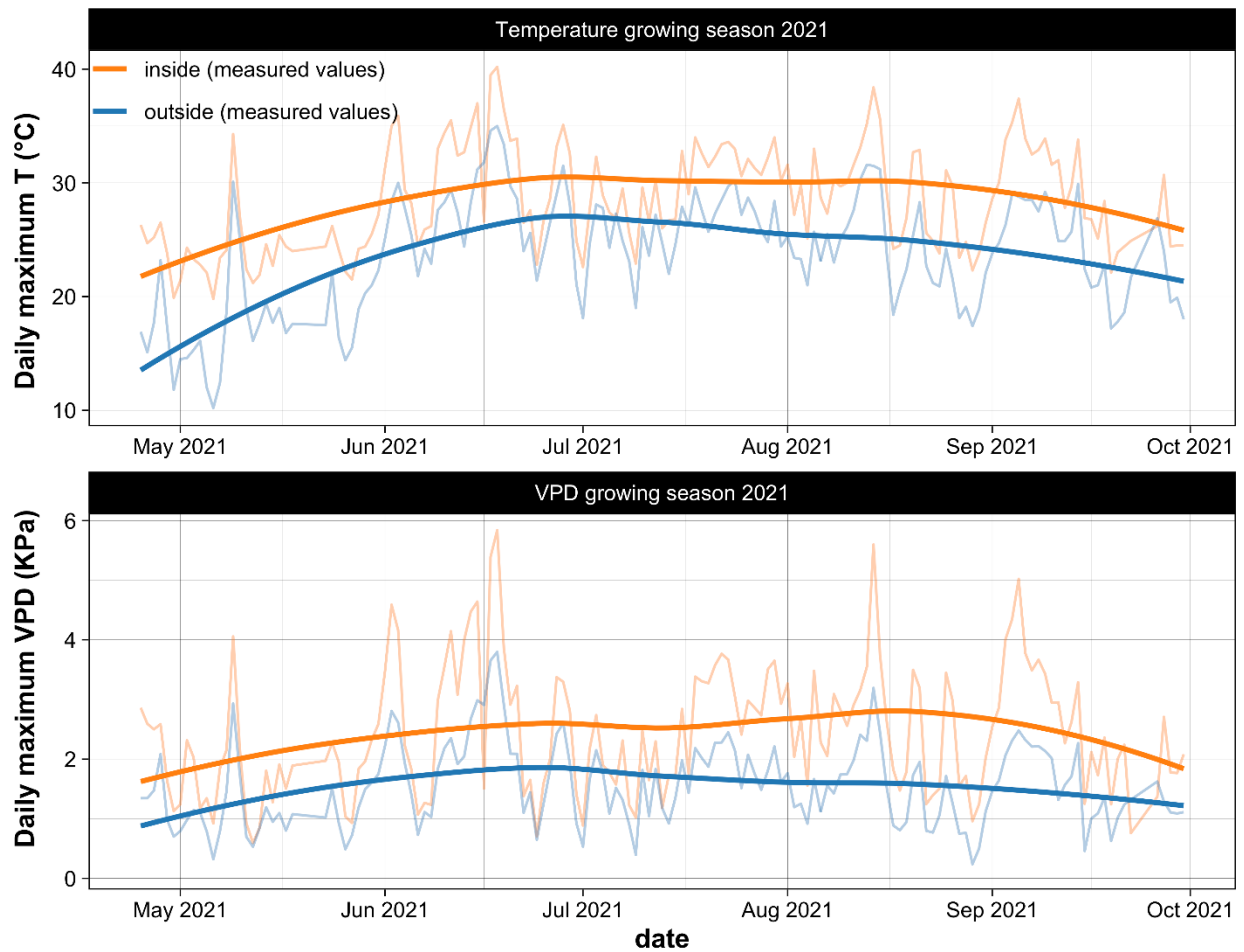


Figure S2.1: Measured daily maximum temperature (top) and daily maximum vapour pressure deficit (bottom) for the growing season from May to September in 2022. The blue line refers to open-field (outside) measurements, and the orange line to measurements inside the growing chamber of the greenhouse.

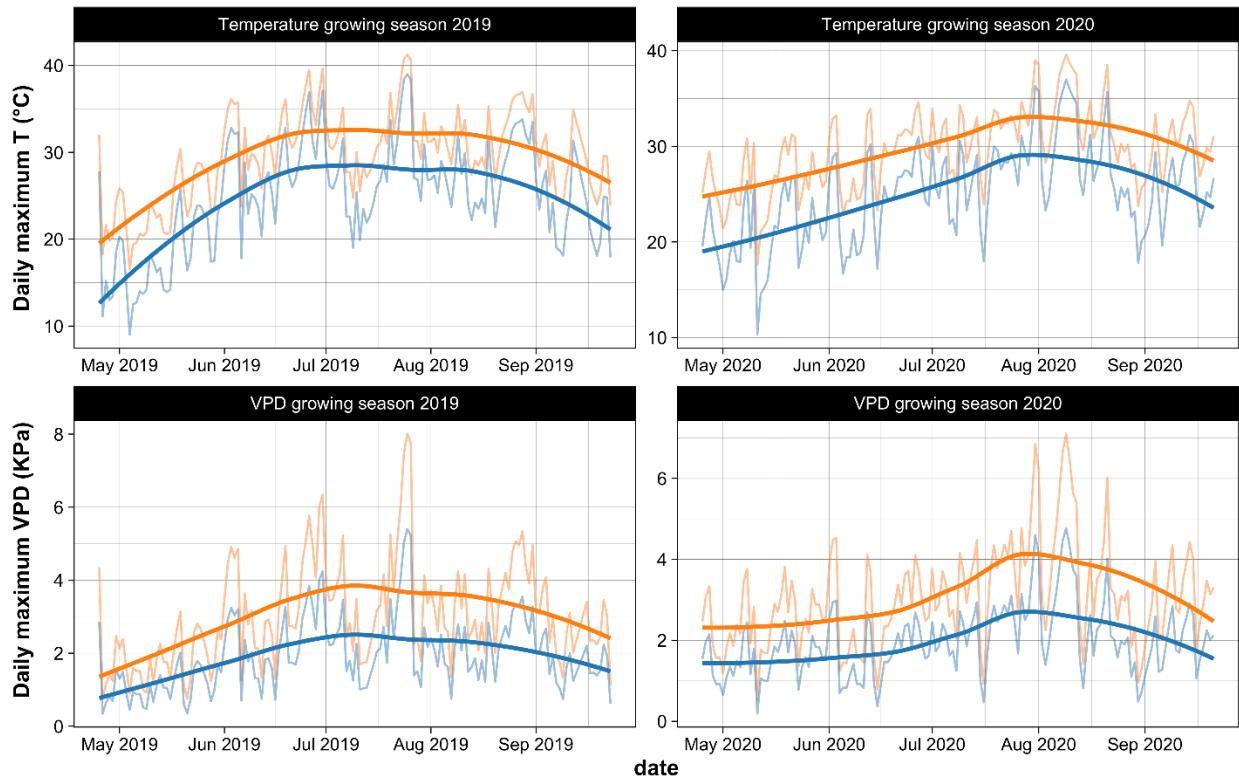


Figure S2.2: Daily maximum temperature (top) and daily maximum vapour pressure deficit (bottom) for the growing season from May to September in 2019 and 2020. The blue line refers to open-field (outside) measurements, and the orange line to measurements inside the growing chamber of the greenhouse. Please note that only the outside values have been empirically measured, inside values were modelled according to available data from 2022 (Figure S2.1).

Table S2.1: Summary of all major variables explored (means \pm SE). The number of investigated plants is given in parentheses. Species abbreviations are as follows: ACPS: *A. pseudoplatanus*; BEPE: *B. pendula*; SOAU: *S. aucuparia*; the treatment is indicated by C for control or S for stress. Small letters indicate significant differences between the control and stress treatment within a given species. For details on the abbreviations, please refer to Table 2.1.

| Variables | Unit | ACPS_C | ACPS_S | BEPE_C | BEPE_S | SOAU_C | SOAU_S |
|--|---|--------------------------------------|-------------------------------------|--------------------------------------|-------------------------------------|--------------------------------------|--------------------------------------|
| Growth-related traits | | | | | | | |
| RCD | mm | 17.31 \pm 0.38 ^a (16) | 10.59 \pm 0.20 ^b (12) | 20.75 \pm 0.42 ^a (18) | 11.39 \pm 0.38 ^b (12) | 19.50 \pm 0.54 ^a (14) | 11.671 \pm 0.27 ^b (10) |
| Shoot length | cm | 209.38 \pm 10.71 ^a (16) | 103.42 \pm 4.80 ^b (12) | 264.11 \pm 3.42 ^a (18) | 139.11 \pm 5.41 ^b (12) | 234.07 \pm 11.44 ^a (14) | 156.90 \pm 4.13 ^b (10) |
| AGB | g | 158.56 \pm 15.30 ^a (11) | 30.58 \pm 2.02 ^b (12) | 222.39 \pm 9.16 ^a (10) | 39.58 \pm 3.61 ^b (11) | 168.30 \pm 11.63 ^a (11) | 58.00 \pm 4.54 ^b (10) |
| ABI | mg d ⁻¹ | 287.07 \pm 23.39 ^a (10) | 60.72 \pm 3.99 ^b (12) | 424.22 \pm 18.65 ^a (9) | 79.28 \pm 7.25 ^b (11) | 323.97 \pm 19.69 ^a (9) | 116.95 \pm 9.81 ^b (9) |
| Branch-related traits | | | | | | | |
| A _{leaf} | cm ² | 35.56 \pm 2.53 ^a (11) | 30.87 \pm 1.85 ^a (12) | 31.72 \pm 4.53 ^a (10) | 9.15 \pm 0.73 ^b (11) | 46.64 \pm 2.43 ^a (11) | 44.38 \pm 6.45 ^a (10) |
| HV | 10 ⁻⁴ m ² m ⁻² | 2.32 \pm 0.23 ^a (16) | 3.04 \pm 0.20 ^b (12) | 1.42 \pm 0.09 ^a (17) | 3.01 \pm 0.25 ^b (11) | 3.91 \pm 0.32 ^a (14) | 4.10 \pm 0.21 ^a (10) |
| SLA | cm ² g ⁻¹ | 163.77 \pm 11.09 ^a (11) | 205.92 \pm 5.72 ^b (12) | 234.31 \pm 17.71 ^a (10) | 180.91 \pm 6.49 ^b (11) | 162.64 \pm 5.75 ^a (11) | 131.15 \pm 3.02 ^b (10) |
| Wood Anatomical traits | | | | | | | |
| D | μm | 33.93 \pm 1.01 ^a (16) | 27.12 \pm 0.46 ^b (12) | 32.35 \pm 0.43 ^a (17) | 26.83 \pm 0.41 ^b (11) | 26.07 \pm 0.86 ^a (14) | 25.56 \pm 0.53 ^a (10) |
| D _h | μm | 42.21 \pm 1.23 ^a (16) | 34.01 \pm 0.68 ^b (12) | 42.06 \pm 0.62 ^a (17) | 33.74 \pm 0.73 ^b (11) | 30.60 \pm 1.07 ^a (14) | 29.00 \pm 0.55 ^a (10) |
| D _h ^{std} | μm | 41.50 \pm 1.36 ^a (16) | 34.67 \pm 0.72 ^b (12) | 40.18 \pm 0.63 ^a (17) | 31.86 \pm 0.74 ^b (11) | 30.21 \pm 1.18 ^a (14) | 28.08 \pm 0.55 ^a (10) |
| VD | n mm ⁻² | 105.21 \pm 5.84 ^a (16) | 114.67 \pm 8.00 ^a (12) | 196.86 \pm 6.97 ^a (17) | 191.39 \pm 9.18 ^a (11) | 323.30 \pm 19.84 ^a (14) | 349.37 \pm 10.19 ^a (10) |
| A _{lumen} :A _{xylem} | % | 10.64 \pm 0.85 ^a (16) | 7.33 \pm 0.56 ^b (12) | 18.38 \pm 0.69 ^a (17) | 12.07 \pm 0.66 ^b (11) | 18.15 \pm 1.11 ^a (14) | 18.93 \pm 0.65 ^a (10) |
| Hydraulic traits | | | | | | | |
| P ₁₂ | MPa | -2.79 \pm 0.21 ^a (9) | -3.04 \pm 0.12 ^a (12) | -1.71 \pm 0.04 ^a (8) | -1.64 \pm 0.02 ^a (10) | -2.70 \pm 0.09 ^a (10) | -3.17 \pm 0.23 ^b (10) |
| P ₅₀ | MPa | -3.32 \pm 0.27 ^a (9) | -3.70 \pm 0.08 ^a (12) | -1.97 \pm 0.03 ^a (8) | -1.86 \pm 0.02 ^b (10) | -3.87 \pm 0.09 ^a (10) | -4.24 \pm 0.14 ^b (10) |
| P ₈₈ | MPa | -3.85 \pm 0.34 ^a (9) | -4.37 \pm 0.08 ^a (12) | -2.22 \pm 0.03 ^a (8) | -2.08 \pm 0.03 ^b (10) | -5.04 \pm 0.12 ^a (10) | -5.31 \pm 0.10 ^a (10) |
| K _S | kg m ⁻¹ MPa ⁻¹ s ⁻¹ | 0.71 \pm 0.09 ^a (10) | 0.41 \pm 0.05 ^b (10) | 1.83 \pm 0.18 ^a (11) | 0.97 \pm 0.05 ^b (11) | 1.22 \pm 0.12 ^a (11) | 1.13 \pm 0.10 ^a (10) |
| K _L | 10 ⁻⁴ kg m ⁻¹ MPa ⁻¹ s ⁻¹ | 1.76 \pm 0.24 ^a (10) | 1.31 \pm 0.17 ^a (10) | 2.87 \pm 0.38 ^a (11) | 2.88 \pm 0.22 ^a (10) | 5.21 \pm 0.67 ^a (11) | 4.63 \pm 0.50 ^a (10) |
| K _{pit} | kg m ⁻¹ MPa ⁻¹ s ⁻¹ | 0.85 \pm 0.11 ^a (10) | 0.50 \pm 0.07 ^b (10) | 2.41 \pm 0.28 ^a (11) | 1.32 \pm 0.09 ^b (10) | 1.66 \pm 0.20 ^a (11) | 1.53 \pm 0.16 ^a (10) |
| K _p | kg m ⁻¹ MPa ⁻¹ s ⁻¹ | 5.39 \pm 0.68 ^a (16) | 2.25 \pm 0.21 ^b (12) | 8.50 \pm 0.47 ^a (17) | 3.60 \pm 0.29 ^b (11) | 4.83 \pm 0.47 ^a (14) | 4.56 \pm 0.30 ^a (10) |

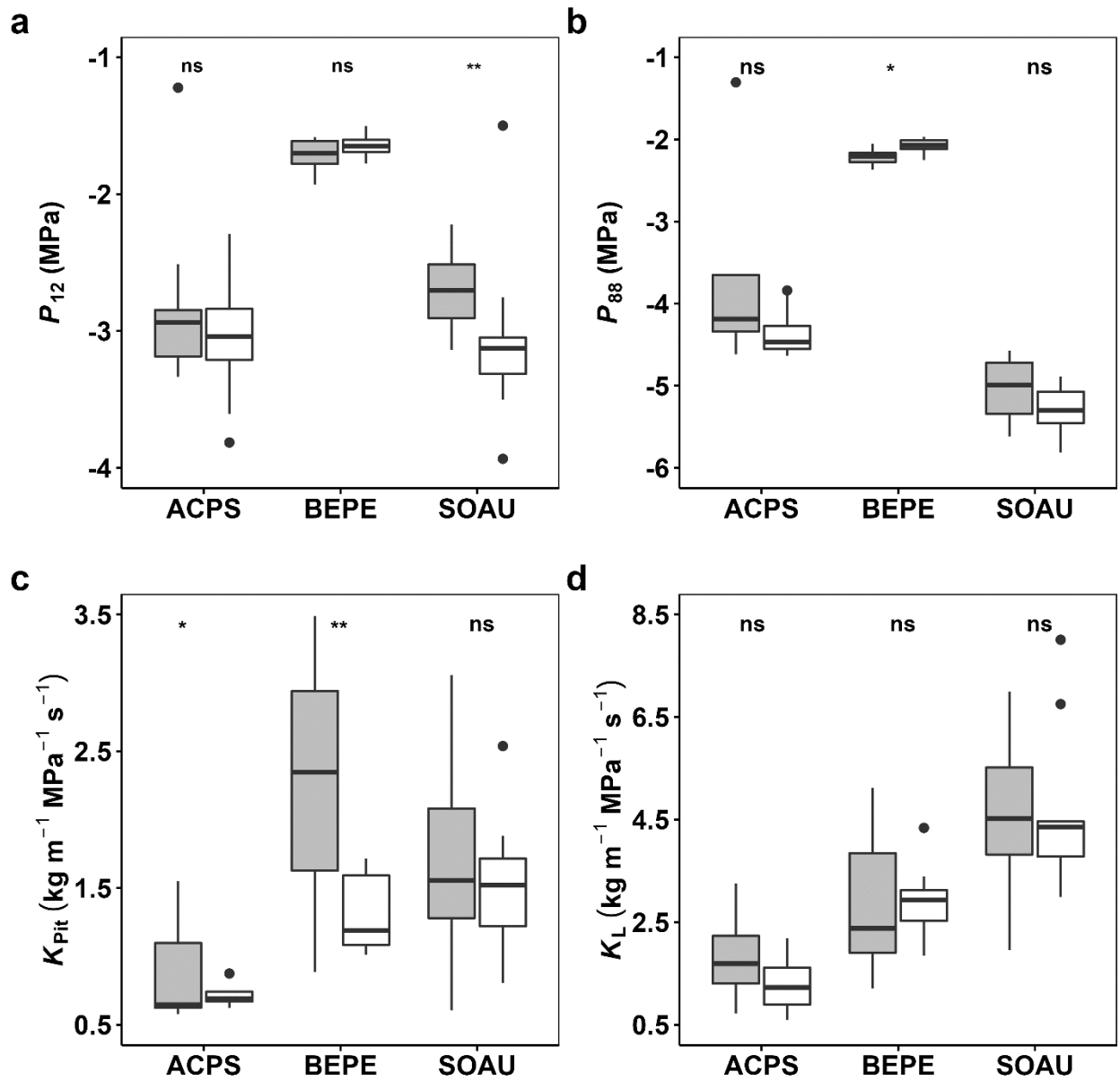


Figure S2.3: Boxplot depicting the plasticity of additional safety - efficiency traits for three tree species. Given are (a) water potential at 12 % loss of hydraulic conductivity (P_{12}), (b) water potential at 88 % loss of hydraulic conductivity (P_{88}), (c) pit conductivity (K_{pit}), (d) leaf specific conductivity (K_L) for the control (grey) and stress (white) treatment. Asterisks indicate the level of significance (*, $p < 0.05$; **, $p < 0.001$; ns, for non-significant). For species abbreviation, see Figure 2.2.

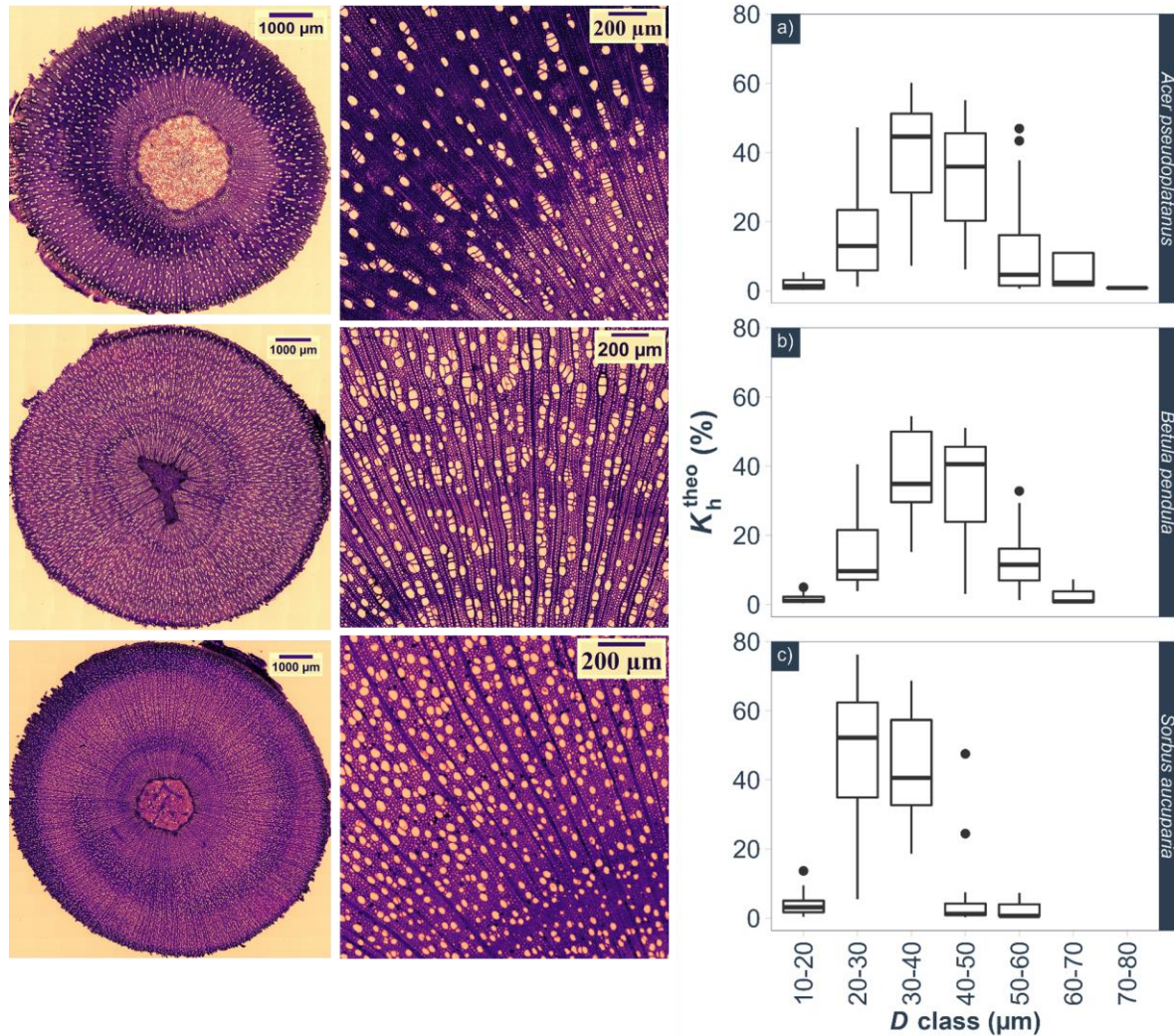


Figure S2.4: In the left column, exemplary cross-sectional images of the stem wood of (top) *A. pseudoplatanus*, (middle), *B. pendula* and (bottom) *S. aucuparia* are given. In the central column, sections of sapwood at 5-fold magnification are shown. The right column, i.e., boxplot depicting shows the contribution of seven vessel size classes (10-80 μm) to K_h^{theo} for the three tree species. Given are (a) *A. pseudoplatanus*, (b) *B. pendula*, and (c) *S. aucuparia*. Scales are indicated in each picture.

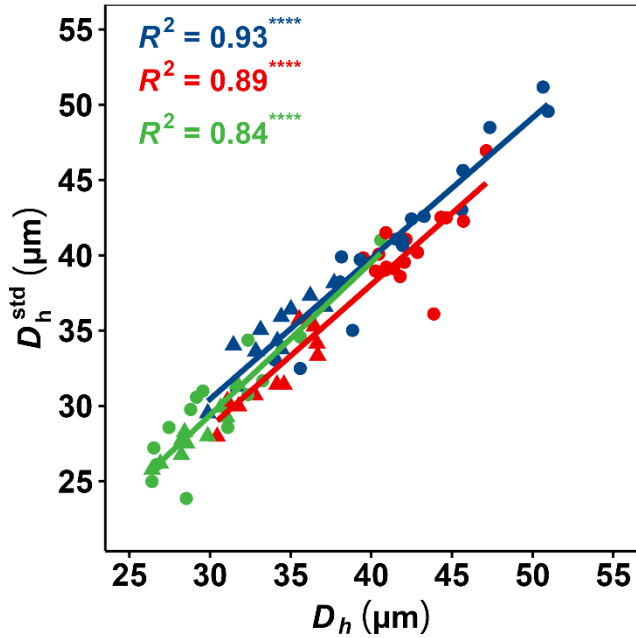


Figure S2.5: Standardized vessel diameter (D_h^{std}) in relation to hydraulically-weighted vessel diameter (D_h). The results from the linear regression analyses are given. Different colours and symbols represent different species and treatments (blue: *A. pseudoplatanus*; red: *B. pendula*; green: *S. aucuparia*; filled circles: control treatment; triangles: stress treatment). Indicated for each species are the coefficients of determination, i.e., R^2 , for the investigated relationships. Asterisks indicate the level of significance (*, $p < 0.05$; **, $p < 0.01$; ***, $p < 0.001$; ns, for non-significant).

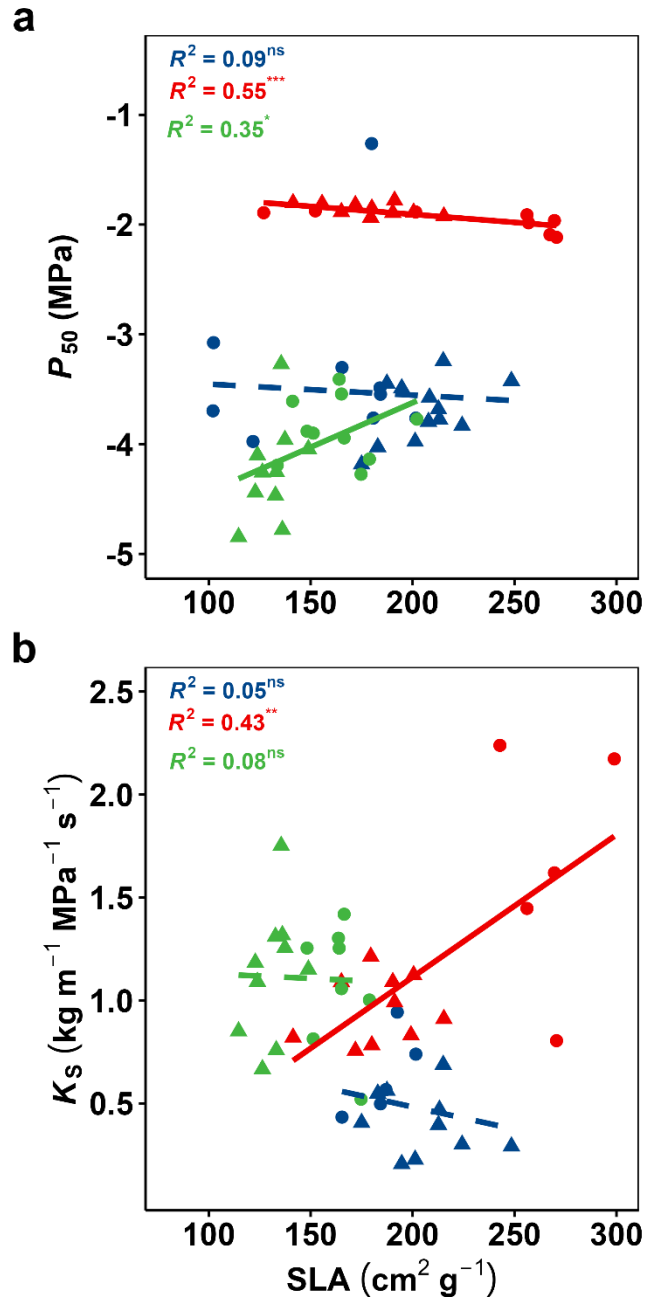


Figure S2.6: Water potential at 50% loss of hydraulic conductivity (P_{50}) in relation to (a) specific leaf area (SLA) and (b) specific conductivity (K_s) in relation to SLA. The results from the linear regression analyses are given. Different colours and symbols represent different species and treatments (blue: *A. pseudoplatanus*; red: *B. pendula*; green: *S. aucuparia*; filled circles: control treatment; triangles: stress treatment). Indicated for each species are the coefficients of determination, i.e., R^2 , for the investigated relationships. Full lines indicate significant effects of variable x on variable y; Dashed lines indicate a non-significant relationship. Asterisks indicate the level of significance (*, $p < 0.05$; **, $p < 0.01$; ***, $p < 0.001$; ns, for non-significant).

References:

- Anfodillo T, Petit G, Crivellaro A (2013) Axial conduit widening in woody species: a still neglected anatomical pattern. *IAWA Journal* 34:352–364.
- Awad H, Barigah T, Badel E, Cochard H, Herbette S (2010) Poplar vulnerability to xylem cavitation acclimates to drier soil conditions. *Physiologia Plantarum* 139:280–288.
- Beikircher B, Sack L, Ganthaler A, Losso A, Mayr S (2021) Hydraulic-stomatal coordination in tree seedlings: tight correlation across environments and ontogeny in *Acer pseudoplatanus*. *New Phytologist* 232:1297–1310.
- Britton TG, Brodribb TJ, Richards SA, Ridley C, Hovenden MJ (2022) Canopy damage during a natural drought depends on species identity, physiology and stand composition. *New Phytologist* 233:2058–2070.
- Brodribb TJ (2009) Xylem hydraulic physiology: The functional backbone of terrestrial plant productivity. *Plant Science* 177:245–251.
- Chaturvedi RK, Raghubanshi AS, Singh JS (2013) Growth of tree seedlings in a tropical dry forest in relation to soil moisture and leaf traits. *Journal of Plant Ecology* 6:158–170.
- Choat B, Brodribb TJ, Brodersen CR, Duursma RA, López R, Medlyn BE (2018) Triggers of tree mortality under drought. *Nature* 558:531–539.
- Choat B, Cobb AR, Jansen S (2008) Structure and function of bordered pits: new discoveries and impacts on whole-plant hydraulic function. *New Phytologist* 177:608–626.
- Choat B, Jansen S, Brodribb TJ, Cochard H, Delzon S, Bhaskar R, Bucci SJ, Feild TS, Gleason SM, Hacke UG, Jacobsen AL, Lens F, Maherali H, Martínez-Vilalta J, Mayr S, Mencuccini M, Mitchell PJ, Nardini A, Pittermann J, Pratt RB, Sperry JS, Westoby M, Wright IJ, Zanne AE (2012) Global convergence in the vulnerability of forests to drought. *Nature* 491:752–755.
- Clark JS, Iverson L, Woodall CW, Allen CD, Bell DM, Bragg DC, D’Amato AW, Davis FW, Hersh MH, Ibanez I, Jackson ST, Matthews S, Pederson N, Peters M, Schwartz MW, Waring KM, Zimmermann NE (2016) The impacts of increasing drought on forest dynamics, structure, and biodiversity in the United States. *Global Change Biology* 22:2329–2352.
- Cochard H, Casella E, Mencuccini M (2007) Xylem vulnerability to cavitation varies among poplar and willow clones and correlates with yield. *Tree Physiology* 27:1761–1767.
- Cochard H, Damour G, Bodet C, Tharwat I, Poirier M, Améglio T (2005) Evaluation of a new centrifuge technique for rapid generation of xylem vulnerability curves. *Physiologia Plantarum* 124:410–418.
- Cunningham SA, Summerhayes B, Westoby M (1999) Evolutionary divergences in leaf structure and chemistry, comparing rainfall and soil nutrient gradients. *Ecological Monographs* 69:569–588.

- Domec J, King JS, Noormets A, Treasure E, Gavazzi MJ, Sun G, McNulty SG (2010) Hydraulic redistribution of soil water by roots affects whole-stand evapotranspiration and net ecosystem carbon exchange. *New Phytologist* 187:171–183.
- Domec J-C, Gartner BL (2003) Relationship between growth rates and xylem hydraulic characteristics in young, mature and old-growth ponderosa pine trees. *Plant, Cell & Environment* 26:471–483.
- Ducrey M, Huc R, Ladjal M, Guehl J-M (2008) Variability in growth, carbon isotope composition, leaf gas exchange and hydraulic traits in the eastern Mediterranean cedars *Cedrus libani* and *C. brevifolia*. *Tree Physiology* 28:689–701.
- Duursma RA, Blackman CJ, Lopéz R, Martin-StPaul NK, Cochard H, Medlyn BE (2019) On the minimum leaf conductance: its role in models of plant water use, and ecological and environmental controls. *New Phytologist* 221:693–705.
- Ellenberg H, Leuschner C (2010) Vegetation Mitteleuropas mit den Alpen. In *Ökologischer, Dynamischer und Historischer Sicht*, Utb GmbH: Stuttgart, Germany.
- Eller CB, de V. Barros F, R.L. Bittencourt P, Rowland L, Mencuccini M, S. Oliveira R (2018) Xylem hydraulic safety and construction costs determine tropical tree growth. *Plant, Cell & Environment* 41:548–562.
- Eziz A, Yan Z, Tian D, Han W, Tang Z, Fang J (2017) Drought effect on plant biomass allocation: A meta-analysis. *Ecology and Evolution* 7:11002–11010.
- Fan Z-X, Zhang S-B, Hao G-Y, Ferry Slik JW, Cao K-F (2012) Hydraulic conductivity traits predict growth rates and adult stature of 40 Asian tropical tree species better than wood density. *Journal of Ecology* 100:732–741.
- Fichot R, Barigah TS, Chamaillard S, Le Thiec D, Laurans F, Cochard H, Brignolas F (2010) Common trade-offs between xylem resistance to cavitation and other physiological traits do not hold among unrelated *Populus deltoides*×*Populus nigra* hybrids. *Plant, Cell & Environment* 1553–1568.
- Fichot R, Chamaillard S, Depardieu C, Le Thiec D, Cochard H, Barigah TS, Brignolas F (2011) Hydraulic efficiency and coordination with xylem resistance to cavitation, leaf function, and growth performance among eight unrelated *Populus deltoides*×*Populus nigra* hybrids. *Journal of Experimental Botany* 62:2093–2106.
- Fuchs S, Schuldt B, Leuschner C (2021) Identification of drought-tolerant tree species through climate sensitivity analysis of radial growth in Central European mixed broadleaf forests. *Forest Ecology and Management* 494:119287.
- Gleason SM, Butler DW, Ziemińska K, Waryszak P, Westoby M (2012) Stem xylem conductivity is key to plant water balance across Australian angiosperm species. *Functional Ecology* 26:343–352.
- Gleason SM, Stephens AEA, Tozer WC, Blackman CJ, Butler DW, Chang Y, Cook AM, Cooke J, Laws CA, Rosell JA, Stuart SA, Westoby M (2018) Shoot growth of woody trees and shrubs is predicted by maximum plant height and associated traits. *Functional Ecology* 32:247–259.

- Gleason SM, Westoby M, Jansen S, Choat B, Hacke UG, Pratt RB, Bhaskar R, Brodrribb TJ, Bucci SJ, Cao K, Cochard H, Delzon S, Domec J, Fan Z, Feild TS, Jacobsen AL, Johnson DM, Lens F, Maherali H, Martínez-Vilalta J, Mayr S, McCulloh KA, Mencuccini M, Mitchell PJ, Morris H, Nardini A, Pittermann J, Plavcová L, Schreiber SG, Sperry JS, Wright IJ, Zanne AE (2016) Weak tradeoff between xylem safety and xylem-specific hydraulic efficiency across the world's woody plant species. *New Phytologist* 209:123–136.
- González-Muñoz N, Sterck F, Torres-Ruiz JM, Petit G, Cochard H, von Arx G, Lintunen A, Caldeira MC, Capdeville G, Copini P, Gebauer R, Grönlund L, Hölttä T, Lobo-do-Vale R, Peltoniemi M, Stritih A, Urban J, Delzon S (2018) Quantifying in situ phenotypic variability in the hydraulic properties of four tree species across their distribution range in Europe *PLoS ONE* 13:e0196075.
- Guet J, Fichot R, Lédée C, Laurans F, Cochard H, Delzon S, Bastien C, Brignolas F (2015) Stem xylem resistance to cavitation is related to xylem structure but not to growth and water-use efficiency at the within-population level in *Populus nigra* L. *Journal of Experimental Botany* 66:4643–4652.
- Hacke UG, Sperry JS, Wheeler JK, Castro L (2006) Scaling of angiosperm xylem structure with safety and efficiency. *Tree Physiology* 26:689–701.
- Hajek P, Kurjak D, von Wühlisch G, Delzon S, Schuldt B (2016) Intraspecific Variation in Wood Anatomical, Hydraulic, and Foliar Traits in Ten European Beech Provenances Differing in Growth Yield. *Frontiers in Plant Science* 7:791.
- Hajek P, Leuschner C, Hertel D, Delzon S, Schuldt B (2014) Trade-offs between xylem hydraulic properties, wood anatomy and yield in *Populus*. *Tree Physiology* 34:744–756.
- Hajek P, Link RM, Nock CA, Bauhus J, Gebauer T, Gessler A, Kovach K, Messier C, Paquette A, Saurer M, Scherer-Lorenzen M, Rose L, Schuldt B (2022) Mutually inclusive mechanisms of drought-induced tree mortality. *Global Change Biology* 28:3365–3378.
- Hari V, Rakovec O, Markonis Y, Hanel M, Kumar R (2020) Increased future occurrences of the exceptional 2018–2019 Central European drought under global warming. *Science Reports* 10:12207.
- Hartmann H, Link RM, Schuldt B (2021) A whole-plant perspective of isohydry: stem-level support for leaf-level plant water regulation. *Tree Physiology* 41:901–905.
- Herbette S, Charrier O, Cochard H, Barigah TS (2021) Delayed effect of drought on xylem vulnerability to embolism in *Fagus sylvatica*. *Canadian Journal of Forest Research* 51:622–626.
- Hoerber S, Leuschner C, Köhler L, Arias-Aguilar D, Schuldt B (2014) The importance of hydraulic conductivity and wood density to growth performance in eight tree species from a tropical semi-dry climate. *Forest Ecology and Management* 330:126–136.
- IPCC (2021) *Climate Change 2021: The Physical Science Basis. Contribution of Working Group I to the Sixth Assessment Report of the Intergovernmental Panel on Climate Change* Masson-Delmotte V, Zhai P, Pirani A, Connors SL, Péan C, Berger S, Caud N, Chen Y, Goldfarb L, Gomis MI, Huang M, Leitzell K, Lonnoy E, Matthews JBR, Maycock TK, Waterfield T, Yelekçi R, Yu R, Zhou B (eds). Cambridge University Press: Cambridge, UK.

- Isasa E, Link R, Jansen S, Sarmiento Cabral J, Schuldt B (2021) Addressing controversies in safety-vessel diameter relationships. In Proceedings of the Conference Ecology Across Borders 2021, Liverpool, UK.
- Kaack L, Weber M, Isasa E, Karimi Z, Li S, Pereira L, Trabi CL, Zhang Y, Schenk HJ, Schuldt B, Schmidt V, Jansen S (2021) Pore constrictions in intervessel pit membranes provide a mechanistic explanation for xylem embolism resistance in angiosperms. *New Phytologist* 230:1829–1843.
- Kotowska MM, Hertel D, Rajab YA, Barus H, Schuldt B (2015) Patterns in hydraulic architecture from roots to branches in six tropical tree species from cacao agroforestry and their relation to wood density and stem growth. *Frontiers in Plant Science* 6.
- Kotowska MM, Link RM, Röhl A, Hertel D, Hölscher D, Waite P-A, Moser G, Tjoa A, Leuschner C, Schuldt B (2021) Effects of Wood Hydraulic Properties on Water Use and Productivity of Tropical Rainforest Trees. *Frontiers in Forests and Global Change* 3:598759.
- Larter M, Pfautsch S, Domec J-C, Trueba S, Nagalingum N, Delzon S (2017) Aridity drove the evolution of extreme embolism resistance and the radiation of conifer genus *Callitris*. *New Phytologist* 215:97–112.
- Lens F, Sperry JS, Christman MA, Choat B, Rabaey D, Jansen S (2011) Testing hypotheses that link wood anatomy to cavitation resistance and hydraulic conductivity in the genus *Acer*. *New Phytologist* 190:709–723.
- Leuschner C, Meier IC (2018) The ecology of Central European tree species: Trait spectra, functional trade-offs, and ecological classification of adult trees. *Perspectives in Plant Ecology, Evolution and Systematics* 33:89–103.
- Leuschner C, Wedde P, Lübke T (2019) The relation between pressure–volume curve traits and stomatal regulation of water potential in five temperate broadleaf tree species. *Annals of Forest Science* 76:1–14.
- Li S, Lens F, Espino S, Karimi Z, Klepsch M, Schenk HJ, Schmitt M, Schuldt B, Jansen S (2016) Intervessel pit membrane thickness as a key determinant of embolism resistance in angiosperm xylem. *IAWA Journal* 37:152–171.
- Liu H, Ye Q, Gleason SM, He P, Yin D (2021) Weak tradeoff between xylem hydraulic efficiency and safety: climatic seasonality matters. *New Phytologist* 229:1440–1452.
- Lübke T, Lamarque LJ, Delzon S, Torres Ruiz JM, Burlett R, Leuschner C, Schuldt B (2022) High variation in hydraulic efficiency but not xylem safety between roots and branches in four temperate broad-leaved tree species. *Functional Ecology* 36:699–712.
- Maherali H, Moura CF, Caldeira MC, Willson CJ, Jackson RB (2006) Functional coordination between leaf gas exchange and vulnerability to xylem cavitation in temperate forest trees. *Plant, Cell & Environment* 29:571–583.
- Markesteyn L, Poorter L, Bongers F, Paz H, Sack L (2011) Hydraulics and life history of tropical dry forest tree species: coordination of species' drought and shade tolerance. *New Phytologist* 191:480–495.

- McDowell N, Pockman WT, Allen CD, Breshears DD, Cobb N, Kolb T, Plaut J, Sperry J, West A, Williams DG, Yezzer EA (2008) Mechanisms of plant survival and mortality during drought: why do some plants survive while others succumb to drought? *New Phytologist* 178:719–739.
- Nolan RH, Gauthey A, Losso A, Medlyn BE, Smith R, Chhajer SS, Fuller K, Song M, Li X, Beaumont LJ, Boer MM, Wright IJ, Choat B (2021) Hydraulic failure and tree size linked with canopy die-back in eucalypt forest during extreme drought. *New Phytologist* 230:1354–1365.
- Pammenter NW, Van der Willigen C (1998) A mathematical and statistical analysis of the curves illustrating vulnerability of xylem to cavitation. *Tree Physiology* 18:589–593.
- R Core Team. R: A Language and Environment for Statistical Computing; R Core Team: Vienna, Austria, 2020.
- Robson TM, Hartikainen SM, Aphalo PJ (2015) How does solar ultraviolet-B radiation improve drought tolerance of silver birch (*Betula pendula* Roth.) seedlings? *Plant, Cell & Environment* 38:953–967.
- Rosas T, Mencuccini M, Barba J, Cochard H, Saura-Mas S, Martínez-Vilalta J (2019) Adjustments and coordination of hydraulic, leaf and stem traits along a water availability gradient. *New Phytologist* 223:632–646.
- Rowland L, da Costa ACL, Galbraith DR, Oliveira RS, Binks OJ, Oliveira A a. R, Pullen AM, Doughty CE, Metcalfe DB, Vasconcelos SS, Ferreira LV, Malhi Y, Grace J, Mencuccini M, Meir P (2015) Death from drought in tropical forests is triggered by hydraulics not carbon starvation. *Nature* 528:119–122.
- Schreiber SG, Hacke UG, Chamberland S, Lowe CW, Kamelchuk D, Bräutigam K, Campbell MM, Thomas BR (2016) Leaf size serves as a proxy for xylem vulnerability to cavitation in plantation trees. *Plant, Cell & Environment* 39:272–281.
- Schuldt B, Knutzen F, Delzon S, Jansen S, Müller-Haubold H, Burlett R, Clough Y, Leuschner C (2016) How adaptable is the hydraulic system of European beech in the face of climate change-related precipitation reduction? *New Phytologist* 210:443–458.
- Schumann K, Leuschner C, Schuldt B (2019) Xylem hydraulic safety and efficiency in relation to leaf and wood traits in three temperate *Acer* species differing in habitat preferences. *Trees* 33:1475–1490.
- Sperry JS, Nichols KL, Sullivan JEM, Eastlack SE (1994) Xylem Embolism in Ring-Porous, Diffuse-Porous, and Coniferous Trees of Northern Utah and Interior Alaska. *Ecology* 75:1736–1752.
- Sperry JS, Tyree MT (1990) Water-stress-induced xylem embolism in three species of conifers. *Plant, Cell & Environment* 13:427–436.
- Sterck FJ, Martínez-Vilalta J, Mencuccini M, Cochard H, Gerrits P, Zweifel R, Herrero A, Korhonen JFJ, Llorens P, Nikinmaa E, Nolè A, Poyatos R, Ripullone F, Sass-Klaassen U (2012) Understanding trait interactions and their impacts on growth in Scots pine branches across Europe: Functional branch trait coordination. *Functional Ecology* 26:541–549.

- Torres-Ruiz JM, Cochard H, Fonseca E, Badel E, Gazarini L, Vaz M (2017) Differences in functional and xylem anatomical features allow *Cistus* species to co-occur and cope differently with drought in the Mediterranean region. *Tree Physiology* 37:755–766.
- Torres-Ruiz JM, Jansen S, Choat B, McElrone AJ, Cochard H, Brodribb TJ, Badel E, Burlett R, Bouche PS, Brodersen CR, Li S, Morris H, Delzon S (2015) Direct X-Ray Microtomography Observation Confirms the Induction of Embolism upon Xylem Cutting under Tension. *Plant Physiology* 167:40–43.
- Tyree MT (2003) Hydraulic limits on tree performance: transpiration, carbon gain and growth of trees. *Trees* 17:95–100.
- Tyree MT, Davis SD, Cochard H (1994) Biophysical Perspectives of Xylem Evolution: is there a Tradeoff of Hydraulic Efficiency for Vulnerability to Dysfunction? *IAWA Journal* 15:335–360.
- Tyree MT, Zimmermann MH (2002) *Xylem Structure and the Ascent of Sap*, 2nd edn. Springer-Verlag, Berlin Heidelberg, Germany, pp. 143–174.
- Vogt UK (2001) Hydraulic vulnerability, vessel refilling, and seasonal courses of stem water potential of *Sorbus aucuparia* L. and *Sambucus nigra* L. *Journal of Experimental Botany* 52:1527–1536.
- Weithmann G, Schuldt B, Link RM, Heil D, Hoerber S, John H, Müller-Haubold H, Schüller L - M., Schumann K, Leuschner C (2022) Leaf trait modification in European beech trees in response to climatic and edaphic drought. *Plant Biology* 24:1272–1286.
- West GB, Brown JH, Enquist BJ (1999) A general model for the structure and allometry of plant vascular systems. *Nature* 400:664–667.
- White FM (1991) *Viscous fluid flow*. McGraw-Hill, New York, USA.
- Wickham H, Averick M, Bryan J, Chang W, McGowan LD, François R, Grolemund G, Hayes A, Henry L, Hester J, Kuhn M, Pedersen TL, Miller E, Bache SM, Müller K, Ooms J, Robinson D, Seidel DP, Spinu V, Takahashi K, Vaughan D, Wilke C, Woo K, Yutani H (2019) Welcome to the Tidyverse. *Journal of Open Source* 4:1686.
- Wikberg J, Ögren E (2004) Interrelationships between water use and growth traits in biomass-producing willows. *Trees-Structure and Function* 18:70–76.
- Wright IJ, Reich PB, Westoby M, Ackerly DD, Baruch Z, Bongers F, Cavender-Bares J, Chapin T, Cornelissen JHC, Diemer M, Flexas J, Garnier E, Groom PK, Gulias J, Hikosaka K, Lamont BB, Lee T, Lee W, Lusk C, Midgley JJ, Navas M-L, Niinemets Ü, Oleksyn J, Osada N, Poorter H, Poot P, Prior L, Pyankov VI, Roumet C, Thomas SC, Tjoelker MG, Veneklaas EJ, Villar R (2004) The worldwide leaf economics spectrum. *Nature* 428:821–827.
- Zhang J-L, Cao K-F (2009) Stem hydraulics mediates leaf water status, carbon gain, nutrient use efficiencies and plant growth rates across dipterocarp species. *Functional Ecology* 23:658–667.

Chapter-3:

Coordinated drought responses determine the time to hydraulic failure in five temperate tree species differing in their degree of isohydry

Manish Kumar^{1,2}, Pierre-André Waite^{1,3}, Roman M. Link^{1,3}, Bernhard Schuldt^{1,3*}

¹ *University of Würzburg, Julius-von-Sachs-Institute of Biological Sciences, Ecophysiology and Vegetation Ecology, Julius-von-Sachs-Platz 3, 97082 Würzburg, Germany.*

² *ICAR—Central Soil Salinity Research Institute (CSSRI), Karnal, 132001, India.*

³ *Technische Universität Dresden, Institute of Forest Botany and Forest Zoology, Cott-Bau, Pienner Straße 7, 01737, Tharandt, Germany.*

Draft submitted.

Abstract

Drought-induced mortality is widespread and affects forest health and productivity. However, the complex mechanisms involved make it difficult to anticipate these effects fully. This study examined the temporal progression of stomatal regulation and plant water potential through a dry-down experiment. We aim to examine plant behaviour by estimating the time it takes to reach stomatal closure and subsequently critical levels of hydraulic failure in response to drought. In addition, we investigate how the traits affecting desiccation time are coordinated along the isohydry continuum across five species with different drought resistance strategies and hydraulic behaviours. We found a strong association between a species' hydroscape area (HSA) and the water potential at 90% stomatal closure (P_{s90}). Species closing their stomata at lower water potential notably had a larger HSA. Isohydry species closed their stomata early with declining water potential to avoid embolism formation, while anisohydric species continued gas exchange until the loss of turgor. Isohydry was mostly associated with leaf hydraulic traits and poorly with xylem safety traits. It was unrelated to the species' time to hydraulic failure during drying-out experiments. We show plant responses to drought can be divided into two phases, with the first phase lasting from the onset of drought to stomatal closure and the second phase from stomatal closure to death. We found traits are coordinated along two major axes related to these two phases. The degree of isohydry of a plant was found to be predominantly associated with the first axis linked to the time to stomatal closure (T_{sc}) and HSA but largely unrelated to the time to critical hydraulic failure. The second axis is associated with hydraulic safety and reflects that species with wider hydraulic safety margins and a lower P_{88} take longer to reach critical levels of hydraulic failure (T_{crit}). This supports the idea that iso-and-anisohydric behaviours are linked to water use strategies rather than to drought tolerance. Overall, our results suggest that there are multiple strategies plants can adapt to cope with drought that rely on adjustments of different traits. The insight into the mechanism determining the time to hydraulic failure recommends considering multiple structural and functional characteristics for sustainable forest plantation management decisions.

Keywords: Stomatal closure, desiccation time, hydraulic traits, hydroscape, cuticular conductance, capacitance, hydraulic safety margin.

3.1 Introduction

Drought-induced tree mortality is widespread and well-documented in almost all forest types across the globe (Allen *et al.* 2010, Peng *et al.* 2011, Anderegg *et al.* 2013). Over the past decades, reduced precipitation and rising temperatures have amplified the intensity and frequency of drought events (Allen *et al.* 2010, Allen *et al.* 2015, Adams *et al.* 2017). The increasing evaporative demand has been linked to reductions in biomass productivity (Kotowska *et al.* 2021, Kumar *et al.* 2022, Ramesha *et al.* 2022) and rises tree mortality (Schuldt *et al.* 2020, McDowell *et al.* 2022, Schönbeck *et al.* 2022). Therefore, there is an urgent need to understand the mechanisms involved in drought-induced tree mortality (O'Brien *et al.* 2017, Hartmann *et al.* 2018). On that matter, growing evidence suggests that a disruption of the plant water transport system (hydraulic failure) is a near-universal pattern in drought-induced tree mortality (Brodribb and Cochard 2009, Mitchell *et al.* 2014, Urli *et al.* 2013, Adams *et al.* 2017). Ultimately, mortality risk during drought depends on how long plants can maintain a tissue water content sufficient to sustain their biochemical functionality (Mantova *et al.* 2022).

Under drought, a plant's internal water transport system endures stress due to decreasing xylem water potentials. The progression of plant drought responses can be divided into two fundamental phases: A first phase before stomatal closure, when the plant is still actively transpiring, and a second phase from stomatal closure to deadly levels of desiccation (cf. Choat *et al.* 2018). Before stomatal closure, stomatal regulation is the main driver of plant water relations, as the conductance of open stomata exceeds other water losses by orders of magnitude (Kerstiens 1996). Under water deficit, stomata gradually close to minimize water loss and xylem water potential drop (Brodribb *et al.* 2003, Nolf *et al.* 2015). After stomatal closure, plant water potentials continue to decrease through uncontrollable water losses via the cuticle, bark and residual stomatal conductance until finally reaching levels that cause the spread of embolism in the xylem (Blackman *et al.* 2016, Blackman *et al.* 2019b, Hammond and Adams 2019).

A number of traits related to the aforementioned processes are routinely quantified to describe plant behaviour under drought. Hydraulic impairment is usually described using xylem embolism thresholds derived from vulnerability curves, such as the water potential at 50% and 88% loss of hydraulic conductivity (P_{50} and P_{88} , respectively, Brodribb and Cochard 2009, Urli *et al.* 2013). In addition, species' performance under drought depends on changes in other critical leaf, xylem and morphological characteristics timely coordinated among each other (Skelton *et al.*

2021, Li *et al.* 2022). One important aspect of plant drought responses is avoiding the onset of xylem embolism formation by adjusting the internal water balance through stomatal regulation (Li *et al.* 2018). The water potential at 90% stomatal closure (P_{s90}) has been shown to be coordinated with embolism thresholds and to be linked to plant mortality risk during drought (Klein 2014, Bartlett *et al.* 2016, Martin-StPaul *et al.* 2017, Li *et al.* 2018). Likewise, leaf turgor loss point (Ψ_{tlp}) is a good predictor of plant hydraulic safety (Bartlett *et al.* 2012b). Ψ_{tlp} is often linked to embolism resistance due to the coordination between the onset of xylem embolism and stomatal closure, the latter of which depends on leaf turgor (Brodribb *et al.* 2003, Bartlett *et al.* 2016, Rodriguez-Dominguez *et al.* 2016, Farrell *et al.* 2017). Coordination between the first and the second phase of drought response is described using the hydraulic safety margin (HSM) between leaf water potential at stomatal closure (i.e. P_{s90}) or turgor loss point (i.e., Ψ_{tlp}) and critical embolism thresholds (e.g., P_{88} , Skelton *et al.* 2015, Martin-StPaul *et al.* 2017). Finally, water losses after stomatal closure are quantified by the cuticular and residual conductance (g_{min}) (Duursma *et al.* 2019). Altogether, these coordinated leaf and xylem traits influence plant mortality risk (Hammond and Adams 2019, Hammond *et al.* 2019).

Due to the many traits involved, the negative effects of a water deficit period can be mitigated in multiple ways (Pivovarov *et al.* 2016). One way to achieve this is via plant hydraulic capacitance, i.e., the ability to store water in tissues and gradually release it during increasing drought stress. Capacitance seems to be a key trait that dynamically modulates both hydraulic safety and efficiency (Meinzer *et al.* 2003, Sperry *et al.* 2008). Its importance to buffer intense periods of water shortage is unequivocally accepted (Steppe and Lemeur 2007, Vergeynst *et al.* 2015, De Baerdemaeker *et al.* 2017, Epila *et al.* 2017). However, no real consensus has emerged regarding its measurement method, and the term hydraulic capacitance is often used to refer to different tissue and plant properties (e.g., leaf, sapwood or branch hydraulic properties). Moreover, the trait has rarely been experimentally studied as part of coordinated plant hydraulic strategies (Barnard *et al.* 2011, Scholz *et al.* 2011, Santiago *et al.* 2018, Blackman *et al.* 2019a).

Hydraulic strategies are frequently categorized by their degree of isohydry, i.e., the stringency of their stomatal control during increasing evaporative demand. In drier environments, more isohydric species tend to close their stomata earlier to limit the decrease in xylem water potentials (Tardieu and Simonneau 1998). Isohydric species, thus, are assumed to delay the onset of xylem embolism formation at the cost of reduced carbon uptake. In contrast, more anisohydric

species maintain their stomata open longer at the cost of decreasing water potentials, preserving assimilation but increasing embolism risk (Tardieu and Simonneau 1998, Roman *et al.* 2015, Hartmann *et al.* 2021). Stomatal sensitivity to water potential has been shown to be species-specific and to vary along a continuum (Klein 2014), suggesting that plant stomatal control strategies form a continuous axis from more to less stringent stomatal control. In addition, it has been shown that some species can switch from isohydric to anisohydric behaviour in response to changing conditions (Rogiers *et al.* 2012, Zhang *et al.* 2012). For these reasons, the relevance of a dichotomic nomenclature has recently been widely discussed, while a clear definition of the underlying mechanisms is yet to come (Martínez-Vilalta and Garcia-Forner 2017, Hochberg *et al.* 2018, Feng *et al.* 2019). In addition to the stomatal response, a set of associated characteristics has been both theoretically and experimentally associated to the isohydric continuum. More anisohydric species tend to have more embolism-resistant xylem (Klein *et al.* 2014), a more negative leaf turgor loss point (Chen *et al.* 2021), a higher carbon invested in stem (Reich 2014, Chen *et al.* 2021), and a higher wood density (Chen *et al.* 2021, Fu and Meinzer 2019).

The lack of clarity about the underlying mechanism is reflected by the large amount of existing metrics to quantify the degree of isohydry of a species, for example, stomatal response curves (e.g. Klein 2014), water potentials at given percentages of loss of stomatal conductance (e.g. Chen *et al.* 2021), the slope of the relationship of midday vs predawn water potential (e.g. Martínez-Vilalta *et al.* 2014), the water potential difference between stomatal closure and P_{50} (Skelton *et al.* 2015), or the so-called hydroscape area (Fu and Meinzer 2019, Fu *et al.* 2019, Li *et al.* 2019, Salvi *et al.* 2022). The conceptual uncertainties about the mechanisms underlying isohydry, as well as a large amount of often disparate metrics to quantify it, illustrate the need to incorporate the concept of isohydry into a more integrative and complete understanding of the coordinated plant response to drought.

Dry-down experiments are an important tool for understanding the relationships between drought tolerance and avoidance traits with critical timings of plant response to drought (Blackman *et al.* 2019b, Li *et al.* 2022). The idea behind these experiments is to measure a set of hydraulic traits and monitor the plant water status on replicate plant samples over a period of progressing desiccation to determine the time necessary to exceed critical desiccation thresholds (e.g. time of stomatal closure or time to critical hydraulic failure). There is an urgent need for dry-down experiments under controlled conditions to be able to identify which traits drive species differences

in desiccation time (Choat *et al.* 2018). While a number of studies have focused on determining the time a plant spends in the second phase of the drying process, from stomatal closure to critical hydraulic failure (Blackman *et al.* 2016, 2019b, Challis *et al.* 2022), so far to our knowledge there are no studies that focus on the time plants spend in the first phase from full hydration to stomatal closure. Moreover, it is largely unknown how different hydraulic strategies in terms of the degree of isohydry relate to drying times.

In the present study, we investigated the drought response and hydraulic strategies of five widespread, economically important central European forest tree species. We conducted drying-down experiments on potted saplings of the species *Acer pseudoplatanus*, *Betula pendula*, *Fagus sylvatica*, *Sorbus aucuparia*, and *Tilia cordata* to quantify their degree of isohydry in terms of the hydroscape area (HSA), and to estimate the time to both stomatal closure (T_{sc}) and critical hydraulic failure (T_{crit}). We further measured a set of water potentials associated with critical points throughout the drying process, namely the xylem water potential at stomatal closure (P_{s90}), at the turgor loss point (Ψ_{tlp}) and at major hydraulic failure (P_{88}). In addition, we measured various traits linked to drought response, such as the hydraulic safety margin (HSM), minimum leaf conductance (g_{min}) and shoot capacitance (C). The aims of our study are, first, to determine the position of these tree species along the isohydric continuum according to P_{s90} and HSA; second, to test how hydraulic traits are related to the degree of isohydry; and third, to test how P_{s90} , HSA and other hydraulic traits are related to T_{sc} and T_{crit} . We hypothesized that (1) the P_{s90} of a species is negatively associated with its HSA, and consistent with its degree of isohydry as described in previous studies, (2) more isohydric species have higher C , less negative P_{88} , wider HSM, and a less negative Ψ_{tlp} , (3) time to stomatal closure (T_{sc}) is associated with P_{s90} , Ψ_{tlp} , HSA, and C , and (4) time to critical hydraulic failure (T_{crit}) is associated with g_{min} , HSM, critical embolism thresholds, and C .

3.2 Material and methods

3.2.1 Species description

Seeds of three species, *Acer pseudoplatanus* L. (ACPS), *Betula pendula* Roth (BEPE), and *Sorbus aucuparia* L. (SOAU), were collected and grown in March 2019 at the botanical garden of the University of Würzburg (cf. Kumar *et al.* 2022). Measurements of these species took place on

similar, healthy individuals aged approx. 28–29 months in July–August 2021. Two other species, *Fagus sylvatica* L. (FASY) and *Tilia cordata* Mill. (TICO), were grown in a nursery near Würzburg from 2019 to 2021, moved to the botanical garden Würzburg and repotted in December 2021. Measurements took place in July–August 2022. Because most of the measurements are destructive, we divided individuals into experiments to estimate a maximum of traits at the species level, using different subsets of trees for drying-out experiments, xylem vulnerability, hydraulic capacitance, etc. The investigated traits are shown in Table 3.1.

The study species were selected for their importance in central European forests and their reportedly contrasting stomatal behaviour. FASY and SOAU have been described as clearly anisohydric (Vogt 2001, Rötzer *et al.* 2017, Leuschner *et al.* 2019, 2020, 2022), while ACPS and BEPE have consistently been described as isohydric (Robson *et al.* 2015, Li *et al.* 2016, Leuschner *et al.* 2019, Beikircher *et al.* 2021, Kumar *et al.* 2022). Finally, published accounts regarding the stomatal behaviour of TICO are mixed, with some studies reporting a fairly isohydric behaviour (Köcher *et al.* 2009, 2013, Leuschner *et al.* 2019) and others a more anisohydric strategy (Moser *et al.* 2016, Gillner *et al.* 2017, Moser-Reischl *et al.* 2019).

3.2.2 Drying-out experiments

Before the dry-down experiments began, we irrigated the saplings daily in a shaded but open environment. We then placed similarly sized saplings in a climate-controlled greenhouse chamber at the Chair of Botany II, University of Würzburg, both in 2021 and 2022. We measured ACPS (n = 8, collar diameter (CD) = 26.81 ± 0.77 cm), BEPE (n = 8, CD = 31.36 ± 1.15 cm), FASY (n = 6, CD = 15.12 ± 1.17 cm), SOAU (n = 7, CD = 26.32 ± 1.23 cm), and TICO (n = 11, CD = 14.09 ± 2.25 cm). At the start of the dry-down period, pots were irrigated to soil saturation and covered with black polythene to reduce evaporation from the topsoil and to ensure water loss is only driven by transpiration. Saplings were randomly assigned in a completely randomized design. We installed a microclimate sensor (1-800-LOGGER, HOBO Onset, Bourne, MA 02532 USA) just above the saplings (height = 1.3 m) to record temperature and humidity every 10 minutes throughout the experiments. Irrigation was then suspended, allowing a progressive decrease in water potential until the plants reached their P_{88} (measured on conspecific saplings from the same batch of plants prior to the experiment). We monitored leaf water potential regularly with a pressure chamber (Model 1505D, PMS Instruments, Albany, OR 97322 USA). We selected each

one leaf per individual at predawn (Ψ_{pd} from 5:00 to 6:00 h) and midday (Ψ_{md} from 12:00 to 13:00 h), and measured water potential within 1 min after excision.

During the dry-out period, all leaves lost due to measurements or leaf shedding were collected and oven-dried at 75 °C for 72 h to estimate the initial leaf mass and area of each sapling and its change over time. We also oven-dried the saplings at 75 °C at the end of the experiments to estimate their aboveground stem and leaf mass. We obtained leaf area per plant by multiplying leaf dry mass (g) by species-specific leaf area (SLA, $\text{cm}^2 \text{g}^{-1}$) measured on different fully hydrated saplings. Maximum leaf area (L_m , cm^2) of the dried-out saplings was estimated from SLA based on the sum of the dry mass of the leaves removed daily and the dry mass of the leaves remaining at the end of the experiment. Likewise, we obtained the amount of water stored in the aboveground fraction of the dried-out plants (V_w , g) by multiplying the total aboveground dry mass (i.e., removed + remaining leaves + stems in g) with species saturated shoot water content (g g^{-1}). Species-level saturated water content was measured on saplings used for hydraulic capacitance measurements as (wet mass - dry mass) / dry mass.

3.2.3 Plant stomatal response during drought

We measured stomatal conductance (g_s , $\text{mmol m}^{-2} \text{s}^{-1}$) on the drying plants to estimate water potential at stomatal closure (i.e., P_{s90} , necessary for the calculation of T_{sc} and the determination of species degree of isohydry). On each tree, we selected three fully expanded, healthy leaves at different locations (i.e., top, middle and lower) and measured their g_s daily using a portable porometer (model AP4, Delta-T Devices Ltd, Cambridge, UK). We measured at the same time each day to record the maximum attainable g_s while accounting for daily patterns. We computed the percent of stomatal conductance using the highest recorded individual g_s as a reference. Finally, we estimated species stomatal response to drought by fitting a sigmoidal curve on the relationship between percent of stomatal conductance and water potential (Li *et al.* 2018). P_{s90} was defined as the predicted water potential at 90% loss of stomatal conductance (Li *et al.* 2018, Blackman *et al.* 2019b).

3.2.4 Embolism resistance and hydraulic safety margin

To determine species death (necessary for T_{crit} and T_{hf}), we measured xylem embolism vulnerability on additional saplings with the flow-centrifuge method (Cochard *et al.* 2005). Measurements were performed in 2021 in the framework of our previous study (Kumar *et al.* 2022) for ACPS, BEPE, and SOAU and in 2022 for FASY and TICO. We shortened the main stems of 5–10 replicates per species to a length of ca. 27 cm and removed the bark at both ends. We then inserted the samples into a custom-made Cavitron rotor chamber attached to a centrifuge (Cavitron device built from a customized Sorvall RC-5C centrifuge) and constantly maintained them under a flow of water. We increased rotor speed by small increments to simulate the decrease of xylem water potential and recorded hydraulic conductivity until a percent loss of hydraulic conductivity (PLC) of at least 90%. We used the Cavisoft software (Cavisoft version 5.2.1, University of Bordeaux, Bordeaux, France) to perform the measurements. Vulnerability curves were fitted using an exponential-sigmoidal model (Pammenter and Vander Willigen 1998) and subsequently used to determine the water potential at 88 % loss of conductivity (P_{88} , Domec and Gartner 2003). In this study, we define the hydraulic safety margin (HSM) as the difference between P_{s90} and P_{88} .

3.2.5 Determination of plant desiccation times

We defined time to hydraulic failure (T_{hf}) as the species average standardized time to reach the water potential at 88% loss of hydraulic conductivity starting from a fully hydrated state. T_{hf} was determined for each species by fitting a non-linear relationship between the observed standardized drying time (i.e. time in hours multiplied by daily average VPD to account for differences in evaporative demand across the drying-out experiments) and Ψ_{pd} of the dried-out trees. In the present study, we consider an individual as dead when $\Psi_{pd} = P_{88}$. We divided T_{hf} into the time to stomatal closure (T_{sc}) and the time from stomatal closure to critical hydraulic failure (T_{crit} , Blackman *et al.* 2016, 2019b). Because plant size influences desiccation time (Blackman *et al.* 2019b, Challis *et al.* 2022), we further standardized T_{sc} and T_{crit} to account for leaf area and water storage (eq. (1)):

$$T_{x_stan} = T_x \cdot \frac{L_m \cdot \rho_w}{V_w}, \quad (1)$$

where T_{x_stan} is the standardized desiccation time x (h cm^{-1}), T_x is the desiccation time for the same tree in VPD hours ($\text{mol mol}^{-1} \text{h}$), L_m (cm^2) is its initial leaf area, and V_w (g) is the mass of water

stored in the wood. V_w was divided by the density of water ρ_w (i.e. 0.996 g cm^{-3} at $30 \text{ }^\circ\text{C}$) to convert it to cm^3 (cf. Challis *et al.* 2022).

3.2.6 Plant hydroscape

To estimate species hydroscape area (HSA, MPa^2), we followed the methodology described by Meinzer *et al.* (2016). Briefly, we calculated HSA as the area of the triangle formed by the regression line between Ψ_{pd} versus Ψ_{md} and the 1:1 line (eq. 2):

$$\text{HSA} = \frac{a \times b}{2}, \quad (2)$$

where a is the intercept of the ordinary linear regression of Ψ_{pd} vs. Ψ_{md} , which represents the most negative Ψ_{md} when $\Psi_{pd}=0$, and b is the intersection of Ψ_{pd} vs. Ψ_{md} and the 1:1 line, which is at $\Psi_{pd} = \Psi_{md}$.

3.2.7 Shoot hydraulic capacitance

Hydraulic capacitance (C) measurements were made on the complete aboveground fraction of well-watered saplings (ACPS: $n = 5$, BEPE: $n = 4$, SOAU: $n = 5$, FASY: $n = 9$, TICO: $n = 5$, Length = 1.0–1.2 m, diameter = 10–14 mm). We followed an updated version of the method described in Li *et al.* (2018) and Blackman *et al.* (2019b). After storing the plants overnight in a cool and humid environment in opaque plastic bags to ensure full water saturation, we cut whole-shoot samples at the root collar, sealed the cut surface with wax and proceeded to bench-dry them. We weighted each shoot at increasing time intervals using an analytical scale (0.01 g) to estimate the amount of water loss. At each time interval (hereafter: drying steps), we measured the water potential of two leaves per shoot using a pressure chamber. We then allowed the shoots to dry slowly until mass constancy or reaching the maximum water potential measurable by the pressure chamber (-10 MPa). The initial mass at the beginning of the experiment corresponds to the water-saturated mass (SM). To be sure that each shoot capacitance experiment started at water saturation, we also measured initial water potential, which was always above -0.3 MPa . All subsequent weight measurements (i.e., fresh mass or FM) were done at a series of drying steps with increasing drying intervals (e.g. 15 min, 30 min, 1 h, 2 h, 4 h, etc.) defined depending on species identity. For each drying step, before measuring mass and water potential, shoots were packed into humid, opaque plastic bags for 30–60 min to limit transpiration and equilibrate the water potential. In addition, we tracked the mass of the excised leaves at each drying step before water potential

measurement. All cut-off leaves were weighed and stored with shed leaves to measure their oven-dried mass (DM). In general, shoots took 3 to 4 days to fully dehydrate. Overnight time was treated as a long equilibration period, as shoots were packed into humid plastic bags to prevent further drying. At the end of the dehydration period, the remaining shoots and removed leaves were oven-dried for 72h at 105 °C to determine their DM. Based on the shoot fresh weight at each drying step, the weight of the removed leaves and the corresponding dry masses, we computed shoot relative water content (RWC in g g^{-1} , eq. 3).

$$RWC = \frac{FM-DM}{SM-DM}, \quad (3)$$

RWC was modelled with an exponential decay equation in dependence of water potential to estimate the moisture release pattern of each species (Li *et al.* 2018, Blackman *et al.* 2019b). To compare species, we used the slope of the linear portion of the capacitance after stomatal closure (Figure S1) (Blackman *et al.* 2019b). The slope was then standardized to account for dry shoot mass (eq. 4).

$$C = \frac{\Delta RWC}{\Delta \Psi} \cdot \frac{SM-DM}{DM} \cdot \frac{1}{M_w}, \quad (4)$$

where $\Delta RWC / \Delta \Psi$ is the slope of the relationship between RWC and water potential ($\text{g g}^{-1} \text{MPa}^{-1}$) multiplied by the maximum amount of stored water by the shoot ($SM - DM$, g) and divided by dry shoot mass (DM, kg). The total ($\text{g kg}^{-1} \text{MPa}^{-1}$) was then converted to $\text{mol kg}^{-1} \text{MPa}^{-1}$ by dividing it by the molar mass of water (M_w , 18.01 g mol^{-1}).

3.2.8 Leaf traits

On additional well-watered saplings, we measured leaf turgor loss point (Ψ_{tlp}), specific leaf area (SLA) and leaf residual conductance (g_{min}) on fully expanded leaves from different canopy positions. Ψ_{tlp} was estimated using 2–3 leaves from fully hydrated saplings ($n = 4$ individuals per species) following Bartlett *et al.* (2012a). The leaves were cut-off, cleaned, double bagged with humidified towels, and stored in a refrigerator until measurement. We then cut blade discs with a cork borer, covered them with aluminium foil and submerged them in liquid nitrogen for at least 2 min. Next, we measured osmolality (mmol kg^{-1}) with a VAPRO 5600 vapor pressure osmometer (Wescor, Inc., Ut 84321 USA), which we then converted to osmotic potentials based on the Morse equation. Ψ_{tlp} was estimated from leaf osmotic potential using eq. 5 in Bartlett *et al.* (2012a). SLA ($\text{cm}^2 \text{g}^{-1}$) was measured on 10 to 30 leaves from fully hydrated saplings ($n = 5$ per species). To

compute SLA, we divided the surface area of the leaves (cm^2) computed from scans using FIJI (Schindelin *et al.* 2012) by their oven-dried mass (g).

Leaf residual conductance was measured on 2-3 mature, healthy leaves from the trees used for capacitance measurements. Excised leaves were cleaned and rehydrated overnight in a glass desiccator by immersing their petioles in water. The saturated leaf mass was recorded using a high-precision balance (MC-1 AC210S, 0.1 mg, Sartorius, Göttingen, Germany). Cut petioles were soaked in ABA solution for 30 minutes to ensure the stomatal closure, then sealed with wax. Leaves were desiccated for 7–10 h under low light in an heating cabinets with controlled conditions, having fixed temperature and relative humidity setting to 25 °C and 70%, respectively. Temperature and humidity were examined inside the incubator with a digital thermo-hygrometer (Testoterm 6010, Testo) to ensure controlled conditions. In addition, silica gel was placed inside to control the humidity in the incubator. Fresh mass was recorded at 30 min intervals. When leaf mass was constant, oven-dry mass was recorded, excluding the wax. Leaves were scanned to calculate the leaf area using FIJI. The projected leaf area (A) was multiplied by two to account for the total leaf surface. Flow rate of water (g / s) was derived from the linear regression slope of change in fresh weight (ΔFM) with time (t), which normalize by the total leaf surface area i.e., adaxial and abaxial (A, m^2) to ascertain a transpiration rate ($J, \text{g m}^{-2} \text{s}^{-1}$).

$$J = \frac{\Delta FM}{\Delta t * A}, \quad (5)$$

Then, cuticular conductance ($g_{\min}, \text{mmol m}^{-2} \text{s}^{-1}$) was calculated by dividing the transpiration rate (J) by driving force to water loss which is the concentration difference of water across the cuticular membrane (cf. Schuster *et al.* 2017, Bueno *et al.* 2019). Then divided by the molar mass of water (g / mol) and multiplied by the mole fraction (VPD / P).

3.2.9 Data analysis

All data visualizations and statistical analyses were performed using R (version 4.1.2, R Development Core Team 2021). We computed vulnerability and stomatal response curves using a sigmoidal model from nlme package (Pinheiro *et al.* 2000) and $T_{\text{hf}}, T_{\text{sc}}, T_{\text{crit}}, C$ and g_{\min} using linear models from base R. We compared characteristics across species using one-way ANOVA and post hoc tests (Tukey's HSD) for pairwise comparisons using the package multcompView (Piepho 2004, Donaghue 2004). Subsequently, we assessed traits correlation using a correlation matrix

from the corrplot package (Wei and Simko 2021). Finally, we performed a principal component analysis (PCA) using prcomp() function and ggbiplot (Vincent 2011) package used to examine the results of PCA for multivariate association among the different traits.

Table 3.1: Summary of investigated traits with their symbols, units and definition.

| Symbols | Units | Definition |
|-------------------------|--------------------------------------|--|
| Ψ_L | MPa | Leaf water potential: indicators of plant water status |
| Ψ_{pd} / Ψ_{md} | MPa | Water potential at predawn (between 5:00 and 6:00) and midday (between 11:30 and 12:30) |
| P_{88} | MPa | Xylem pressure at 88% loss of hydraulic conductance |
| P_{s90} | MPa | Water potential at 10% of maximum stomatal conductance |
| Ψ_{tip} | MPa | Water potential at leaf turgor loss point |
| HSM | MPa | (Stomatal) hydraulic safety margin defined as the difference between P_{s90} and P_{88} |
| C | $\text{mol kg}^{-1} \text{MPa}^{-1}$ | Hydraulic capacitance: amount of releasable water in the saplings' tissues per unit change in xylem tension and dry mass. |
| HSA | MPa^2 | Hydroscape area (HSA): area of the triangle formed between the 1:1 line and the regression line made between $\Psi_{predawn}$ and Ψ_{midday} |
| g_{min} | $\text{mmol m}^{-2} \text{s}^{-1}$ | Leaf cuticular conductance: moles of water lost per area and per time (normalized by vapour pressure deficit) |
| T_{sc_stan} | h cm^{-1} | Standardized time to stomatal closure (T_{sc}) standardized by the ratio of L_m and V_w |
| T_{crit_stan} | h cm^{-1} | Standardized time to critical level of hydraulic failure starting from stomatal closure (T_{crit}) standardized by the ratio of L_m and V_w (as a model component in Blackman <i>et al.</i> 2019b) |

3.3 Results

3.3.1 Stomatal behaviour and relative degree of isohydry

Stomatal conductance varied considerably across species and, after experimentally controlling for measurement time by performing measurements at the same time each day, was driven by leaf water potential decline (Figure 3.1, Table 3.2). Maximum g_s was particularly high in ACPS and BEPE (species previously described as isohydric, Table 3.2) and declined quickly under stress. Likewise, the estimated P_{s90} mirrored previously recorded patterns of isohydry, with more negative P_{s90} values for more anisohydric species (FASY and SOAU). Moreover, isohydric species closed their stomata well before the Ψ_{tip} (Table 3.2), while P_{s90} coincided well with Ψ_{tip} in more anisohydric species.

In addition, the three species positioned on the anisohydric end of the spectrum had an $\text{HSA} > 1$, while the more isohydric species had a much lower HSA (Figure 3.2, Table 3.2). We recorded a six-fold difference between the two most extreme HSA (0.29 and 1.85 MPa^2 for ACPS and FASY, respectively), which showed a similarly pronounced variation across species as P_{s90} (Table 3.2). As expected, HSA was strongly associated with P_{s90} (Figure S3.2, $R^2 = 0.91$, $P = 0.01$), and resulted in the same ranking of species.

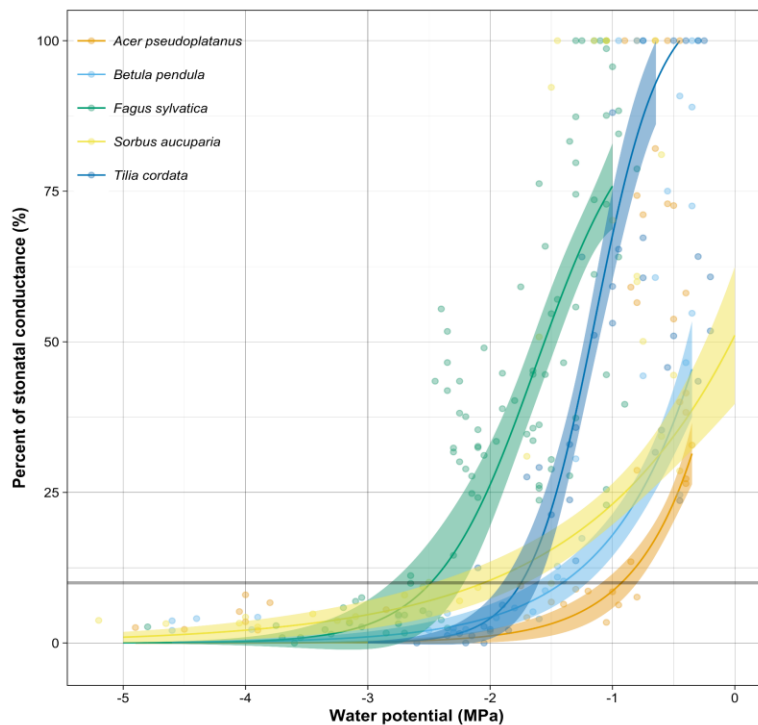


Figure 3.1: Stomatal response curves of dried-out saplings from the five investigated temperate tree species ($n=4-5$). Presented are percentage of maximal stomatal conductance (see Table 3.2) measured daily until complete stomatal closure against leaf water potential. Fitted lines and 95% confidence intervals (coloured ribbons) were shown. Water potential at 90 % loss of stomatal conductance is represented by the horizontal grey line.

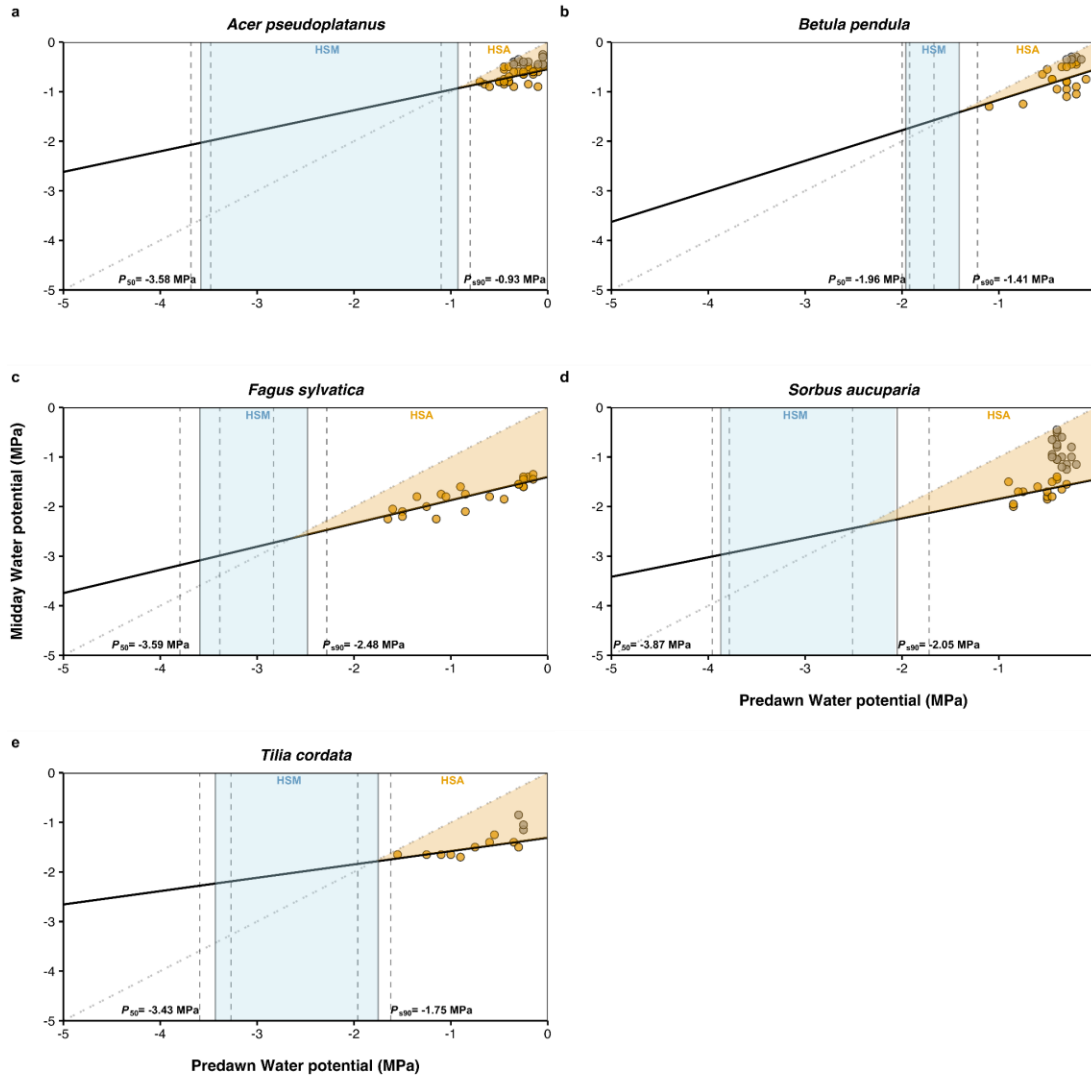


Figure 3.2: Plots of leaf water potential at predawn (Ψ_{pd}) versus midday (Ψ_{md}) associated with the 1:1 line. Presented are data from dried-out saplings from the five investigated temperate tree species ($n = 5 - 8$). Each point represents one measurement day on one plant with Ψ_{pd} measured before 6:00 against Ψ_{md} measured between 11:30 and 13:30. Orange points were included in the linear regression while grey points were excluded as they represent data collected under humid conditions when Ψ_{md} likely varied independently of Ψ_{pd} (Fu and Meinzer, 2019). The hydroscape area (HSA) coloured in light orange was calculated from the area of the triangle formed by the regression line between Ψ_{pd} versus Ψ_{md} and the 1:1 line. Data points beyond $\Psi_{pd} = \Psi_{md}$ were removed according to Meinzer *et al.* (2016). Species water potential at 10% stomatal closure (P_{50}) and at 88% loss of hydraulic conductivity (P_{88}) are represented by vertical full lines (\pm SE = dashed lines). The hydraulic safety margin (HSM, $P_{50} - P_{88}$) is coloured in light blue.

3.3.2 Species differences in drought response traits

Our drying-out experiments revealed a broad range in the time to complete hydraulic failure (T_{hf} , see Figure S3.2). The unstandardized T_{hf} ranged from 464 VPD hours (i.e. time adjusted by daily VPD) for ACPS to 282 VPD hours for BEPE, seemingly independently of

species hydraulic behaviour. After accounting for differences in plant size, the contribution of the time to stomatal closure (T_{sc_stan}) to the total time to hydraulic failure (T_{hf_stan}) was larger than the contribution of the time from P_{s90} to P_{88} (T_{crit_stan}) for all species (ranging from 62% to 75%, Figure 3.3, Table 3.2) As expected, with 16%, the T_{crit_stan} contribution to T_{hf_stan} was the lowest in FASY.

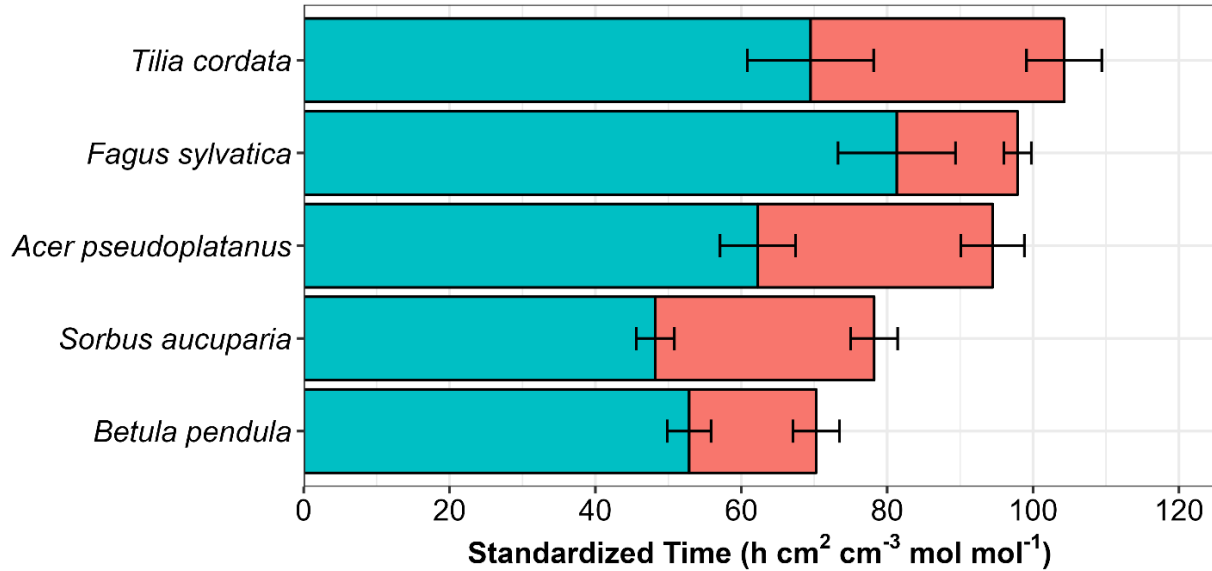


Figure 3.3: Stacked bar chart depicting time to hydraulic failure (T_{hf}) divided into two main phases: time to stomatal closure (T_{sc}) and time to critical water potential after stomatal closure (T_{crit}). To account for evaporative demand and morphological differences across the five investigated tree species, cumulative time was adjusted by vapour pressure deficit and standardized by ratio of total leaf area and volume of water stored. T_{sc} (\pm SE), is represented in green, while T_{crit} (\pm SE) is represented in red colour.

We also found that branch-related traits such as P_{88} and hydraulic capacitance (C) differed across the five species ($f(4) = 85.26$ and 10.30 , $P < 0.001$, Figures 3.4a and 3.4d). The lowest C was recorded for the most anisohydric species (2.47 ± 0.40 and 4.76 ± 0.67 mol kg⁻¹ MPa⁻¹ for FASY and SOAU, respectively), while the highest C was recorded for one of the most isohydric species (10.98 ± 2.31 mol kg⁻¹ MPa⁻¹ for BEPE). On the opposite, more anisohydric species presented the most negative P_{88} , while the highest P_{88} was found for BEPE (-2.21 ± 0.04 MPa). However, the isohydric ACPS had a P_{88} similar to the anisohydric species (-4.24 ± 0.13 MPa).

Likewise, we found leaf traits differ significantly across species ($f(4) = 9.86$ for Ψ_{tlp} and 16.21 for g_{min} , $P < 0.001$, Figure 3.4b and 3.4c, Table 3.2). Leaf turgor loss point (Ψ_{tlp}) was the lowest for the most anisohydric species (-2.48 and -2.37 MPa for FASY and SOAU, respectively). Finally, we found a slight variation in leaf residual conductance (g_{min} ranging from 1.28 to 3.33 mmol m⁻² s⁻¹) across species, with a significantly higher g_{min} for ACPS (Figure 3.4c, Table 3.2).

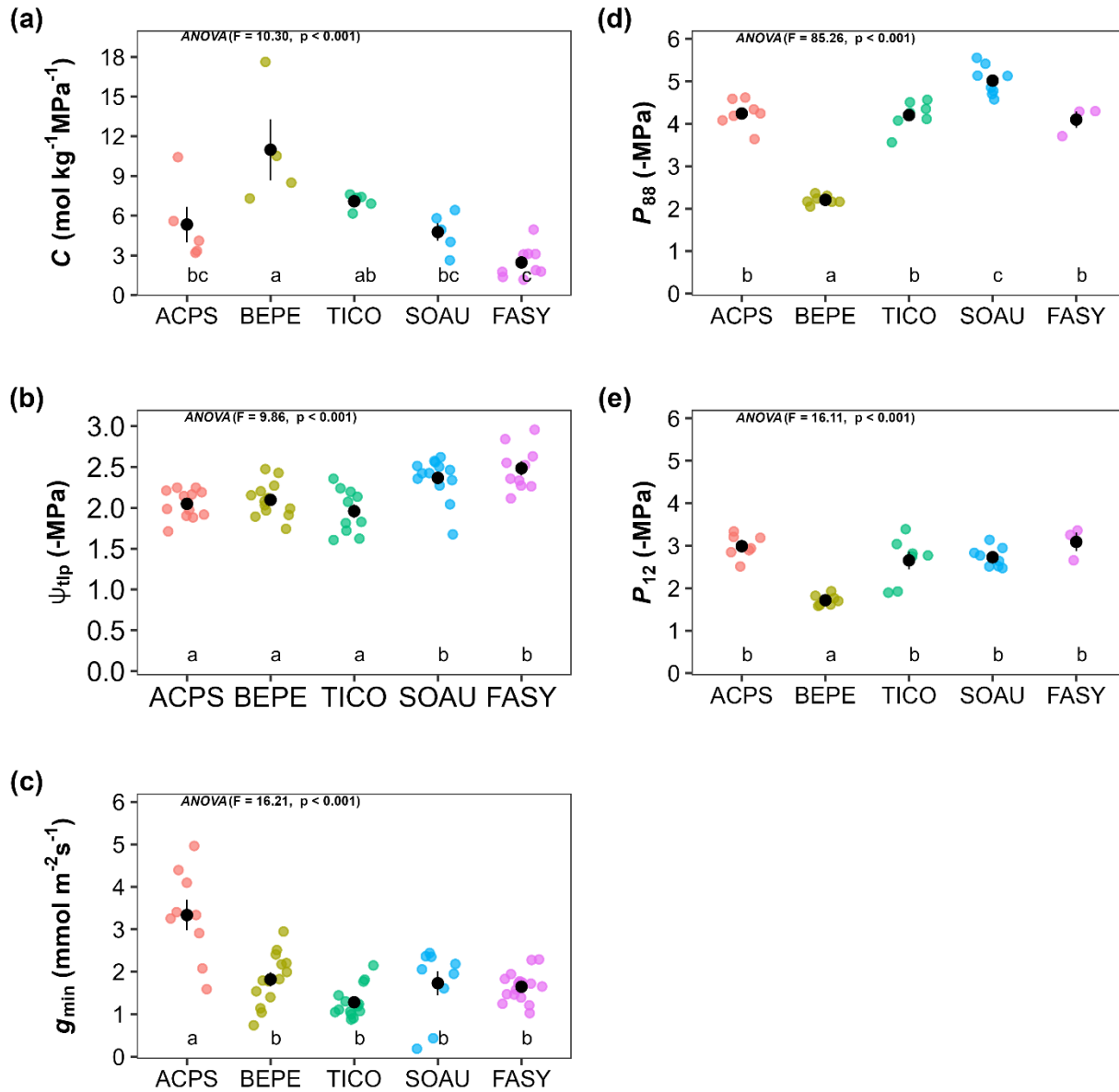


Figure 3.4: Point and range plots of hydraulic traits across five temperate tree species. Presented here are (a) sapling hydraulic capacitance (C), (b) leaf water potential at turgor loss point (Ψ_{tlp}), (c) leaf residual conductance (g_{min}), (d) xylem water potential at 88 % loss of hydraulic conductivity (P_{88}) and (e) xylem water potential at 12 % loss of hydraulic conductivity (P_{12}) for each species. Coloured points represent individual measurements done on entire saplings (C , $n = 5 - 8$), on the main stem (P_{12} , P_{88} , $n = 4 - 8$) or on healthy sun-exposed leaves (Ψ_{tlp} and g_{min} , $n = 8 - 13$). Black points represent mean (\pm SE). Significant differences across species were estimated using one-way ANOVA (F statistic and p -values are given on the top-left of each panel) and post hoc tests (Tukey HSD; represented by letters). Species abbreviations; ACPS: *Acer pseudoplatanus*; BEPE: *Betula pendula*; TICO: *Tilia cordata*, SOAU: *Sorbus aucuparia*; FASY: *Fagus sylvatica*.

3.3.3 Coordination between drought response traits

We found that the degree of isohydry of a species as quantified by P_{s90} and HSA was most strongly associated with leaf safety (e.g. Ψ_{tlp} and g_{min}) and drought avoidance traits (e.g. C). Species closing their stomata at lower leaf water potentials or having a larger hydroscape, i.e. more anisohydric species, had a more negative Ψ_{tlp} ($R = -0.79$ with HSA, Figure 3.5), a lower g_{min} ($R = -0.70$ with HSA) and a lower hydraulic capacitance ($R = -0.53$ with HSA). Likewise, anisohydric species had a more negative P_{88} ($R = -0.41$ with HSA), although they did not possess wider hydraulic safety margins ($R = 0.09$ between HSA and HSM).

As expected, HSA and P_{s90} were related to time to stomatal closure (T_{sc_stan}), with more anisohydric species having a longer T_{sc_stan} ($R = -0.42$ between P_{s90} and T_{sc_stan} , Figure 3.5). Species with a more negative P_{s90} also tended to have a lower capacitance, while there was no relationship to HSM or P_{88} (Figure 3.5). While T_{sc_stan} appeared largely decoupled from most other investigated characteristics, T_{crit_stan} was highly correlated with safety traits at the wood (i.e. with P_{88} : $R = -0.72$, Figure 3.5), at the leaf (i.e. with Ψ_{tlp} : $R = 0.47$) and at the plant level (i.e. with HSM: $R = 0.87$).

In our PCA, the observed traits cluster along two main axes of variation that reflect their association with different phases of their drought response in consistent hydraulic strategies (Figure 3.6). The two primary axes of traits variability collectively explained 74.5 % of the total variation in the dataset. The first PCA axis (PC1) is linked to traits associated with stomatal stringency and isohydric plant behaviour and reflects that species with larger HSA close their stomata and lose their leaf turgor at a more negative water potential, resulting in a longer time until stomatal closure. The second PCA axis (PC2) is associated with hydraulic safety and reflects that species with wider hydraulic safety margins and a lower P_{88} take longer to reach critical levels of hydraulic failure. Finally, hydraulic capacitance and residual conductance seem to be associated to both stomatal stringency and hydraulic safety, however with a tendency for species closing their stomata later to have lower C and g_{min} .

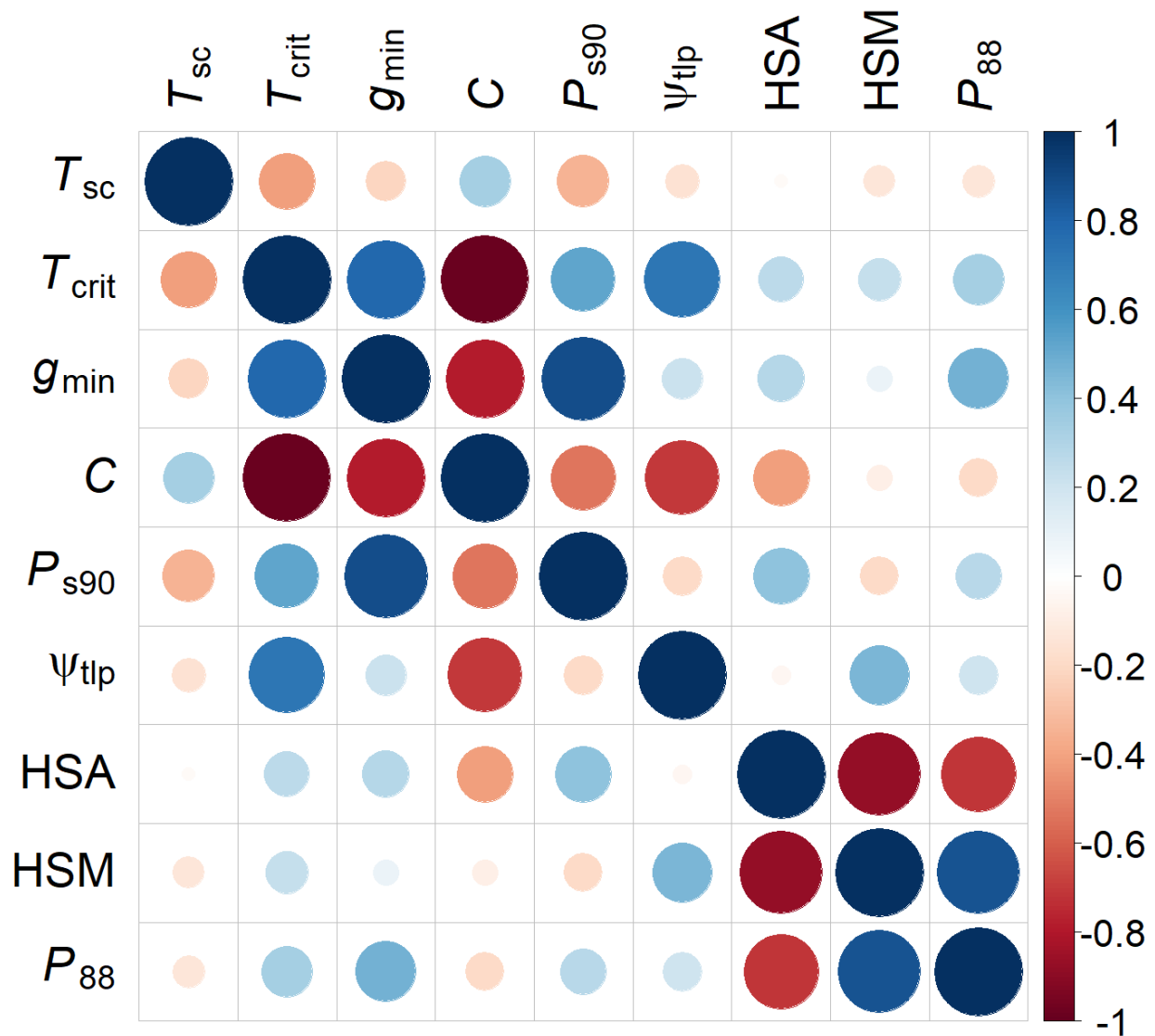


Figure 3.5: Clustered correlation matrix of investigated hydraulic traits and drying-out threshold times. Presented here are time to stomatal closure (T_{sc}), time to critical water potential (T_{crit}), hydraulic capacitance (C), water potential at 88% loss of hydraulic conductivity (P_{88}), at leaf turgor loss point (Ψ_{tip}), and at 90% loss of stomatal conductance (P_{s90}), as well as leaf residual conductance (g_{min}), hydraulic safety margin (HSM), hydroscape area (HSA). (See table 3.1 for units and descriptions).

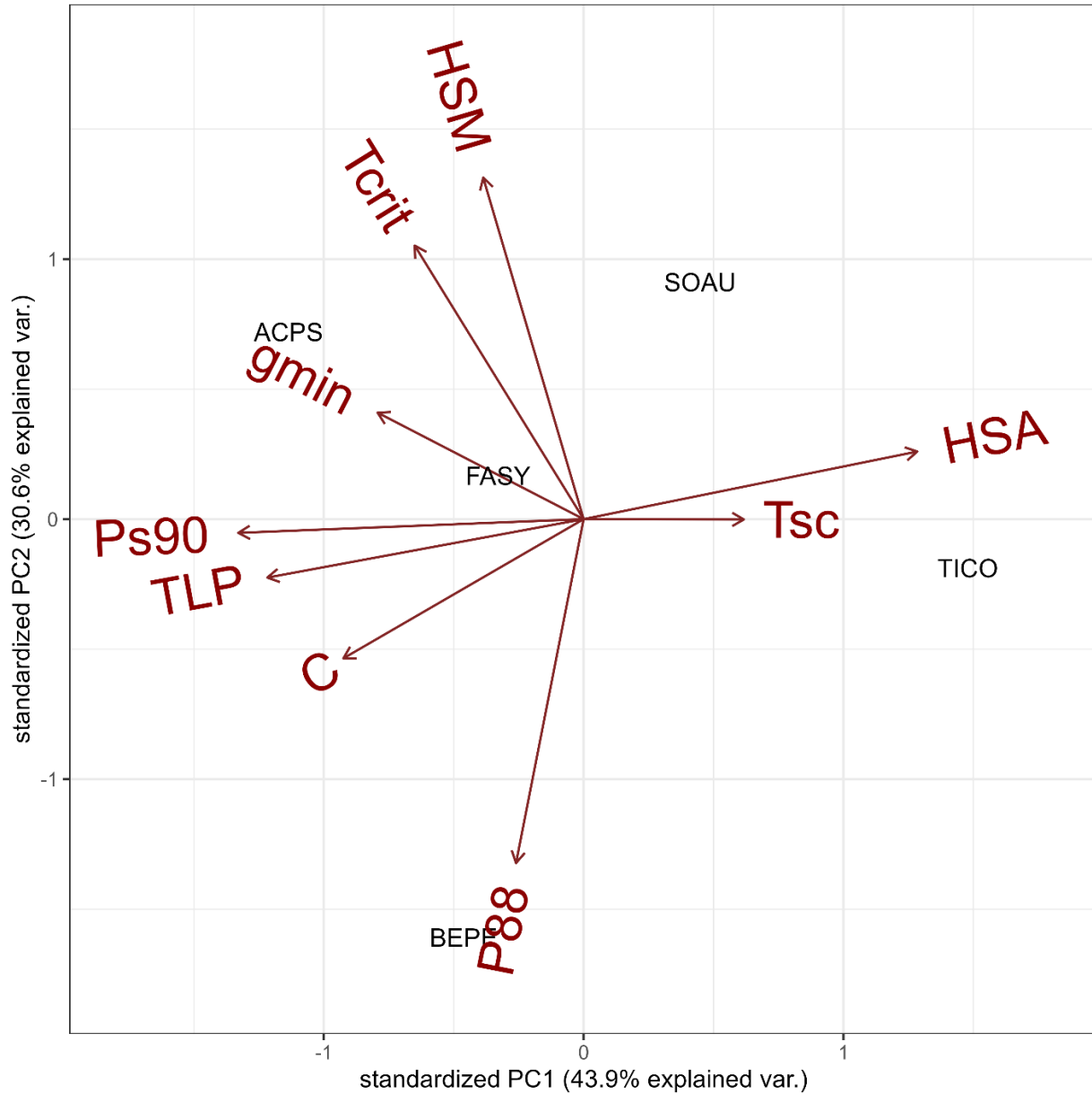


Figure 3.6: Principal component analysis (PCA) of nine hydraulic characteristics across five temperate tree species. The x-axis and y-axis represent species stomatal stringency and hydraulic safety, respectively. Presented here are time to stomatal closure (T_{sc}), time to critical water potential (T_{crit}), hydraulic capacitance (C), water potential at 88% loss of hydraulic conductivity (P_{88}), at leaf turgor loss point (Ψ_{tlp}), and at 90% loss of stomatal conductance (P_{s90}), as well as leaf residual conductance (g_{min}), hydraulic safety margin (HSM), hydroscape area (HSA). (See table 3.1 for units and descriptions).

3.4 Discussion

The results of this study are consistent with the assumption that plant responses to drought are divided into two discrete phases, the first one lasting from the onset of drought to stomatal closure and the second one from stomatal closure to death. We find that the duration of the first phase is mostly determined by traits related to stomatal regulation, while the duration of the second phase is more strongly associated with traits related to xylem resistance. Our results suggest a coordination of drought response traits along two major axes related to these two phases. We further find that the degree of isohydry of a plant is predominantly associated with the first axis linked to the time to stomatal closure but largely unrelated to the time to critical hydraulic failure. This supports the idea that iso- and anisohydric behaviours are linked to water use strategies rather than to drought survival strategies.

3.4.1 The temporal progression of plant drought responses

To understand and predict the behaviour of plants under drought, it is paramount to shift the focus from merely comparing critical water potentials to estimating the time it takes to reach them (Arend *et al.* 2021). Our results illustrate that by separating the total time to hydraulic failure into a component before and a component after stomatal closure, it is possible to gain insights about the coordination of plant drought responses that are unavailable otherwise. A similar approach has been proposed in the conceptual framework of Hammond and Adams (2019). However, these authors divided the dynamics of plant desiccation into phases based on mortality risk rather than on critical water potentials, with the first phase lasting from the onset of drought to incipient mortality risk (cf. Sapes *et al.* 2019) and the second phase from this point to the ‘point of no return’ (defined as 50% mortality risk, Hammond *et al.* 2019). As the mortality risk of individual plants is very difficult to quantify (cf. Hajek *et al.* 2022), in this study, we prefer to work with water potential thresholds, which have the additional advantage to be defined in terms of the most important state variable used to describe plant water status (cf. De Swaef *et al.* 2022). In addition, these definitions allow intuitive interpretations of T_{sc} as the time to stomatal closure and T_{crit} as the time needed to cross the stomatal hydraulic safety margin. As stomatal closure consistently happens before the onset of embolism formation and hence prior to the point of incipient mortality risk (Martin-StPaul *et al.* 2017, Sperry *et al.* 2017), the two definitions of the

two phases in our paper are not identical to those in Hammond and Adams (2019). Thus, the associations between drying times and hydraulic partially observed here partially differ from the trait associations predicted by these authors.

As long as stomata are open, their conductance dwarves cuticular and residual conductance (Duursma *et al.* 2019) and bark conductance (Wolfe *et al.* 2020). For that reason, the contribution of the latter to total plant water loss is negligible in the first phase. Consistent with this, we found T_{sc_stan} to be more strongly associated with P_{s90} and the mechanistically closely related Ψ_{tlp} than with g_{min} . However, the correlation between g_{min} and the standardized drying time after stomatal closure (T_{crit_stan}) was equally low, possibly due to the relatively low range of g_{min} of 1.28–3.33 $\text{mmol m}^{-2} \text{s}^{-1}$ covered by our dataset compared to the wide range reported for this trait (cf. Duursma *et al.* 2019). The strong association of T_{crit_stan} with hydraulic safety margins and critical embolism thresholds reinforces its interpretation as the time needed to cross the hydraulic safety margin. Interestingly, the standardized average times plants of a species spent in each of the two phases were correlated neither with each other nor with the average total desiccation time. This illustrates that a focus only on drying times after stomatal closure (cf. Blackman *et al.* 2016, 2019b) may not always be sufficient to predict the time to death of a plant under natural drought conditions, and shows that there are multiple strategies for plants to cope with drought that rely on adjustments of different traits.

3.4.2 Coordination of drought response traits

Our results indicate that drought response traits among the studied tree species are consistent in line with their theoretically expected sequence (Bartlett *et al.* 2016). For all species, stomatal closure occurred and, for all species with the exception of BEPE, turgor loss happened before reaching water potentials associated with the onset of embolism formation (P_{12}). This strict avoidance of loss of xylem function has been documented elsewhere (Martin-StPaul *et al.* 2017, Hochberg *et al.* 2017, Li *et al.* 2018) and illustrates the strong selection in favour of trait combinations that protect the functionality of the plant conductive system. BEPE relies on early leaf shedding as a drought response strategy (Gao *et al.* 2017, Hajek *et al.* 2022), which decouples leaf and stem water potentials and may explain the relatively negative Ψ_{tlp} for that species considering its low embolism resistance. Moreover, the species is known to adjust its leaf osmotic potentials under drought plastically and thus to drop its Ψ_{tlp} in response to drought (Aspelmeier

and Leuschner 2004). In either case, the low time to hydraulic failure observed for BEPE indicates that they crossed deadly embolism thresholds early in the drought, which is in accordance with the high mortality rates observed for saplings of that species in the wake of the extreme 2018 drought event (Hajek *et al.* 2022).

The observed patterns in the stomatal response of the studied species were largely consistent with published accounts of their degree of isohydry, with species reported to be more anisohydric having a larger HSA and closing their stomata as well as losing their turgor at more negative water potentials. An exception to this pattern is TICO, which had a relatively high Ψ_{tip} and P_{s90} as well as an intermediate HSA. However, there seems a lack of consensus for TICO (Köcher *et al.* 2009), and our results are more in line with Leuschner *et al.* (2019), who reported fairly isohydric behaviour for that species. In our experiment, the large internal water storage of TICO combined with its relatively high embolism resistance and early stomatal closure led to the highest average standardized drying time for that species.

Counter to our expectations, neither embolism resistance nor the associated hydraulic safety margins were related to metrics of isohydry. Instead, our results indicate traits associated with plant drought response to cluster along two largely independent axes of variation. In our PCA, both HSA and P_{s90} scored strongly on the first axis, which suggests that this axis is linked to the isohydry continuum. The high scores of whole-plant capacitance on that axis further indicate that the position of a species on that axis is associated with drought avoidance traits. The second axis was associated with critical embolism thresholds and HSM, and can hence be interpreted as an axis of xylem safety. This implies that plants may be able to adjust their drought response along two largely independent axes reflecting different underlying trade-offs rather than reducing to a single axis of variation defining a spectrum of drought tolerance strategies, as suggested by Choat *et al.* (2018). While these results clearly have to be interpreted with care due to the low number of investigated species, in our dataset, stomatal stringency and xylem resistance to drought-induced embolism formation were largely decoupled. This finding contrasts with many published accounts on the isohydry spectrum (Martínez-Vilalta *et al.* 2014, Klein *et al.* 2014, Pivovarovoff *et al.* 2018, Fu and Meinzer 2019), but may reflect the lack of a direct mechanistic link between both characteristics. While a coordination between stomatal response and embolism formation requires stomata to close before the onset of embolism formation (Martin-StPaul *et al.* 2017), there is no mechanism that dictates how wide the water potential range from stomatal closure to critical

hydraulic failure should be for a given P_{s90} (cf. McCulloh *et al.* 2019). Hence, potential associations between stomatal sensitivity and xylem vulnerability traits may reflect their independent roles in drought tolerance rather than coordinated function (Bartlett *et al.* 2016). It is, therefore, possible that many viable strategies exist that are based on different combinations of stomatal response and xylem resistance traits. Ultimately, studies on larger numbers of species from different biomes will be necessary to determine the level of integration between these different groups of drought response traits (He *et al.* 2021), as well as their link to trade-offs associated with other environmental stressors (Puglielli *et al.* 2021) and main axes of plant trait variation above- (Wright *et al.* 2004) and belowground (Weemstra *et al.* 2016).

3.4.3 Metrics of the degree of isohydry

To quantify the degree of isohydry of plants, a large amount of different metrics have been developed that often result in contrasting results (Martínez-Vilalta and Garcia-Forner 2017, Feng *et al.* 2019). Here, we found a high correlation between two common metrics of isohydry, the HSA (Meinzer *et al.* 2016) and the water potential at stomatal closure (cf. Chen *et al.* 2021). This relationship is in line with previous assessments of the HSA (Li *et al.* 2019) and illustrates that the latter indeed reflects how stomatal response regulates water potential during drought events, highlighting its value as a general metric of isohydry. However, mapping hydroscares requires continuous monitoring of plant water potentials during drought events, which is associated with a high measurement effort and can be challenging under field conditions. While the measurement of stomatal response curves can be achieved over shorter time scales, the required measurement effort is still substantial. Moreover, stomatal conductance does not only depend on water potential, but is also sensitive to temperature, light intensity and abscisic acid (ABA) concentrations (Brodribb and McAdam 2013, Klein *et al.* 2014), which can induce a high uncertainty in P_{s90} estimates if not measured under appropriately controlled conditions. For these reasons, measuring isohydry metrics like the HSA or P_{s90} for large numbers of species remains challenging.

In the last decade, the need for easily measurable proxy traits describing leaf-level drought adaptations has led to a resurgence of interest in pressure-volume curve traits such as the turgor loss point (Bartlett *et al.* 2012b, 2014). Ψ_{tlp} can be estimated rapidly based on leaf osmometry (cf. Bartlett *et al.* 2012a), has immediate mechanistic importance and has been shown to be strongly associated with parameters of stomatal response curves (Bartlett *et al.* 2016). Due to its often high

correlation with other isohydry metrics like the HSA, Ψ_{tip} has been proposed as a robust proxy of isohydry (Meinzer *et al.* 2016, Fu and Meinzer 2019). Leaf turgor is directly involved in passive pathways of stomatal closure, as stomatal closure is driven by guard cell turgor, which is directly influenced by bulk leaf water status (McAdam and Brodribb 2014). In addition, changes in leaf turgor may actively trigger ABA release in leaves (McAdam *et al.* 2016). Indeed, recent work indicates that turgor-mediated control of stomatal response is central for the stomatal closure of most woody plants (Rodríguez-Domínguez *et al.* 2016). The close mechanistic link to stomatal control is reflected in the strong association of Ψ_{tip} with both P_{s90} and HSA found in our study, which corroborates the value of Ψ_{tip} estimates as an easily measurable, mechanistically proximate trait directly linked to the stomatal response.

In a study of plant drought responses of species from the Cape region, Skelton *et al.* (2015) proposed the water potential range between stomatal closure and P_{50} as a further metric of isohydry that merges stomatal and xylem hydraulic strategies. This metric is essentially a stomatal hydraulic safety margin (cf. Martin-StPaul *et al.* 2017, Li *et al.* 2019). While the HSM reported here was based on P_{88} to match the definition of T_{crit} , there was no significant association between either the HSM based on P_{50} and P_{88} with any of the variables associated with the isohydry spectrum. Rather, HSM was related to xylem resistance traits and the duration of the second phase of drought response. Accordingly, stomatal HSMs may not be ideal to describe the stringency of stomatal response. Rather, our results support the proposed use of the HSA as a complement to the HSM to describe plant drought responses before and after stomatal closure (Hartmann *et al.* 2021).

In recent years, the concept of isohydry itself increasingly has become the subject of criticism. One point of contention is the missing evidence for a link between mid- and long-term regulation of plant water potentials on the one hand and the stringency of stomatal control on the other hand (Martínez-Vilalta and Garcia-Forner 2017). While in our study, we found metrics associated with both processes to be strongly correlated, the data by Martínez-Vilalta and Garcia-Forner (2017) clearly demonstrate that this is not always the case. Further, in a modelling experiment, Hochberg *et al.* (2018) showed that isohydry metrics are sensitive to environmental conditions, potentially resulting in different ranking orders for the same species. Hochberg *et al.* (2018), therefore, argue that to study differences in plant hydraulic strategies, it is simpler and more robust to focus on the physical parameters that drive plant-environment interactions rather than to focus on behaviours that derive from these interactions. Indeed, a better way forward to understand the coordination of

plant drought response traits into consistent syndromes may be to identify common patterns of shared variation between physiological “hard” traits with a clear mechanistic interpretation, and to use process-based models to understand how they jointly affect water potential regulation.

3.5 Conclusion

Our study confirms the hypothesized agreement between the water potential at stomatal closure and the hydroscape area, corroborating the value of a latter as an index of stomatal stringency. Consistent with our assumptions, more isohydric species had larger internal water storage and lost their leaf turgor at less negative water potentials. However, counter to our expectations, the degree of isohydry was entirely unrelated to embolism resistance and hydraulic safety margins. The latter formed a separate axis of variation linked to the duration of time from stomatal closure to lethal levels of desiccation, while the traits related to stomatal control, as expected, were more strongly associated with the time to stomatal closure. Our results highlight the importance of the temporal dynamics of plant drought responses and show that different traits affect drying time before and after stomatal closure. Notably, stomatal stringency was largely decoupled from the standardized drying time, which illustrates that isohydry alone paints an incomplete picture of plant drought responses. To improve our understanding of the coordination of plant traits and their role in different phases of desiccation, it will be necessary to study whether the observed trait patterns generalize onto larger species samples from different biomes both in situ and in dry-down experiments under controlled conditions.

Acknowledgements

The first author is grateful to the Indian Council of Agricultural Research (ICAR), New Delhi, India, for providing financial support through the Netaji Subhas - ICAR International Fellowship Program. Logistical and scientific assistance from the University of Würzburg, Germany, is acknowledged. We thank C. Gernert and Y. Heppenstiel for their skilful support in the laboratory during microscopic work and wood anatomical analyses, and Jutta Winkler-Steinbeck for regular supervision of the plants.

Table 3.2: Hydraulic properties of the five investigated temperate tree species. Shown are mean \pm standard error values for each species ($n = 5-8$ saplings), except for P_{s90} and HSA for which 95% confidence intervals are given. Provided are stomatal stringency categories as described in previous studies (see materials and methods section), time to hydraulic failure (T_{hf} , h cm^{-1}), water potential at 10% stomatal conductance (P_{s90} , MPa), hydroscape area (HSA, MPa^2), leaf turgor loss point (Ψ_{tlp} , MPa), hydraulic safety margin (HSM as $P_{s90} - P_{88}$, MPa), branch hydraulic capacitance (C), leaf residual conductance (g_{min} , $mmol m^{-2} s^{-1}$) and xylem water potential at 12, 50 and 88% loss of hydraulic conductivity (P_{12}, P_{50}, P_{88} , MPa). Letters indicate significant differences across species (One-way ANOVA and Tukey HSD).

| Traits measured | Unit | <i>Acer pseudoplatanus</i> | <i>Betula pendula</i> | <i>Tilia cordata</i> | <i>Sorbus aucuparia</i> | <i>Fagus sylvatica</i> |
|--------------------|------------------------|----------------------------|-------------------------|-------------------------|-------------------------|-------------------------|
| Stomata Stringency | - | Isohydic | Isohydic | Isohydic | Anisohydric | Anisohydric |
| HSA | MPa^2 | 0.29 (0.25, 0.36) | 0.65 (0.55, 0.82) | 1.17 (1.06, 1.31) | 1.63 (1.36, 2.72) | 1.85 (1.65, 2.14) |
| P_{s90} | MPa | -0.93 (-1.10, -0.80) | -1.41 (-1.67, -1.22) | -1.75 (-1.96, -1.62) | -2.05 (-2.51, -1.71) | -2.49 (-2.83, -2.28) |
| g_{smax} | $mmol m^{-2} s^{-1}$ | 309.35 ± 7.89 | 286.26 ± 15.02 | 55.85 ± 1.98 | 301.59 ± 6.30 | 74.28 ± 1.58 |
| T_{hf} | h cm^{-1} | 92.94 ± 6.97^{ab} | 70.27 ± 4.32^b | 106.17 ± 10.17^a | 78.22 ± 4.99^{ab} | 101.43 ± 9.02^{ab} |
| T_{sc} | h cm^{-1} | 62.27 ± 5.17^a | 52.86 ± 2.99^a | 69.50 ± 8.65^a | 48.22 ± 2.60^a | 81.31 ± 8.04^a |
| T_{crit} | h cm^{-1} | 32.18 ± 4.35^{ab} | 17.41 ± 3.20^b | 34.77 ± 5.15^a | 30.00 ± 3.21^{ab} | 16.57 ± 1.88^b |
| Ψ_{tlp} | MPa | -2.05 ± 0.05^a | -2.10 ± 0.06^a | -1.96 ± 0.09^a | -2.37 ± 0.07^b | -2.48 ± 0.08^b |
| HSM | MPa | 3.24 | 0.80 | 2.45 | 2.97 | 1.62 |
| C | $mol kg^{-1} MPa^{-1}$ | 5.33 ± 1.34^{bc} | 10.98 ± 2.31^a | 7.09 ± 0.26^{ab} | 4.76 ± 0.67^b | 2.47 ± 0.40^c |
| g_{min} | $mmol m^{-2} s^{-1}$ | 3.33 ± 0.36^a | 1.82 ± 0.16^b | 1.28 ± 0.09^b | 1.73 ± 0.28^b | 1.65 ± 0.09^b |
| P_{12} | MPa | -2.99 ± 0.11^b | -1.72 ± 0.05^a | -2.65 ± 0.21^b | -2.73 ± 0.08^b | -3.09 ± 0.22^b |
| P_{50} | MPa | -3.62 ± 0.11^{bc} | -1.96 ± 0.04^a | -3.43 ± 0.16^b | -3.87 ± 0.08^c | -3.59 ± 0.21^{bc} |
| P_{88} | MPa | -4.24 ± 0.13^b | -2.21 ± 0.04^a | -4.20 ± 0.13^b | -5.02 ± 0.12^c | -4.10 ± 0.19^b |

Supplementary information

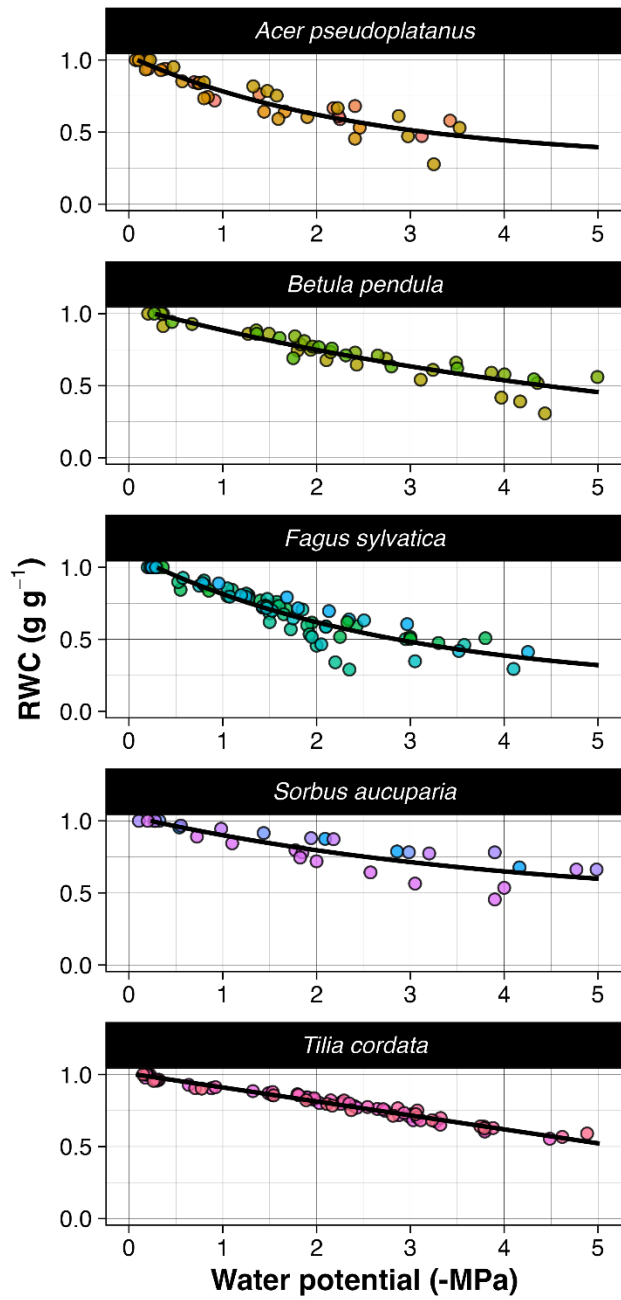


Figure S3.1: Shoot hydraulic capacitance (C) of the five investigated temperate tree species ($n = 4 - 9$). Presented curve are obtained by modelled RWC with water potential using an exponential decay equation. The mean value with post hoc test shown in Table 3.2. The slope was also standardized to account for dry shoot mass.

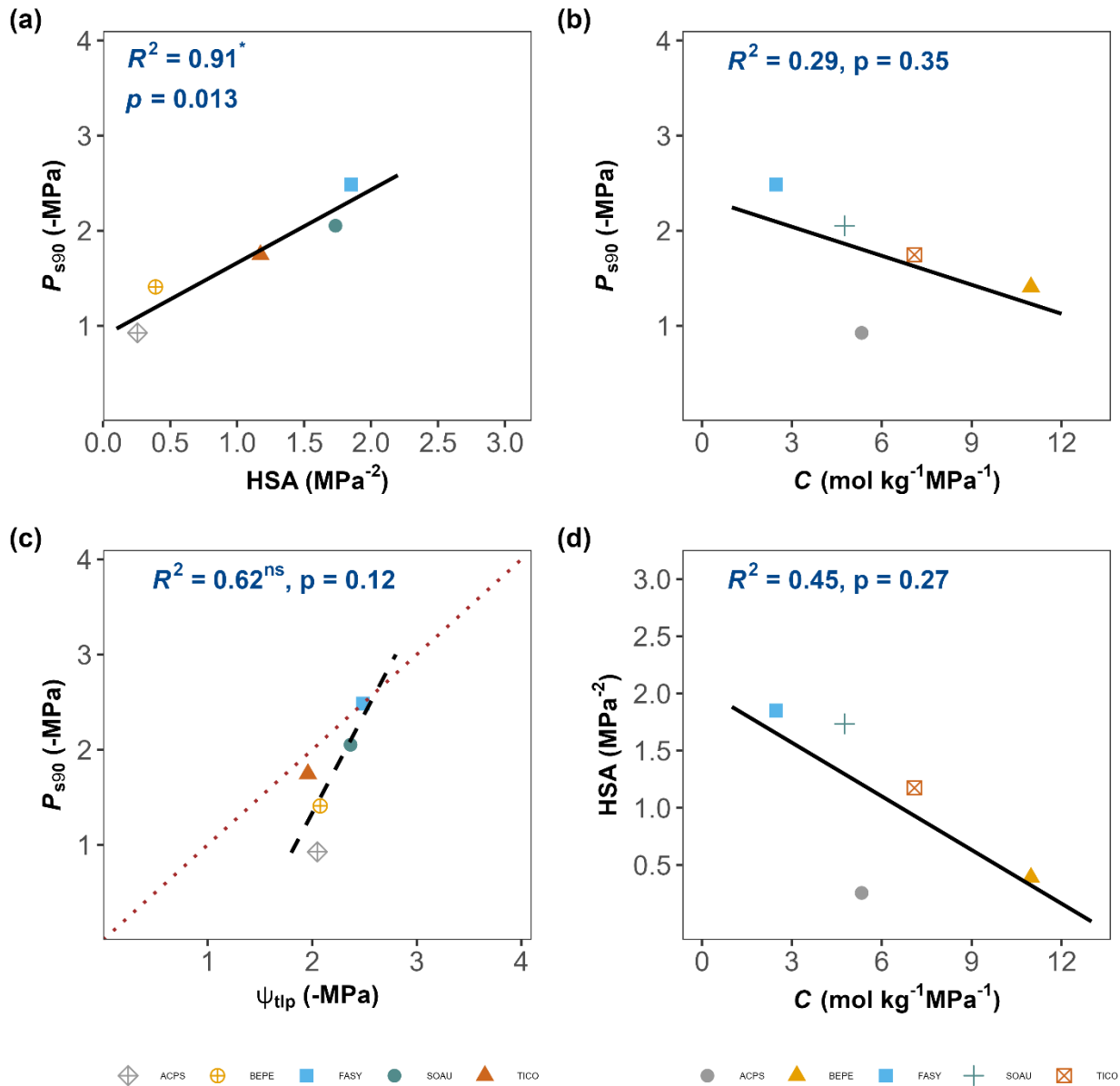


Figure S3.2: Relationship of stomatal closure (P_{s90}) with hydroscape area, HSA (a); capacitance, C (b); Turgor loss point, ψ_{tip} (c); and (d) relationship between HSA and C across five temperate tree species. The symbols used for species are diamond: ACPS, plus sign circle: BEPE, filled square: FASY, filled circle: SOAU, filled triangle: TICO. Asterisks indicate the level of significance (*, $p < 0.05$; **, $p < 0.01$; ns, for non-significant).

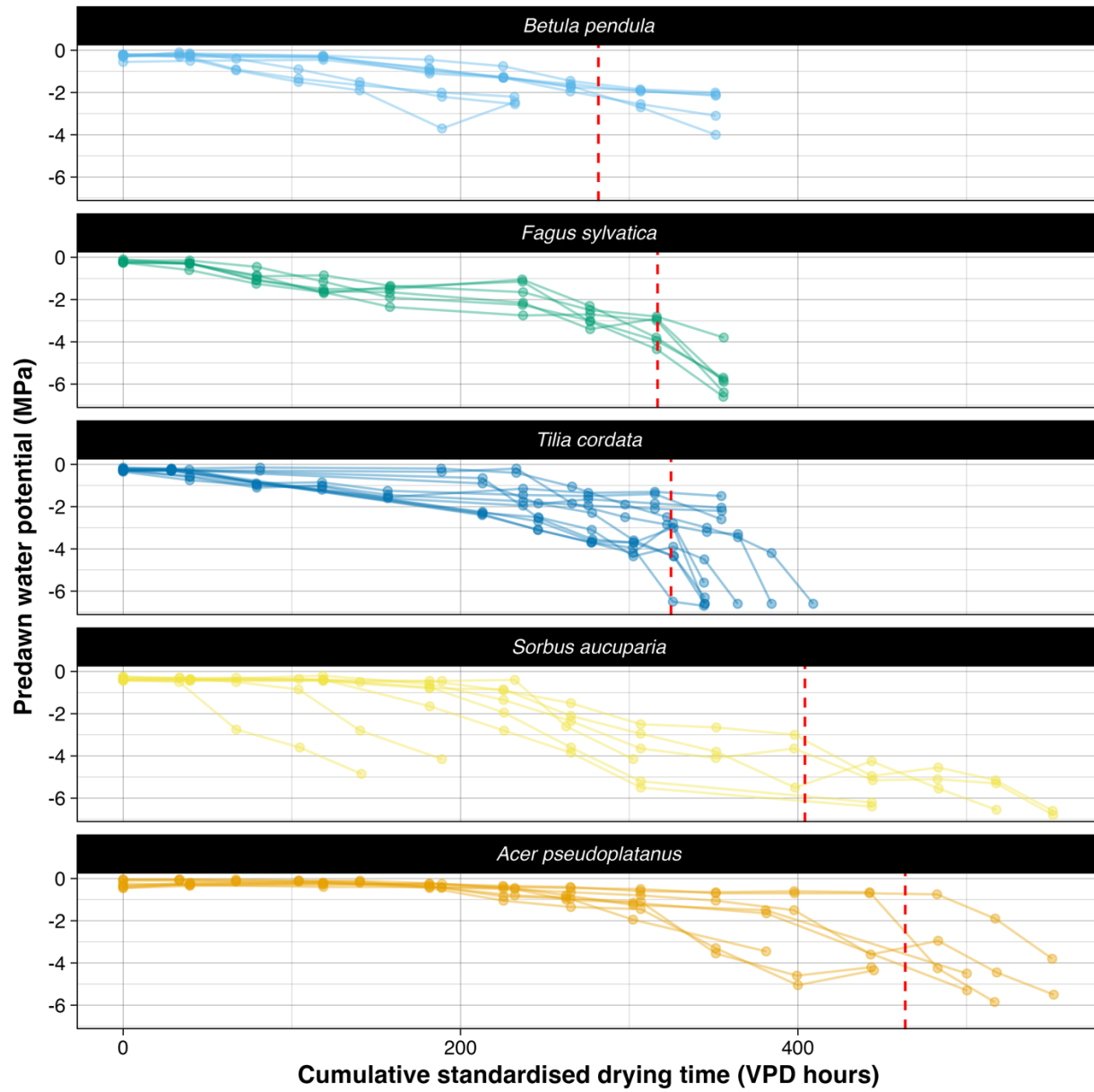


Figure S3.3: Predawn water potential course of dried-out saplings from five temperate tree species. Cumulative drying time was adjusted by daily vapor pressure deficit to account for differences in evaporative demand. Each data point represents a water potential measurement on one plant. Vertical red lines stand for species P_{88} measured on sapling replicates (see Table 3.2).

References:

- Adams HD, Barron-Gafford GA, Minor RL, Gardea AA, Bentley LP, Law DJ, Breshears DD, McDowell NG, Huxman TE (2017) Temperature response surfaces for mortality risk of tree species with future drought. *Environmental Research Letters* 12:115014.
- Allen CD, Breshears DD, McDowell NG (2015) On underestimation of global vulnerability to tree mortality and forest die-off from hotter drought in the Anthropocene. *Ecosphere* 6:129.
- Allen CD, Macalady AK, Chenchouni H, Bachelet D, McDowell N, Vennetier M, Kitzberger T, Rigling A, Breshears DD, Hogg EH (Ted), Gonzalez P, Fensham R, Zhang Z, Castro J, Demidova N, Lim J-H, Allard G, Running SW, Semerci A, Cobb N (2010) A global overview of drought and heat-induced tree mortality reveals emerging climate change risks for forests. *Forest Ecology and Management* 259:660–684.
- Anderegg WRL, Kane JM, Anderegg LDL (2013) Consequences of widespread tree mortality triggered by drought and temperature stress. *Nature Climate Change* 3:30–36.
- Arend M, Link RM, Patthey R, Hoch G, Schuldt B, Kahmen A (2021) Rapid hydraulic collapse as cause of drought-induced mortality in conifers. *Proceedings of the National Academy of Sciences* 118:e2025251118.
- Aspelmeier S, Leuschner C (2004) Genotypic variation in drought response of silver birch (*Betula pendula*): leaf water status and carbon gain. *Tree Physiology* 24:517–528.
- Barnard DM, Meinzer FC, Lachenbruch B, Mcculloh KA, Johnson DM, Woodruff DR (2011) Climate-related trends in sapwood biophysical properties in two conifers: avoidance of hydraulic dysfunction through coordinated adjustments in xylem efficiency, safety and capacitance. *Plant, Cell & Environment* 34:643–654.
- Bartlett MK, Klein T, Jansen S, Choat B, Sack L (2016) The correlations and sequence of plant stomatal, hydraulic, and wilting responses to drought. *Proceedings of the National Academy of Sciences* 113:13098–13103.
- Bartlett MK, Scoffoni C, Ardy R, Zhang Y, Sun S, Cao K, Sack L (2012a) Rapid determination of comparative drought tolerance traits: using an osmometer to predict turgor loss point. *Methods in Ecology and Evolution* 3:880–888.
- Bartlett MK, Scoffoni C, Sack L (2012b) The determinants of leaf turgor loss point and prediction of drought tolerance of species and biomes: a global meta-analysis: Drivers of plant drought tolerance. *Ecology Letters* 15:393–405.
- Bartlett MK, Zhang Y, Kreidler N, Sun S, Ardy R, Cao K, Sack L (2014) Global analysis of plasticity in turgor loss point, a key drought tolerance trait. *Ecology Letters* 17:1580–1590.
- Beikircher B, Sack L, Ganthaler A, Losso A, Mayr S (2021) Hydraulic-stomatal coordination in tree seedlings: tight correlation across environments and ontogeny in *Acer pseudoplatanus*. *New Phytologist* 232:1297–1310.
- Blackman CJ, Creek D, Maier C, Aspinwall MJ, Drake JE, Pfautsch S, O’Grady A, Delzon S, Medlyn BE, Tissue DT, Choat B (2019a) Drought response strategies and hydraulic traits

- contribute to mechanistic understanding of plant dry-down to hydraulic failure. *Tree Physiology* 39:910–924.
- Blackman CJ, Li X, Choat B, Rymer PD, De Kauwe MG, Duursma RA, Tissue DT, Medlyn BE (2019b) Desiccation time during drought is highly predictable across species of *Eucalyptus* from contrasting climates. *New Phytologist* 224:632–643.
- Blackman CJ, Pfautsch S, Choat B, Delzon S, Gleason SM, Duursma RA (2016) Toward an index of desiccation time to tree mortality under drought: Desiccation time to tree mortality. *Plant, Cell & Environment* 39:2342–2345.
- Brodribb TJ, Cochard H (2009) Hydraulic Failure Defines the Recovery and Point of Death in Water-Stressed Conifers. *Plant Physiology* 149:575–584.
- Brodribb TJ, Holbrook NM, Edwards EJ, Gutierrez MV (2003) Relations between stomatal closure, leaf turgor and xylem vulnerability in eight tropical dry forest trees. *Plant, Cell & Environment* 26:443–450.
- Brodribb TJ, McAdam SAM (2013) Abscisic Acid Mediates a Divergence in the Drought Response of Two Conifers. *Plant Physiology* 162:1370–1377.
- Bueno A, Alfarhan A, Arand K, Burghardt M, Deininger A-C, Hedrich R, Leide J, Seufert P, Staiger S, Riederer M (2019) Effects of temperature on the cuticular transpiration barrier of two desert plants with water-spender and water-saver strategies. *Journal of Experimental Botany* 70:1613–1625.
- Challis A, Blackman C, Ahrens C, Medlyn B, Rymer P, Tissue D (2022) Adaptive plasticity in plant traits increases time to hydraulic failure under drought in a foundation tree. *Tree Physiology* 42:708–721.
- Chen Z, Zhang Y, Yuan W, Zhu S, Pan R, Wan X, Liu S (2021) Coordinated variation in stem and leaf functional traits of temperate broadleaf tree species in the isohydric–anisohydric spectrum. *Tree Physiology* 41:1601–1610.
- Choat B, Brodribb TJ, Brodersen CR, Duursma RA, López R, Medlyn BE (2018) Triggers of tree mortality under drought. *Nature* 558:531–539.
- Cochard H, Damour G, Bodet C, Tharwat I, Poirier M, Améglio T (2005) Evaluation of a new centrifuge technique for rapid generation of xylem vulnerability curves. *Physiologia Plantarum* 124:410–418.
- De Baerdemaeker NJF, Salomón RL, De Roo L, Steppe K (2017) Sugars from woody tissue photosynthesis reduce xylem vulnerability to cavitation. *New Phytologist* 216:720–727.
- De Swaef T, Pieters O, Appeltans S, Borra-Serrano I, Coudron W, Couvreur V, Garré S, Lootens P, Nicolai B, Pols L, Saint Cast C, Šalagovič J, Van Haeverbeke M, Stock M, wyffels F (2022) On the pivotal role of water potential to model plant physiological processes. *in silico Plants* 4:diab038.
- Domec J-C, Gartner BL (2003) Relationship between growth rates and xylem hydraulic characteristics in young, mature and old-growth ponderosa pine trees. *Plant, Cell & Environment* 26:471–483.

- Donoghue JR (2004) Implementing Shaffer's multiple comparison procedure for a large number of groups. *Recent Developments in Multiple Comparison Procedures* 47:1–24.
- Duursma RA, Blackman CJ, Lopéz R, Martin-StPaul NK, Cochard H, Medlyn BE (2019) On the minimum leaf conductance: its role in models of plant water use, and ecological and environmental controls. *New Phytologist* 221:693–705.
- Epila J, De Baerdemaeker NJF, Vergeynst LL, Maes WH, Beeckman H, Steppe K (2017) Capacitive water release and internal leaf water relocation delay drought-induced cavitation in African *Maesopsis eminii*. *Tree Physiology* 37:481–490.
- Farrell C, Szota C, Arndt SK (2017) Does the turgor loss point characterize drought response in dryland plants? *Plant, Cell & Environment* 40:1500–1511.
- Feng X, Ackerly DD, Dawson TE, Manzoni S, McLaughlin B, Skelton RP, Vico G, Weitz AP, Thompson SE (2019) Beyond isohydricity: The role of environmental variability in determining plant drought responses. *Plant, Cell & Environment* 42:1104–1111.
- Fu X, Meinzer FC (2019) Metrics and proxies for stringency of regulation of plant water status (iso/anisohdry): a global data set reveals coordination and trade-offs among water transport traits. *Tree Physiology* 39:122–134.
- Fu X, Meinzer FC, Woodruff DR, Liu Y-Y, Smith DD, McCulloh KA, Howard AR (2019) Coordination and trade-offs between leaf and stem hydraulic traits and stomatal regulation along a spectrum of isohydry to anisohydry. *Plant, Cell & Environment* 42:2245–2258.
- Gao R, Shi X, Wang JR (2017) Comparative studies of the response of larch and birch seedlings from two origins to water deficit. *New Zealand Journal of Forestry Science* 47:14.
- Gillner S, Korn S, Hofmann M, Roloff A (2017) Contrasting strategies for tree species to cope with heat and dry conditions at urban sites. *Urban Ecosystems* 20:853–865.
- Hajek P, Link RM, Nock CA, Bauhus J, Gebauer T, Gessler A, Kovach K, Messier C, Paquette A, Saurer M, Scherer-Lorenzen M, Rose L, Schuldt B (2022) Mutually inclusive mechanisms of drought-induced tree mortality. *Global Change Biology* 28:3365–3378.
- Hammond WM, Adams HD (2019) Dying on time: traits influencing the dynamics of tree mortality risk from drought. *Tree Physiology* 39:906–909.
- Hammond WM, Yu K, Wilson LA, Will RE, Anderegg WRL, Adams HD (2019) Dead or dying? Quantifying the point of no return from hydraulic failure in drought-induced tree mortality. *New Phytologist* 223:1834–1843.
- Hartmann H, Link RM, Schuldt B (2021) A whole-plant perspective of isohydry: stem-level support for leaf-level plant water regulation. *Tree Physiology* 41:901–905.
- Hartmann H, Moura CF, Anderegg WRL, Ruehr NK, Salmon Y, Allen CD, Arndt SK, Breshears DD, Davi H, Galbraith D, Ruthrof KX, Wunder J, Adams HD, Bloemen J, Cailleret M, Cobb R, Gessler A, Grams TEE, Jansen S, Kautz M, Lloret F, O'Brien M (2018) Research frontiers for improving our understanding of drought-induced tree and forest mortality. *New Phytologist* 218:15–28.

- He D, Biswas SR, Xu M-S, Yang T-H, You W-H, Yan E-R (2021) The importance of intraspecific trait variability in promoting functional niche dimensionality. *Ecography* 44:380–390.
- Hochberg U, Rockwell FE, Holbrook NM, Cochard H (2018) Iso/Anisohdry: A Plant–Environment Interaction Rather Than a Simple Hydraulic Trait. *Trends in Plant Science* 23:112–120.
- Hochberg U, Windt CW, Ponomarenko A, Zhang Y-J, Gersony J, Rockwell FE, Holbrook NM (2017) Stomatal closure, basal leaf embolism, and shedding protect the hydraulic integrity of grape stems. *Plant Physiology* 174:764–775.
- Kerstiens G (1996) Cuticular water permeability and its physiological significance. *Journal of Experimental Botany* 47:1813–1832.
- Klein T (2014) The variability of stomatal sensitivity to leaf water potential across tree species indicates a continuum between isohydric and anisohydric behaviours. *Functional Ecology* 28:1313–1320.
- Klein T, Yakir D, Buchmann N, Grünzweig JM (2014) Towards an advanced assessment of the hydrological vulnerability of forests to climate change-induced drought. *New Phytologist* 201:712–716.
- Köcher P, Gebauer T, Horna V, Leuschner C (2009) Leaf water status and stem xylem flux in relation to soil drought in five temperate broad-leaved tree species with contrasting water use strategies. *Annals of Forest Science* 66:101–101.
- Köcher P, Horna V, Leuschner C (2013) Stem water storage in five coexisting temperate broad-leaved tree species: significance, temporal dynamics and dependence on tree functional traits. *Tree Physiology* 33:817–832.
- Kotowska MM, Link RM, Röhl A, Hertel D, Hölscher D, Waite P-A, Moser G, Tjoa A, Leuschner C, Schuldt B (2021) Effects of Wood Hydraulic Properties on Water Use and Productivity of Tropical Rainforest Trees. *Frontiers in Forests and Global Change* 3:598759.
- Kumar M, Waite P-A, Paligi SS, Schuldt B (2022) Influence of Juvenile Growth on Xylem Safety and Efficiency in Three Temperate Tree Species. *Forests* 13:909.
- Leuschner C (2020) Drought response of European beech (*Fagus sylvatica* L.)—A review. *Perspectives in Plant Ecology, Evolution and Systematics* 47:125576.
- Leuschner C, Schipka F, Backes K (2022) Stomatal regulation and water potential variation in European beech: challenging the iso/anisohdry concept. *Tree Physiology* 42:365–378.
- Leuschner C, Wedde P, Lübke T (2019) The relation between pressure–volume curve traits and stomatal regulation of water potential in five temperate broadleaf tree species. *Annals of Forest Science* 76:1–14.
- Li S, Feifel M, Karimi Z, Schuldt B, Choat B, Jansen S (2016) Leaf gas exchange performance and the lethal water potential of five European species during drought. *Tree Physiology* 36:179–192.

- Li X, Blackman CJ, Choat B, Duursma RA, Rymer PD, Medlyn BE, Tissue DT (2018) Tree hydraulic traits are coordinated and strongly linked to climate-of-origin across a rainfall gradient. *Plant, Cell & Environment* 41:646–660.
- Li X, Blackman CJ, Peters JMR, Choat B, Rymer PD, Medlyn BE, Tissue DT (2019) More than iso/anisohdry: Hydroscares integrate plant water use and drought tolerance traits in 10 eucalypt species from contrasting climates. *Functional Ecology* 33:1035–1049.
- Li X, Xi B, Wu X, Choat B, Feng J, Jiang M, Tissue D (2022) Unlocking Drought-Induced Tree Mortality: Physiological Mechanisms to Modeling. *Frontiers in Plant Science* 13.
- Mantova M, Herbette S, Cochard H, Torres-Ruiz JM (2022) Hydraulic failure and tree mortality: from correlation to causation. *Trends in Plant Science* 27:335–345.
- Martínez-Vilalta J, Garcia-Fornier N (2017) Water potential regulation, stomatal behaviour and hydraulic transport under drought: deconstructing the iso/anisohydric concept. *Plant, Cell & Environment* 40:962–976.
- Martínez-Vilalta J, Poyatos R, Aguadé D, Retana J, Mencuccini M (2014) A new look at water transport regulation in plants. *New Phytologist* 204:105–115.
- Martin-StPaul N, Delzon S, Cochard H (2017) Plant resistance to drought depends on timely stomatal closure. *Ecology Letters* 20:1437–1447.
- McAdam SAM, Brodribb TJ (2014) Separating Active and Passive Influences on Stomatal Control of Transpiration. *Plant Physiology* 164:1578–1586.
- McAdam SAM, Susmilch FC, Brodribb TJ (2016) Stomatal responses to vapour pressure deficit are regulated by high speed gene expression in angiosperms. *Plant, Cell & Environment* 39:485–491.
- McCulloh KA, Domec J-C, Johnson DM, Smith DD, Meinzer FC (2019) A dynamic yet vulnerable pipeline: Integration and coordination of hydraulic traits across whole plants. *Plant, Cell & Environment* 42:2789–2807.
- McDowell NG, Sapes G, Pivovarov A, Adams HD, Allen CD, Anderegg WRL, Arend M, Breshears DD, Brodribb T, Choat B, Cochard H, De Cáceres M, De Kauwe MG, Grossiord C, Hammond WM, Hartmann H, Hoch G, Kahmen A, Klein T, Mackay DS, Mantova M, Martínez-Vilalta J, Medlyn BE, Mencuccini M, Nardini A, Oliveira RS, Sala A, Tissue DT, Torres-Ruiz JM, Trowbridge AM, Trugman AT, Wiley E, Xu C (2022) Mechanisms of woody-plant mortality under rising drought, CO₂ and vapour pressure deficit. *Nature Reviews Earth & Environment* 3:294–308.
- Meinzer FC, James SA, Goldstein G, Woodruff D (2003) Whole-tree water transport scales with sapwood capacitance in tropical forest canopy trees. *Plant, Cell & Environment* 26:1147–1155.
- Meinzer FC, Woodruff DR, Marias DE, Smith DD, McCulloh KA, Howard AR, Magedman AL (2016) Mapping ‘hydroscares’ along the iso- to anisohydric continuum of stomatal regulation of plant water status. *Ecology Letters* 19:1343–1352.
- Mitchell PJ, O’Grady AP, Tissue DT, Worledge D, Pinkard EA (2014) Co-ordination of growth, gas exchange and hydraulics define the carbon safety margin in tree species with contrasting drought strategies. *Tree Physiology* 34:443–458.

- Moser A, Rötzer T, Pauleit S, Pretzsch H (2016) The Urban Environment Can Modify Drought Stress of Small-Leaved Lime (*Tilia cordata* Mill.) and Black Locust (*Robinia pseudoacacia* L.). *Forests* 7:71.
- Moser-Reischl A, Rahman MA, Pauleit S, Pretzsch H, Rötzer T (2019) Growth patterns and effects of urban micro-climate on two physiologically contrasting urban tree species. *Landscape and Urban Planning* 183:88–99.
- Nolf M, Creek D, Duursma R, Holtum J, Mayr S, Choat B (2015) Stem and leaf hydraulic properties are finely coordinated in three tropical rain forest tree species. *Plant, Cell & Environment* 38:2652–2661.
- O'Brien MJ, Engelbrecht BMJ, Joswig J, Pereyra G, Schuldt B, Jansen S, Kattge J, Landhäuser SM, Levick SR, Preisler Y, Väinänen P, Macinnis-Ng C (2017) A synthesis of tree functional traits related to drought-induced mortality in forests across climatic zones. *Journal of Applied Ecology* 54:1669–1686.
- Pammenter NW, Van der Willigen C (1998) A mathematical and statistical analysis of the curves illustrating vulnerability of xylem to cavitation. *Tree Physiology* 18:589–593.
- Peng S, Chen A, Xu L, Cao C, Fang J, Myneni RB, Pinzon JE, Tucker CJ, Piao S (2011) Recent change of vegetation growth trend in China. *Environmental Research Letters* 6:044027.
- Piepho H-P (2004) An Algorithm for a Letter-Based Representation of All-Pairwise Comparisons. *Journal of Computational and Graphical Statistics* 13:456–466.
- Pinheiro J, Bates D, DebRoy S, Sarkar D, and R Core Team (2020). nlme: linear and nonlinear mixed effects models. R package version 3.1–145.
- Pivovarov AL, Cook VMW, Santiago LS (2018) Stomatal behaviour and stem xylem traits are coordinated for woody plant species under exceptional drought conditions. *Plant, Cell & Environment* 41:2617–2626.
- Pivovarov AL, Pasquini SC, De Guzman ME, Alstad KP, Stemke JS, Santiago LS (2016) Multiple strategies for drought survival among woody plant species. *Functional Ecology* 30:517–526.
- Puglielli G, Hutchings MJ, Laanisto L (2021) The triangular space of abiotic stress tolerance in woody species: a unified trade-off model. *New Phytologist* 229:1354–1362.
- R Development Core Team (2021) *R: a language and environment for statistical computing*. Vienna, Austria: R Foundation for Statistical Computing. <https://www.R-project.org/>.
- Ramesha MN, Link RM, Paligi SS, Hertel D, Röhl A, Hölscher D, Schuldt B (2022) Variability in growth-determining hydraulic wood and leaf traits in *Melia dubia* across a steep water availability gradient in southern India. *Forest Ecology and Management* 505:119875.
- Reich PB (2014) The world-wide ‘fast–slow’ plant economics spectrum: a traits manifesto. *Journal of Ecology* 102:275–301.
- Robson TM, Hartikainen SM, Aphalo PJ (2015) How does solar ultraviolet-B radiation improve drought tolerance of silver birch (*Betula pendula* Roth.) seedlings? *Plant, Cell & Environment* 38:953–967.

- Rodriguez-Dominguez CM, Buckley TN, Egea G, de Cires A, Hernandez-Santana V, Martorell S, Diaz-Espejo A (2016) Most stomatal closure in woody species under moderate drought can be explained by stomatal responses to leaf turgor. *Plant, Cell & Environment* 39:2014–2026.
- Rogiers SY, Greer DH, Hatfield JM, Hutton RJ, Clarke SJ, Hutchinson PA, Somers A (2012) Stomatal response of an anisohydric grapevine cultivar to evaporative demand, available soil moisture and abscisic acid. *Tree Physiology* 32:249–261.
- Roman DT, Novick KA, Brzostek ER, Dragoni D, Rahman F, Phillips RP (2015) The role of isohydric and anisohydric species in determining ecosystem-scale response to severe drought. *Oecologia* 179:641–654.
- Rötzer T, Häberle KH, Kallenbach C, Matyssek R, Schütze G, Pretzsch H (2017) Tree species and size drive water consumption of beech/spruce forests - a simulation study highlighting growth under water limitation. *Plant and Soil* 418:337–356.
- Salvi AM, Gosetti SG, Smith DD, Adams MA, Givnish TJ, McCulloh KA (2022) Hydroscares, hydroscape plasticity and relationships to functional traits and mesophyll photosynthetic sensitivity to leaf water potential in *Eucalyptus* species. *Plant, Cell & Environment* 45:2573–2588.
- Santiago LS, De Guzman ME, Baraloto C, Vogenberg JE, Brodie M, Hérault B, Fortunel C, Bonal D (2018) Coordination and trade-offs among hydraulic safety, efficiency and drought avoidance traits in Amazonian rainforest canopy tree species. *New Phytologist* 218:1015–1024.
- Sapes G, Roskilly B, Dobrowski S, Maneta M, Anderegg WRL, Martinez-Vilalta J, Sala A (2019) Plant water content integrates hydraulics and carbon depletion to predict drought-induced seedling mortality. *Tree Physiology* 39:1300–1312.
- Schindelin J, Arganda-Carreras I, Frise E, Kaynig V, Longair M, Pietzsch T, Preibisch S, Rueden C, Saalfeld S, Schmid B, Tinevez J-Y, White DJ, Hartenstein V, Eliceiri K, Tomancak P, Cardona A (2012) Fiji: an open-source platform for biological-image analysis. *Nature Methods* 9:676–682.
- Scholz FG, Phillips NG, Bucci SJ, Meinzer FC, Goldstein G (2011) Hydraulic Capacitance: Biophysics and Functional Significance of Internal Water Sources in Relation to Tree Size. In: Meinzer FC, Lachenbruch B, Dawson TE (eds) *Size- and Age-Related Changes in Tree Structure and Function*. Springer Netherlands, Dordrecht, pp 341–361.
- Schönbeck LC, Schuler P, Lehmann MM, Mas E, Mekarni L, Pivovarov AL, Turberg P, Grossiord C (2022) Increasing temperature and vapour pressure deficit lead to hydraulic damages in the absence of soil drought. *Plant, Cell & Environment* 45:3275–3289.
- Schuldt B, Buras A, Arend M, Vitasse Y, Beierkuhnlein C, Damm A, Gharun M, Grams TEE, Hauck M, Hajek P, Hartmann H, Hiltbrunner E, Hoch G, Holloway-Phillips M, Körner C, Larysch E, Lübke T, Nelson DB, Rammig A, Rigling A, Rose L, Ruehr NK, Schumann K, Weiser F, Werner C, Wohlgemuth T, Zang CS, Kahmen A (2020) A first assessment of the impact of the extreme 2018 summer drought on Central European forests. *Basic and Applied Ecology* 45:86–103.

- Schuster A-C, Burghardt M, Riederer M (2017) The ecophysiology of leaf cuticular transpiration: are cuticular water permeabilities adapted to ecological conditions? *Journal of Experimental Botany* 68:5271–5279.
- Skelton RP, Anderegg LDL, Diaz J, Kling MM, Papper P, Lamarque LJ, Delzon S, Dawson TE, Ackerly DD (2021) Evolutionary relationships between drought-related traits and climate shape large hydraulic safety margins in western North American oaks. *Proceedings of the National Academy of Sciences* 118:e2008987118.
- Skelton RP, West AG, Dawson TE (2015) Predicting plant vulnerability to drought in biodiverse regions using functional traits. *Proceedings of the National Academy of Sciences* 112:5744–5749.
- Sperry JS, Meinzer FC, McCULLOH KA (2008) Safety and efficiency conflicts in hydraulic architecture: scaling from tissues to trees. *Plant, Cell & Environment* 31:632–645.
- Sperry JS, Venturas MD, Anderegg WRL, Mencuccini M, Mackay DS, Wang Y, Love DM (2017) Predicting stomatal responses to the environment from the optimization of photosynthetic gain and hydraulic cost: A stomatal optimization model. *Plant, Cell & Environment* 40:816–830.
- Steppe K, Lemeur R (2007) Effects of ring-porous and diffuse-porous stem wood anatomy on the hydraulic parameters used in a water flow and storage model. *Tree Physiology* 27:43–52.
- Tardieu F, Simonneau T (1998) Variability among species of stomatal control under fluctuating soil water status and evaporative demand: modelling isohydric and anisohydric behaviours. *Journal of Experimental Botany* 49:419–432.
- Urli M, Porte AJ, Cochard H, Guengant Y, Burrett R, Delzon S (2013) Xylem embolism threshold for catastrophic hydraulic failure in angiosperm trees. *Tree Physiology* 33:672–683.
- Vergeynst LL, Dierick M, Bogaerts JAN, Cnudde V, Steppe K (2015) Cavitation: a blessing in disguise? New method to establish vulnerability curves and assess hydraulic capacitance of woody tissues. *Tree Physiology* 35:400–409.
- Vincent Q. Vu (2011). ggbiplot: A ggplot2 based biplot. R package version 0.55. <http://github.com/vqv/ggbiplot>.
- Vogt UK (2001) Hydraulic vulnerability, vessel refilling, and seasonal courses of stem water potential of *Sorbus aucuparia* L. and *Sambucus nigra* L. *Journal of Experimental Botany* 52:1527–1536.
- Weemstra M, Mommer L, Visser EJW, Ruijven J van, Kuyper TW, Mohren GMJ, Sterck FJ (2016) Towards a multidimensional root trait framework: a tree root review. *New Phytologist* 211:1159–1169.
- Wei T and Simko V (2021). R package 'corrplot': Visualization of a Correlation Matrix (Version 0.92). Available from <https://github.com/taiyun/corrplot>.
- Wolfe BT (2020) Bark water vapour conductance is associated with drought performance in tropical trees. *Biology Letters* 16:20200263.

Wright IJ, Reich PB, Westoby M, Ackerly DD, Baruch Z, Bongers F, Cavender-Bares J, Chapin T, Cornelissen JHC, Diemer M, Flexas J, Garnier E, Groom PK, Gulias J, Hikosaka K, Lamont BB, Lee T, Lee W, Lusk C, Midgley JJ, Navas M-L, Niinemets Ü, Oleksyn J, Osada N, Poorter H, Poot P, Prior L, Pyankov VI, Roumet C, Thomas SC, Tjoelker MG, Veneklaas EJ, Villar R (2004) The worldwide leaf economics spectrum. *Nature* 428:821–827.

Zhang Y, Oren R, Kang S (2012) Spatiotemporal variation of crown-scale stomatal conductance in an arid *Vitis vinifera* L. cv. Merlot vineyard: direct effects of hydraulic properties and indirect effects of canopy leaf area. *Tree Physiology* 32:262–279.

Chapter-4: Synthesis (General discussion)

4.1 Juvenile growth trade-off with hydraulic efficiency-safety

Plant growth and survival depend on regulating internal water transport and maintaining tissue water balance under different environmental conditions. This study found that all plants grew faster in normal growing conditions than stressed plants. Biomass production (ABI, mg d^{-1}) was more pronounced in the control plants, with an average of 2.8- to 5.3-fold higher (see Chapter-2, Figure 2.2). Our results also indicate that the aboveground biomass allocation was linked to either both or one trait, likely hydraulic safety and efficiency for all three species studied. Furthermore, it is associated with anatomical and leaf traits (Figures 2.4, 2.5, 4.1). The general trend of growth rate linkage with xylem safety-efficiency negotiation across the species is lacking, supporting to the notion of species-specific hydraulic strategies. Across the species, higher biomass allocation (growth) was strongly and positively linked to larger hydraulic efficiency (K_s) in two species (ACPS, SOAU), which is expected to be associated with D_h . On the other hand, a clear pattern of xylem safety (P_{50}) is lacking due to opposite trends; negative association in BEPE and positive in the case of SOAU. The association between hydraulic safety-efficiency is complex and depends on many factors, such as xylem anatomy, plant allometry, and growing environment. Generally, a plant prioritizes hydraulic efficiency over safety may be more susceptible to water stress and vice-versa. If plants prefer to develop more resistance xylem over hydraulic efficiency, growth rates are less likely to be impacted by drought. SOAU's growth rate (Table S2.1) is comparatively less affected among the species under drought due to higher embolism resistance.

In contrast, BEPE with the highest K_s shows a severely affected growth rate due to stress. Efficiency-related traits (K_s and D_h) were linked to higher biomass allocation, which reliably agreed with the previous finding (Fichot *et al.* 2010, Hoeber *et al.* 2014, Gleason *et al.* 2018, Kotowska *et al.* 2021, Ramesha *et al.* 2022). Hydraulic efficiency-safety association likely exists as faster growth often requires a higher hydraulic efficiency attained through larger vessel diameters. The xylem capacity to transport water is directly proportional to the size of the conduit diameter, i.e., scales of the fourth power. However, the growth rate associated with the efficiency-safety trade-off agreement is ambiguous (Domec and Gartner 2003, Wikberg and Ögren 2004, Zhang and Cao 2009, Fichot *et al.* 2011, Fan *et al.* 2012, Hoeber *et al.* 2014, Guet *et al.* 2015, Gleason *et al.* 2016, Hajek *et al.* 2016, Schuldt *et al.* 2016, Eller *et al.* 2018).

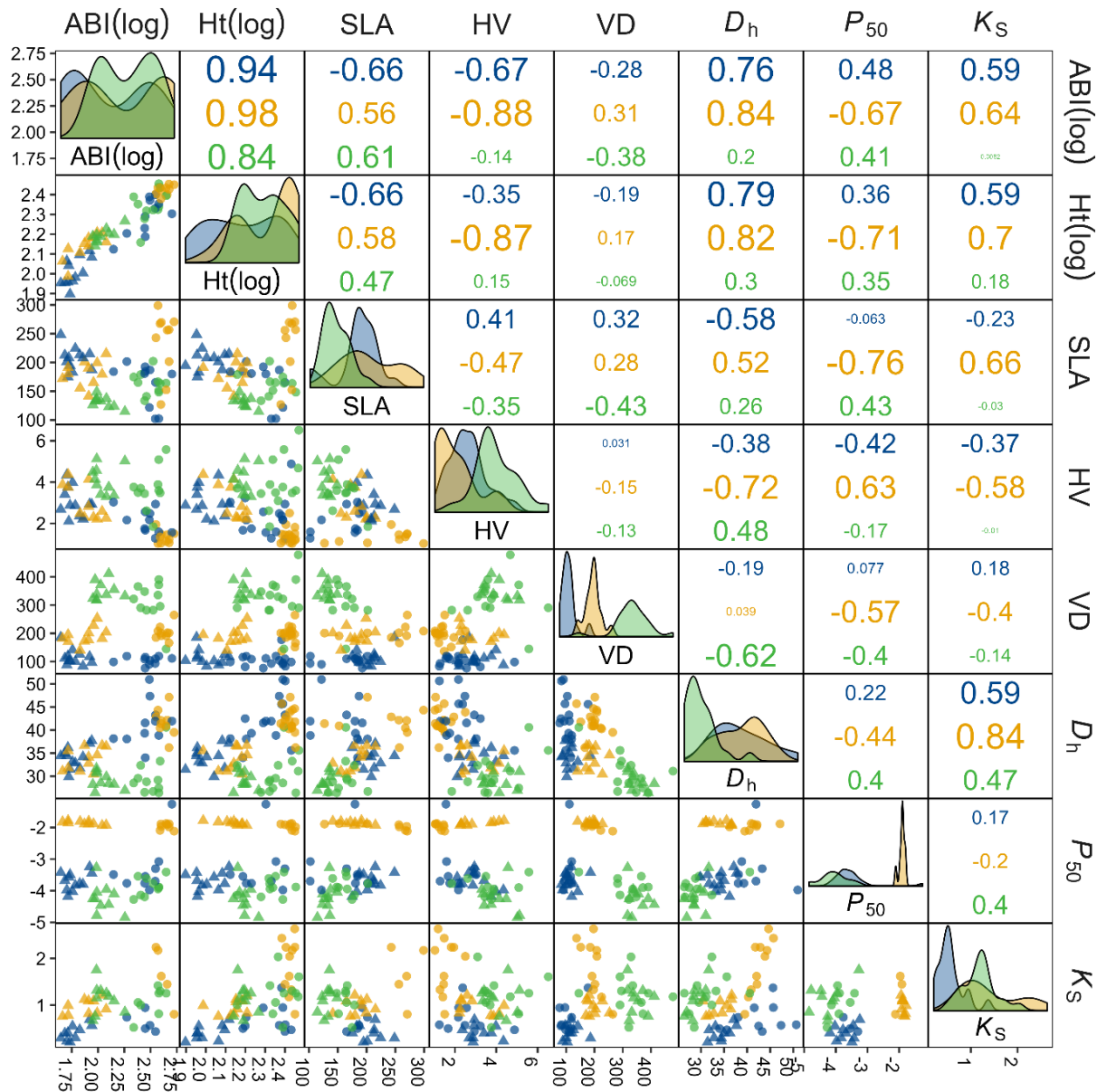


Figure 4.1: Correlation matrix of hydraulic, morphological, and anatomical traits of the three species. Different colours and symbols represent species and treatments (blue: *A. pseudoplatanus*; orange: *B. pendula*; green: *S. aucuparia*; filled circles: control; triangles: stress). Shown are the biomass increment (ABI, mg d^{-1}), the shoot height from ground to uppermost leaf (Ht, cm), the specific leaf area (SLA, $\text{cm}^2 \text{g}^{-1}$), the sapwood-to-leaf area ratio (HV, $10^{-4} \text{m}^2 \text{m}^{-2}$), the vessel density (VD, n mm^{-2}), the hydraulically-weighted vessel diameter (D_h , μm), the xylem pressure at 50% loss of hydraulic conductance (P_{50} , MPa), the specific conductivity (K_s , $\text{kg m}^{-1} \text{MPa}^{-1} \text{s}^{-1}$). The variables ABI and Ht are log-transformed. The three panels plot shows the Pearson correlations (upper triangle), the relation of variables on the x-axis and y-axis with a scatterplot (lower triangle), and the density plots for corresponding variables (diagonal). Figure produced with R package *corrormorant* v. 0.0.0.9007 (<https://github.com/r-link/corrormorant>).

4.2 Xylem safety-efficiency trade-off and anatomical factors

Our results show that wider vessels, associated with higher hydraulic efficiency (K_s), are linked to higher growth rates in control plants than in water-stressed plants. Xylem safety (denoted by P_{50}) signifies the percent loss of conductivity of the stem with increasing xylem pressure (Figure 4.2). Further, anatomical analysis of the studied plants revealed significant differences in vascular arrangement, which is strongly influenced by the environmental conditions in which the plants grew. Specifically, we found that the frequency of wider vessels is consistently higher in the control condition of all species (Figure 4.3). But the contribution of these vessels to the potential hydraulic conductivity (K_P) is considerably higher in ACPS and BEPE than SOAU (Figure 4.4), which has a greater number of narrower vessels and is associated with a considerable contribution to K_P . The higher frequency of smaller vessels under stress suggests that evolutionary trade-offs and phenotypic adaptations occur at the level of wood anatomy. Furthermore, we found that SOAU tends to have a shorter stature (shrub or tree, Vogt 2001) in nature, as smaller plants are known to develop narrower vessels and more drought-resistant xylem networks. Narrow vessels are more resistant to cavitation and provide a smaller vessel area that is less prone to air seeding pressure, which agrees with previous findings (Wheeler *et al.* 2005, Hacke *et al.* 2006, Christman *et al.* 2012). Moreover, SOAU's high wood density indicates a greater investment in xylem vessels. Tree species with higher wood density are more likely to survive drought conditions (Hoffmann *et al.* 2011, Nardini *et al.* 2013, Greenwood *et al.* 2017, Fu and Meinzer 2019, Liang *et al.* 2021).

The xylem efficiency-safety trade-off at the anatomical level has traditionally been assumed (Sperry and Tyree 1990). Empirical evidence shows that wider conduits supported by large areas are more susceptible to water stress-induced cavitation due to the greater likelihood of presenting inter-vessel pits area to low air-seeding pressure (Wheeler *et al.* 2005, Hacke *et al.* 2006, Christman *et al.* 2009, 2012). On this note, larger vessels are more likely to increase the risks of water-conducting tissue to the cavitation (forming air emboli in the xylem that can disrupt water transport) to the decline of the water potential. Additionally, wider vessels can have thinner and more porous pit membranes that could increase the risk of water-conducting tissue to cavitation (Scholz *et al.* 2013, Li *et al.* 2016b, Schuldt *et al.* 2016, Hacke *et al.* 2017). The trade-off relationship is influenced by vessel length and grouping, pit fraction, and contact fraction (Wheeler *et al.* 2005, Loepfe *et al.* 2007). So, thicker membranes, shallower chambers, and fewer and smaller apertures are some features of the pit that could support greater cavitation (Lens *et al.*

2011). Further, wider conduits incline to develop thicker inter-vessel pit membranes to safeguard water transport integrity, which could be a reason for the weak trade-off safety-efficiency in angiosperms (Gleason *et al.* 2016). The safety-efficiency trade-off most likely influenced by various wood anatomical features, not only vessel diameter (Schuldt *et al.* 2016).

In plants, a trade-off between hydraulic efficiency-safety could be beneficial for optimizing xylem capacity to achieve better performance. However, achieving xylem optimization is challenging because it requires balancing extreme frugality borders on a scale of functional traits that facilitate drought-tolerance mechanisms. On a parsimonious bottleneck, plants often compromise one trait over another to promote growth and survival under stress.

Our study supports the notion that different evolutionary pathways exist to achieve xylem safety and efficiency and that the trade-off may be species- and scale-dependent (Lübbe *et al.* 2022). Additionally, xylem safety appears to be a conservative trait (cf. Rosas *et al.* 2019, Fuchs *et al.* 2021), while hydraulic efficiency is more plastic to meet the water demand of higher growth with the supported foliage. Xylem efficiency and safety are expected to reflect ecological and evolutionary differences among species (Gleason *et al.* 2016). Considering evolutionary adaptation, the traits trade-off may likely exist for optimizing the xylem function within the growing environment (Hacke *et al.* 2006, Gleason *et al.* 2016), and optimal xylem conduits should have a high conductive efficiency (Franklin *et al.* 2022). However, empirical evidence is equivocal, and recent studies could find only weak or no relations between hydraulic efficiency and safety (Maherali *et al.* 2006, Hajek *et al.* 2014, Gleason *et al.* 2016, Schumann *et al.* 2019, Liu *et al.* 2021).

4.3 Adjustment of leaf traits in response to environmental stress

Leaves trait modifications in response to drought are perhaps the most complex as they control the gas exchange through stomatal regulation. However, understanding the association of functional leaf traits with hydraulic traits is limited. Specific leaf area (SLA) evaluates the light-intercepting leaf area per unit of dry leaf mass. A species with a high SLA tends to have thinner and lighter leaves. Further, in order to control supply capacity per unit of water demand, allocation to sapwood cross-sectional area relative to leaf area (Huber value, HV) is a crucial element of plant hydraulic architecture (Mencuccini and Bonosi 2001). On this note, leaf-related traits exhibited

inevitable differential responses to water stress. This study (Chapter 2, Table S2.1, and Figure 4.1) shows that the water deficit setting considerably influences the specific leaf area (SLA) and the Huber value (HV), i.e., the sapwood-to-leaf area ratio. Growth rates are negatively associated with HV and decrease consistently with a water deficit. In contrast, SLA is progressively linked to the growth rate in two species but adversely with ACPS.

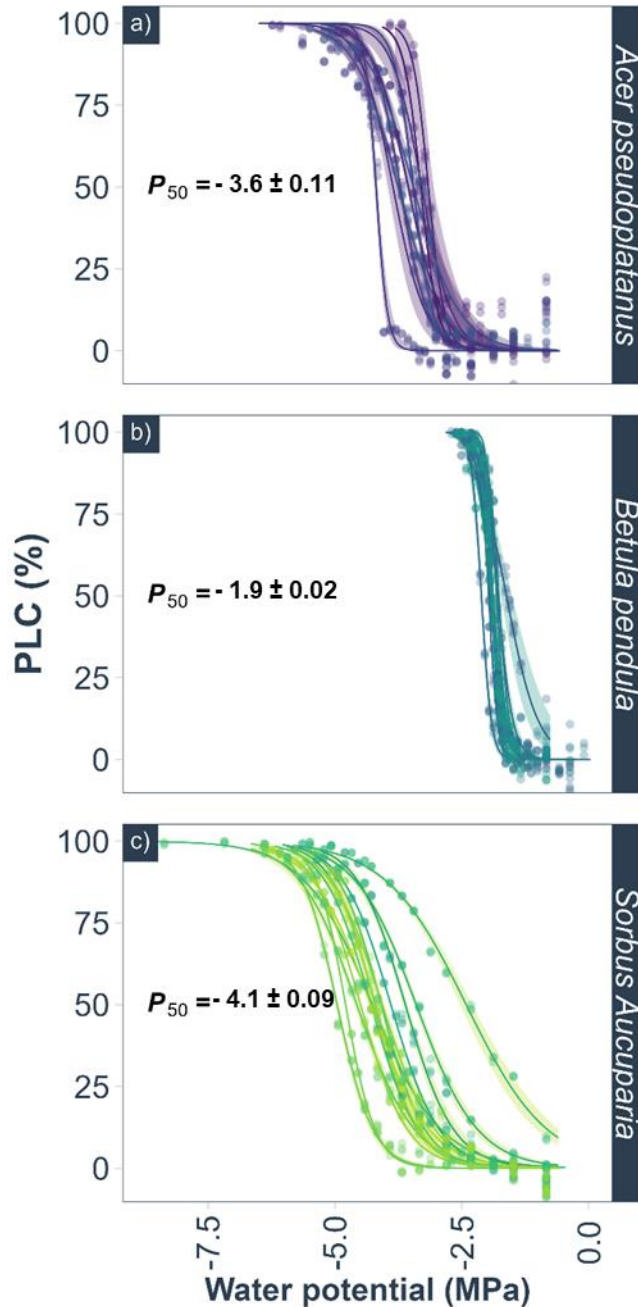


Figure 4.2: Vulnerability curves depicting the percent loss of conductivity (PLC) of stem samples against decreasing xylem pressure for each species. Shown are the observed PLC and the predicted vulnerability curves with their bootstrapped $\pm 95\%$ confidence (shaded areas) and the mean P_{50} of the corresponding species (middle left). Measured species were the three temperate tree species such as *A. Pseudoplatanus* (a); *B. pendula* (b); and *S. aucuparia* (c).

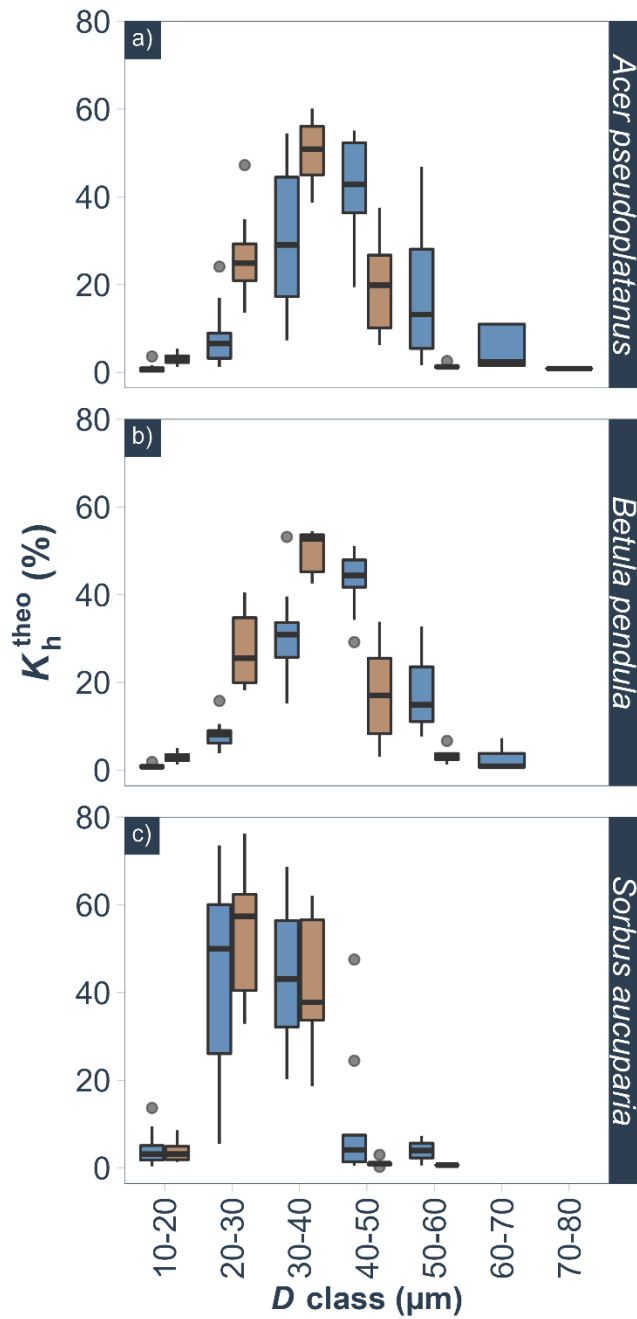


Figure 4.3: Boxplot showing the proportional contribution of different vessels class to the theoretical conductivity of sapwood for three temperate tree species: *A. pseudoplatanus* (a), *B. pendula* (b), and *S. aucuparia* (c). Different colours indicate the treatment levels: Blue (control) and brown (stress).

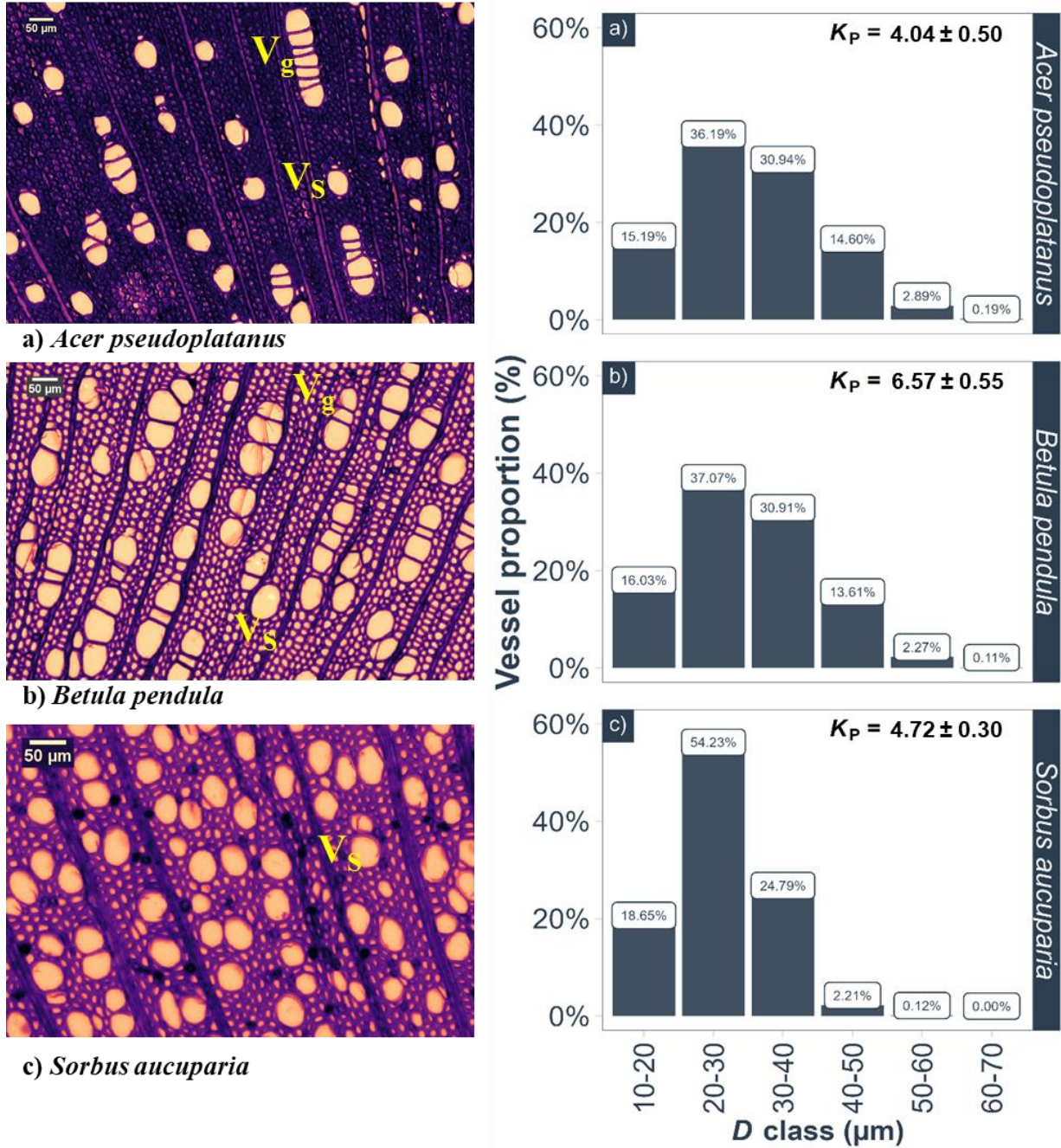


Figure 4.4: Anatomical sections of the stems and vessels distribution at different diameter categories show the species' distinctive vascular architecture. Bar graph showing the proportion of the vessel (%) of diameter class for three temperate tree species: *A. pseudoplatanus* (a), *B. pendula* (b), and *S. aucuparia* (c). Potential conductivity (K_p , mean \pm SE) are given for the species, respectively: 4.04 ± 0.5 , 6.57 ± 0.55 , and 4.72 ± 0.30 $\text{kg m}^{-1} \text{s}^{-1} \text{MPa}^{-1}$ (top right). Scales are indicated at 50 μm in each cross-sectional image of sapwood. The species shows two types of vessels (Vg:

Hence, a clear trend is lacking in SLA modification, most likely due to the low number of species covered by these studies. The lower SLA is recorded with stress conditions in two species, whereas it is the opposite trend in the case of ACPS. Across the species, BEPE has a higher SLA and tends to invest less resources in leaf structure, which is likely more vulnerable to low water availability. This agrees with the findings that low leaf dry mass investment per unit of leaf area is linked to high K_s and high embolism vulnerability (Rosas *et al.* 2019). On the contrary, ACPS and SOAU have a lower SLA, providing more resistance to cavitation under stress.

Furthermore, leaf size also decreased with stress conditions, consistent with previous findings that showed a decrease in leaf size and SLA with decreasing water availability (Poorter *et al.* 2012, Wright *et al.* 2017, Zhu *et al.* 2022). In addition, the leaf traits (dimension, SLA, HV) are more strongly influenced by environmental factors than xylem traits (Bartlett *et al.* 2016, Powell *et al.* 2017, Weithmann *et al.* 2022). However, in beech, the opposite trend (Meier and Leuschner 2008) or no relation (Schuldt *et al.* 2016) was recorded at the intraspecific level. Thus, the plasticity of leaf-level traits to water deficits may provide valuable insights into species' growth and performance. However, it is likely to depend on species-specific differential drought resistance mechanisms.

4.4 Stomatal stringency and relative degree of isohydry

Stomatal stringency is crucial in determining drought resistance strategies on the spectrum of iso-anisohydric. In this connection, stomatal regulation of plant water potential (Ψ_x) is paramount to discerning species' survival ability. The relative degree of stomatal stringency represents the two extremes of plant water regulation strategies. Isohydric plants rapidly lower their stomatal conductance, keeping the water potential in their cells essentially constant and delaying xylem cavitation in response to drought. Yet, it also reduces carbon uptake (Tardieu and Simonneau 1998). Anisohydric plants, on the other hand, typically maintain increased stomatal conductance with decreasing water potential, preserving carbon assimilation but incurring a higher risk of embolism formation in their xylem conduits (Martínez-Vilalta and Garcia-Forner 2017, Meinzer *et al.* 2017, Hartmann *et al.* 2021). Although it has been highlighted, there is no universally accepted definition of this continuum (reviewed in Hochberg *et al.* 2018, Feng *et al.* 2019).

4.4.1 Metrics and proxies for plant water potential regulation

The isohydricity indices used for species characterization have been extensively reviewed, and various metrics have been established (Hochberg *et al.* 2018, Feng *et al.* 2019). For example, the aptitude of stomatal conductance and their closure during stress could be underpinning the difference between isohydric and anisohydric plants (Tardieu and Simonneau 1998), the daily fluctuation in Ψ_L (Klein 2014); the slope of Ψ_{md} versus Ψ_{pd} (Martínez-Vilalta *et al.* 2014); hydroscape area (Meinzer *et al.* 2016). In the connection, the most relevant distinction between partial isohydry and extreme anisohydry can be inferred by comparing the observed and predicted Ψ_{md} and $\Delta\Psi$ (i.e., $\Psi_{pd}-\Psi_{md}$), which serve as indices of the risk of hydraulic failure and carbon starvation, respectively. Low values of Ψ_{md} are directly linked to a decline in hydraulic conductivity (Pockman and Sperry 2000), while low values of $\Delta\Psi$ reduce the transpiration capacity and make the plant more vulnerable to carbon starvation (Sperry *et al.* 2002).

Despite the modest success of species classification based on isohydricity indices, there remains a lack of a universally accepted definition (Hochberg *et al.* 2018, Feng *et al.* 2019). In this study, we tested different methods to estimate plant degree of isohydry, which is associated with hydraulic strategies during increasing drought. We explicitly wanted to quantify the variability of water potential to describe the species' water use strategy of the five temperate trees, for which physiological data are limited. As per the species' distinct aptitudes, we expected to assess variations in hydraulic behaviour among species. Therefore, we mainly examined the five most common definitions of isohydricity along the continuum. They are the following: First, isohydricity could be defined modestly only by the minimum Ψ_{md} experienced by a species (Figure 4.5, Figure 4.6a). However, it has limitations due to the influence by drought severity (see Martínez-Vilalta and Garcia-Forner 2017). Second, a maximum range of daily leaf water potential variation ($\Delta\Psi_L$) could describe isohydricity (Figure 4.7a), and species with less diurnal variation are considered more isohydric (see Klein 2014). Third, a linear regression slope fitted to the relationship between Ψ_{md} and Ψ_{pd} defines isohydry (Figure 4.6b, Table A4.1), species with flatter slopes designating more isohydric behaviours (Martínez-Vilalta *et al.* 2014). Fourth, another option would be to use the relationship between $\Delta\Psi_L$ against Ψ_{pd} (Meinzer *et al.* 2016, depicted in Figure 4.7b). Finally, the hydroscape area (Fu and Meinzer 2019, Fu *et al.* 2019, Li *et al.* 2019, Salvi *et al.* 2022), most recently intended to describe the isohydricity of the plant. However, these definitions do not necessarily agree with each another. Further, we examined the relationship of

diurnal changes in leaf water potentials ($\Delta\Psi_L$) and Ψ_{md} with g_s along with VPD to describe the water use strategies of species.

4.4.2 Estimating plant degree of isohdry and testing species-specific variability using linear mixed-effects models

Model Description:

We modeled Ψ_L by applying linear mixed-effect using the following parameterization and the parameter estimates for the fixed and random effect of a linear mixed effect models showing the relationship between different variables (response and predictor or explanatory), depicted in appendix Table (Table A4.1, Table A4.2, Table A4.3, Table A4.4). The models are:

(Model: a) $\Psi_{md} \sim (\text{VPD} * \text{species}) + \text{days} + (1 | \text{treeID})$

(Model: b) $\Psi_{md} \sim (\Psi_{pd} * \text{VPD}) + \text{species} + \text{days} + (1 | \text{treeID})$

(Model: c) $\Delta\Psi_L \sim \text{VPD} + \text{species} + \text{days} + (1 | \text{treeID})$

(Model: d) $\Delta\Psi_L \sim (\Psi_{pd} * \text{VPD}) + \text{species} + \text{days} + (1 | \text{treeID})$

Model test (Fixed and random effects):

we tested the water potential on every tree individually multiple times. So, the tree identity was fitted as a random effect. We simply want to control for the variation coming from tree identity. We tested the species difference in the Ψ_{md} throughout the desiccation event. Here, we used a linear-mixed-effects model with Ψ_{md} as a response variable; and VPD, species along with their interaction, and days as fixed effects. The tree ID was envisaged as a random effect. Linear-mixed-effects model was applied using the package lme4 in R (Bates *et al.* 2015) to show the species-specific variation difference. VPD was standardized by mean and standard deviation, and the day shifts to starting point 0 for more easy interpretation. We also conducted the ANOVA to determine the significance level between variables. In second model, we used Ψ_{md} as a response variable; Ψ_{pd} and VPD, their interaction, species, and days as fixed effects, and tree ID as a random effect. In third, we tested the daily range of variation in $\Delta\Psi_L$ from Ψ_{pd} to Ψ_{md} of the species throughout the desiccation event, therefore, chosen as a response variable. VPD, species, and days were fixed effects, and tree ID was treated as a random effect. Similarly, in fourth, $\Delta\Psi_L$ was chosen as a

response variable; Ψ_{pd} and VPD with interaction, species, and days were fixed effects, along with tree ID treated as a random effect. The fifth matrix, hydroscape area, is explained in Chapter-3. Further, we analyzed the stomatal conductance (g_s) with a linear model—Ordinary least squares (OLS)—to show the species-specific variation difference (Figure 4.8 and Figure 4.9).

We performed multiple models fitting to choose the best model from them according to model selection criteria (AIC, BIC, and log-likelihood ratio). The model fit and comparison of models were made with the chi-squared test. First, we run a Null model and then model(s) with fixed and random effects. After fitting the model, we checked the model assumptions by examine the residuals versus fitted values for each group of random intercept level and Q-Q plots. Moreover, we also checked the multi-collinearity among the variables using variance inflation factors (VIFs). We use maximum likelihood (ML) when comparing models with different fixed effects, as it does not rely on the coefficients of the fixed effects. However, we exercised the restricted maximum likelihood (REML) in the linear mixed models for parameter estimation criterion due to the biaseness nature of ML variance estimates.

4.4.3 Challenges to the isohydry concept and variability in plant water potential dynamics

Along the spectrum, isohydric linked to drought avoidance strategies and anisohydric to drought tolerance are commonly accepted. However, conflicting results of previous findings present challenges to the iso-anisohydry concept, especially considering the hydraulic swing behaviour in response to changing conditions (Rogiers *et al.* 2012, Zhang *et al.* 2012, Martínez-Vilalta and Garcia-Forner 2017, Hochberg *et al.* 2018, Feng *et al.* 2019, Leuschner *et al.* 2022). Studies showed that plant water potential dynamics could vary over space and time within an individual along a continuum from isohydry to anisohydry. For instance, *Larrea tridentate* exhibit extreme anisohydry under wet soil conditions and partial isohydry under prolonged dry or cold conditions (Guo *et al.* 2020). It showed a substantial variation in daily predawn (Ψ_{pd}) and midday (Ψ_{md}) water potential that was linked to episodic moisture and seasonal temperature (Oren *et al.* 1999, Ogle *et al.* 2012). Similarly, Grapevine may have an advantage in dry ecosystems with isohydric grapevines (Chave *et al.* 2010). However, anisohydric behaviour improves performance (Pou *et al.* 2012).

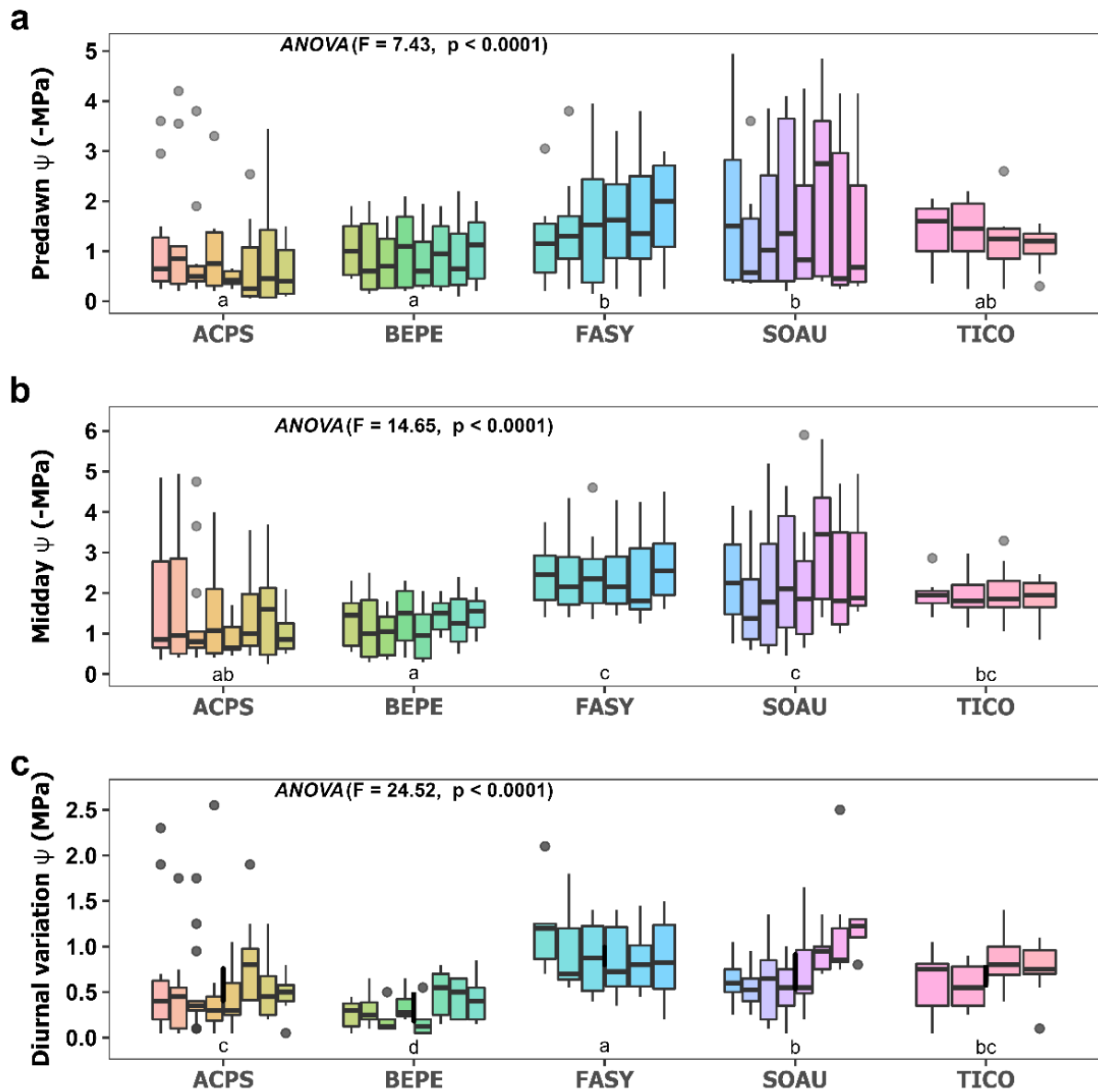


Figure 4.5: Water potential variation among the five temperate tree species. (a) Ψ_{pd} variation, (b) Ψ_{md} variation, and (c) Variation in the diurnal range of Ψ_L (i.e., $\Psi_{pd} - \Psi_{md}$) variation. Tukey's post-hoc test with a different letter indicates significant differences across the species.

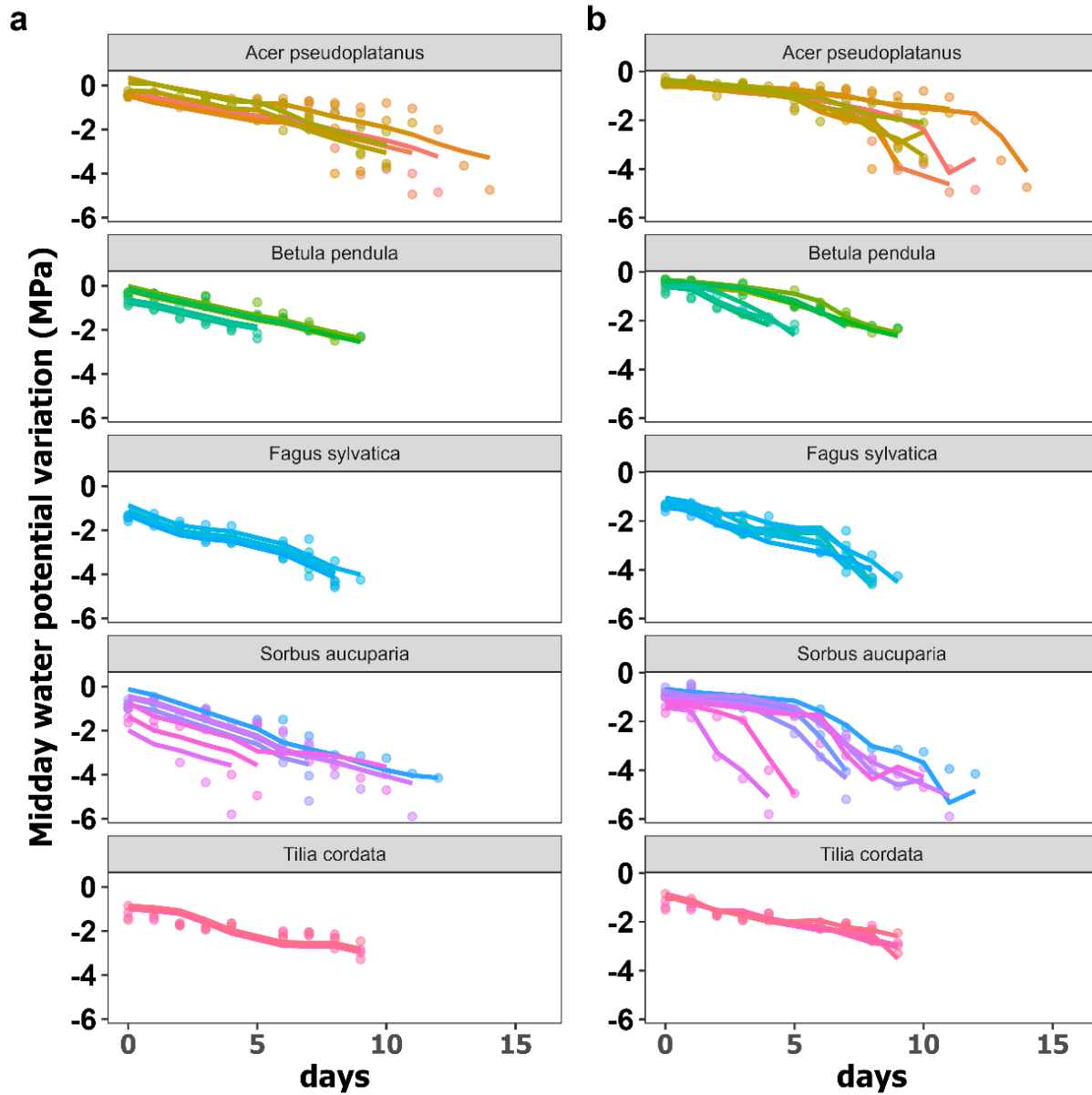


Figure 4.6: Linear mixed effect modelled the midday water potential (Ψ_{md}) variation among the species, which could describe the isohyricity. The first model (a) is a random intercept model independent of Ψ_{pd} , and the second model (b) is the random intercept model that includes the Ψ_{pd} as a predictor variable. VPD, days, and species are fixed effects and treeID as a random factor. The syntax used for model building in R would look like this: (Note—model: a, $\Psi_{md} \sim \text{days} + (\text{VPD} * \text{species}) + (1 | \text{treeID})$); and model: b, $\Psi_{md} \sim (\Psi_{pd} * \text{VPD}) + \text{species} + \text{days} + (1 | \text{treeID})$.

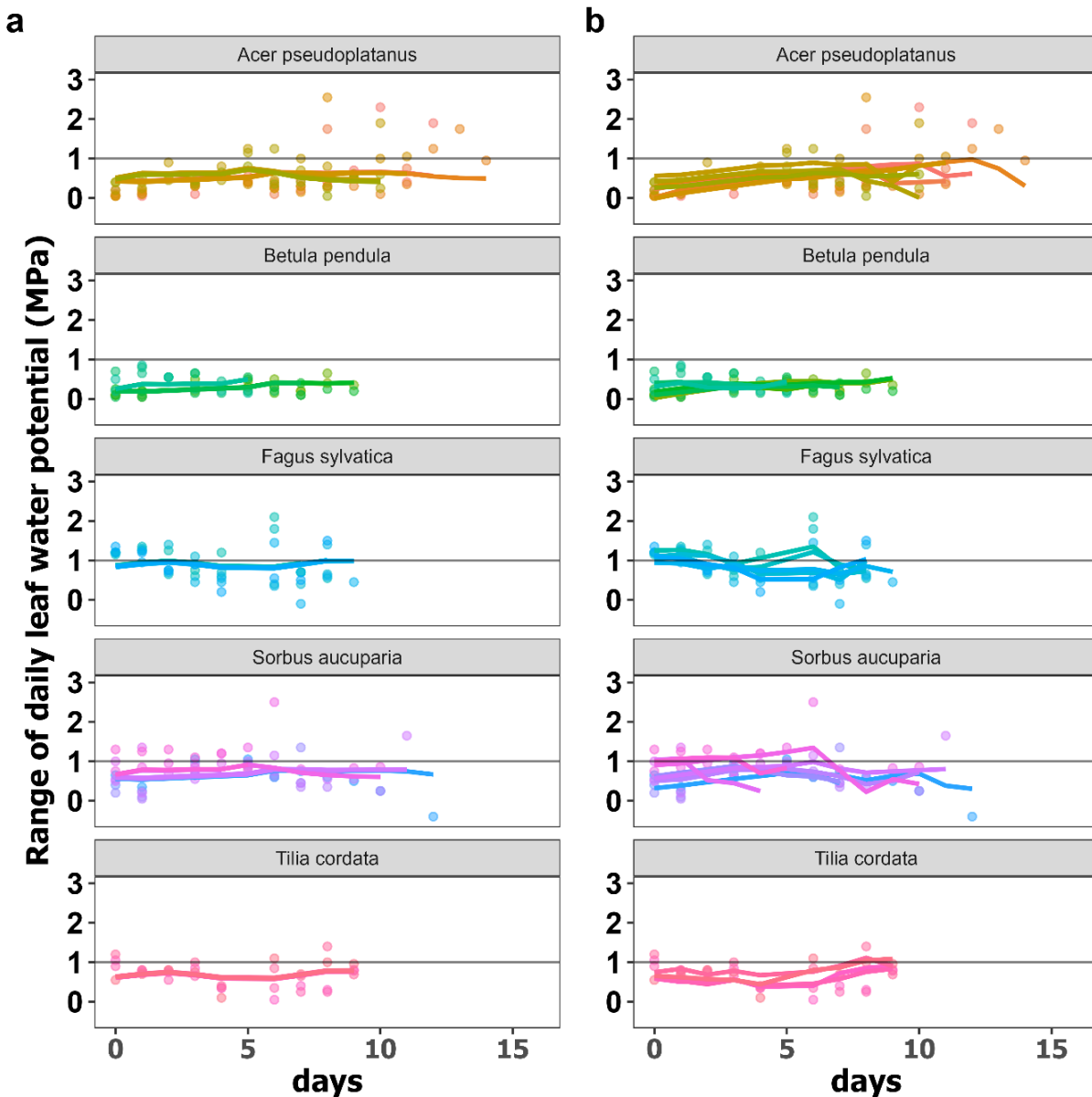


Figure 4.7: Linear mixed effect modelled a maximum range of variation for the daily leaf water potential ($\Delta\Psi_L$, i.e., $\Psi_{pd} - \Psi_{md}$), which could describe the isohydricity, and species with less diurnal variation are considered to be more isohydric (Klein 2014). Model (a) is a random intercept model which is independent of Ψ_{pd} , and the second model (b) includes the Ψ_{pd} as a predictor variable. VPD, days, and species are fixed effects and treeID as a random factor. The syntax used for model building in R would look like this: (Note—model: a, $\Delta\Psi_L \sim \text{VPD} + \text{species} + \text{days} + (1 | \text{treeID})$; and model: b, $\Delta\Psi_L \sim (\Psi_{pd} * \text{VPD}) + \text{species} + \text{days} + (1 | \text{treeID})$).

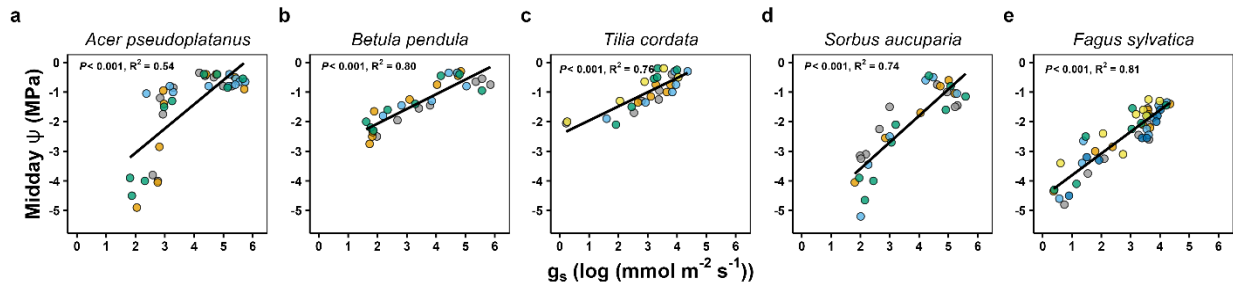


Figure 4.8: Linear regression show the stomatal conductance (g_s) versus midday water potential (Ψ_{md}) relationship from the five temperate tree species (a–e). Ψ_{md} was restricted to P_{88} , representing the hydraulic failure associated with tree mortality. Different colour points denote a water potential measurement on each individual. Each figure panel shows the significance level (p -value) and the coefficient of determination, i.e., R^2 for the investigated relationship for the species.

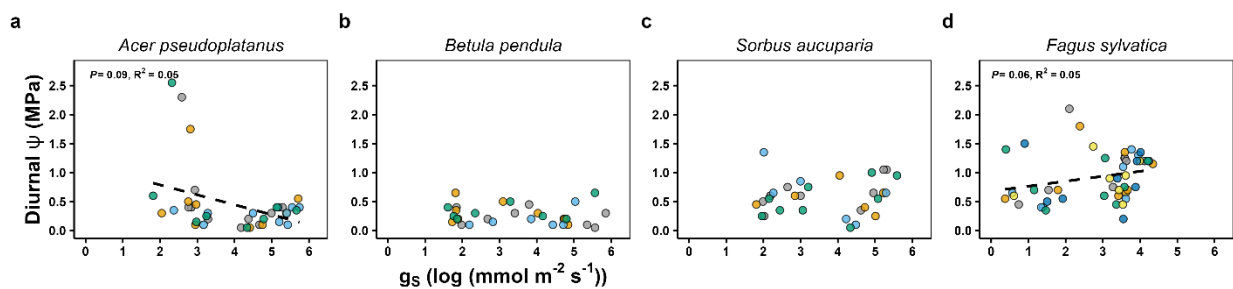


Figure 4.9: Stomatal conductance (g_s) versus a diurnal range of variation of leaf water potential ($\Delta\Psi_L$, i.e., $\Psi_{pd} - \Psi_{md}$) show a non-association relationship through a linear regression among four temperate tree species (a–d). Broken lines indicate a marginal association between both. Ψ_{md} was restricted to P_{88} , representing the hydraulic failure associated with tree mortality. Different colour points denote a water potential measurement on each individual. Each figure panel shows the significance level (p -value) and the coefficient of determination, i.e., R^2 for the investigated relationship for the species.

Grapevines have been shown to regulate their isohydricity during the growth season and switch from isohydric to anisohydric with varying soil moisture (Domec and Johnson 2012, Rogiers *et al.* 2012, Zhang *et al.* 2012). Likewise, *Quercus douglasii* was found to vary spatially across different moisture conditions and temporally between seasons and exhibited more anisohydric behaviour during wet spring than dry summer, suggesting that variable hydraulic behaviour could be adaptive in seasonally dry climates (Feng *et al.* 2019). Additionally, isohydric species are not inevitably always carbon starved (Garcia-Forner *et al.* 2017). However, the differential growth rates of poplar genotypes affect their ability to adapt to drought, with fast-growing genotypes being more susceptible to hydraulic damage under water scarcity, and showing isohydric stomatal behavior (Zhang *et al.* 2020).

Further, plant survival probability during drought along the continuum is also equivocal. For example, studies have witnessed that the co-occurring isohydric *Pinus edulis* was more susceptible to drought-induced mortality than the anisohydric *Juniperus monosperma* (McDowell *et al.* 2008, McDowell 2011, Meinzer *et al.* 2014, Garcia-Forner *et al.* 2016). Adding to the list, the most isohydric species of southern pines forests, *Pinus taeda* and *Pinus echinata*, are more vulnerable to drought (Roman *et al.* 2015); *Pinus radiata* survive longer than anisohydric *Eucalyptus* (Mitchell *et al.* 2013). *Acacia aptaneura* showed more isohydric-like behavior after repeated droughts than after a single drought (Nolan *et al.* 2017). In contrast, White oak (*Quercus alba* L.) endures drought better than isohydric black walnut (*Juglans nigra* L.) (Loewenstein and Pallardy 1998). Further, anisohydric S/R20 cultivar of *Prunus* is more drought-tolerant than isohydric R20 cultivar (Álvarez-Maldini *et al.* 2021) due to the longer photosynthesis period during water stress. *Morus indica* exhibit anisohydric behaviour during seasonal summer drought, which is advantageous in maintaining photosynthetic assimilation (Guha and Reddy 2014). *Eucalyptus comaldulensis* and *Melia dubia* showed isohydric stomatal behaviour and sustained higher carbon assimilation under moisture stress (Tolia *et al.* 2019).

This conflicting finding highlights the varying dynamics of plant water potential across individuals and species, and exhibit both isohydric and anisohydric behavior under different conditions. We acknowledge the plant-environment interaction impact their survival during drought, which emphasises the need for further research.

4.5 Plant desiccation time thresholds

Stomatal regulation of plant water potential (Ψ_x) is paramount to discerning species' ability to survive. It makes a bridge between carbon starvation and hydraulic failure (Mackay *et al.* 2015, Anderegg *et al.* 2015, Blackman *et al.* 2019b). Plant water loss occurs in two critical stages, which decide desiccation tolerance; the first response phase is until the stomata close and enables to balance the stomatal conductance relative to carbon gain. The second phase starts after stomatal closure and ends with catastrophic hydraulic failure. So, plants continue to lose water even after stomatal closure through cuticular conductance. On this note, the time to hydraulic failure (T_{hf}) has two main components: the time to stomata closure (T_{sc}) and the time to critical hydraulic failure starting from stomatal closure (T_{crit} ; Blackman *et al.* 2016, 2019b), which collectively decide plant

mortality. The mechanisms prior to and following the stomatal closure are primarily involved: (1) desiccation delay (or avoidance strategy) and (2) desiccation tolerance (see Figure 4.10). T_{sc} linked to drought avoidance strategy and was persuaded by the coordinated traits response of P_{s90} , Ψ_{t1p} , and HSA. Following a stomata closure, plants prefer to delay the time of tissue desiccation, which depends on traits like higher resistance to embolism (P_{88}), lower Ψ_{t1p} , high HSM, and lower g_{min} . This countermeasure against the decreasing lethal water potential is linked to T_{crit} , supported by the development of resistant xylem or an increased safety margin (Tyree *et al.* 2003, Hacke and Sperry 2001, Li *et al.* 2019). Additionally, species with higher levels of hydraulic safety had lower rates of photosynthesis (Reich 2014).

We show that T_{hf} is influenced by the interplay of various traits, which is endorsed by other studies. For instance, *Pinus radiata* took nearly three times longer to reach critical hydraulic failure compared to angiosperm species despite having lower embolism resistance (Blackman *et al.* 2019a). This indicates that embolism resistance alone cannot predict the time to plant mortality. Our study also highlights the importance of coordinated traits in preview of drought resistance strategy in determining the timing of hydraulic failure. The critical point of stomatal closure plays a crucial role in composing the coordination of various traits and hydraulic strategies. It marks the transition from incipient cavitation to catastrophic hydraulic failure. Various researchers supported this view. For example, stomata are usually closed before incipient cavitation events (Delzon and Cochard 2014, Martin-StPaul *et al.* 2017, Sperry *et al.* 2017, Choat *et al.* 2018); stomata function (opening-closing ratio) facilitates the gas exchange balance, embolism resistance, and pathogen defence (Xie *et al.* 2022), decisive in the timing of catastrophic hydraulic failure (Mcdowell *et al.* 2008, Arend *et al.* 2021, Joshi *et al.* 2022), adjusting physiological and morphological traits such as leaf conductance, turgor loss, cuticular conductance, hydraulic safety margins, and embolism resistance (Blackman *et al.* 2019b, Hammond and Adams 2019, Lemaire *et al.* 2021, Ruffault *et al.* 2022). Additionally, the xylem and stomata functions are closely interconnected and could explain growth and mortality (Skelton *et al.* 2015, Brodribb 2017, Martin-StPaul *et al.* 2017).

4.6 Traits significance and their coordination along the spectrum

The trade-offs and linkages between stomatal and hydraulic traits are crucial for determining species' drought response strategy. Therefore, our study combines different methods

to estimate the plant degree of isohydry to explain the species' hydraulic strategies. On this note, we elucidate hydroscape area (HSA), and their association with other physiological traits in determining the desiccation time (please see chapter-3). We found that the species' hydroscape area matches their stomatal stringency, confirming the link between stomatal response and the decline of leaf water potential. We also show that isohydric behaviour was mostly associated with leaf hydraulic traits and poorly with xylem safety traits.

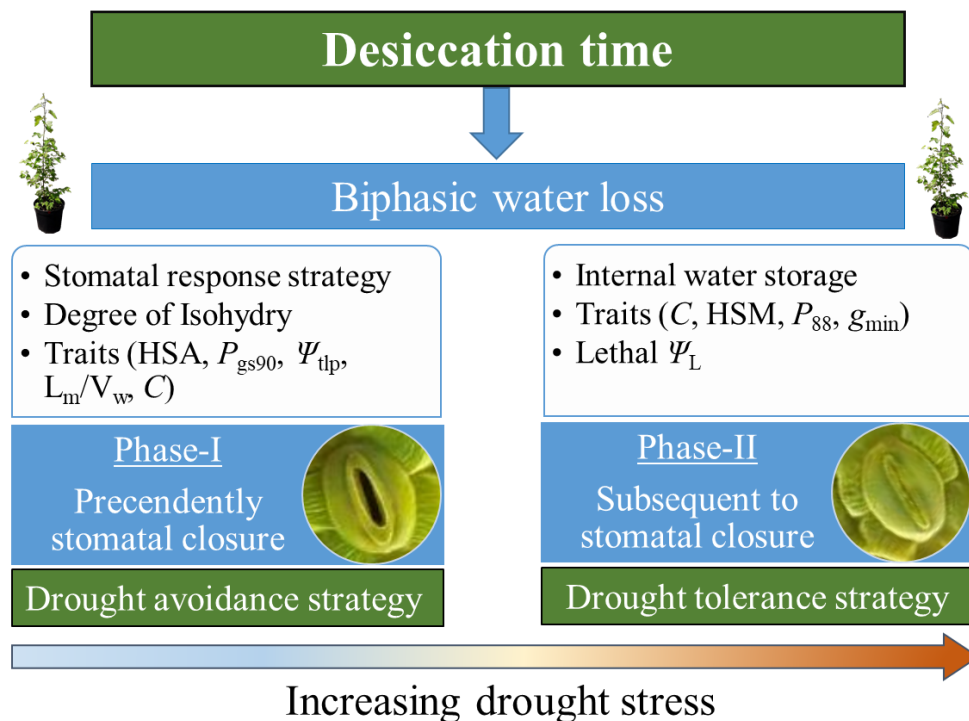


Figure 4.10: Species drought response strategy shaped the desiccation time. Stomatal closure marks the transition from incipient cavitation to catastrophic hydraulic failure and is crucial in organizing and coordinating the various physiological traits. Hydroscape area (HSA) signifies the stomatal stringency. The traits involved in drought avoidance are early stomatal closure (P_{s90}), lower turgor loss (Ψ_{tlp}), a lower ratio of the leaf area (L_m) to the volume of water contained (V_w), capacitance (C), while tolerance strategy linked to high embolism resistance (P_{88}), low cuticular conductance (g_{min}), and increased hydraulic safety margin (HSM).

In addition, we advocate that HSA and P_{s90} are closely related to growth and productivity as they are linked to the time to stomatal closure. Species that close stomata at lower water potential notably had a larger HSA. So, anisohydric species (SOAU and FASY) tend to maximize stomatal function to gain carbon at the risk of xylem embolism. Thus, they are rather linked to water use strategies rather than drought tolerance strategies. Moreover, due to less stringent stomatal regulation, higher embolism resistance could be an adaptation in anisohydric species that allows

for the free exchange of gases up to a certain limit to maximize carbon gain, however, at the expense of risk to hydraulic failure (Mcdowell *et al.* 2008, Arend *et al.* 2021, Hartmann *et al.* 2021), and more resistant xylem helps to tolerate lower xylem pressure, consistent with previous findings (Moser *et al.* 2016, Leuschner *et al.* 2022). More anisohydric species tend to have a higher tolerance to drought-induced embolism, faster assimilation and growth rates, a more negative leaf turgor loss point, and a lower wood density (Attia *et al.* 2015, Roman *et al.* 2015, Ratzmann *et al.* 2019, Chen *et al.* 2021). In contrast, isohydric species (ACPS and BEPE) responded to drought stress quickly and tend to close the stomata prior to (or close to) the onset of cavitation, making them more susceptible to carbon starvation. This corroborates the finding of (Li *et al.* 2018). TICO had a relatively high Ψ_{tlp} and P_{s90} as well as an intermediate HSA. However, there seems a lack of consensus for TICO (Köcher *et al.* 2009), and our results are more in line with Leuschner *et al.* (2019), who reported fairly isohydric behaviour for that species.

4.6.1 Turgor loss point and stomata closure

In this study, a mechanistic link to stomatal control is reflected in the strong association of Ψ_{tlp} with both P_{s90} and HSA, which corroborates the value of Ψ_{tlp} estimates as an easily measurable, directly linked to the stomatal response. With the exception of BEPE, stomatal closure for all species linked to turgor loss, which happened before reaching water potentials associated with the onset of embolism formation (P_{12}), consistent to findings of other studies (Skelton *et al.* 2015, Hochberg *et al.* 2017, Martin-StPaul *et al.* 2017, Li *et al.* 2018).

More isohydric species may adapt the strategy to act on conserving more water than anisohydric as a response to drought. Further, the small margin between P_{s90} and P_{50} or P_{88} in an anisohydric species probably indicates that the organs could be saved from being damaged and maintain their functionality until the integrity of cell turgor at declining water potential, which is in line with a study (Meinzer *et al.* 2016). However, contrasting findings reported by some studies that did not witness an association of Ψ_{tlp} with P_{s90} (Farrell *et al.* 2017, Johnson *et al.* 2018, Blackman *et al.* 2019a, Jacob *et al.* 2022), and suggested to use with care as Ψ_{tlp} stand-alone metrics to the drought tolerance traits. While most of the studies advocated the notion of association of Ψ_{tlp} and P_{s90} , which is proxy of stomatal closure (Brodribb *et al.* 2003, Bartlett *et al.* 2014, 2016, Martin-StPaul *et al.* 2017).

4.6.2 Embolism resistance and hydraulic safety margin

Our results show the two primary axes of trait variability describe the isohydric plant behaviour. Counter to our expectations, neither embolism resistance nor the associated hydraulic safety margins were related to metrics of isohydry. Instead, our results indicate traits associated with plant drought response to cluster along two largely independent axes of variation. On the temporal desiccation response, the first axis is linked to T_{sc} , which reflects stomatal stringency and HSA. The second axis is associated with hydraulic safety and reflects that species with wider hydraulic safety margins and a lower P_{88} take longer to reach critical levels of hydraulic failure (T_{crit}). HSM has been recognized as the most important trait in the desiccation tolerance strategy (Tyree *et al.* 2003, Skelton *et al.* 2015, Martin-StPaul *et al.* 2017, Blackman *et al.* 2019a). However, we did not observe a consistency between HSM and time to hydraulic failure along the iso-anisohydric continuum (Table A4.1). Additionally, higher HSM facilitates embolism repair and prevents catastrophic failure (Johnson *et al.* 2012, Martin-StPaul *et al.* 2017). Chir pine show less sensitivity to extreme droughts due to wide safety margin in the Central Himalaya (Tyagi *et al.* 2023).

4.6.3 Cuticular conductance

T_{crit} during drought should be influenced by g_{min} , the minimum water loss from leaves following stomata closure. Plants can circumvent tissue desiccation by reducing g_{min} , which regulates the rate of water loss. In our study, TICO and FASY had the lowest absolute g_{min} , possibly contributing to a longer desiccation time. This is consistent with previous findings that low g_{min} is adaptive to drought tolerance (Burghardt and Riederer 2003, Brodribb *et al.* 2014, Blackman *et al.* 2016, Martin-StPaul *et al.* 2017). However, some studies show the desiccation time has also been found to be unrelated to g_{min} (Blackman *et al.* 2019b) and highly responsive to growth conditions (Duursma *et al.* 2019).

Further, lower g_{min} contributes to slow plant water loss, thereby influencing plant desiccation time. Plants that tend to reduce leaf area under drought confer an advantage through a more conservative water use strategy. The smallest leaf area and lowest g_{min} contribute to slow plant water loss, translating into greater drought tolerance by increasing T_{hf} under severe water deficit. On this note, the ratio of L_m and V_w appraises drought tolerance as providing a measure of the proportion of surface area for water loss and the total stored water, which is portrayed as a

reserve for extending plant survival following stomata closure when plants fail to extract soil water. Plant size influences desiccation time (Blackman *et al.* 2019b, Challis *et al.* 2022). We, therefore, standardized T_{sc} and T_{crit} to account for leaf area and water storage (please refer to Chapter 3).

4.6.4 Shoot capacitance

In the isohydric framework, plant water regulation depends on its dynamic plant–environment interaction (Sade *et al.* 2012, Hochberg *et al.* 2018, Feng *et al.* 2019, Guo *et al.* 2020). We observed that isohydric species typically maintain the constant Ψ_L , which is also reflected in the stem's high relative water content (RWC). Our results supported this notion, which may likely be one of the reasons for the high capacitance (C) with species such as BEPE, ACPS, and TICO. On this bases, we expect that isohydric plants regulate the RWC more strictly along with stomatal stringency. Theoretically, a plant with higher C can delay stress periods by agreeing on a drought-avoidance strategy (Scholz *et al.* 2011, Wolfe 2017, Blackman *et al.* 2019a, Jiang *et al.* 2021). Further, C helps to stabilize stem water potentials during changes in transpiration under stress by avoiding the embolism process (Meinzer *et al.* 2009, Anderegg and Meinzer 2015), supported by our study findings that species having higher C close their stomata at high water potentials (For example, BEPE, ACPS, and TICO).

Further, Capacitance facilitates to supply of 45 % of total diurnal transpiration during seasonal drought (Preisler *et al.* 2022). Thus, the contribution of internal water storage capacitance is very crucial for tree survival under drought as they stabilize the declining stem water potential and avoids reaching the Ψ_{min} value that causes catastrophic hydraulic failure (Meinzer *et al.* 2009, Anderegg and Meinzer 2015, Salomón *et al.* 2017, Preisler *et al.* 2022). Furthermore, we show that iso-anisohydric behaviours are rather linked to water use strategies. Thus, mapping RWC is essential to defining plant water balance which, in turn, C a role in desiccation tolerance and avoidance strategies.

FASY, with a lower C , achieved a longer desiccation time successfully. In contrast, isohydric species (ACPS and BEPE) failed to achieve longer desiccation times despite higher C . This is consistent with the previous findings that showed longer desiccation time with decreased C (Gleason *et al.* 2014, Blackman *et al.* 2019b). Furthermore, the role of C regulation cannot be denied in both phases, i.e., before and after the stomatal closure in drought response. However, the

mechanism behind it is still unclear. Their role in desiccation time is a matter of debate. It may involve trade-offs with traits such as cavitation resistance, Ψ_{tp} , and HSM, as suggested by earlier studies (Scholz *et al.* 2011, Meinzer *et al.* 2009, Gleason *et al.* 2014, Li *et al.* 2018, Blackman *et al.* 2019b).

Supplementary information

Table A4.1: A list of all the main variables explored in the study was given with units and summary (means \pm SE) for five temperate species. Values were mean \pm SE, 95% confidence intervals (CIs) were shown in parenthesis for P_{s90} and HSA, and the coefficients of determination, i.e., R^2 , for the relationships using a linear model (Slope of Ψ_{pd} vs. Ψ_{md}). Species abbreviations are as follows: ACPS: *A. pseudoplatanus*; BEPE: *B. pendula*; TICO: *T. Cordata*; SOAU: *S. aucuparia*; FASY: *F. Sylvatica*.

| | Species | Unit | ACPS | BEPE | TICO | SOAU | FASY |
|---|---------|------------------|-----------------------|-----------------------|------------------------|-----------------------|-----------------------|
| Traits | | | | | | | |
| <i>Stomata stringency</i> | | | | | | | |
| Stomatal closure (P_{s90}) | | MPa | -0.93 (-1.1, -0.8) | -1.41 (-1.7, -1.2) | -1.75 (-1.96, -1.6) | -2.05 (-2.5, -1.7) | -2.49 (-2.8, -2.3) |
| Hydroscape area (HSA) | | MPa ² | 0.29 (0.25, 0.36) | 0.65 (0.55, 0.82) | 1.17 (1.06, 1.31) | 1.63 (1.36, 2.72) | 1.85 (1.65, 2.14) |
| Midday water potential (Ψ_{md}) | | MPa | -1.65 \pm 0.15 | -1.43 \pm 0.10 | -1.93 \pm 0.09 | -2.51 \pm 0.19 | -2.52 \pm 0.14 |
| Diurnal range of water potential ($\Delta\Psi = \Psi_{pd} - \Psi_{md}$) | | MPa | 0.54 \pm 0.05 | 0.32 \pm 0.03 | 0.68 \pm 0.05 | 0.70 \pm 0.07 | 0.89 \pm 0.06 |

Table A4.1: (Continued...)

| Traits | Species | Unit | ACPS | BEPE | TICO | SOAU | FASY |
|---------------------------------------|----------------|---|---------------------|--------------------|-------------------|---------------------|-------------------|
| <i>Foliar - level</i> | | | | | | | |
| Specific leaf area | | cm ² g ⁻¹ | 138.71 ± 3.2 | 169.96 ± 6.4 | 199.96 ± 8.0 | 170.16 ± 9.1 | 209.50 ± 1.9 |
| Huber value | | 10 ⁻⁴ m ² m ⁻² | 4.77 ± 0.3 | 4.28 ± 0.3 | 7.56 ± 1.6 | 3.81 ± 0.4 | 5.18 ± 0.7 |
| Mean Leaf area | | cm ² | 62.73 ± 6.5 | 18.23 ± 1.2 | 25.61 ± 1.8 | 65.44 ± 7.4 | 14.15 ± 1.3 |
| Leaf density | | kg m ⁻³ | 409.97 ± 29.1 | 379.72 ± 18.2 | 402.66 ± 40.9 | 487.05 ± 53.5 | 483.25 ± 20.1 |
| Maximum leaf area | | cm ² | 12123.4 ± 1331.7 | 16994.4 ± 850.3 | 2269.8 ± 143.8 | 15411.3 ± 1633.7 | 3647.3 ± 415.8 |
| Cuticular conductance | | mmol m ⁻² s ⁻¹ | 3.33 ± 0.36 | 1.82 ± 0.16 | 1.28 ± 0.09 | 1.73 ± 0.28 | 1.65 ± 0.09 |
| Mean maximal stomatal conductance | | mmol m ⁻² s ⁻¹ | 98.38 ± 15.32 | 67.98 ± 14.45 | 22.73 ± 3.08 | 75.09 ± 13.60 | 32.31 ± 3.34 |
| Absolute maximal stomatal conductance | | mmol m ⁻² s ⁻¹ | 309.35 ± 7.89 | 286.26 ± 15.02 | 55.85 ± 1.98 | 301.59 ± 6.30 | 74.28 ± 1.58 |
| 90 % loss of stomatal conductance | | mmol m ⁻² s ⁻¹ | 30.94 ± 0.79 | 28.63 ± 1.50 | 5.59 ± 0.20 | 30.16 ± 0.63 | 7.43 ± 0.16 |
| Percent stomatal conductance | | % | 32.14 ± 4.97 | 24.48 ± 4.79 | 40.76 ± 5.19 | 25.05 ± 4.54 | 44.08 ± 4.45 |
| Turgor loss point | | MPa | -2.05 ± 0.05 | -2.10 ± 0.06 | -1.96 ± 0.09 | -2.37 ± 0.07 | -2.48 ± 0.08 |

Table A4.1: (Continued...)

| Traits | Species | Unit | ACPS | BEPE | TICO | SOAU | FASY |
|------------------------------------|---------|--|------------------|------------------|------------------|------------------|------------------|
| <i>Stem-level</i> | | | | | | | |
| P_x at 12% loss of conductance | | MPa | -2.99 ± 0.11 | -1.72 ± 0.05 | -2.65 ± 0.21 | -2.73 ± 0.08 | -3.09 ± 0.22 |
| P_x at 50% loss of conductance | | MPa | -3.62 ± 0.11 | -1.96 ± 0.04 | -3.43 ± 0.16 | -3.87 ± 0.08 | -3.59 ± 0.21 |
| P_x at 88% loss of conductance | | MPa | -4.24 ± 0.13 | -2.21 ± 0.04 | -4.20 ± 0.13 | -5.02 ± 0.12 | -4.10 ± 0.19 |
| Specific conductivity | | $\text{kg m}^{-1} \text{MPa}^{-1} \text{s}^{-1}$ | 0.71 ± 0.09 | 1.83 ± 0.18 | - | 1.22 ± 0.12 | - |
| Pit conductivity | | $\text{kg m}^{-1} \text{MPa}^{-1} \text{s}^{-1}$ | 0.85 ± 0.11 | 2.41 ± 0.28 | - | 1.66 ± 0.20 | - |
| Potential conductivity | | $\text{kg m}^{-1} \text{MPa}^{-1} \text{s}^{-1}$ | 5.39 ± 0.68 | 8.50 ± 0.47 | - | 4.83 ± 0.47 | - |
| Shoot capacitance | | $\text{mol kg}^{-1} \text{MPa}^{-1}$ | 5.33 ± 1.34 | 10.98 ± 2.31 | 7.09 ± 0.26 | 4.76 ± 0.67 | 2.47 ± 0.40 |
| Wood density | | g cm^{-3} | 0.52 ± 0.02 | 0.42 ± 0.01 | 0.35 ± 0.02 | 0.58 ± 0.05 | 0.49 ± 0.01 |
| Saturated water content | | g g^{-1} | 59.39 | 54.77 | 56.31 | 60.18 | 42.15 |
| Amount of water available in plant | | g | 622.3 ± 58.5 | 797.5 ± 58.3 | 101.6 ± 6.3 | 790.9 ± 80.5 | 122.8 ± 16.6 |

Table A4.1: (Continued...)

| Traits | Species | Unit | ACPS | BEPE | TICO | SOAU | FASY |
|---|----------------|--------------------|---------------|---------------|----------------|----------------|---------------|
| <i>Safety margin limits</i> | | | | | | | |
| Hydraulic safety margin ($P_{s90} - P_{88}$) | | MPa | 3.24 | 0.80 | 2.45 | 2.97 | 1.62 |
| Relative water content at stomatal closure | | % | 64.32 | 79.92 | 84.35 | 80.34 | 49.64 |
| Relative water content at hydraulic failure | | % | 47.27 | 72.01 | 58.42 | 66.46 | 42.92 |
| <i>Desiccation time</i> | | | | | | | |
| Standardized time to stomatal closure (T_{sc}) | | h cm ⁻¹ | 62.27 ± 5.17 | 52.86 ± 2.99 | 69.50 ± 8.65 | 48.22 ± 2.60 | 81.31 ± 8.04 |
| Standardized time from stomatal closure to hydraulic failure (T_{crit}) | | h cm ⁻¹ | 32.18 ± 4.35 | 17.41 ± 3.20 | 34.77 ± 5.15 | 30.00 ± 3.21 | 16.57 ± 1.88 |
| Standardized total time to hydraulic failure (T_{hf}) | | h cm ⁻¹ | 92.94 ± 6.97 | 70.27 ± 4.32 | 106.17 ± 10.17 | 78.22 ± 4.99 | 101.43 ± 9.02 |
| <i>Wood anatomy</i> | | | | | | | |
| Hydraulically weighted vessel diameter | | μm | 42.21 ± 1.23 | 42.06 ± 0.62 | - | 30.60 ± 1.07 | - |
| Vessel density | | n mm ⁻² | 105.21 ± 5.84 | 196.86 ± 6.97 | - | 323.30 ± 19.84 | - |

Analysis results of the Linear mixed effect model are summarised here.

(Model: a) $\Psi_{md} \sim (\text{VPD} * \text{species}) + \text{days} + (1 | \text{treeID})$

(Model: b) $\Psi_{md} \sim (\Psi_{pd} * \text{VPD}) + \text{species} + \text{days} + (1 | \text{treeID})$

(Model: c) $\Delta\Psi_L \sim \text{VPD} + \text{species} + \text{days} + (1 | \text{treeID})$

(Model: d) $\Delta\Psi_L \sim (\Psi_{pd} * \text{VPD}) + \text{species} + \text{days} + (1 | \text{treeID})$

Table S4.1: Parameter estimates of the linear mixed effect models show the midday water potential (Ψ_{md}) relationship as an f(x) of the interaction of VPD * species and days as fixed effects and treeID as a random factor. VPD was standardised by mean and standard deviation, and the day shifts to starting point 0 for more easy interpretation. The model syntax used for model building: $\Psi_{md} \sim (\text{VPD} * \text{species}) + \text{days} + (1 | \text{treeID})$. Shown is an estimate of the fixed effects of a linear mixed model with their model selection fit criteria. (AIC = 559.6, n = 282, groups= 34).

| Effect | Estimate | Std. Error | Pr(> t) | |
|------------------------------|----------|------------|----------|-----|
| (Intercept) | 0.12747 | 0.16665 | 0.44862 | |
| days | -0.28601 | 0.0146 | 2.00E-16 | *** |
| VPD | 0.21231 | 0.07104 | 0.003086 | ** |
| <i>Betula pendula</i> | -0.39652 | 0.21823 | 0.078849 | . |
| <i>Fagus sylvatica</i> | -1.67704 | 0.24672 | 4.92E-08 | *** |
| <i>Sorbus aucuparia</i> | -1.25244 | 0.21566 | 2.49E-06 | *** |
| <i>Tilia cordata</i> | -0.6395 | 0.26848 | 0.023358 | * |
| VPD: <i>Betula pendula</i> | -0.13677 | 0.1035 | 0.18758 | |
| VPD: <i>Fagus sylvatica</i> | -0.47488 | 0.1412 | 0.000894 | *** |
| VPD: <i>Sorbus aucuparia</i> | -0.50229 | 0.09846 | 6.71E-07 | *** |
| VPD: <i>Tilia cordata</i> | 0.06781 | 0.14104 | 0.631117 | |

Table S4.1a: Shown is an estimate of the random effects of the linear mixed model. (Note: ~ 30% variance explained by the treeID, and “left-over” explained by a fixed effect).

| Parameter | Estimate |
|-----------------------|----------|
| Variance of intercept | 0.14 |
| Residual variance | 0.32 |

Table S4.2: Parameter estimates of the linear mixed effect models show the midday water potential (Ψ_{md}) relationship as an f(x) of the interaction of Ψ_{pd} * VPD and days as fixed effects and treeID as a random factor. VPD was standardised, and the day shifts to starting point 0 for more easy interpretation. The model syntax used for model building: $\Psi_{md} \sim (\Psi_{pd} * VPD) + \text{species} + \text{days} + (1 | \text{treeID})$. Shown is an estimate of the fixed effects of a linear mixed model with their model selection fit criteria. (AIC = 295, n = 282, groups= 34). Significant relationships are asterisk.

| Effect | Estimate | Std. Error | Pr(> t) | |
|-------------------------|----------|------------|----------|-----|
| (Intercept) | -0.30371 | 0.09555 | 0.002851 | ** |
| predawn | 0.68113 | 0.04098 | 2.00E-16 | *** |
| VPD | 0.05502 | 0.04829 | 0.255587 | |
| days | -0.08859 | 0.01485 | 7.60E-09 | *** |
| <i>Betula pendula</i> | 0.0494 | 0.11751 | 0.677786 | |
| <i>Fagus sylvatica</i> | -0.78517 | 0.1315 | 1.78E-06 | *** |
| <i>Sorbus aucuparia</i> | -0.4704 | 0.12006 | 0.000562 | *** |
| <i>Tilia cordata</i> | -0.39737 | 0.14014 | 0.009407 | ** |
| predawn:VPD | 0.09546 | 0.02778 | 0.000679 | *** |

Table S4.2a: Shown is an estimate of the random effects of the linear mixed model. (Note: ~ 21% variance explained by the treeID, and “left-over” explained by a fixed effect).

| Parameter | Estimate |
|-----------------------|----------|
| Variance of intercept | 0.035 |
| Residual variance | 0.134 |

Table S4.3: Parameter estimate of the linear mixed effect models shows the relationship of a maximum daily range of water potential variation ($\Delta\Psi_L$, i.e., $\Psi_{pd} - \Psi_{md}$) as an $f(x)$ of VPD, species and days as fixed effects and treeID as a random factor. VPD was standardised, and the day shifts to starting point 0 for more easy interpretation. The model syntax used for model building: $\Delta\Psi_L \sim \text{VPD} + \text{species} + \text{days} + (1 | \text{treeID})$. An estimate of fixed effects of a linear mixed model is shown with their model selection fit criteria and satterthwaite's t-tests. (AIC = 334.1, n = 282, groups = 34). Significant relationships are shown with an asterisk.

| Effect | Estimate | Std. Error | Pr(> t) | |
|-------------------------|----------|------------|----------|-----|
| (Intercept) | 0.574 | 0.071 | < 0.001 | *** |
| VPD | 0.106 | 0.036 | 0.003 | ** |
| <i>Betula pendula</i> | -0.233 | 0.08 | 0.006 | ** |
| <i>Fagus sylvatica</i> | 0.434 | 0.086 | < 0.001 | *** |
| <i>Sorbus aucuparia</i> | 0.157 | 0.075 | 0.045 | * |
| <i>Tilia cordata</i> | 0.206 | 0.092 | 0.03 | * |
| days | -0.009 | 0.01 | 0.4 | |

Table S4.3a: Shown is an estimate of the random effects of the linear mixed model. (Note: ~ 1% variance explained by the treeID, and “left-over” explained by a fixed effect).

| Parameter | Estimate |
|-----------------------|----------|
| Variance of intercept | 0.002 |
| Residual variance | 0.177 |

Table S4.4: Parameter estimate of the linear mixed effect models depict the relationship of a maximum daily range of water potential variation ($\Delta\Psi_L$, i.e., $\Psi_{pd} - \Psi_{md}$) as an f(x) of interaction between Ψ_{pd} and VPD, species, and days as fixed effects; and treeID as a random factor. VPD was standardised, and the day shifts to starting point 0 for more easy interpretation. The model syntax used for model building: $\Delta\Psi_L \sim (\Psi_{pd} * VPD) + \text{species} + \text{days} + (1 | \text{treeID})$. An estimate of the fixed effects of a linear mixed model is shown with their model selection fit criteria and satterthwaite's t-tests (AIC = 295, n = 282, groups= 34). Significant relationships are shown with an asterisk.

| Effect | Estimate | Std. Error | Pr(> t) | |
|-------------------------|-----------------|-------------------|--------------------|-----|
| (Intercept) | 0.30371 | 0.09555 | 0.002851 | ** |
| predawn | 0.31887 | 0.04098 | 1.40E-13 | *** |
| VPD | -0.05502 | 0.04829 | 0.255587 | |
| <i>Betula pendula</i> | -0.0494 | 0.11751 | 0.677786 | |
| <i>Fagus sylvatica</i> | 0.78517 | 0.1315 | 1.78E-06 | *** |
| <i>Sorbus aucuparia</i> | 0.4704 | 0.12006 | 0.000562 | *** |
| <i>Tilia cordata</i> | 0.39737 | 0.14014 | 0.009407 | ** |
| days | 0.08859 | 0.01485 | 7.60E-09 | *** |
| predawn:VPD | -0.09546 | 0.02778 | 0.000679 | *** |

Table S4.4a: Shown is an estimate of the random effects of the linear mixed model. (Note: ~ 21% variance explained by the treeID, and “left-over” explained by a fixed effect).

| Parameter | Estimate |
|-----------------------|-----------------|
| Variance of intercept | 0.04 |
| Residual variance | 0.13 |

Table S4.5: The parameter estimates of ANOVA with the Tukey post-hoc test shows the multiple comparisons of overall change in midday leaf water potential (Ψ_{md}) across the five species (Figure 4.5b) during dry-out events. Significant differences between species are shown with a asterisk.

| Species | diff | lwr | upr | adj p-value | |
|-------------|---------|---------|---------|-------------|-----|
| BEPE - ACPS | 0.14542 | -0.3845 | 0.67535 | 0.94344 | |
| FASY - ACPS | -1.0467 | -1.5901 | -0.5033 | 0.00000 | *** |
| SOAU - ACPS | -0.9819 | -1.4847 | -0.479 | 0.00000 | *** |
| TICO - ACPS | -0.5083 | -1.1065 | 0.09 | 0.13770 | |
| FASY - BEPE | -1.1921 | -1.7933 | -0.591 | 0.00000 | *** |
| SOAU - BEPE | -1.1273 | -1.692 | -0.5626 | 0.00000 | *** |
| TICO - BEPE | -0.6537 | -1.3048 | -0.0025 | 0.04858 | * |
| SOAU- FASY | 0.06485 | -0.5125 | 0.64224 | 0.99803 | |
| TICO - FASY | 0.53847 | -0.1237 | 1.20062 | 0.17068 | |
| TICO- SOAU | 0.47362 | -0.1557 | 1.10291 | 0.23765 | |

Table S4.6: The parameter estimates of ANOVA with the Tukey post-hoc test shows the multiple comparisons of the overall daily range of water potential variation ($\Delta\Psi_L$) across the five species (Figure 4.5c) during dry-out events. Significant differences between species are shown with a asterisk.

| Species | diff | lwr | upr | adj p-value | |
|-------------|----------|----------|----------|-------------|-----|
| BEPE - ACPS | -0.23403 | -0.38215 | -0.08591 | 0.00018 | *** |
| FASY - ACPS | 0.339048 | 0.187167 | 0.490928 | 0.00000 | *** |
| SOAU - ACPS | 0.154209 | 0.013663 | 0.294754 | 0.02332 | * |
| TICO - ACPS | 0.123492 | -0.04372 | 0.290707 | 0.25716 | |
| FASY - BEPE | 0.573077 | 0.40506 | 0.741094 | 0.00000 | *** |
| SOAU - BEPE | 0.388238 | 0.230393 | 0.546083 | 0.00000 | *** |
| TICO - BEPE | 0.357521 | 0.175524 | 0.539518 | 0.00000 | *** |
| SOAU- FASY | -0.18484 | -0.34622 | -0.02346 | 0.01552 | * |
| TICO - FASY | -0.21556 | -0.40063 | -0.03048 | 0.01311 | * |
| TICO- SOAU | -0.03072 | -0.20661 | 0.145173 | 0.98933 | |

References:

- Álvarez-Maldini C, Acevedo M, Pinto M (2021) Hydroscales: A Useful Metric for Distinguishing Iso-/Anisohydric Behavior in Almond Cultivars. *Plants* 10:1249.
- Anderegg WRL, Hicke JA, Fisher RA, Allen CD, Aukema J, Bentz B, Hood S, Lichstein JW, Macalady AK, McDowell N, Pan Y, Raffa K, Sala A, Shaw JD, Stephenson NL, Tague C, Zeppel M (2015) Tree mortality from drought, insects, and their interactions in a changing climate. *New Phytologist* 208:674–683.
- Anderegg WRL, Meinzer FC (2015) Wood Anatomy and Plant Hydraulics in a Changing Climate. In: Hacke U (ed) *Functional and Ecological Xylem Anatomy*. Springer International Publishing, Cham, pp 235–253.
- Arend M, Link RM, Patthey R, Hoch G, Schuldt B, Kahmen A (2021) Rapid hydraulic collapse as cause of drought-induced mortality in conifers. *Proceedings of the National Academy of Sciences* 118:e2025251118.
- Attia Z, Domec J-C, Oren R, Way DA, Moshelion M (2015) Growth and physiological responses of isohydric and anisohydric poplars to drought. *Journal of Experimental Botany* 66:4373–4381.
- Bartlett MK, Klein T, Jansen S, Choat B, Sack L (2016) The correlations and sequence of plant stomatal, hydraulic, and wilting responses to drought. *Proceedings of the National Academy of Sciences* 113:13098–13103.
- Bartlett MK, Zhang Y, Kreidler N, Sun S, Ardy R, Cao K, Sack L (2014) Global analysis of plasticity in turgor loss point, a key drought tolerance trait. *Ecology Letters* 17:1580–1590.
- Bates D, Mächler M, Bolker B, Walker S (2015) Fitting Linear Mixed-Effects Models Using lme4. *Journal of Statistical Software* 67.
- Blackman CJ, Creek D, Maier C, Aspinwall MJ, Drake JE, Pfautsch S, O’Grady A, Delzon S, Medlyn BE, Tissue DT, Choat B (2019a) Drought response strategies and hydraulic traits contribute to mechanistic understanding of plant dry-down to hydraulic failure. *Tree Physiology* 39:910–924.
- Blackman CJ, Li X, Choat B, Rymer PD, De Kauwe MG, Duursma RA, Tissue DT, Medlyn BE (2019b) Desiccation time during drought is highly predictable across species of *Eucalyptus* from contrasting climates. *New Phytologist* 224:632–643.
- Blackman CJ, Pfautsch S, Choat B, Delzon S, Gleason SM, Duursma RA (2016) Toward an index of desiccation time to tree mortality under drought: Desiccation time to tree mortality. *Plant, Cell & Environment* 39:2342–2345.
- Brodribb TJ (2017) Progressing from ‘functional’ to mechanistic traits. *New Phytologist* 215:9–11.
- Brodribb TJ, Holbrook NM, Edwards EJ, Gutiérrez MV (2003) Relations between stomatal closure, leaf turgor and xylem vulnerability in eight tropical dry forest trees. *Plant, Cell & Environment* 26:443–450.

- Brodrribb TJ, McAdam SAM, Jordan GJ, Martins SCV (2014) Conifer species adapt to low-rainfall climates by following one of two divergent pathways. *Proceedings of the National Academy of Sciences* 111:14489–14493.
- Burghardt M, Riederer M (2003) Ecophysiological relevance of cuticular transpiration of deciduous and evergreen plants in relation to stomatal closure and leaf water potential. *Journal of Experimental Botany* 54:1941–1949.
- Challis A, Blackman C, Ahrens C, Medlyn B, Rymer P, Tissue D (2022) Adaptive plasticity in plant traits increases time to hydraulic failure under drought in a foundation tree. *Tree Physiology* 42:708–721.
- Chaves MM, Zarrouk O, Francisco R, Costa JM, Santos T, Regalado AP, Rodrigues ML, Lopes CM (2010) Grapevine under deficit irrigation: hints from physiological and molecular data. *Annals of Botany* 105:661–676.
- Chen Z, Zhang Y, Yuan W, Zhu S, Pan R, Wan X, Liu S (2021) Coordinated variation in stem and leaf functional traits of temperate broadleaf tree species in the isohydric–anisohydric spectrum. *Tree Physiology* 41:1601–1610.
- Choat B, Brodrribb TJ, Brodersen CR, Duursma RA, López R, Medlyn BE (2018) Triggers of tree mortality under drought. *Nature* 558:531–539.
- Christman MA, Sperry JS, Adler FR (2009) Testing the ‘rare pit’ hypothesis for xylem cavitation resistance in three species of *Acer*. *New Phytologist* 182:664–674.
- Christman MA, Sperry JS, Smith DD (2012) Rare pits, large vessels and extreme vulnerability to cavitation in a ring-porous tree species. *New Phytologist* 193:713–720.
- Delzon S, Cochard H (2014) Recent advances in tree hydraulics highlight the ecological significance of the hydraulic safety margin. *New Phytologist* 203:355–358.
- Domec J-C, Gartner BL (2003) Relationship between growth rates and xylem hydraulic characteristics in young, mature and old-growth ponderosa pine trees. *Plant, Cell & Environment* 26:471–483.
- Domec J-C, Johnson DM (2012) Does homeostasis or disturbance of homeostasis in minimum leaf water potential explain the isohydric versus anisohydric behavior of *Vitis vinifera* L. cultivars? *Tree Physiology* 32:245–248.
- Duursma RA, Blackman CJ, López R, Martin-StPaul NK, Cochard H, Medlyn BE (2019) On the minimum leaf conductance: its role in models of plant water use, and ecological and environmental controls. *New Phytologist* 221:693–705.
- Eller CB, Rowland L, Oliveira RS, Bittencourt PRL, Barros FV, da Costa ACL, Meir P, Friend AD, Mencuccini M, Sitch S, Cox P (2018) Modelling tropical forest responses to drought and El Niño with a stomatal optimization model based on xylem hydraulics. *Philosophical Transactions of the Royal Society B: Biological Sciences* 373:20170315.
- Fan Z-X, Zhang S-B, Hao G-Y, Ferry Slik JW, Cao K-F (2012) Hydraulic conductivity traits predict growth rates and adult stature of 40 Asian tropical tree species better than wood density. *Journal of Ecology* 100:732–741.

- Farrell C, Szota C, Arndt SK (2017) Does the turgor loss point characterize drought response in dryland plants? *Plant, Cell & Environment* 40:1500–1511.
- Feng X, Ackerly DD, Dawson TE, Manzoni S, McLaughlin B, Skelton RP, Vico G, Weitz AP, Thompson SE (2019) Beyond isohydricity: The role of environmental variability in determining plant drought responses. *Plant, Cell & Environment* 42:1104–1111.
- Fichot R, Barigah TS, Chamaillard S, Le Thiec D, Laurans F, Cochard H, Brignolas F (2010) Common trade-offs between xylem resistance to cavitation and other physiological traits do not hold among unrelated *Populus deltoides*×*Populus nigra* hybrids: Xylem resistance to cavitation and water relations in poplar. *Plant, Cell & Environment*:1553–1568.
- Fichot R, Chamaillard S, Depardieu C, Le Thiec D, Cochard H, Barigah TS, Brignolas F (2011) Hydraulic efficiency and coordination with xylem resistance to cavitation, leaf function, and growth performance among eight unrelated *Populus deltoides*×*Populus nigra* hybrids. *Journal of Experimental Botany* 62:2093–2106.
- Franklin O, Fransson P, Hofhansl F, Joshi J (2022) Optimal balancing of xylem efficiency and safety explains plant vulnerability to drought. *bioRxiv*: 10.1101/2022.05.16.491812.
- Fu X, Meinzer FC (2019) Metrics and proxies for stringency of regulation of plant water status (iso/anisohdry): a global data set reveals coordination and trade-offs among water transport traits. *Tree Physiology* 39:122–134.
- Fu X, Meinzer FC, Woodruff DR, Liu Y-Y, Smith DD, McCulloh KA, Howard AR (2019) Coordination and trade-offs between leaf and stem hydraulic traits and stomatal regulation along a spectrum of isohydry to anisohdry. *Plant, Cell & Environment* 42:2245–2258.
- Fuchs S, Schuldt B, Leuschner C (2021) Identification of drought-tolerant tree species through climate sensitivity analysis of radial growth in Central European mixed broadleaf forests. *Forest Ecology and Management* 494:119287.
- Garcia-Forner N, Adams HD, Sevanto S, Collins AD, Dickman LT, Hudson PJ, Zeppel MJB, Jenkins MW, Powers H, Martínez-Vilalta J, McDowell NG (2016) Responses of two semiarid conifer tree species to reduced precipitation and warming reveal new perspectives for stomatal regulation: Stomatal regulation in piñon and juniper trees. *Plant, Cell & Environment* 39:38–49.
- Garcia-Forner N, Biel C, Savé R, Martínez-Vilalta J (2017) Isohydric species are not necessarily more carbon limited than anisohydric species during drought. *Tree Physiology* 37:441–455.
- Gleason SM, Blackman CJ, Cook AM, Laws CA, Westoby M (2014) Whole-plant capacitance, embolism resistance and slow transpiration rates all contribute to longer desiccation times in woody angiosperms from arid and wet habitats. *Tree Physiology* 34:275–284.
- Gleason SM, Stephens AEA, Tozer WC, Blackman CJ, Butler DW, Chang Y, Cook AM, Cooke J, Laws CA, Rosell JA, Stuart SA, Westoby M (2018) Shoot growth of woody trees and shrubs is predicted by maximum plant height and associated traits. *Functional Ecology* 32:247–259.
- Gleason SM, Westoby M, Jansen S, Choat B, Hacke UG, Pratt RB, Bhaskar R, Brodribb TJ, Bucci SJ, Cao K, Cochard H, Delzon S, Domec J, Fan Z, Feild TS, Jacobsen AL, Johnson DM,

- Lens F, Maherali H, Martínez-Vilalta J, Mayr S, McCulloh KA, Mencuccini M, Mitchell PJ, Morris H, Nardini A, Pittermann J, Plavcová L, Schreiber SG, Sperry JS, Wright IJ, Zanne AE (2016) Weak tradeoff between xylem safety and xylem-specific hydraulic efficiency across the world's woody plant species. *New Phytologist* 209:123–136.
- Greenwood S, Ruiz-Benito P, Martínez-Vilalta J, Lloret F, Kitzberger T, Allen CD, Fensham R, Laughlin DC, Kattge J, Bönisch G, Kraft NJB, Jump AS (2017) Tree mortality across biomes is promoted by drought intensity, lower wood density and higher specific leaf area. *Ecology Letters* 20:539–553.
- Guet J, Fichot R, Lédée C, Laurans F, Cochard H, Delzon S, Bastien C, Brignolas F (2015) Stem xylem resistance to cavitation is related to xylem structure but not to growth and water-use efficiency at the within-population level in *Populus nigra* L. *EXBOTJ* 66:4643–4652.
- Guha A, Reddy AR (2014) Leaf gas exchange, water relations and photosystem-II functionality depict anisohydric behavior of drought-stressed mulberry (*Morus indica*, cv. V1) in the hot semi-arid steppe agroclimate of Southern India. *Flora - Morphology, Distribution, Functional Ecology of Plants* 209:142–152.
- Guo JS, Hultine KR, Koch GW, Kropp H, Ogle K (2020) Temporal shifts in iso/anisohdry revealed from daily observations of plant water potential in a dominant desert shrub. *New Phytologist* 225:713–726.
- Hacke UG, Sperry JS (2001) Functional and ecological xylem anatomy. *Perspectives in Plant Ecology, Evolution and Systematics* 4:97–115.
- Hacke UG, Sperry JS, Wheeler JK, Castro L (2006) Scaling of angiosperm xylem structure with safety and efficiency. *Tree physiology* 26:689–701.
- Hacke UG, Spicer R, Schreiber SG, Plavcová L (2017) An ecophysiological and developmental perspective on variation in vessel diameter: Variation in xylem vessel diameter. *Plant, Cell & Environment* 40:831–845.
- Hajek P, Kurjak D, von Wühlisch G, Delzon S, Schuldt B (2016) Intraspecific Variation in Wood Anatomical, Hydraulic, and Foliar Traits in Ten European Beech Provenances Differing in Growth Yield. *Frontiers in Plant Science* 7:791.
- Hajek P, Leuschner C, Hertel D, Delzon S, Schuldt B (2014) Trade-offs between xylem hydraulic properties, wood anatomy and yield in *Populus*. *Tree Physiology* 34:744–756.
- Hammond WM, Adams HD (2019) Dying on time: traits influencing the dynamics of tree mortality risk from drought. *Tree Physiology* 39:906–909.
- Hartmann H, Link RM, Schuldt B (2021) A whole-plant perspective of isohydry: stem-level support for leaf-level plant water regulation. *Tree Physiology* 41:901–905.
- Hochberg U, Rockwell FE, Holbrook NM, Cochard H (2018) Iso/Anisohdry: A plant–environment interaction rather than a simple hydraulic trait. *Trends in Plant Science* 23:112–120.
- Hochberg U, Windt CW, Ponomarenko A, Zhang Y-J, Gersony J, Rockwell FE, Holbrook NM (2017) Stomatal closure, basal leaf embolism, and shedding protect the hydraulic integrity of grape stems. *Plant Physiology* 174:764–775.

- Hoerber S, Leuschner C, Köhler L, Arias-Aguilar D, Schuldt B (2014) The importance of hydraulic conductivity and wood density to growth performance in eight tree species from a tropical semi-dry climate. *Forest Ecology and Management* 330:126–136.
- Hoffmann WA, Marchin RM, Abit P, Lau OL (2011) Hydraulic failure and tree dieback are associated with high wood density in a temperate forest under extreme drought. *Global Change Biology* 17:2731–2742.
- Jacob V, Choat B, Churchill AC, Zhang H, Barton CVM, Krishnananthaselvan A, Post AK, Power SA, Medlyn BE, Tissue DT (2022) High safety margins to drought-induced hydraulic failure found in five pasture grasses. *Plant, Cell & Environment* 45:1631–1646.
- Jiang P, Meinzer FC, Fu X, Kou L, Dai X, Wang H (2021) Trade-offs between xylem water and carbohydrate storage among 24 coexisting subtropical understory shrub species spanning a spectrum of isohydry. *Tree Physiology* 41:403–415.
- Johnson DM, Domec J-C, Carter Berry Z, Schwantes AM, McCulloh KA, Woodruff DR, Wayne Polley H, Wortemann R, Swenson JJ, Scott Mackay D, McDowell NG, Jackson RB (2018) Co-occurring woody species have diverse hydraulic strategies and mortality rates during an extreme drought. *Plant, Cell & Environment* 41:576–588.
- Johnson DM, McCulloh KA, Woodruff DR, Meinzer FC (2012) Hydraulic safety margins and embolism reversal in stems and leaves: Why are conifers and angiosperms so different? *Plant Science* 195:48–53.
- Joshi J, Stocker BD, Hofhansl F, Zhou S, Dieckmann U, Prentice IC (2022) Towards a unified theory of plant photosynthesis and hydraulics. *Nature Plants*:1–13.
- Klein T (2014) The variability of stomatal sensitivity to leaf water potential across tree species indicates a continuum between isohydric and anisohydric behaviours. *Functional Ecology* 28:1313–1320.
- Köcher P, Gebauer T, Horna V, Leuschner C (2009) Leaf water status and stem xylem flux in relation to soil drought in five temperate broad-leaved tree species with contrasting water use strategies. *Annals of Forest Science* 66:101–101.
- Kotowska MM, Link RM, Röhl A, Hertel D, Hölscher D, Waite P-A, Moser G, Tjoa A, Leuschner C, Schuldt B (2021) Effects of Wood Hydraulic Properties on Water Use and Productivity of Tropical Rainforest Trees. *Frontiers in Forests and Global Change* 3:598759.
- Lemaire C, Blackman CJ, Cochard H, Menezes-Silva PE, Torres-Ruiz JM, Herbette S (2021) Acclimation of hydraulic and morphological traits to water deficit delays hydraulic failure during simulated drought in poplar. *Tree Physiology* 8:2008-2021.
- Lens F, Sperry JS, Christman MA, Choat B, Rabaey D, Jansen S (2011) Testing hypotheses that link wood anatomy to cavitation resistance and hydraulic conductivity in the genus *Acer*. *New Phytologist* 190:709–723.

- Leuschner C, Schipka F, Backes K (2022) Stomatal regulation and water potential variation in European beech: challenging the iso/anisohydry concept. *Tree Physiology* 42:365–378.
- Leuschner C, Wedde P, Lübke T (2019) The relation between pressure–volume curve traits and stomatal regulation of water potential in five temperate broadleaf tree species. *Annals of Forest Science* 76:1–14.
- Li S, Lens F, Espino S, Karimi Z, Klepsch M, Schenk HJ, Schmitt M, Schuldt B, Jansen S (2016b) Intervessel pit membrane thickness as a key determinant of embolism resistance in angiosperm xylem. *IAWA Journal* 37:152–171.
- Li X, Blackman CJ, Choat B, Duursma RA, Rymer PD, Medlyn BE, Tissue DT (2018) Tree hydraulic traits are coordinated and strongly linked to climate-of-origin across a rainfall gradient. *Plant, Cell & Environment* 41:646–660.
- Li X, Blackman CJ, Peters JMR, Choat B, Rymer PD, Medlyn BE, Tissue DT (2019) More than iso/anisohydry: Hydrosapscapes integrate plant water use and drought tolerance traits in 10 eucalypt species from contrasting climates. *Functional Ecology* 33:1035–1049.
- Liang X, Ye Q, Liu H, Brodribb TJ (2021) Wood density predicts mortality threshold for diverse trees. *New Phytologist* 229:3053–3057.
- Liu H, Ye Q, Gleason SM, He P, Yin D (2021) Weak tradeoff between xylem hydraulic efficiency and safety: climatic seasonality matters. *New Phytologist* 229:1440–1452.
- Loepfe L, Martinez-Vilalta J, Piñol J, Mencuccini M (2007) The relevance of xylem network structure for plant hydraulic efficiency and safety. *Journal of Theoretical Biology* 247:788–803.
- Loewenstein NJ, Pallardy SG (1998) Drought tolerance, xylem sap abscisic acid and stomatal conductance during soil drying: a comparison of young plants of four temperate deciduous angiosperms. *Tree Physiology* 18:421–430.
- Lübke T, Lamarque LJ, Delzon S, Torres Ruiz JM, Burlett R, Leuschner C, Schuldt B (2022) High variation in hydraulic efficiency but not xylem safety between roots and branches in four temperate broad-leaved tree species. *Functional Ecology*:1365-2435.13975.
- Mackay DS, Roberts DE, Ewers BE, Sperry JS, McDowell NG, Pockman WT (2015) Interdependence of chronic hydraulic dysfunction and canopy processes can improve integrated models of tree response to drought. *Water Resources Research* 51:6156–6176.
- Maherali H, Moura CF, Caldeira MC, Willson CJ, Jackson RB (2006) Functional coordination between leaf gas exchange and vulnerability to xylem cavitation in temperate forest trees. *Plant Cell Environment* 29:571–583.
- Martínez-Vilalta J, Garcia-Forner N (2017) Water potential regulation, stomatal behaviour and hydraulic transport under drought: deconstructing the iso/anisohydric concept: Deconstructing the iso/anisohydric concept. *Plant, Cell & Environment* 40:962–976.
- Martínez-Vilalta J, Poyatos R, Aguadé D, Retana J, Mencuccini M (2014) A new look at water transport regulation in plants. *New Phytologist* 204:105–115.

- Martin-StPaul N, Delzon S, Cochard H (2017) Plant resistance to drought depends on timely stomatal closure. *Ecology Letters* 20:1437–1447.
- McDowell N, Pockman WT, Allen CD, Breshears DD, Cobb N, Kolb T, Plaut J, Sperry J, West A, Williams DG, Yezzer EA (2008) Mechanisms of plant survival and mortality during drought: why do some plants survive while others succumb to drought? *New Phytologist* 178:719–739.
- McDowell NG (2011) Mechanisms Linking Drought, Hydraulics, Carbon Metabolism, and Vegetation Mortality. *Plant Physiology* 155:1051–1059.
- Meier IC, Leuschner C (2008) Leaf Size and Leaf Area Index in *Fagus sylvatica* Forests: Competing Effects of Precipitation, Temperature, and Nitrogen Availability. *Ecosystems* 11:655–669.
- Meinzer FC, Johnson DM, Lachenbruch B, McCulloh KA, Woodruff DR (2009) Xylem hydraulic safety margins in woody plants: coordination of stomatal control of xylem tension with hydraulic capacitance. *Functional Ecology* 23:922–930.
- Meinzer FC, Smith DD, Woodruff DR, Marias DE, McCulloh KA, Howard AR, Magedman AL (2017) Stomatal kinetics and photosynthetic gas exchange along a continuum of isohydric to anisohydric regulation of plant water status. *Plant, Cell & Environment* 40:1618–1628.
- Meinzer FC, Woodruff DR, Marias DE, McCulloh KA, Sevanto S (2014) Dynamics of leaf water relations components in co-occurring iso- and anisohydric conifer species: Dynamics of leaf water relations components. *Plant, Cell & Environment* 37:2577–2586.
- Meinzer FC, Woodruff DR, Marias DE, Smith DD, McCulloh KA, Howard AR, Magedman AL (2016) Mapping ‘hydroscares’ along the iso- to anisohydric continuum of stomatal regulation of plant water status. *Ecology Letters* 19:1343–1352.
- Mencuccini M, Bonosi L (2001) Leaf/sapwood area ratios in Scots pine show acclimation across Europe. *Canadian Journal of Forest Research* 31:442–456.
- Mitchell PJ, O’Grady AP, Tissue DT, White DA, Ottenschlaeger ML, Pinkard EA (2013) Drought response strategies define the relative contributions of hydraulic dysfunction and carbohydrate depletion during tree mortality. *New Phytologist* 197:862–872.
- Moser A, Rötzer T, Pauleit S, Pretzsch H (2016) The Urban Environment Can Modify Drought Stress of Small-Leaved Lime (*Tilia cordata* Mill.) and Black Locust (*Robinia pseudoacacia* L.). *Forests* 7:71.
- Nardini A, Battistuzzo M, Savi T (2013) Shoot desiccation and hydraulic failure in temperate woody angiosperms during an extreme summer drought. *New Phytologist* 200:322–329.
- Nolan RH, Tarin T, Santini NS, McAdam SAM, Ruman R, Eamus D (2017) Differences in osmotic adjustment, foliar abscisic acid dynamics, and stomatal regulation between an isohydric and anisohydric woody angiosperm during drought. *Plant, Cell & Environment* 40:3122–3134.
- Ogle K, Lucas RW, Bentley LP, Cable JM, Barron-Gafford GA, Griffith A, Ignace D, Jenerette GD, Tyler A, Huxman TE, Loik ME, Smith SD, Tissue DT (2012) Differential daytime and

- night-time stomatal behavior in plants from North American deserts. *New Phytologist* 194:464–476.
- Oren R, Sperry JS, Katul GG, Pataki DE, Ewers BE, Phillips N, Schäfer KVR (1999) Survey and synthesis of intra- and interspecific variation in stomatal sensitivity to vapour pressure deficit. *Plant, Cell & Environment* 22:1515–1526.
- Pockman WT, Sperry JS (2000) Vulnerability to xylem cavitation and the distribution of Sonoran Desert vegetation. *American Journal of Botany* 87:1287–1299.
- Poorter H, Niklas KJ, Reich PB, Oleksyn J, Poot P, Mommer L (2012) Biomass allocation to leaves, stems and roots: meta-analyses of interspecific variation and environmental control. *New Phytologist* 193:30–50.
- Pou A, Medrano H, Tomàs M, Martorell S, Ribas-Carbó M, Flexas J (2012) Anisohydric behaviour in grapevines results in better performance under moderate water stress and recovery than isohydric behaviour. *Plant Soil* 359:335–349.
- Powell TL, Wheeler JK, de Oliveira AAR, da Costa ACL, Saleska SR, Meir P, Moorcroft PR (2017) Differences in xylem and leaf hydraulic traits explain differences in drought tolerance among mature Amazon rainforest trees. *Global Change Biology* 23:4280–4293.
- Preisler Y, Hölttä T, Grünzweig JM, Oz I, Tatarinov F, Ruehr NK, Rotenberg E, Yakir D (2022) The importance of tree internal water storage under drought conditions. *Tree Physiology* 42:771–783.
- Ramesha MN, Link RM, Paligi SS, Hertel D, Röhl A, Hölscher D, Schuldt B (2022) Variability in growth-determining hydraulic wood and leaf traits in *Melia dubia* across a steep water availability gradient in southern India. *Forest Ecology and Management* 505:119875.
- Ratzmann G, Meinzer FC, Tietjen B (2019) Iso/Anisohdry: Still a Useful Concept. *Trends in Plant Science* 24:191–194.
- Reich PB (2014) The world-wide ‘fast–slow’ plant economics spectrum: a traits manifesto. *Journal of Ecology* 102:275–301.
- Rogiers SY, Greer DH, Hatfield JM, Hutton RJ, Clarke SJ, Hutchinson PA, Somers A (2012) Stomatal response of an anisohydric grapevine cultivar to evaporative demand, available soil moisture and abscisic acid. *Tree Physiology* 32:249–261.
- Roman DT, Novick KA, Brzostek ER, Dragoni D, Rahman F, Phillips RP (2015) The role of isohydric and anisohydric species in determining ecosystem-scale response to severe drought. *Oecologia* 179:641–654.
- Rosas T, Mencuccini M, Barba J, Cochard H, Saura-Mas S, Martínez-Vilalta J (2019) Adjustments and coordination of hydraulic, leaf and stem traits along a water availability gradient. *New Phytologist* 223:632–646.
- Ruffault J, Pimont F, Cochard H, Dupuy J-L, Martin-StPaul N (2022) SurEau-Ecos v2.0: a trait-based plant hydraulics model for simulations of plant water status and drought-induced mortality at the ecosystem level. *Geoscientific Model Development* 15:5593–5626.

- Sade N, Gebremedhin A, Moshelion M (2012) Risk-taking plants Anisohydric behavior as a stress-resistance trait. *Plant Signaling & Behavior* 7:767–770.
- Salomón RL, Limousin J-M, Ourcival J-M, Rodríguez-Calcerrada J, Steppe K (2017) Stem hydraulic capacitance decreases with drought stress: implications for modelling tree hydraulics in the Mediterranean oak *Quercus ilex*. *Plant, Cell & Environment* 40:1379–1391.
- Salvi AM, Gosetti SG, Smith DD, Adams MA, Givnish TJ, McCulloh KA (2022) Hydroscares, hydroscape plasticity and relationships to functional traits and mesophyll photosynthetic sensitivity to leaf water potential in *Eucalyptus* species. *Plant, Cell & Environment* 45:2573–2588.
- Scholz A, Rabaey D, Stein A, Cochard H, Smets E, Jansen S (2013) The evolution and function of vessel and pit characters with respect to cavitation resistance across 10 *Prunus* species. *Tree Physiology* 33:684–694.
- Scholz FG, Phillips NG, Bucci SJ, Meinzer FC, Goldstein G (2011) Hydraulic Capacitance: Biophysics and Functional Significance of Internal Water Sources in Relation to Tree Size. In: Meinzer FC, Lachenbruch B, Dawson TE (eds) *Size- and Age-Related Changes in Tree Structure and Function*. Springer Netherlands, Dordrecht, pp 341–361.
- Schuldt B, Knutzen F, Delzon S, Jansen S, Müller-Haubold H, Burlett R, Clough Y, Leuschner C (2016) How adaptable is the hydraulic system of European beech in the face of climate change-related precipitation reduction? *New Phytologist* 210:443–458.
- Schumann K, Leuschner C, Schuldt B (2019) Xylem hydraulic safety and efficiency in relation to leaf and wood traits in three temperate *Acer* species differing in habitat preferences. *Trees* 33:1475–1490.
- Skelton RP, West AG, Dawson TE (2015) Predicting plant vulnerability to drought in biodiverse regions using functional traits. *Proceedings of the National Academy of Sciences* 112:5744–5749.
- Sperry JS, Hacke UG, Oren R, Comstock JP (2002) Water deficits and hydraulic limits to leaf water supply. *Plant, Cell & Environment* 25:251–263.
- Sperry JS, Tyree MT (1990) Water-stress-induced xylem embolism in three species of conifers. *Plant, Cell & Environment* 13:427–436.
- Sperry JS, Venturas MD, Anderegg WRL, Mencuccini M, Mackay DS, Wang Y, Love DM (2017) Predicting stomatal responses to the environment from the optimization of photosynthetic gain and hydraulic cost: A stomatal optimization model. *Plant, Cell & Environment* 40:816–830.
- Tardieu F, Simonneau T (1998) Variability among species of stomatal control under fluctuating soil water status and evaporative demand: modelling isohydric and anisohydric behaviours. *Journal of Experimental Botany* 49:419–432.
- Tolia N, Devakumar AS, Sheshshayee MS, Kambalimath S (2019) Growth performance of six multipurpose tree species based on the carbon assimilation capacity: a functional approach. *Agroforestry Systems* 93:1031–1043.

- Tyagi V, Singh SP, Singh RD, Gumber S (2023) Chir pine and banj oak responses to pre-monsoon drought across slope aspects and positions in Central Himalaya. *Environmental Monitoring and Assessment* 195:258.
- Tyree MT, Engelbrecht BMJ, Vargas G, Kursar TA (2003) Desiccation Tolerance of Five Tropical Seedlings in Panama. Relationship to a Field Assessment of Drought Performance. *Plant Physiology* 132:1439–1447.
- Vogt UK (2001) Hydraulic vulnerability, vessel refilling, and seasonal courses of stem water potential of *Sorbus aucuparia* L. and *Sambucus nigra* L. *Journal of Experimental Botany* 52:1527–1536.
- Weithmann G, Schuldt B, Link RM, Heil D, Hoeber S, John H, Müller-Haubold H, Schüller L-M, Schumann K, Leuschner C (2022) Leaf trait modification in European beech trees in response to climatic and edaphic drought. *Plant Biology* 24:1272–1286.
- Wheeler JK, Sperry JS, Hacke UGWE, Hoang N (2005) Inter-vessel pitting and cavitation in woody Rosaceae and other vesselled plants: a basis for a safety versus efficiency trade-off in xylem transport. *Plant, Cell & Environment* 28:800–812.
- Wikberg J, Ögren E (2004) Interrelationships between water use and growth traits in biomass-producing willows. *Trees - Structure and Function* 18:70–76.
- Wolfe BT (2017) Retention of stored water enables tropical tree saplings to survive extreme drought conditions. *Tree Physiology* 37:469–480.
- Wright IJ, Dong N, Maire V, Prentice IC, Westoby M, Díaz S, Gallagher RV, Jacobs BF, Kooyman R, Law EA, Leishman MR, Niinemets Ü, Reich PB, Sack L, Villar R, Wang H, Wilf P (2017) Global climatic drivers of leaf size. *Science* 357:917–921.
- Xie J, Wang Z, Li Y (2022) Stomatal opening ratio mediates trait coordinating network adaptation to environmental gradients. *New Phytologist* 235:907–922.
- Zhang J-L, Cao K-F (2009) Stem hydraulics mediates leaf water status, carbon gain, nutrient use efficiencies and plant growth rates across dipterocarp species. *Functional Ecology* 23:658–667.
- Zhang L, Liu L, Zhao H, Jiang Z, Cai J (2020) Differences in Near Isohydic and Anisohydic Behavior of Contrasting Poplar Hybrids (I-101 (*Populus alba* L.) × 84K (*Populus alba* L. × *Populus glandulosa* Uyeki)) under Drought-Rehydration Treatments. *Forests* 11:402.
- Zhang Y, Oren R, Kang S (2012) Spatiotemporal variation of crown-scale stomatal conductance in an arid *Vitis vinifera* L. cv. Merlot vineyard: direct effects of hydraulic properties and indirect effects of canopy leaf area. *Tree Physiology* 32:262–279.
- Zhu J, Thimonier A, Etzold S, Meusburger K, Waldner P, Schmitt M, Schleppei P, Schaub M, Thormann J-J, Lehmann MM (2022) Variation in leaf morphological traits of European beech and Norway spruce over two decades in Switzerland. *Frontiers in Forests and Global Change* 4:778351.

Chapter-5: General conclusion

5.1 Conclusion

The dissertation highlights the diversity of species' traits coordination, acclimatization, and strategies along the degree of isohydry at species-specific levels in responses to drought. In general, the acclimatization of species to a changing environment can be attributed to the plastic response of traits. Studying these responses is essential for the better function of forest ecosystems in changing climates, especially with increasing VPD associated with high temperatures. Based on the findings of the present dissertation (Chapter-2 and 3, Table A4.1), we here elucidate the species-specific traits adjustment to understand the growth and survival mechanism in response to drought.

In the study, *Acer pseudoplatanus*, the most isohydric species, showed higher growth rates linked to higher K_S but not P_{50} , which depends on large vessel diameter. Under stress, the species experienced a strong reduction in hydraulic conductivity and vessel diameter, but xylem safety remained unaffected. Huber values (HV) linked to growth performance had a decreasing trend under stress conditions. In the first study (Chapter-2), all three species exhibited a similar tendency in HV, indicating that more resources were used for water transportation. The species also adjusted their leaf-level water supply by reducing the size of leaves and potentially their numbers in response to more stressful climatic conditions. Furthermore, on the framework of iso-anisohydric, ACPS prefers to close its stomata well before the loss of cell turgor, resulting in the highest hydraulic safety margins. Additionally, higher capacitance and wood density play important roles in drought tolerance. In contrast, the higher Ψ_{tp} in the species signifies the loss of cell turgor at higher water potentials. The species' higher cuticular conductance offers a disadvantage as it contributes to speedy water loss after stomata closure, which can influence plant desiccation time.

Betula pendula, an isohydric species with stringent stomatal control, showed a higher biomass production that was negatively linked with the P_{50} value (more negative) while positively with higher K_S . The species exhibited reduced vessel diameter, associated with specific conductivity under stress, resulting in a lower growth rate. Despite higher capacitance and early stomatal closure strategy supporting to avoid of cavitation, BEPE failed to achieve longer desiccation times due to lower embolism resistance and hydraulic safety margin. Contrary to expectation, species exhibited lower Ψ_{tp} , which does not ally with the onset of embolism formation (P_{12}). However, BEPE relies on early leaf shedding as a drought response strategy (Gao *et al.*

2017, Hajek *et al.* 2022), which decouples leaf and stem water potentials and may explain the relatively negative Ψ_{tip} for that species considering its low embolism resistance. Moreover, the species is known to adjust its leaf osmotic potentials under drought plastically and thus to drop its Ψ_{tip} (Aspelmeier and Leuschner 2004). Additionally, higher C appeared not to hold the promise to negotiate with declining water potential.

The stomatal behaviour of *Tilia cordata* is mixed in the published accounts of their degree of isohydry; the species had a relatively high Ψ_{tip} and P_{s90} as well as an intermediate HSA, even though it and other species from the genus *Tilia* are often classified as anisohydric (Moser *et al.* 2016, Gillner *et al.* 2017, Kiorapostolou *et al.* 2018, Moser-Reischl *et al.* 2019). However, there seems a lack of consensus for TICO (Köcher *et al.* 2009), and our results are more in line with Leuschner *et al.* (2019), who reported fairly isohydric behaviour for that species. In our study, the large internal water storage combined with its relatively high embolism resistance and early stomatal closure led to the highest average standardized drying time for that species. In addition, longer desiccation times for the species also supported by the lowest cuticular conductance and large hydraulic safety margin ($P_{s90} - P_{s88}$).

Sorbus aucuparia is reported to be more anisohydric, having a larger HSA and displays higher embolism resistance but lower biomass production under stress conditions. However, hydraulic efficiency and the primary anatomical determinant (i.e., vessel diameter) are unaffected. So, it suggests that embolism resistance could be favoured when a plant is grown under stress. This could be likely the reason for building more resistance xylem to support the longer stomata functioning with declining water potential. Further, the species has high wood density, indicating a greater investment in xylem vessels, which allows for better survival in drought conditions (Hoffmann *et al.* 2011, Nardini *et al.* 2013, Greenwood *et al.* 2017, Liang *et al.* 2021), and denser wood has a lower Ψ_{tip} (Fu and Meinzer 2019). Additionally, the species has a more negative P_{s90} and Ψ_{tip} , which allows for prolonged stomatal function and higher C -assimilation. A lower Ψ_{tip} is an asset in holding cell turgor for longer with declining water potential, while a high hydraulic safety margin enables the species to endure drought better. However, smaller C and higher supported leaf areas prove inadequate for longer desiccation times.

Fagus sylvatica is the most anisohydric species due to its largest HSA in our studied species and exhibiting the lowest P_{s90} and Ψ_{tip} values, enabling it to achieve a longer desiccation time. The species adopts a strategy of keeping stomata open for longer, allowing for greater carbon gain and

5. Conclusion

posing a risk of embolism. However, the lower Ψ_{tp} value is advantageous in maintaining cell turgor for longer periods under decreasing water potential. The more negative P_{88} value and less supported leaf area also supported the species' longer desiccation time.

5.2 Scopes and Limitations

Millions of recently planted tree saplings died, and mature trees were damaged during a past drought in central Europe (Schuldt *et al.* 2020, Rukh *et al.* 2023). To alleviate the climate change impact of forthcoming droughts and mitigate the situation, the European Commission plans to plant three billion trees across the EU by 2030. Studies suggested that mixed-species stand can be more productive and shows resilience to drought than the monoculture plantation (Liu *et al.* 2018, Vitali *et al.* 2018, Grossiord 2019, Hajek *et al.* 2022, Feng *et al.* 2022). The advantage of mixed-species plantations over monocultures can be attributed to the complementary and selection effects (Isbell *et al.* 2009, Grossiord *et al.* 2014, Grossiord 2019, Hajek *et al.* 2022). Large-sized trees can facilitate resource access at different temporal or spatial scales, thereby reducing interspecific competition and providing shelter from wind to neighbourhood species, which is important for species survival (Grossiord 2019, Hajek *et al.* 2022). Furthermore, mixed-species stands are preferred when interspecific interactions are generally more beneficial than intraspecific interactions (Hajek *et al.* 2022). Therefore, the selection of species and their combinations in forest stands can significantly affect tree mortality and productivity, thereby having important implications for reforestation programs and plantation management decisions.

To achieve the target of mixed-species reforestation, profound knowledge of the hydraulic characteristics is needed. Further, it is essential to understand the mechanisms of drought resistance and identify saplings that are resistant to drought. This requires a solid understanding of the relationship between traits related to xylem safety and the desiccation time of saplings (most notably P_{88} , HSM). We introduce the concepts of drought tolerance and isohydricity as a plant-environment interaction that can help describe a species' hydraulic strategy. Chapter-2 discusses the relationship between high growth rate, K_S , and large vessel diameter. In addition, it deliberated that P_{50} does not consistently vary with juvenile growth rate. In chapter-3, we examined how the stomatal stringency, HSM, and hydraulic-related traits impact the desiccation time and whether a species adopts a desiccation delay or avoidance and tolerance strategy. We believe that the catastrophic hydraulic failure coincides with plant mortality (P_{88}), so HSM calculated based on P_{88} could be more appropriate to understand the desiccation time.

However, Greenhouse studies of saplings have some limitations and considerations. For this, field studies are necessary confirming these relationships to understand the effects of drought on tree growth and mortality. Other traits, such as non-structural carbohydrate (NSC) storage (O'Brien *et al.* 2014, Sapes *et al.* 2019, Jiang *et al.* 2021, Challis *et al.* 2022), rooting depth (Nardini *et al.* 2016), and nature of embolism repair (Brodersen and McElrone 2013, Arend *et al.* 2022) are essential for mitigating drought stress under field conditions. Additionally, species mixtures in forest stands can promote greater drought resilience and affect forest productivity (Klein *et al.* 2014, Meinzer *et al.* 2014, Garcia-Forner *et al.* 2016). Leaf trait responses to environmental gradients and stomatal acclimation contribute to drought resistance (Dong *et al.* 2020, Joshi *et al.* 2022). Furthermore, the lack of consistency of trait-environment relationships along the iso-anisohydric spectrum narrows our expectations of simple trait trade-offs that unify multiple facets of plant response to drought.

5.3 Future perspectives

Future research should investigate additional plant functional traits under increasing drought stress to confirm our study results. Ψ_{\min} provides a reliable measure of plant function during periods of high evaporative demand and indicates its hydraulic performance close to critical failure (Meinzer *et al.* 2009, Choat *et al.* 2012). In addition, it is combined with stomatal behaviour, which exerts significant selective pressure on the xylem (Joshi *et al.* 2022). Specifically, for identifying drought-tolerant species for reforestation, future research directives should focus on determining the drought threshold on which anisohydric strategy-adapted species lose their advantage due to the high risk of embolism. Additionally, the substantial contribution of internal water storage and shoot capacitance in mitigating the effects of drought should be investigated as they have the potential to predict the difference between mortality and survival accurately and can be remotely sensed (Salomón *et al.* 2017, Sapes and Sala 2021, Preisler *et al.* 2022). Further, a more detailed investigation on controversial issues, such as growth trade-offs with hydraulic safety-efficiency and the xylem safety-vessel diameter association, is required. Moreover, on the note of the dynamic issue of plant-environment interaction and the controversial definition of iso-anisohydric, a more integrative and holistic approach to coordinated functional traits in response to drought is necessary.

References:

- Arend M, Link RM, Zahnd C, Hoch G, Schuldt B, Kahmen A (2022) Lack of hydraulic recovery as cause of post-drought foliage reduction and canopy decline in European beech. *New Phytologist* 234:1195-1205.
- Aspelmeier S, Leuschner C (2004) Genotypic variation in drought response of silver birch (*Betula pendula*): leaf water status and carbon gain. *Tree Physiology* 24:517–528.
- Brodersen C, McElrone A (2013) Maintenance of xylem Network Transport Capacity: A Review of Embolism Repair in Vascular Plants. *Frontiers in Plant Science* 4:108.
- Challis A, Blackman C, Ahrens C, Medlyn B, Rymer P, Tissue D (2022) Adaptive plasticity in plant traits increases time to hydraulic failure under drought in a foundation tree. *Tree Physiology* 42:708–721.
- Choat B, Jansen S, Brodribb TJ, Cochard H, Delzon S, Bhaskar R, Bucci SJ, Feild TS, Gleason SM, Hacke UG, Jacobsen AL, Lens F, Maherali H, Martínez-Vilalta J, Mayr S, Mencuccini M, Mitchell PJ, Nardini A, Pittermann J, Pratt RB, Sperry JS, Westoby M, Wright IJ, Zanne AE (2012) Global convergence in the vulnerability of forests to drought. *Nature* 491:752–755.
- Dong N, Prentice IC, Wright IJ, Evans BJ, Togashi HF, Caddy-Retalic S, McInerney FA, Sparrow B, Leitch E, Lowe AJ (2020) Components of leaf-trait variation along environmental gradients. *New Phytologist* 228:82–94.
- Feng Y, Schmid B, Loreau M, Forrester DI, Fei S, Zhu J, Tang Z, Zhu J, Hong P, Ji C, Shi Y, Su H, Xiong X, Xiao J, Wang S, Fang J (2022) Multispecies forest plantations outyield monocultures across a broad range of conditions. *Science* 376:865–868.
- Fu X, Meinzer FC (2019) Metrics and proxies for stringency of regulation of plant water status (iso/anisohydry): a global data set reveals coordination and trade-offs among water transport traits. *Tree Physiology* 39:122–134.
- Gao R, Shi X, Wang JR (2017) Comparative studies of the response of larch and birch seedlings from two origins to water deficit. *New Zealand Journal of Forestry Science* 47:14.
- Garcia-Forner N, Adams HD, Sevanto S, Collins AD, Dickman LT, Hudson PJ, Zeppel MJB, Jenkins MW, Powers H, Martínez-Vilalta J, McDowell NG (2016) Responses of two semiarid conifer tree species to reduced precipitation and warming reveal new perspectives for stomatal regulation: Stomatal regulation in piñon and juniper trees. *Plant, Cell & Environment* 39:38–49.
- Gillner S, Korn S, Hofmann M, Roloff A (2017) Contrasting strategies for tree species to cope with heat and dry conditions at urban sites. *Urban Ecosystems* 20:853–865.
- Greenwood S, Ruiz-Benito P, Martínez-Vilalta J, Lloret F, Kitzberger T, Allen CD, Fensham R, Laughlin DC, Kattge J, Bönisch G, Kraft NJB, Jump AS (2017) Tree mortality across biomes is promoted by drought intensity, lower wood density and higher specific leaf area. *Ecology Letters* 20:539–553.
- Grossiord C (2019) Having the right neighbors: how tree species diversity modulates drought impacts on forests. *New Phytologist* 228:42–49.

- Grossiord C, Granier A, Ratcliffe S, Bouriaud O, Bruelheide H, Čećko E, Forrester DI, Dawud SM, Finér L, Pollastrini M, Scherer-Lorenzen M, Valladares F, Bonal D, Gessler A (2014) Tree diversity does not always improve resistance of forest ecosystems to drought. *Proceedings of the National Academy of Sciences USA* 111:14812–14815.
- Hajek P, Link RM, Nock CA, Bauhus J, Gebauer T, Gessler A, Kovach K, Messier C, Paquette A, Saurer M, Scherer-Lorenzen M, Rose L, Schuldt B (2022) Mutually inclusive mechanisms of drought-induced tree mortality. *Global Change Biology* 28:3365–3378.
- Hoffmann WA, Marchin RM, Abit P, Lau OL (2011) Hydraulic failure and tree dieback are associated with high wood density in a temperate forest under extreme drought. *Global Change Biology* 17:2731–2742.
- Isbell FI, Polley HW, Wilsey BJ (2009) Biodiversity, productivity and the temporal stability of productivity: patterns and processes. *Ecology Letters* 12:443–451.
- Jiang P, Meinzer FC, Fu X, Kou L, Dai X, Wang H (2021) Trade-offs between xylem water and carbohydrate storage among 24 coexisting subtropical understory shrub species spanning a spectrum of isohydry. *Tree Physiology* 41:403–415.
- Joshi J, Stocker BD, Hofhansl F, Zhou S, Dieckmann U, Prentice IC (2022) Towards a unified theory of plant photosynthesis and hydraulics. *Nature Plants*:1–13.
- Kiorapostolou N, Galiano-Pérez L, von Arx G, Gessler A, Petit G (2018) Structural and anatomical responses of *Pinus sylvestris* and *Tilia platyphyllos* seedlings exposed to water shortage. *Trees* 32:1211–1218.
- Klein T, Yakir D, Buchmann N, Grünzweig JM (2014) Towards an advanced assessment of the hydrological vulnerability of forests to climate change-induced drought. *New Phytologist* 201:712–716.
- Köcher P, Gebauer T, Horna V, Leuschner C (2009) Leaf water status and stem xylem flux in relation to soil drought in five temperate broad-leaved tree species with contrasting water use strategies. *Annals of Forest Science* 66:101–101.
- Leuschner C, Wedde P, Lübke T (2019) The relation between pressure–volume curve traits and stomatal regulation of water potential in five temperate broadleaf tree species. *Annals of Forest Science* 76:1–14.
- Liang X, Ye Q, Liu H, Brodribb TJ (2021) Wood density predicts mortality threshold for diverse trees. *New Phytologist* 229:3053–3057.
- Liu CLC, Kuchma O, Krutovsky KV (2018) Mixed-species versus monocultures in plantation forestry: Development, benefits, ecosystem services and perspectives for the future. *Global Ecology and Conservation* 15:e00419.
- Meinzer FC, Johnson DM, Lachenbruch B, McCulloh KA, Woodruff DR (2009) Xylem hydraulic safety margins in woody plants: coordination of stomatal control of xylem tension with hydraulic capacitance. *Functional Ecology* 23:922–930.

5. Conclusion

- Meinzer FC, Woodruff DR, Marias DE, Mcculloh KA, Sevanto S (2014) Dynamics of leaf water relations components in co-occurring iso- and anisohydric conifer species: Dynamics of leaf water relations components. *Plant, Cell & Environment* 37:2577–2586.
- Moser A, Rötzer T, Pauleit S, Pretzsch H (2016) The Urban Environment Can Modify Drought Stress of Small-Leaved Lime (*Tilia cordata* Mill.) and Black Locust (*Robinia pseudoacacia* L.). *Forests* 7:71.
- Moser-Reischl A, Rahman MA, Pauleit S, Pretzsch H, Rötzer T (2019) Growth patterns and effects of urban micro-climate on two physiologically contrasting urban tree species. *Landscape and Urban Planning* 183:88–99.
- Nardini A, Battistuzzo M, Savi T (2013) Shoot desiccation and hydraulic failure in temperate woody angiosperms during an extreme summer drought. *New Phytologist* 200:322–329.
- Nardini A, Casolo V, Dal Borgo A, Savi T, Stenni B, Bertoincin P, Zini L, McDowell NG (2016) Rooting depth, water relations and non-structural carbohydrate dynamics in three woody angiosperms differentially affected by an extreme summer drought. *Plant, Cell & Environment* 39:618–627.
- O'Brien MJ, Leuzinger S, Philipson CD, Tay J, Hector A (2014) Drought survival of tropical tree seedlings enhanced by non-structural carbohydrate levels. *Nature Climate Change* 4:710–714.
- Preisler Y, Hölttä T, Grünzweig JM, Oz I, Tatarinov F, Ruehr NK, Rotenberg E, Yakir D (2022) The importance of tree internal water storage under drought conditions. *Tree Physiology* 42:771–783.
- Rukh S, Sanders TGM, Krüger I, Schad T, Bolte A (2023) Distinct Responses of European Beech (*Fagus sylvatica* L.) to Drought Intensity and Length—A Review of the Impacts of the 2003 and 2018–2019 Drought Events in Central Europe. *Forests* 14:248.
- Salomón RL, Limousin J-M, Ourcival J-M, Rodríguez-Calcerrada J, Steppe K (2017) Stem hydraulic capacitance decreases with drought stress: implications for modelling tree hydraulics in the Mediterranean oak *Quercus ilex*. *Plant, Cell & Environment* 40:1379–1391.
- Sapes G, Roskilly B, Dobrowski S, Maneta M, Anderegg WRL, Martinez-Vilalta J, Sala A (2019) Plant water content integrates hydraulics and carbon depletion to predict drought-induced seedling mortality. *Tree Physiology* 39:1300–1312.
- Sapes G, Sala A (2021) Relative water content consistently predicts drought mortality risk in seedling populations with different morphology, physiology and times to death. *Plant, Cell & Environment* 44:3322–3335.
- Schuldt B, Buras A, Arend M, Vitasse Y, Beierkuhnlein C, Damm A, Gharun M, Grams TEE, Hauck M, Hajek P, Hartmann H, Hiltbrunner E, Hoch G, Holloway-Phillips M, Körner C, Larysch E, Lübke T, Nelson DB, Rammig A, Rigling A, Rose L, Ruehr NK, Schumann K, Weiser F, Werner C, Wohlgemuth T, Zang CS, Kahmen A (2020) A first assessment of the impact of the extreme 2018 summer drought on Central European forests. *Basic and Applied Ecology* 45:86–103.
- Vitali V, Forrester DI, Bauhus J (2018) Know Your Neighbours: Drought Response of Norway Spruce, Silver Fir and Douglas Fir in Mixed Forests Depends on Species Identity and Diversity of Tree Neighbourhoods. *Ecosystems* 21:1215–1229.

Index of Figures

| | |
|---|-----|
| Figure 1.1 Water transportation routes, in general..... | 5 |
| Figure 1.2 A conceptual perspective of the eco-evolutionary trade-off..... | 6 |
| Figure 1.3 Anatomical traits affecting the relationship between xylem safety and efficiency. | 7 |
| Figure 1.4 Exemplary distribution maps of investigated | 10 |
| Figure 1.5 Plausible growth trade-offs within conducting xylem system..... | 12 |
| Figure 1.6 Logical flow of the chapters in the dissertation. | 14 |
| | |
| Figure 2.1 Boxplots showing the micro-climatic growing conditions..... | 32 |
| Figure 2.2 Boxplots of growth-related traits | 39 |
| Figure 2.3 Boxplot depicting the variability between treatments for hydraulic, wood anatomical, and leaf. ... | 40 |
| Figure 2.4 Effect of growth performance on the water potential at 50% loss of hydraulic conductivity (P_{50}).. | 42 |
| Figure 2.5 Dependency of growth rate on wood anatomical and leaf morphological traits..... | 43 |
| Figure 2.6 Water potential at 50% loss of hydraulic conductivity. | 44 |
| | |
| Figure 3.1: Stomatal response curves of dried-out saplings from the five investigated temperate tree..... | 76 |
| Figure 3.2: Plots of leaf water potential at predawn (Ψ_{pd}) versus midday (Ψ_{md})..... | 77 |
| Figure 3.3: Stacked bar chart depicting time to hydraulic failure (T_{hf})..... | 78 |
| Figure 3.4: Point and range plots of hydraulic traits across five temperate tree species. | 79 |
| Figure 3.5: Clustered correlation matrix of investigated hydraulic traits..... | 81 |
| Figure 3.6: Principal component analysis (PCA) of nine hydraulic characteristics | 82 |
| | |
| Figure 4.1: Correlation matrix of hydraulic, morphological, and anatomical traits | 103 |
| Figure 4.2: Vulnerability curves depicting the percent loss of conductivity (PLC) | 106 |
| Figure 4.3: Boxplot showing the proportional contribution of different vessels class. | 107 |
| Figure 4.4: Anatomical sections of the stems and vessels distribution at different diameter..... | 108 |
| Figure 4.5: Water potential variation among the five temperate tree species..... | 113 |
| Figure 4.6: Linear mixed effect modelled the midday water potential (Ψ_{md}) variation | 114 |
| Figure 4.7: Linear mixed effect modelled a maximum range of variation ($\Delta\Psi_L$, i.e., $\Psi_{pd}-\Psi_{md}$) | 115 |
| Figure 4.8: Linear regression show the stomatal conductance (g_s) versus midday water potential (Ψ_{md})..... | 116 |
| Figure 4.9: Stomatal conductance (g_s) versus a diurnal range of variation ($\Delta\Psi_L$, i.e., $\Psi_{pd}-\Psi_{md}$) | 116 |
| Figure 4.10: Species drought response strategy shaped the desiccation time..... | 119 |

Index of Tables

| | |
|---|-----|
| Table 2.1 List of variables included in this study with their definitions and units. | 34 |
| Table S2.1 Summary of all major variables explored | 52 |
| Table 3.1: Summary of investigated traits with their symbols, units and definition. | 75 |
| Table 3.2: Hydraulic properties of the five investigated temperate tree species | 89 |
| Table A4.1: A list of all the main variables explored in the study was given with units and summary | 124 |
| Table S4.1: Parameter estimates of the linear mixed effect models show the midday water potential (Ψ_{md}) relationship as an f(x) of the interaction of VPD * species and days | 128 |
| Table S4.2: Parameter estimates of the linear mixed effect models show the midday water potential (Ψ_{md}) relationship as an f(x) of the interaction of Ψ_{pd} * VPD and days | 129 |
| Table S4.3: Parameter estimate of the linear mixed effect models shows the relationship of a maximum daily range of water potential variation ($\Delta\Psi_L$, i.e., $\Psi_{pd} - \Psi_{md}$) as an f(x) of VPD, species and days | 130 |
| Table S4.4: Parameter estimate of the linear mixed effect models depict the relationship of a maximum daily range of water potential variation ($\Delta\Psi_L$, i.e., $\Psi_{pd} - \Psi_{md}$) as an f(x) of interaction between Ψ_{pd} and VPD | 131 |
| Table S4.5: The parameter estimate of ANOVA with the Tukey post-hoc test shows the multiple comparisons of overall change in midday leaf water potential (Ψ_{md}) | 132 |
| Table S4.6: The parameter estimate of ANOVA with the Tukey post-hoc test shows the multiple comparisons of the overall daily range of water potential variation ($\Delta\Psi_L$) | 132 |

Publications:

Publications presented for the dissertation

Kumar M, Waite P-A, Paligi SS, Schuldt B (2022) Influence of Juvenile Growth on Xylem Safety and Efficiency in Three Temperate Tree Species. *Forests* 13:909.

Kumar M, Waite P-A, Link R M, Schuldt B (2023) Coordinated drought responses determine the time to hydraulic failure in five temperate tree species differing in their degree of isohydry. (draft).

Additional publications from earlier work during my PhD

Peer reviewed publications

Fahad S, Chavan SB, Chichaghare AR, Uthappa AR, **Kumar M**, Kakade V, Pradhan A, Jinger D, Rawale G, Yadav DK, Kumar V, Farooq TH, Ali B, Sawant AV, Saud S, Chen S, Poczai P (2022) Agroforestry Systems for Soil Health Improvement and Maintenance. *Sustainability* 14:14877.

Kumar R, Kumar A, Banyal R, **Kumar M**, Singh A, Yadav RK, Dobhal S, Sharma S (2022) Seed and seedling diversity delimitation and differentiation of Indian populations of *Melia dubia* cav. *Saudi Journal of Biological Sciences* 29:489–498.

Kumar R, Mehta H, Kumar A, Bhardwaj AK, Kaushal R, Dobhal S, Gupta AK, Banyal R, **Kumar M**, Kumar S, Verma K (2021) Seed source variation affects the growth, biomass, carbon stock, and climate resilience potential: A case study of *Celtis australis* in Indian Himalayas. *Global Ecology and Conservation* 26:e01469.

Chavan SB, Uthappa AR, **Kumar M**, Handa AK, Sirohi C, Chichaghare AR, Rawale GB, Sawant AV, Dhoke S (2022) Stalwarts who globally shaped the concept and science called agroforestry. *Indian Journal of Agroforestry*:1–12.

Ranjan R, Pramanik M, Tiwari SP, **Kumar M**, Yadav RS (2020) Rain Water Harvesting in Non-arable Land using Staggered Trenching in Semi-arid Climate of Bundelkhand. *Journal of Agricultural Physics* 20:69–74.

Acknowledgements

Acknowledgement in true essence is to remember and express our gratitude and appreciation for those who have supported me throughout my PhD journey. First and foremost, I take this opportunity to express my heartfelt thanks to my prudent mentor Prof. Dr. Bernhard Schuldt, for offering me the opportunity to conduct my research in his laboratory at the University of Würzburg, Germany. His support, expert guidance, kind cooperation and meticulous supervision have been invaluable throughout my dissertation. I am excited and looking forward to collaborating with him on future projects!

I further want to give sincere thanks and a deep appreciation to my advisory committee members, Prof. Dr. Dirk Hölscher and Prof. Dr. Juliano Cabral, for their timely cooperation, encouragement, and feedback on my research work. Special thanks to co-author Dr. Pierre-André Waite and Dr. Roman Mathias Link, who facilitated and supported me with methodological and statistical questions during my study. Thanks to Mr Sharath Shyamappa Paligi, who first guided me when I arrived in Germany, and also for their support, contribution and suggestions on my manuscripts.

The financial help provided by the Indian Council of Agricultural Research (ICAR), New Delhi, India, through the Netaji Subhas - ICAR International Fellowship programme 2019-22 to pursue PhD degree in Germany is duly acknowledged. I thank Dr. T. Mohapatra, Director General, Dr. G. Venkateswarlu and Dr. Seema Jaggi, ADG (EQR), ICAR, India, for approving my fellowship grant file. Mr. Bhagwat Singh, ACTO (EQR), ICAR, for timely processing and release of fellowship. Special thanks to Dr. P. C. Sharma, Director, and R. K. Yadav, head, HCM, ICAR-CSSRI, Karnal, for the support and encouragement to apply ICAR fellowship. I gratefully acknowledge the logistics and scientific assistance from the University of Würzburg, Germany. I am thankful for the technical support provided by Christine Gernert, Yvonne Heppenstiel, and Jutta Winkler-Steinbeck from the University of Würzburg, Germany.

I am grateful to my colleagues and friends, Vincent Riedel, Emilie Isasa, Julia Rieder, Fon Robinson, and Dr. Amauri Bergmann Bueno, Dr. Aline Xavier de Souza. Thanks to my friends Dr. Sridhar Patra, Dr. Mundre Ningappa Ramesha and Dr. Surekha Rajkumar, who have supported and encouraged me throughout my PhD journey. Special thanks go to Dr. Praveen Kumar Rai and Asim Swain, who provided me with a sense of comfort during my stay in Germany and helped me navigate the challenges that came along the way. Thanks to Dr Rajesh Kaushal for proofreading my thesis.

At this pivotal moment, I am overwhelmed with emotion and struggle to find words that adequately express my profound gratitude to my beloved family. To my dear mother and father, Ruby, Drishti, Ishani, Kamlesh, Shashi, and Rajani, I am forever grateful for your unconditional love, patience, support, and encouragement throughout life. You are a constant source of strength and inspiration, and I can't thank you enough for everything you have done for me.

Finally, thank you all for being a part of this incredible journey. Your support and encouragement have made me overcome the challenges throughout the journey. Last but not least, I sincerely thank all beloved, respected people who helped me directly or indirectly, but I could not find a separate mention.

Manish Kumar
(Author)

Affidavit

I hereby confirm that my thesis entitled “Structural and compositional effects on tree-water relation” is the result of my own work. I did not receive any help or support from commercial consultants. All sources and / or materials applied are listed and specified in the thesis.

Furthermore, I confirm that this thesis has not yet been submitted as part of another examination process neither in identical nor in similar form.

Würzburg, 29.03.2023

Place, Date

Signature

Eidesstattliche Erklärung

Hiermit erkläre ich an Eides statt, die Dissertation “Strukturelle und Zusammensetzungs effekte auf die Beziehung zwischen Baum und Wasser” eigenständig, d.h. insbesondere selbständig und ohne Hilfe eines kommerziellen Promotionsberaters, angefertigt und keine anderen als die von mir angegebenen Quellen und Hilfsmittel verwendet zu haben.

Ich erkläre außerdem, dass die Dissertation weder in gleicher noch in ähnlicher Form bereits in einem anderen Prüfungsverfahren vorgelegen hat.

Würzburg, 29.03.2023

Ort, Datum

Unterschrif

Curriculum vitae

| | |
|------------|------------|
| [Redacted] | [Redacted] |
| [Redacted] | [Redacted] |
| [Redacted] | [Redacted] |
| [Redacted] | [Redacted] |
| [Redacted] | [Redacted] |
| [Redacted] | [Redacted] |

[Redacted]

[Redacted]

[Redacted]

[Redacted]

[Redacted]

[Redacted]

[Redacted]

[Redacted]

[Redacted]

[Redacted]

[Redacted]

[Redacted]

[Redacted]

[Redacted]

[Redacted]

[Redacted]

[Redacted]

[Redacted]

[Redacted]

[Redacted]

[Redacted]

[Redacted]

[Redacted]

[Redacted]

[Redacted]

[Redacted]

[Redacted]

[Redacted]

[Redacted]

[Redacted]

[Redacted]

[Redacted]

[Redacted]

[Redacted]

[Redacted text block]

[Redacted text block]

[Redacted text block]

[Redacted text block]

[Redacted text block]

[Redacted text block]

[Redacted text block]

[Redacted text block]

[Redacted text block]

[Redacted text block]

[Redacted text block]

Authors contributions statement

[Redacted text]